Spring 2019

Feasibility and assessment of using recycled rubber for infrastructure applications

Ahmed A. Gheni

Department: Civil, Architectural and Environmental Engineering

FEASIBILITY AND ASSESSMENT OF USING RECYCLED RUBBER FOR INFRASTRUCTURE APPLICATIONS

by

AHMED ADNAN GHENI

A DISSERTATION

Presented to the Faculty of the Graduate School of the

MISSOURI UNIVERSITY OF SCIENCE AND TECHNOLOGY

In Partial Fulfillment of the Requirements for the Degree

DOCTOR OF PHILOSOPHY

IN

CIVIL ENGINEERING

2019

Approved by:

Mohamed A. ElGawady; Advisor
John J. Myers
Lesley H. Sneed
Stuart Baur
K. Chandrashekhara

PUBLICATION DISSERTATION OPTION

This dissertation consists of the following eight articles.

Paper I: Pg. 13-54 “Mechanical Characterization of Concrete Masonry Units Manufactured with Crumb Rubber Aggregate." was published in the *ACI Materials Journal*.

Paper II: Pg. 55-96 “Thermal Characterization of Cleaner and Eco-Efficient Masonry Units Using Sustainable Aggregates." was published in *Journal of Cleaner Production*.

Paper III: Pg. 97-138 “Retention Behavior of Crumb Rubber as An Aggregate in Innovative Chip Seal Surfacing." was published in *Journal of Cleaner Production.*

Paper IV: Pg. 139-200 “Texture and Design of Green Chip Seal Using Recycled Crumb Rubber Aggregate." was published in *Journal of Cleaner Production.*

Paper V: Pg. 201-230 “Leaching Assessment of Eco-Friendly Rubberized Chip Seal Pavement." was published in *Journal of Transportation Research Record.*

Paper VI: Pg. 231-272 “Durability Properties of Cleaner Cement Mortar with By-Products of Tire Recycling." was submitted for publication in *Journal of Cleaner Production.*

Paper VII: Pg. 273-304 “Recycled Additive to Improve Freeze-Thaw Durability of High Fly Ash Content Mortar." was submitted for publication in the *ACI Materials Journal.*

Paper VIII: Pg. 305-360 “Thermal and Acoustic Retrofitting of Masonry Elements Using Sustainable Alternative." will be submitted for publication in *Journal of Applied Energy*.

ABSTRACT

The United States needs to mine billions of tons of raw natural aggregate each year. At the same time, millions of scrap tires are stockpiled every year. Therefore, replacing natural aggregate with recycled crumb rubber aggregate will be beneficial to the construction industry and environment. This research aimed to investigate the feasibility of using recycled rubber in new construction applications. Based on size, recycled rubber was selected to match its natural counterpart. Different ratios of recycled crumb rubber were used as a fine aggregate replacement in concrete masonry units (CMUs) where the rubberized units showed a lower unit weight, higher ultimate strain, and better durability. In addition, the thermal conductivity of rubberized masonry units decreased with increasing the rubber content resulting in a reduction in heating energy consumption. In a different application, recycled crumb rubber was used as a full or partial replacement of coarse aggregate in chip seal surfacing where it shows better retention especially with longer curing time. The rubberized chip seal had a rougher surface which increases driving safety. Environmentally, the toxic heavy metals leached from the rubberized chip were below that of the EPA drinking water standards with a significant reduction of heavy metal leaching when rubber was used with emulsion in the form of chip seal. The third application was utilizing the waste of scrap tire processing in a form of rubber- fiber powder (RFP) as a sand replacement within cement mortar. RFP was used as an additive to provide more corrosion resistance and less heat of hydration of cement mortar. Incorporating RFP within plastering mortar disclosed that RFP can be used as an eco-friendly additive to provide better crack resistance, thermal and acoustical insulation as well as noise reduction.

ACKNOWLEDGMENTS

First and foremost, I thank God for making all things possible. I would like to express my sincere gratitude to my advisor Dr. ElGawady for his support, patience, motivation, and immense knowledge. Dr. ElGawady believed in me like nobody else did and gave me endless support. He taught me how to define a research problem, propose and investigate a solution to it, and publish the results. On a personal level, Dr. ElGawady inspired me by his hardworking and passionate attitude. To summarize, I would give him most of the credit for becoming the kind of Ph.D. candidate I am today. Special thanks to my advisory committee members, Dr. John J. Myers, Dr. Lesley H. Sneed, Dr. Stuart Baur, and Dr. K. Chandrashekhara, for their time and input. I would also like to acknowledge my fellow students in the CArE Department (too many to list here but you know who you are!) for providing support and friendship. Special thanks go to Dr. Zuhair Al-Jaberi for being my chosen brother and Dr. Hesham Tuwair for his continuous advice. Thanks also go to CArE Department staff: John Bullock, Greg Leckrone, Gary Abbott, Brian Swift, Mike Lusher, Jason Cox, and Delbert Hampton, for their technical support.

I dedicate this to the memory of my father Adnan Gheni, the special man who sacrificed everything toward putting his children in the right way. Love you Dad and I hope I can transfer some of your genes to my kids. Thank you, Mam, for your daily prayers, I couldn't survive without them. I would like to thank my family: my wife and my three adorable kids for their daily love as well as my sisters and brother for their encouragement. Last but not least, I extend my gratitude to all those who made this work possible through financial and in-kind contributions including Missouri DNR, Missouri DOT, HCED Iraq, Midwest Brick & Block, Williams Form Engineering Corp, and Vance Brothers.

TABLE OF CONTENTS

Page

LIST OF ILLUSTRATIONS

PAPER IV

PAPER VI

PAPER VII

PAPER VIII

LIST OF TABLES

SECTION

1. INTRODUCTION

1.1. BACKGROUND

Statistics shows continues increase in the consumption of construction material leaded by extensive use of sand and gravel. As shown in Figure 1, the U.S. consumption of construction materials is incomparable to any other material. During the year of 1998, 73% of all materials used in U.S., by weight, were crushed stone, sand, and gravel (Horvath 2004), which should raise a serious concern about the continuous depletion of these natural resources.

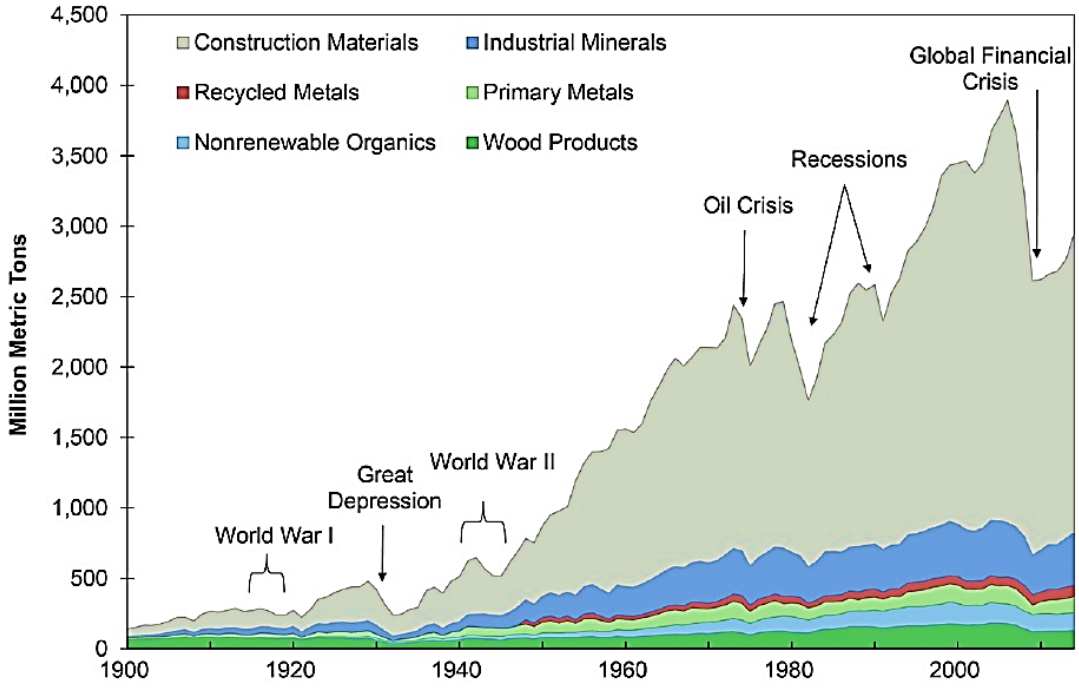

Figure 1.1. U.S. Nonfuel Material Consumption, 1900-2014 (Matos 2012).

Since the construction activities are responsible for exhausting the environment and natural resources, there is an opportunity for reducing the impact of the construction industry on the environment by replacing a portion of the mineral aggregate with a recycled one. For example, replacing only 10% of the used mineral aggregate with recycled materials resulting in cutting of the annual total consumption of the natural aggregate by 112 million ton.

The world is facing a serious problem dealing with scrap tires. As shown in Figure 2, approximately more than four million tons of scrap tires were dumped in the U.S. during 2017 alone taking up valuable space in landfill and wasting valuable resources in the form of the rubber material, textile, and metal cord (RMA 2018). During the year of 2017, U.S. created about 256 million scrap tires (RMA 2018); furthermore, it is expected that the number of vehicles will nearly double worldwide by 2040, which results in even larger environmental concerns of how to properly address the challenges related to the disposal of scrap tires. Since scrap tires are not a biodegradable material, there is a major concern with fire hazards. Rubber tires burn very quickly and are very difficult to extinguish, which can lead to months of fire with a high rate of toxic gas emissions as well as surface and groundwater pollution due to the melted oily residue from the burned tires. It is very difficult to prevent or quench the oxygen supply of the donut-shaped tire since it contains 75% void space, which increases the fire exposure risk of scrap tires in landfills. In addition, scrap tires serve as a fertile breeding ground for mosquitoes and other insects due to their ability to collect and retain water and heat. With the serious threat of the mosquito-borne Zika virus, the focus not only on dealing with the new generated scrap tires but also cleaning up old stockpiles of scrap tires.

Reusing scrap tires is the best practical approach to deal with them due to the lack of both technical and economical disposal mechanisms for scrap tires. Current popular use of scrap tires includes using their recycled crumb rubber as mulch in farms or playgrounds and a binder modifier in asphalt; however, as shown in Figure 2, civil engineering market consumes a very small portion from the total generated scrap tires because of the lack of practical application. Another widely used application for the scrap tires was using them as a fuel in cement production kilns; however, their use resulted in higher CO2 and Sulphur dioxide emissions during the burning process which affect the chemical composition of cement, which resulted in delayed ettringite formation and potential cracking in concrete members (Olorunniwo 1994). Therefore, there is an urgent need to find new applications for scrap tires that can consume large quantities of crap tires.

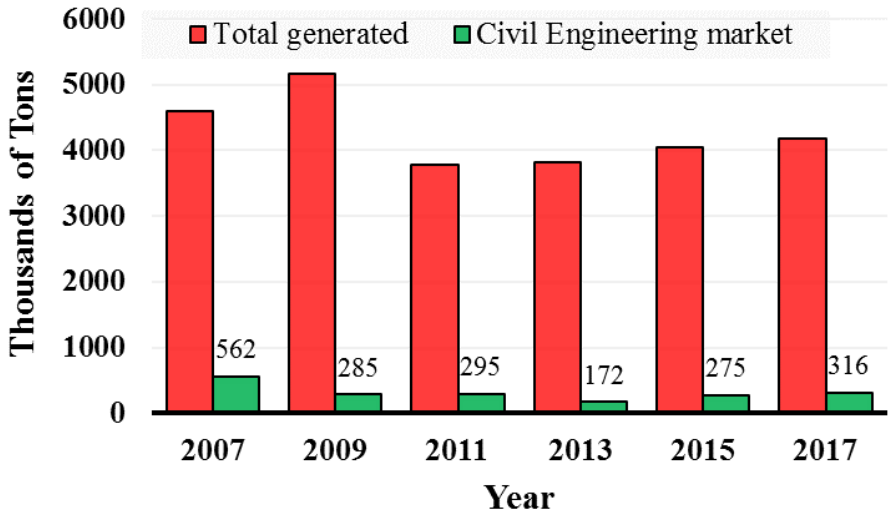

Figure 1.2. U.S. Scrap Tire Trends 2007 – 2017 (RMA 2018).

Since there is a need for an alternative material to replace natural aggregate in construction applications and another need for new applications for scrap tires, this

dissertation investigated using crumb rubber derived from scrap tires as an aggregate in construction which, if successful, would address both issues. Furthermore, the selected niche market should be applications where the construction will benefit from the high performance of tires as a durable, sound and thermal insulator, high strain capacity, and high viscous damping material while does not necessarily need high strength.

1.2. OBJECTIVES AND SCOPE OF WORK

The overarching objective of this work is to find new applications in the area of civil engineering that consume a big portion of the yearly generated scrap tires. In particular, this dissertation aims to:

1. Determine the mechanical and physical properties of rubberized mortar where mineral fine aggregate is replaced by rubber powder. The developed rubberized mortar can be used for plastering as a thermal and sound repair for existing structures or as part of new construction. Processing the scrap tire results in about 65% crumb rubber in different sizes and 35% solid waste that includes steel cords and fibers, nylon fiber, contaminated rubber, and rubber-fiber powder (Granuband Macon 2017). About 25% of this solid waste, which equates to 8% of the total scrap tires volume, is rubber powder and nylon fiber (RFP), which is still going to landfills under a very strict measured due to its very fine particle sizes. Rubber powder has no current applications at all in the market. Therefore, this is another challenging product that this research is addressing. This application focused on crumb rubber having aggregate size ranging from 0.02 to 0.3 mm.
2. Determine the mechanical and physical properties of rubberized masonry units where crumb rubber is used to replace mineral fine aggregate in conventional

concrete masonry units (CMUs). CMU is one of the most important and widely used construction materials with 4.5 billion structural concrete masonry units been produced in the U.S during 2014 alone. Currently there are a very few studies in the technical literature on using crumb rubber as a recycled material in manufacturing concrete masonry units (CMUs). This study investigated the cyclic and monotonic compressive strength, E-modulus, energy dissipation, sound insulation, and thermal insulation. Furthermore, the long-term durability of the crumb rubber CMUs was investigated as well. This application focused on crumb rubber having aggregate size ranging from 1 to 4 mm

3. Determine the feasibility, mechanical properties, and develop design models for rubberized chip seal where mineral coarse aggregate is replaced with crumb rubber. Previous studies used crumb rubber as asphalt binder modifier but not an aggregate. There has been no research on using crumb rubber as an aggregate in chip seal which, if successful, will significantly increase the sustainability of chip seal and consumes huge amount of scrap tires. This study investigated the adhesion between crumb rubber and different types of binders. Furthermore, the effects of using crumb rubber on chip seal macro-texture was investigated. Field implementations of rubberized chip seal in Sedalia, Rolla, and Boonville were also carried out. This application focused on crumb rubber having aggregate size ranging from 5 to 10 mm.

1.3. DISSERTATION OUTLINE

This dissertation includes three sections. Section 1 includes a brief introduction to the subject area, the objectives and scope of the dissertation, and a literature review establishing the state of the art of the research area. Section 2 contains eight journal papers that discuss three main new application of the recycled rubber based on the size of rubber particles. The waste of scrap tires processing in a form of rubber- fiber powder was used as a sand replacement in mortar. Crumb rubber with particles smaller than 4mm was used as a partial replacement for fine aggregate in masonry units, while recycled rubber with particles larger than 4mm was used as a full or partial replacement for coarse aggregate in chip seal surfacing. Section 3 presents the key findings of all experiments, which were executed during this research study, as well as a proposal for future research.

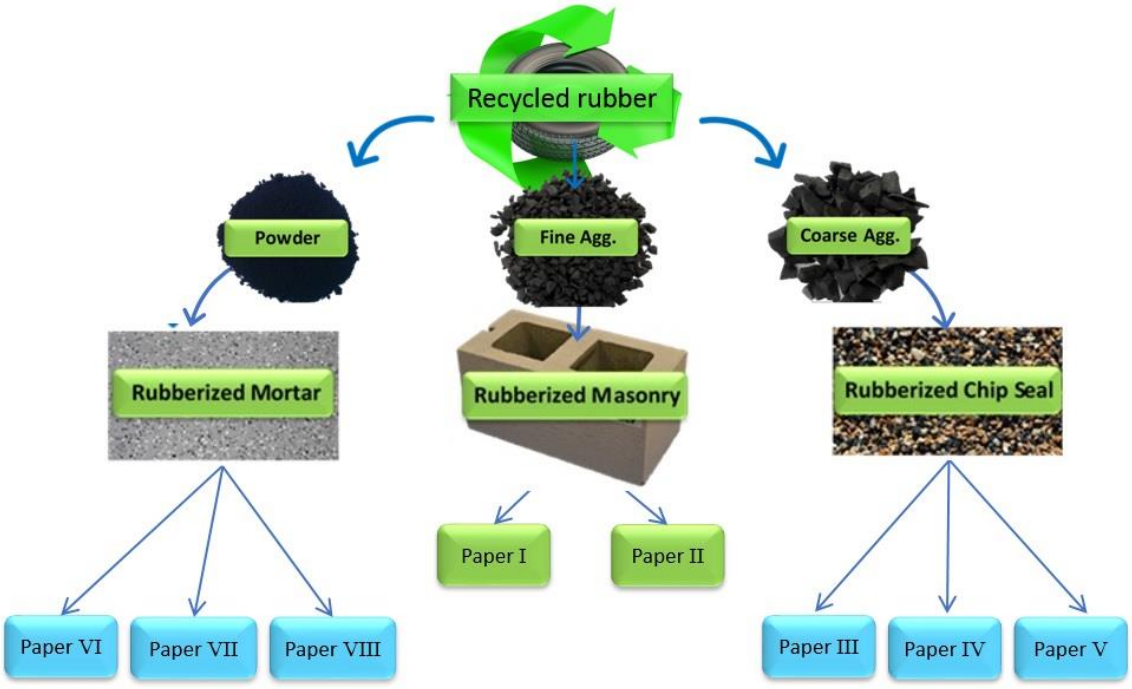

Figure 1.3. Dissertation outline.

2. LITERATURE REVIEW

2.1. USING RECYCLED RUBBER IN CONCRETE

Comprehensive research has been devoted to characterize the fresh and hardened properties of rubberized concrete where crumb rubber replaced cement and/or natural aggregates. A reduction was noted in the unit weight of rubberized concrete because of the rubber particle's low specific gravity and the increase in entrapped air contents. The measured air content was higher in rubberized concrete than in reference mixtures without rubber (Fedroff et al. 1996, Khatib and Bayomy 1999, Siddique and Naik 2004). Researchers reported also that there is a rubber content threshold; before that threshold adding rubber will increase slump values due to the hydrophobic nature of rubber which causes a water film coating on the rubber particles that reduce the friction with other particles. Beyond the threshold, the low unit weight of the rubber causes a reduction in slump (Siddique and Naik 2004, Sukontasukkul and Chaikaew 2006, Gou and Liu 2014).

Both the compressive and flexural strengths were negatively affected when crumb rubber was used as one of the constituent of concrete mixture due to rubber's relatively low stiffness and the poor bond between the rubber particles and cement paste (Siddique and Naik 2004, Batayneh et al. 2008, Najim and Hall 2010, Thomas and Gupta 2013, Gou and Liu 2014, Moustafa and ElGawady 2016, Youssf et al. 2017). Using large rubber particles were also more influential in reducing the compressive strength of rubberized concrete than using small particles. This influence is due to the low stiffness of rubber particles which makes it act like air voids where their effect increase with increasing the volume of each void (Eldin and Senouci 1993, Fattuhi and Clark 1996, Batayneh et al. 2008). Furthermore, the elastic modulus of rubberized concrete decreased with the increase

of rubber content since rubber has lower stiffness compared to aggregate. However, using lower stiffness materials, i.e., rubber increased the ultimate strain of rubberized concrete (Ganjian et al. 2009). Rubberized concrete displayed higher energy dissipation, viscous damping and hysteric damping compared with the corresponding conventional concrete (Hernandez-Olivares et al. 2002, Zheng et al. 2008, Xue and Shinozuka 2013, Moustafa and ElGawady 2015, Youssf et al. 2015, Youssf et al. 2016, Moustafa and ElGawady 2017, Moustafa et al. 2017). Recently, researchers proposed rubberized concrete as a structural material in high seismic regions to enhance energy dissipation capabilities, a crucial feature for structures built in high seismic regions (Xue and Shinozuka 2013). Atahan and Yücel (2012) performed drop-weight tests on rubberized concrete cylinders. They determined that replacing 20-40% of aggregates with crumb rubber creates concrete mixtures that are useful for concrete barriers panels. Moustafa and ElGawady (2015) used free vibration on simply supported beams and static cyclic compression tests on concrete cylinder to investigate the concrete's dynamic properties. They reported that both the viscous damping and the average hysteresis damping increased as the rubber content increased.

Compared with conventional concrete, rubberized concrete provides higher sound and heat insulation, sound absorption, and noise reduction coefficient as well as lower heat transfer properties (Turgut and Yesilata 2008, Sukontasukkul 2009, Hall et al. 2012). It was reported that composite concrete-scrap-tire-pieces walls increased the thermal insulation of a model room by 11% (Yesilata et al. 2011). Using granulated rubber in the concrete of flooring and foundations was enough to have low-rise dwellings meet the UK Building Regulations in term of thermal insulations without the need to any additional insulating layers (Paine and Dhir 2010). Both the amount of rubber and particles sizes has

an impact on the thermal conductivity of rubberized concrete (Abu-Lebdeh et al. 2014). Using larger size of rubber particle in the production of rubberized gypsum board resulted in a better reduction in the thermal conductivity and the same trend was reported with cement mortar as well (Fadiel et al. 2014).

Rubberized concrete exhibited better freeze and thaw durability and sulfate resistance compared to conventional concrete mixtures (Savas et al. 1997, Benazzouk and Queneudec 2002, Yung et al. 2013, Thomas and Gupta 2015, Liu et al. 2016, Richardson et al. 2016, Thomas et al. 2016). The freeze and thaw of rubberized concrete can be further improved should a finer particle size, up to 20 μm, be used (Richardson et al. 2016), which is comparable to the size of cement particles. However, it is very expensive to produce recycled rubber with a particle size smaller than 1.5 mm (Yang et al. 2011, Shu and Huang 2014).

2.2. USING RECYCLED RUBBER IN CONCRETE MASONRY

Researches have shown that crumb rubber obtained from scrap tires can be used to replace mineral aggregate leading to more environment-friendly construction industry (Papagiannakis and Lougheed 1995, Hanson et al. 1996, Amirkhanian 2001, Shuler 2011, Rangaraju and Gadkar 2012, Moustafa and ElGawady 2015, Youssf et al. 2016). However, in the last 10 years, more than 1000 paper were published in Scopus journals related to masonry units. The term “eco-efficient” were mentioned in only 0.3% of those papers, meaning that the eco-efficient concept has not yet successfully entered in the masonry research field (Pacheco-Torgal et al. 2014). More than 4.6 billion CMUs were produced in the United States in 2014 with a nearly 12% annual increase. However, CMUs are manufactured today using conventional materials that have a negative impact on the

environment. In addition, CMUs are quite a brittle material. Hence, a pressing need exists to produce CMUs that are more ductile and sustainable. One potential approach toward this good is to replace some of the natural fine aggregates with crumb rubber produced from scrap tires.

A very few studies investigated the effect of adding crumb rubber to masonry units as a replacement of natural aggregates producing what is known as rubberized concrete masonry units (RCMUs). Very few researchers produced both load-bearing and non-load-bearing rubberized masonry hollow blocks and rubberized brick where mineral aggregates were partially replaced with crumb rubber (Isler 2012, Mohammed et al. 2012, Sadek and El-Attar 2015). The previous researchers focused on finding a new home for recycled rubber, so they can dump it there with target to match the characterizations of the conventional materials. However, in this research, the target is to use the unique features of rubber to improve the current products and get a better performance in different measures.

2.3. USING RECYCLED RUBBER IN PAVEMENT

Transportation infrastructure is a major contributor to global greenhouse gas emissions with 23% of global carbon dioxide (CO2) emissions, which makes it the second largest contributor, only behind electricity generation (Ang and Marchal 2013). As a result, using recycled material in the construction of the transportation infrastructure will help to cut the (CO2) emissions significantly. One application is using scrap tire material in the roadway construction. One application where scrap tire material may prove to be used successfully is in the roadway construction. Previous studies used crumb rubber as asphalt

binder modifier, which improves the general performance of the binders in terms of temperature susceptibility, viscosity, and stiffness(Lee et al. 2008, Presti 2013).

The processes of applying crumb-rubber modifier (CRM) in asphalt mixtures including blending asphalt cement with crumb rubber at a high temperature (177–210 ^{o}C). The Federal Highway Administration (FHWA) and many state agencies have conducted numerous field studies for the feasibility of using recycled rubber tire products in asphalt pavements. The National Cooperative Highway Research Programs (NCHRP) provides a comprehensive review of the use of recycled rubber tires in highways based on a review of nearly 500 references and information recorded from state highway agencies' responses to a 1991 survey of practices (Epps and Mason 1994). Florida DOT began constructing demonstration projects of asphalt pavement with CRM wet processes in 1989 and has reported satisfactory pavement performance (Page 1992). It concluded that the addition of CRM would increase the asphalt film thickness, binder resiliency, viscosity, and shear strength. Virginia DOT constructed pavements containing CRM asphalt mixtures produced by two wet processes and compared the pavement performance to that of conventional asphalt mixtures. Maupin (Maupin Jr 1996) reported that the mixes containing asphalt rubber performed at least as well as conventional mixes. In Virginia mixes, the inclusion of asphalt rubber in hot-mix asphalt (HMA) pavements increased construction cost by 50–100 percent as compared to the cost of conventional mixes. Troy et al. (Troy et al. 1996) conducted a research on CRM pavements in the state of Nevada. In their study, they evaluated a CRM binder using the Superpave binder testing protocols and conducted the mix design using the Hveem procedure. They concluded that the conventional sample

geometry in Superpave binder test protocols cannot be used to test the CRM binders and that the Hveem compaction is inadequate for mixtures containing CRM binders.

This dissertation used another approach to recycle crumb rubber. Crumb rubber was used as an aggregate replacement (not binder modifier) in chip seal. Chip seal is a layer of surfacing treatment that is constructed by spreading binder followed by uniform aggregates. Rollers are used after spreading the aggregates for compaction in order to achieve the required embedment of the aggregates into the layer of binder. Chip seal plays an excellent role in resisting tire-damage actions and creates a macrotexture that provides a good skid-resistant surface to ensure a safe driving atmosphere (Gransberg and James 2005). In addition, chip seal has been widely used for preventive road maintenance to prevent further surface deterioration. One important feature that makes chip seal competitive with the other maintenance techniques is its affordability (Gransberg and James 2005, Karasahin et al. 2014).

According to the best knowledge of the researcher, there has been no research on using crumb rubber as an aggregate into chip seal. This is partially due to the fact that chip seal practice in the U.S. has been developed as an empirical procedure rather than engineering sound practice. This dissertation aims at investigating the potential use of crumb rubber as an aggregate in chip seal which, if successful, will significantly increase the performance and sustainability of chip seal.

PAPER

I. MECHANICAL CHARACTERIZATION OF CONCRETE MASONRY UNITS MANUFACTURED WITH CRUMB RUBBER AGGREGATE

Ahmed A. Gheni, Mohamed A. ElGawady, and John J. Myers

ABSTRACT

An experimental investigation was conducted to investigate the effects of replacing varying percentages of fine natural aggregates with crumb rubber in concrete masonry units (CMUs), creating rubberized concrete masonry units (RCMUs). The mechanical and physical characteristics of RCMUs having 0%, 10%, 20%, and 37% crumb rubber were investigated and presented in this paper. The unit weight and water absorption of RCMUs were measured. A scanning electron microscope (SEM) analysis was used to study the global structure for RCMUs and the interfacial zone. RCMUs were also exposed to extreme weather conditions for 72 days inside an environmental chamber. Furthermore, RCMUs were subjected to rapid freezing and thawing tests. The RCMUs as well as grouted and ungrouted masonry prisms were tested under monotonic and cyclic axial loads.

The results indicated that RCMUs with high rubber content displayed higher values of axial ultimate strains. RCMUs exhibited a significant strain softening; while conversely, failure was quite brittle in CMUs. RCMUs specimens exhibited an improvement in compressive strength after several cycles of severe weather exposure. The CMU specimens, however, exhibited degradation in their compression strength capacity. The water absorption was higher in RCMUs than it was in the CMU prisms.

Keywords: masonry; crumb rubber; rubberized concrete, sustainable materials.

1. INTRODUCTION

A concrete masonry unit (CMU) is an important construction material that is widely used around the world. One pressing need for the construction industry is to use more sustainable material. One approach toward achieving sustainable CMUs is to use recycled materials such as crumb rubber, produced from scrap tires, in replacing natural aggregates during manufacturing CMUs. Scrap tires are already available across the U.S; for example, during 2013 alone, the U.S. generated 233 million scrap tires as reported by the Rubber Manufacturers Association. Scrap tires are considered harmful waste that serves as a home for mosquitoes, rats, and snakes. They also represent a tremendous fire hazard. Once a tire pile catches fire, it is very hard to extinguish. Such fire would emit significant amounts of CO2 and harmful dioxins into the surrounding environment. Many landfill operators do not accept scrap tires in their landfills. Most states in the United States (U.S.) have enacted legislation that restricts or even bans the disposal of tires in landfills. Using recycled tires as a filler to produce CMUs would reduce the amount of scrap tires placed in landfills. Recycled tires also have the potential to improve the mechanical and physical characteristics of CMUs. Yet, a very few studies investigated the effect of adding crumb rubber to masonry units as a replacement of natural aggregates producing what is known as rubberized concrete masonry units (RCMUs). RCMUs can be produced as load-bearing and non-load-bearing blocks1, 2 with the compressive strength of RCMUs is generally smaller than that of their conventional counterpart. While there have been few studies on RCMU, several studies altered the fresh and hardened concrete showed that adding crumb rubber to concrete mixtures as a replacement of aggregate and/or cement. It was stated by Robisson et al.3 that rubber and cement have been successfully combined before without

any negative long-term interaction between them. For example, rubber particles have been added to cement to form a self-healing cement system for long-term durability. Rubberized concrete commonly displays smaller unit weight, compared to conventional concrete. Since rubber particles have significantly lower specific gravity compared to natural aggregates. Furthermore, rubberized concrete has generally higher air entrapped than its content part in conventional concrete. Rubberized concrete also has smaller slump compared to its counterpart conventional concrete. Furthermore, the use of crumb rubber as a partial replacement for aggregate reduces the compressive strength, flexural strengths and dynamic modulus of elasticity4-10. Damping properties, however, of rubberized concrete are higher than that of conventional concrete. Energy absorption and dissipation increased greatly when rubber replaced natural aggregate in concrete11 Recently, researchers proposed rubberized concrete as a structural material in high seismic regions to enhance energy dissipation capabilities, a crucial feature for structures built in high seismic regions12. Atahan and Yücel13 performed drop-weight tests on rubberized concrete cylinders. They determined that replacing 20-40% of aggregates with crumb rubber creates concrete mixtures that are useful for concrete barriers panels. Moustafa and ElGawady14 used free vibration on simply supported beams and static cyclic compression tests on concrete cylinder to investigate the concrete's dynamic properties. They reported that both the viscous damping and the average hysteresis damping increased as the rubber content increased.

Rubber also altered the physical properties of concrete. Rubberized concrete has a higher sound absorption, a higher noise reduction coefficient, and lower heat transfer

properties than those of conventional concrete. As a result, rubberized concrete has a greater ability to retain stored heat energy15-17.

The mechanical and physical characteristics of hollow concrete masonry units having 0%, 10%, 20%, and 37% crumb rubber replacement of natural fine aggregate by volume are presented in this manuscript. The compressive strength and ultimate strain under cyclic loads were investigated for masonry prisms constructed out of RCMUs. Both grouted and ungrouted prisms were examined. Masonry water absorption, unit strength, unit weight, and durability of RCMUs were compared with conventional CMUs. Scanning electron microscopy (SEM) was performed for the different RCMU.

2. RESEARCH SIGNIFICANCE

Concrete masonry unit (CMU) is a wide speared construction material. More than 4.6 billion concrete masonry units were produced in the USA during 2014 with nearly 12% annual increase18. However, CMUs are manufactured today using conventional materials that have a negative impact on the environment. In addition, CMUs are quite a brittle material. Hence, a pressing need exists to produce CMUs that are more ductile and sustainable. One potential approach toward this good is to replace some of the natural aggregates with crumb rubber produced from scrap tires. In addition, finding a new home for non- biodegradable waste like scrap tire, which is an environmental concern, will minimize their negative environmental impacts.

3. EXPERIMENTAL PROGRAM

This manuscript presents the results of the mechanical characterization of RCMUs including unit weight, water absorption, and unit compressive strength. The manuscript

also presents the compressive strengths of RCMUs after they had been subjected to cycles of extreme environmental conditions such as freezing and thawing, high humidity, and high temperature. The results of scanning electron microscopy that was performed to study the interfacial zone between rubber from one side and cement paste from the other side, are also presented in this manuscript. Finally, grouted/ungrouted prisms were subjected to cyclic compressive testing and the results are presented. All results are compared to those of conventional CMUs and prisms constructed out of CMUs.

3.1. MATERIAL PROPERTIES

Hollow concrete masonry units having 0%, 10%, 20%, and 37% crumb rubber replacement of natural fine aggregate by volume were produced by a masonry plant in Jefferson City, Missouri using standard manufacturing process. These blocks were used during the course of this study. Based on earlier studies1, 4, 11, 19, it was decided that a maximum fine natural aggregate replacement of 20% would potentially produce masonry blocks with minimal strength reduction which can be used in structural applications while higher replacement values maybe used for non-structural applications. Hence, one replacement percentage of 40% was targeted during the mixture design. However, during the mixture process, the final rubber replacement was found to be 37% only.

All of the materials used during this research were sampled and tested according to the appropriate ASTM standard as listed in Table 1. The sieve analysis of the rubber and the fine aggregate that were used for blocks manufacturing during this research are illustrated in Figure 1. The mix of rubber that was used came from three different grades of rubber (Figure 2). The grout was sampled and tested according to ASTM C1019 – 13 (Figure 3). The mortar's compressive strength was sampled and tested according to ASTM C270−12a.

3.2. RCMU MECHANICAL CHARACTERIZATION

The unit weight, water absorption, and compressive strength of RCMUs were tested according to ASTM C140/C140M−14b. For each rubber content ratio, three individual RCMUs were tested for compressive strength. A fibrous composite laminated cap was used to distribute the load and prevent the stress concentrations. A rigid 24 x 12 x 2 inch (610 x 305 x 51 mm) steel loading plate was used to apply the loads (Figure 4). The maximum stress was averaged for each rubber ratio. To find the absorption according to ASTM C140/C140M−14b, three RCMUs from each different rubber ratio were placed in an oven at 235°F (113°C) for 25 hours (Figure 5). Whenever two successive RCMUs were weighed at intervals of 2 hours showed an increment of loss not greater than 0.2% of the previous weight, the weight of the specimen was determined. The samples were then left outside the oven until they reached room temperature so that the oven-dry weight (W_d) could be measured. Next, the samples were soaked in a large water container for 24 to 28 hours. The specimens then were removed from the water and weighted while they suspended by a metal wire and completely submerged in water and record (W_i) (immersed weight). Block then was removed from the water and all visible water was wiped before obtaining the saturated weight (W_s). The absorption and unit weight were calculated using equation 1.

$$Absorption, kg/m^3 = \frac{w_s - w_d}{w_s - w_i} * 1000 \quad (1)$$

W_s = saturated weight of specimen, kg

W_i = immersed weight of specimen, kg and

W_d = oven-dry weight of specimen, kg.

3.3. RCMU DURABILITY CHARACTERIZATION

Five RCMUs from each rubber ratio were placed inside an environmental chamber (Figure 6) for 73 days. These specimens were exposed to severe weathering cycles representing 20 years of harsh Midwest weather exposure(Micelli and Myers 2008, Tuwair et al. 2016) (Table 2 and Figure 7.). A computer-controlled environmental chamber was used to simulate 350 different environmental cycles including the following: 50 freeze-thaw cycles representing cold days and 50 alternating cycles of high temperature and high relative humidity representing hot and humid days. The compressive strength of each RCMU was then tested according to ASTM C140/C140M−14b and compared to that of the unexposed RCMUs to better understand the crumb rubber's effect on durability. Similar test was carried out on reference CMUs.

3.4. RAPID FREEZING AND THAWING TEST

A freezing and thawing resistance test was conducted according to ASTM C 666-Procedure A which involves both freezing and thawing specimens in water. Four specimens were tested for each ratio of rubber. The specimens were prepared by cutting an 11 x 3 x 1.5 inch (280 x 76 x 38 mm) prismatic piece from the face shell of RCMU **(Figure 8)**. Freezing and thawing tests began by placing the specimens in the thawing water at the beginning of the thawing phase. Then, the specimens went through cycles of freezing and thawing. After every 36 cycles, the specimens were removed from the apparatus in a thawed condition and the changes in weight and relative dynamic modulus of elasticity were measured for each specimen. The water was changed, and the containers were washed after each set of cycles. The tests were continued and repeated for 300 freezing and thawing

cycles or until the relative dynamic modulus of elasticity reached 60% of the initial dynamic modulus for each specimen whichever occurred first.

The relative dynamic modulus of elasticity was calculated using equation 2:

$$P_c = \frac{n_1^2}{n^2} * 100\% \quad (2)$$

where:

P_c = relative dynamic modulus of elasticity, after c cycles of freezing and thawing, (percent).

n = fundamental transverse frequency at 0 cycles of freezing and thawing, and

n_1 = fundamental transverse frequency after c cycles of freezing and thawing.

At the conclusion of this test, the durability factor for each specimen with different rubber ratios were calculated as follows:

$$DF = \frac{P * c}{M} \quad (3)$$

where:

DF = durability factor of the test specimen,

P = relative dynamic modulus of elasticity at c cycles, %,

c = number of cycles at which P reaches 60% or the 300 cycles, whichever is less.

M = specified number of cycles at which the exposure is to be terminated.

3.5. ULTRASONIC PULSE VELOCITY

An ultrasonic pulse velocity test was carried out on an 11 x 3 x 1.5 inch (280 x 76 x 38 mm) prismatic specimen (Figure 9). Three replicate specimens were for each percentage of rubber tested.

3.6. SCANNING ELECTRON MICROSCOPE (SEM) ANALYSIS

Both light microscope and scanning electron microscope (SEM) analyses were conducted according to ASTM C1723 − 10 to evaluate the characteristics of the interfacial transition zone (ITZ) between crumb rubber particles and cement paste and to compare this with the ITZ between the mineral aggregate and cement paste. Both polished and fractured samples were examined during this investigation. The test was conducted for RCMU specimens having different rubber content.

3.7. MECHANICAL CHARACTERIZATION OF RCMU MASONRY PRISMS

Twenty four masonry prisms, each with a height of four blocks, were constructed and investigated to determine the compressive strength of RCMU's, E-modulus, and ultimate strain. Three fully-grouted and three ungrouted masonry prisms were tested for each rubber ratio.

Each prism specimen was identified as follows: X-KK-Y, where X represents the amount of rubber replacement ratio (i.e., 0, 10, 20, and 37). KK represents either a grouted (G) or an ungrouted (UG) specimen, Y is the specimen replicate number within each replacement group. Thus, code 10-UG-5 refers to the 5th replicate, ungrouted specimen that had a 10% rubber replacement ratio.

Professional masons constructed the masonry prisms according to ASTM C1314-12. A stack bond with a face shell bedding and Portland cement lime mortar type S were used. Both CMUs and RCMUs (each 7.63 x 7.63 x 15.625 inches (194 x 194 x 397 mm)) were used to build up the prisms. Each prism was one-block long and four-blocks high. Grouting was completed immediately after the prisms were constructed. A rod vibrator was used to consolidate the grout in each cell. The prisms were then exposed to ambient temp in the lab conditions until testing.

Material samples were taken during the construction. Mortar cylinders measuring 4 x 2 inches (102 x 51 mm) and grout prisms measuring 4 x 4 x 8 inches (102 x 102 x 204 mm) were sampled according to ASTM C1019 – 11. The samples were tested on the same day the prisms were tested and at 28 days to determine the mortar and grout compressive strengths.

A displacement control compressive cyclic loading was used to test all of the specimens (Figure 10). The cyclic compression consisted of full loading/unloading cycles. Each loading step was repeated for three times at a loading rate of 0.002 in/min (0.0508 mm/min) and with a loading step of 0.05 in. (1.27 mm).

Two LVDTs were fixed between the middle of the top and the bottom CMUs to measure the vertical displacement (Figure 11). These displacements were used to calculate masonry axil strains.

4. EXPERIMENTAL RESULTS AND DISCUSSION

Table 1 presents the properties of the material and blocks used during the course of this study. It also presents any imposed limits by the appropriate ASTM standards. As illustrated in Table 1, RCMUs having up to 20% replacement of fine aggregate with crumb

rubber meet the requirements of the ASTM C90 in term of unit compressive strength and water absorption. These RCMUs are also classified as normal weight blocks since their unit weight exceeds 2000 kg/m^3 (125 lb/ft^3). However, RCMUs having 37% of fine aggregate replacement can't be used for structural applications.

4.1. UNIT WEIGHT

The effect of the rubber replacement on the unit weight of RCMUs and CMUs is illustrated in Figure 12. As shown in the figure, the CMU's unit weight nonlinearly decreased as the rubber content increased. Increasing the rubber content from 0% to 37% decreased the unit weight from 137.7 lb/ft^3 (2206 kg/m^3) to 119.4 lb/ft^3 (1913 kg/m^3) representing a reduction of 13.3% in the RCMU's unit weight while a rubber content of 20% decreased the unit weight from 137.7 lb/ft^3 (2206 kg/m^3) to 128 lb/ft^3 (2050 kg/m^3) representing a reduction of 7.1% in the RCMU's unit weight. This reduction occurred because the rubber particle's specific gravity was only 32% of that of the fine aggregate. Furthermore, the air content increased with increasing the rubber content in the mixture as indicated by the higher absorption rate (Table 1). Figure 13 shows the nature of the rubber particles' surface. The rubber particles have a rough, scratchy, non-polar surface nature that is tends to entrap air within and around the rubber particles, which has been previously reported[19].

As illustrated in Table 1 and Figure 12, RCMUs having up to 20% replacement of fine aggregate with crumb rubber have unit weight exceeding 2000 kg/m^3 (125 lb/ft^3) and hence are classified as normal weight blocks. However, RCMUs having 37% rubber replacement are classified as medium weight blocks.

4.2. WATER ABSORPTION

The effect of rubber content on the water absorption is illustrated in Figure 14. As shown in the figure, the water absorption increases as the rubber content increases. Increasing the rubber content from 0% to 37% increased the water absorption from 6.8 lb/f^3 (109 kg/m^3) to 11 lb/f^3 (176 kg/m^3), representing an increase of 61.7%. Despite this increase, the absorption rate of all RCMUs did not exceed the absorption rate allowed by ASTM C90-12 of 13 lb/f^3 (208 kg/m^3) (Table 1). The increase in the absorption rate occurred because the rubber had a relatively larger particle size than the fine aggregate. This difference in the particle size created extra voids due to the shortage of the fine materials in the rubber particles. Moreover, it is related to the increase in the air voids explained earlier in this manuscript.

4.3. UNIT COMPRESSIVE STRENGTH

The effect of rubber content on the unit compressive strength is shown in Figure 15. As shown in the figure increasing the rubber content nonlinearly decreased the masonry unit compressive strength. Increasing rubber replacement from 0% to 37% decreased the compressive strength by 77.5%. However, increasing rubber replacement from 0% to 20% decreased the compressive strength by 48.3%. Despite this decrease in strength, the compressive strengths of all RCMUs having rubber replacement up to 20% exceeded the minimum required strength of the ASTM C90-12 of 1900 psi (13.1 MPa) (Table 1).

4.4. COMPRESSIVE STRENGTH AND STRESS- STRAIN RELATIONSHIP

As mentioned, forty four-block high prisms grouted and ungrouted constructed out of RCMs and CMUs were tested under axial cyclic loads. The average strengths, strains at

peak loads, and initial stiffnesses of each five replicate specimens are listed in Table 3. Furthermore, the axial stresses vs. axial strains for each prism are calculated. The axial loads measured during testing of each prism were divided by the prism cross sectional area to calculate the axial stresses while the LVDTs shown in Figure11 were used to calculate the average axial strains. The results of representative prisms are presented in Figure 15. The results indicate that the crumb rubber replacement had significant effects on the strength, initial stiffness, and axial strain at peak loads of the investigated masonry prisms.

As shown in Figure 15 and Table 3, using crumb rubber generally reduced the compressive strengths of the investigated ungrouted prisms with rations ranging from 31% to 71% proportional to the rubber content. For grouted prisms, the reduction ranging from 6.3% to 30.5% based on the rubber content. However, the reductions in the case of grouted prisms were not proportional to the rubber content. The strength of the grouted prims results from two different components, namely, the block strength and grout. For a conventional CMU (0% rubber), the block is quite brittle due to the sever stress concentrations which lead to very early failure of CMU face-shells and webs before the filler grout is being subjected to high axial stress. During testing prisms constructed out of CMUs, the grout suffered few micro to macro-cracks at rupture of the prisms (Figure 16). Hence, the contribution of grout to prims strength was limited. Contrarily, RCMUs have the ability to go through higher axial deformation before failure allowing higher grout deformations and higher grout contribution to the prism axial strength. However, the addition of rubber reduces the strength of the CMUs (Table 1). Hence, there are two contradicting mechanisms that influence the strength of fully-grouted masonry prisms constructed out of RCMUs. For example, RCMUs having 37% rubber replacement had the

ability to go through very high axial strains without failure but also the high rubber replacement ratio had sever effect on the strength of the RCMUs. Hence, fully-grouted prisms constructed out of these blocks displayed a strength reduction of 30.5%. Similarly, RCMUs having 10% and 20% rubber replacement displayed a strength reduction of 27.3% and 6.3%, respectively.

Visual observations and calculations revealed a clear influence of RCMUs on prism stiffness (Figure 17). For the grouted prisms, increasing the rubber content from 0% to 37% decreased stiffness from 3400 ksi (23442 MPa) to 1810 ksi (12480 MPa), which represents a reduction of 47%. Regarding the ungrouted prisms, increasing the rubber content from 0% to 37% decreased stiffness from 4500 ksi (31026 MPa) to 955 ksi (6585 MPa), which represents a reduction of 79%. The influence of rubber on stiffness was less pronounced in the grouted prisms because all prisms had the same type of conventional grout (no rubber in the grout).

Prisms constructed using RCMUs displayed also very high axial strains at the peak loads. For the grouted prisms, 630%, 46%, and 4% increases in the axial strains corresponding to the peak loads were recorded when rubber replacement ratios of 37%, 20%, and 10%, respectively, were used (Figure 15a). While 71%, 7%, and 7% increases in the axial strains corresponding to the peak loads were recorded with 37%, 20%, and 10% rubber replacement ratios, respectively, in the ungrouted prisms (Figure 15b).

An observed beneficial feature for the rubberized prisms was the failure mechanism. Failure in the conventional masonry prisms, i.e. 0% rubber replacement, was quiet brittle and sudden (Figure 15a); the tested prisms could not resist any further load beyond the peck load. In contrast, prisms constructed using RCMUs behaved very ductile with a

gradual failure. For example, prims constructed using 20% rubber replacement RCMUs were able to resist three cycles at stress equal to 67% of the f'_m with a corresponding axial strain of 192% of its peak load strain (Figure 15a). This feature represents pseudo ductility for masonry which allows the engineers to do the required repair in particular compression failure zones before the total collapse or failure can occur in a particular masonry element. However, this requires all other failure modes such as shear failure and reinforcement rupture being superseded. Finally, the large axial strains in RCMUs would help a structural masonry element to display higher ductility capacity which is crucial for seismic regions. Furthermore, the large areas enclosed by the stress-strain loops (Figure 15) indicate that RCMUs significantly increased the energy dissipation of the investigated masonry prisms compared to those prisms constructed using CMUs.

4.5. EFFECTS OF EXTREME ENVIRONMENTAL CONDITIONS

As mentioned earlier, CMUs and RCMUs were placed into environmental chamber and subjected to extreme weather cycles. Then, the compressive strengths of these specimens were determined. The compressive strengths of the conditioned RCMUs were higher than that of the conditioned CMUs (Figure 18). As shown in the figure, the conditioned CMU displayed a compressive strength reduction of 4%. The rubber increased the compressive strength of the conditioned RCMUs by 1% to 20%; this increase, however, was not proportional to the rubber content. The compressive strength of the conditioned RCMU was controlled by contradicting parameters. Increasing the rubber content increased the entrapped air which was filled with water during the weathering cycles. Under freezing conditions, the entrapped water volume increased imposing internal pressure on the RCMUs leading to micro cracking and compressive strength reduction.

Similar behavior was observed for CMUs. However, including crumb rubber in RCMUs acts as an internal spring that absorbs the increase in water volume. Furthermore, when rubber is exposed to low temperatures, the rubber particles crystallize, thereby increasing the rubber compressive strength and stiffness(Fuller et al. 2004), which increases the compressive strength of the unit. However, rubber crystallization decreases the spring effect of the crumb rubber particles inside the matrix, which decreases the ability of crumb rubber to release the internal stresses that result from entrapped water expansion. The amount of crystallinity is related to both the length and the temperature of exposure of RCMU. In the cases of having 20% rubber replacement, the positive factors dominated the performance of the RCMUs meaning that the rubber hardening and internal spring action was significantly higher than the increase in the internal pressure due to water freezing. However, this was not the case for 10% and 37% rubber replacement.

4.6. RAPID FREEZING AND THAWING TEST

As explained earlier, rapid freeze-thaw tests were conducted per ASTM C 666-Procedure A. The behavior of RCMU after the rapid freeze-thaw test depends on the percentage of rubber content (Figs. 19 and 20). RCMUs having 10% rubber content behaved better than the conventional CMUs with gradual reduction in the measured dynamic modules of elasticity. RCMUs having 20% and 37% rubber content replacement respectively, however, each behaved worse than the conventional CMUs with rapid reduction in the dynamic modulus of elasticity. Similarly, the durability factor (DF) of RCMUs having 10% rubber content was 19% higher than that of CMUs, while the DFs of RCMUs having 20% and 37% rubber content were 21% and 29% lower than that of CMUs. This occurred, as explained earlier, due to different contradicting factors including the

increase in entrapped water, rubber crystallization, and internal spring. This clarifies the vacillating behavior of the samples with a 37% rubber content replacement ratio. As a result, the strength of RCMU increased in the beginning of the low temperature cycles when some of the rubber crystallized and the other part absorbed the internal stresses. When the entire amount of crumb rubber in the matrix crystallized, the flexibility of rubber decreased, which reduced its ability to absorb the internal stresses. Therefore, the strength started to decrease rapidly.

4.7. ULTRASONIC PULSE VELOCITY AND SOUND INSULATION

Adding rubber particles to CMUs reduced the velocity of ultrasonic waves and had the same effect on the dynamic modulus of elasticity. Increasing the rubber content linearly decreased the velocity of ultrasonic waves (Figure 21). There was a 36% reduction in the velocity of ultrasonic waves when 37% of the fine aggregate was replaced with crumb rubber. This reduction occurred due to the ability of rubber to absorb the waves. Moreover, the increase in the discontinuous air voids, which is related to the increase of crumb rubber in the matrix, impeded the ultrasonic waves and reduced the ultrasonic pulse velocity. This indicates that having crumb rubber in masonry blocks reduced the sound transmission, which is one of the aspects for the sound insulation. Similarly, Sukontasukkul proved that using crumb rubber in concrete increases sound absorption by increasing the sound absorption coefficient (α) and noise reduction coefficient (NRC)(Sukontasukkul 2009). Nehdi and Khan(Nehdi and Khan 2001) stated that using rubber in concrete enhances the sound insulation compared to conventional concrete.

4.8. SCANNING ELECTRON MICROSCOPE (SEM) ANALYSIS

Figure 22 shows the results of the SEM analyses for CMUs and RCMUs. As shown in the figure, the RCMUs samples (Figure 22 b, c, d) had more air voids than the sample with no rubber (Fig 22 a). The size of the air voids increased as the amount of rubber in the matrix increased.

To evaluate the interfacial bond between rubber particles and conventional aggregate from one side and the cement paste to the other side, the Ca/Si (C/S) criterion was used. This criterion considered the bond high if C/S<1.5(Xincheng 2012). For the samples with no rubber, the element analysis of ITZ between the conventional aggregate and the cement paste showed a C/S ratio of 0.483 (Figure 23 a). This number represents a very high bond between the aggregate and the cement paste. On the contrary, the C/S ratio was 1.58 for the interfacial zone between the rubber particles and the cement paste (Figure 23 b). This ratio represents a relatively low bond relationship between the rubber particles and the cement paste.

The weak bond between the rubber particles and the cement paste was clear when the scanning electron microscope analysis was conducted on the cracked samples. These samples were taken from RCMU that failed by compression test. As shown in Figure 24, there was a gap between the rubber particles and cement paste after failure which occurred due to the weak bond between them which clarifies the systematic reduction in the compressive strength of the rubberized masonry blocks. The poor characteristic of the rubberized masonry blocks ITZ was one of the main reasons for this reduction.

5. FINDING AND CONCLUSIONS

Concrete masonry units with four different ratios of crumb rubber were physically and mechanically examined. The results of compressive strength, peak strain, initial stiffness, water absorption, unit weight, durability, ultrasonic waves, and SEM analysis were reported in this manuscript. Based on the experimental investigation, the following findings and conclusions can be drawn:

1. Producing RCMU in a typical masonry plant was undertaken successfully. Crumb rubber can be used up to 20% partial replacement for fine natural aggregate to produce a rubberized masonry block units (RCMUs) that meet the requirements of the ASTM C90.
2. The RCMUs have a lower unit weight; however, they have higher water absorption rate compared to those of CMUs.
3. Despite the reduction in the compressive strength of RCMUs with increasing the rubber content, using 20% rubber replacement in RCMU resulted in a reduction of 6% in compressive strength of four units stacked high masonry prism. However, significant reduction in the initial stiffness was observed causing 34% reduction in initial stiffness when 20% rubber replacement was used.
4. RCMUs displayed significantly higher ultimate strain compared to those of CMUs.
5. The addition of 20% rubber as a partial replacement of fine aggregate improved the durability of the units by increasing the compressive strength after cycles of extreme environmental conditions.

6. Rubberized blocks displayed a reduction in the ultrasonic pulse velocity and sound transmission. However, farther investigations are needed to study the impact of rubber on sound absorption, reflection, and energy reduction.
7. Scanning electron microscope (SEM) analysis of the interfacial transition zone (ITZ) showed that rubber particles have a weaker bond with cement paste than natural aggregates, which explained the systematic reduction in the compressive strength of the rubberized masonry blocks.

ACKNOWLEDGEMENTS

Midwest Block & Brick Inc. manufactured the blocks used in this research. They also provided the professional masons for construction. This support is greatly appreciated. However, any opinions, findings, conclusions, and recommendations presented in this paper are those of the authors and do not necessarily reflect the views of the sponsors.

Table 1. Material properties.

Items	No. of samples	Tests type	Results	ASTM limits
Mortar	6	Compressive strength ASTM C270 − 12a	2820 psi (19.4 MPa)	Type S 1800 psi (12.4 MPa)
Grout	6	Compressive strength ASTM C476 − 10	4240 psi (29.2 MPa)	2000 psi (14 MPa)
RCMU	12	Compressive strength ASTM C90−12	0% rubber 4332 psi (29.8 MPa) 10% rubber 3664 psi (25.3 MPa) 20% rubber 2234 psi (15.4 MPa) 37% rubber 966 psi (6.7 MPa)	1900 psi (13.1 MPa)
RCMU	12	Absorption Testing ASTM C90−12	0% rubber 6.8 lb/ft^3 (109 kg/m^3) 10% rubber 8.3 lb/ft^3 (133 kg/m^3) 20% rubber 9.4 lb/ft^3 (151 kg/m^3) 37% rubber 11 lb/ft^3 (176 kg/m^3)	13 lb/ft^3 (208 kg/m^3) (Max)
RCMU	12	Density Classification ASTM C90−12	0% rubber 137.7 lb/ft^3 (2206 kg/m^3) 10% rubber 132.5 lb/ft^3 (2122 kg/m^3) 20% rubber 128 lb/ft^3 (2050 kg/m^3) 37% rubber 119.4 lb/ft^3 (1913 kg/m^3)	Lightweight less than 105 lb/ft^3 (1680 kg/m^3) Medium weight 105 to less than 125 lb/ft^3 (1680–2000 kg/m^3) Normal weight 125 lb/ft^3 (2000 kg/m^3) or more
Masonry prism	50	Compressive strength ASTM C1314-12	see table 3	
Rubber	----	unit weight	40 lb/ft^3 (641 kg/m^3)	

Table 2. Environmental chamber cycles.

Conditioning Cycles	Conditioning Extreme Limits	Number of Cycles
Freeze- thaw cycles	-20ºC to 10ºC (-4ºF to 50ºF)	50
High temperature cycles	20ºC to 50ºC (68ºF to 122ºF)	150
Relative humidity cycles	60% RH to 95% RH at 20ºC (68ºF)	50
Relative humidity cycles	60% RH to 95% RH at 25ºC (77ºF)	50
Relative humidity cycles	60% RH to 95% RH at 40ºC (104ºF)	50

Table 3. Tests results of four block height prisms.

Specimen name	maximum stress, psi (MPa)	Micro Strain at maximum stress (in/in) (mm/mm)	Initial Stiffness, ksi (GPa)
0-G	3318 (22.88)	0.96*10^3	3400 (23.44)
10-G	2413(16.64)	1.0*10^3	2713 (18.7)
20-G	3108 (21.43)	1.4*10^3	2250 (15.51)
37-G	2307 (15.9)	7.0*10^3	1810 (12.48)
0-UG	3492 (24.1)	0.7*10^3	4500 (31.03)
10-UG	2396 (16.52)	0.75*10^3	2680 (18.48)
20-UG	2396 (16.52)	0.75*10^3	2312 (15.94)
37-UG	1021 (7.04)	1.2*10^3	955 (6.58)

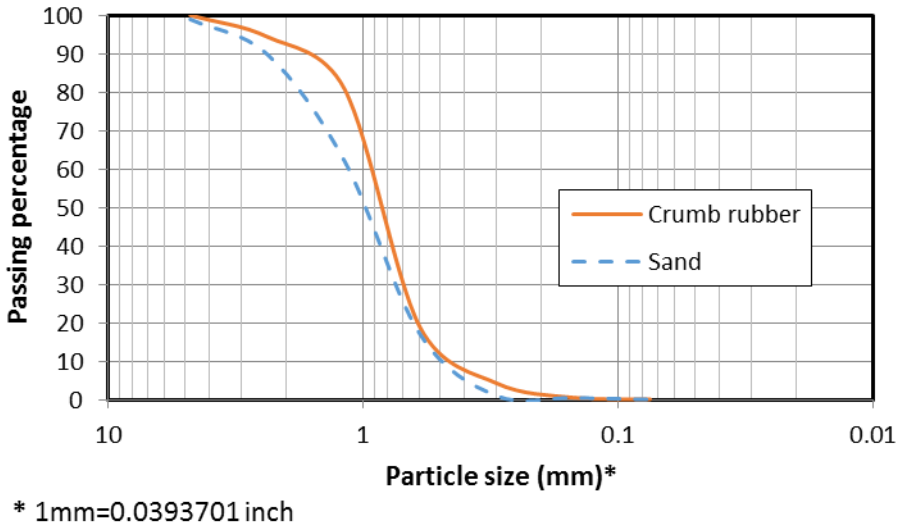

Figure 1. Sieve analysis of the used mix of crumb rubber.

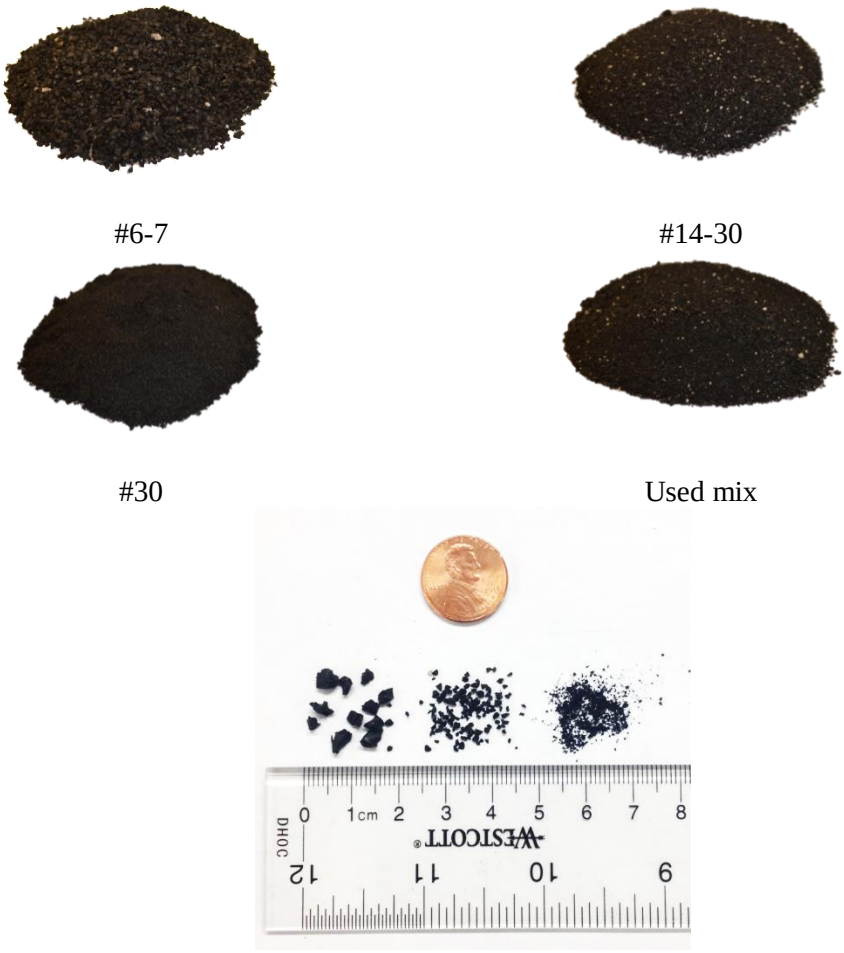

Figure 2. The different sizes of crumb rubber that used in RCMU's production.

(a) (b)

Figure 3. Grout specimens. (a) casting and (b) samples and testing.

Figure 4. Compressive strength test setup.

Figure 5. Water absorption test.

Figure 6. RCMUs in the environmental chamber.

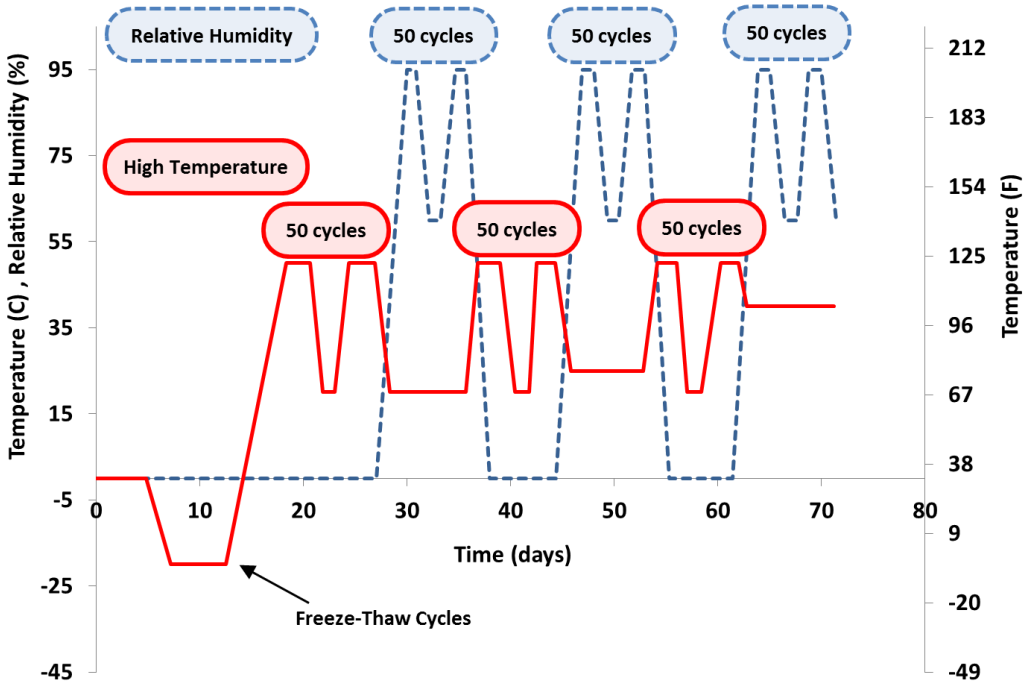

Figure7. Exposure regime for environmental chamber cycles.

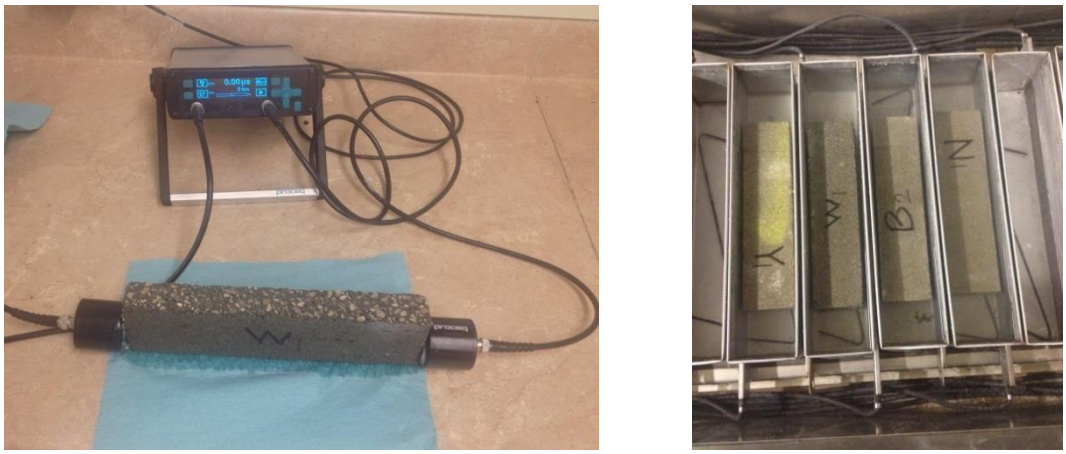

(a) (b)

Figure 8. Rapid freezing and thawing test. (a) ultrasonic test of RCMU sample and (b) samples in freezing and thawing chamber.

Figure 9. Ultrasonic pulse velocity test.

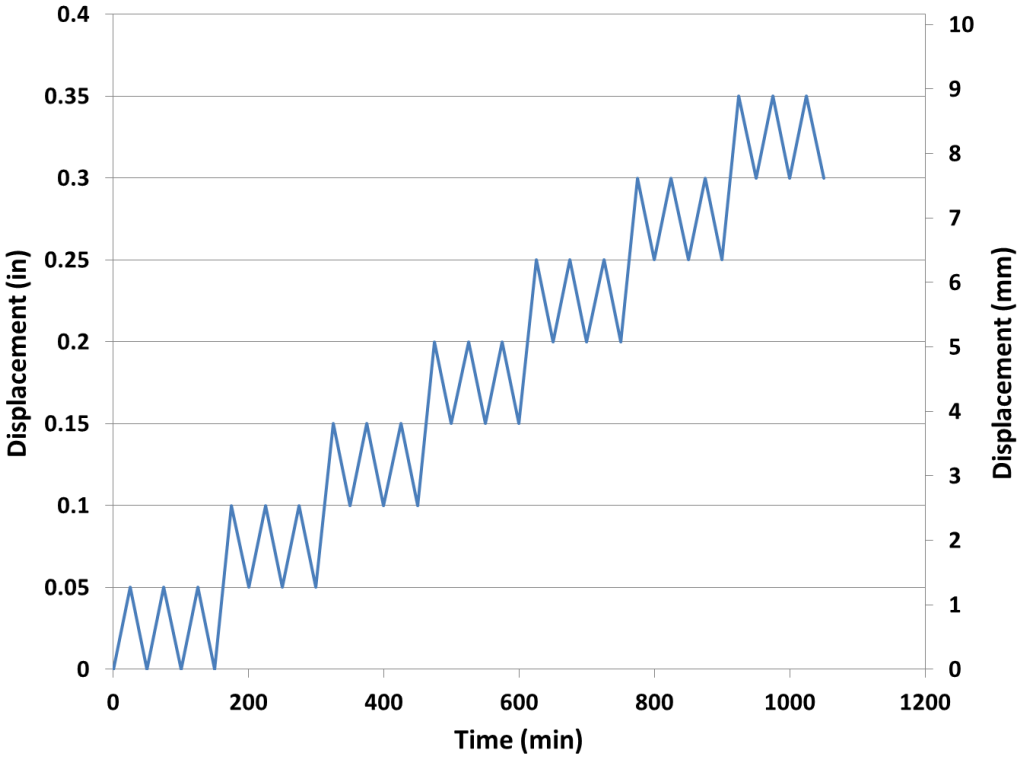

Figure10. Loading protocol.

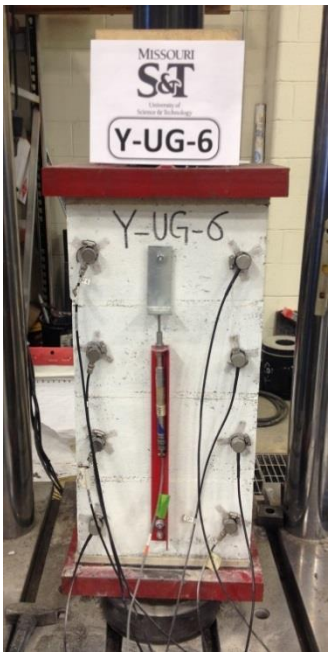

Figure11. Measuring strain of four blocks height masonry prism.

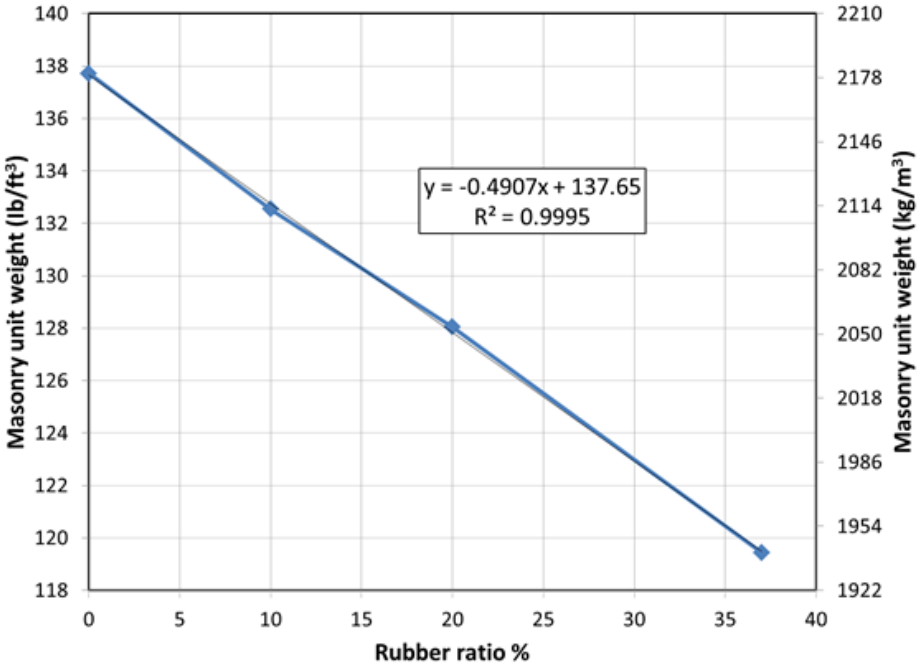

Figure 12. Effect of rubber replacement ratios on the unit weight of masonry unit.

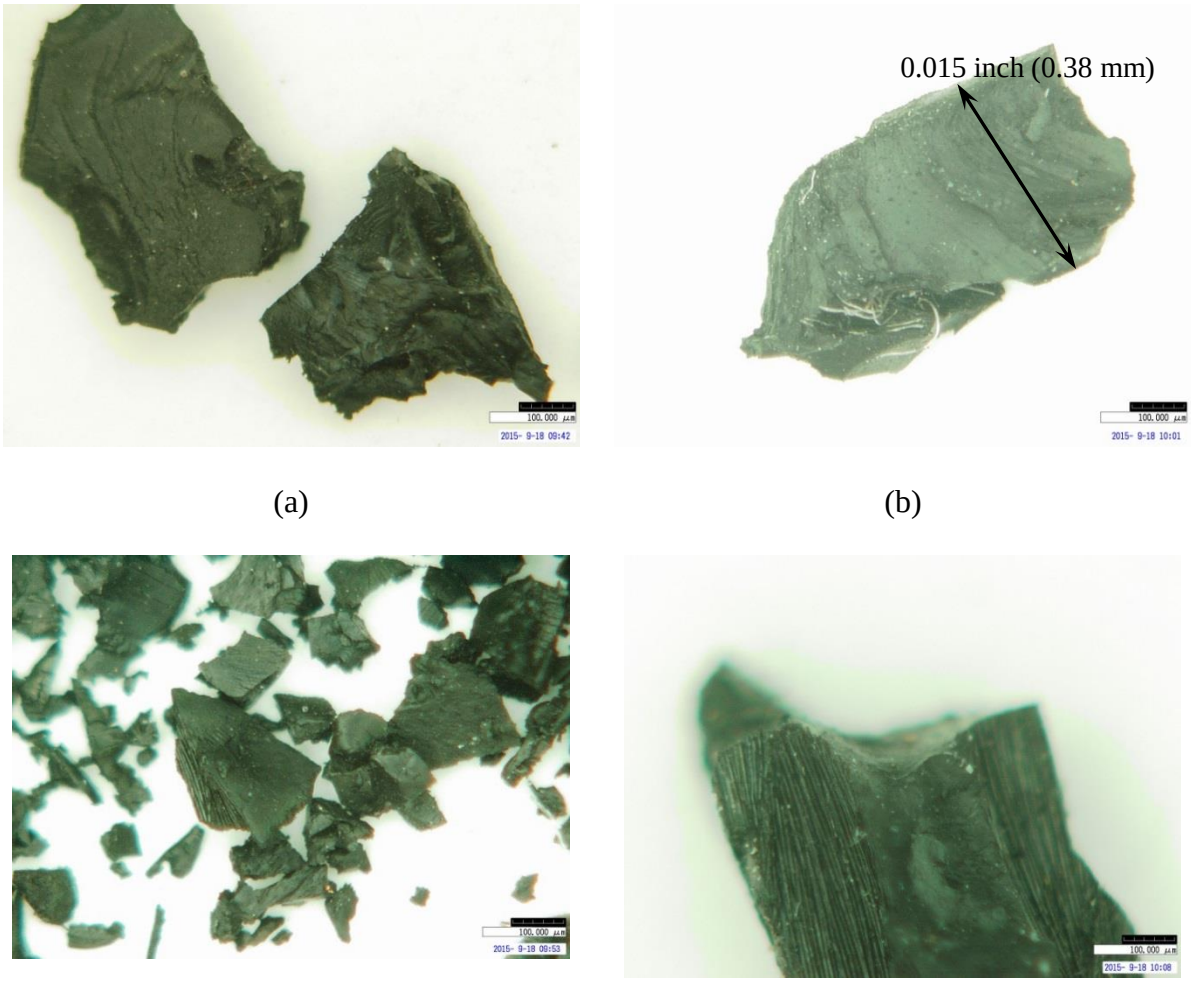

Figure 13. The non-polar nature of the crumb rubber particles' surface.

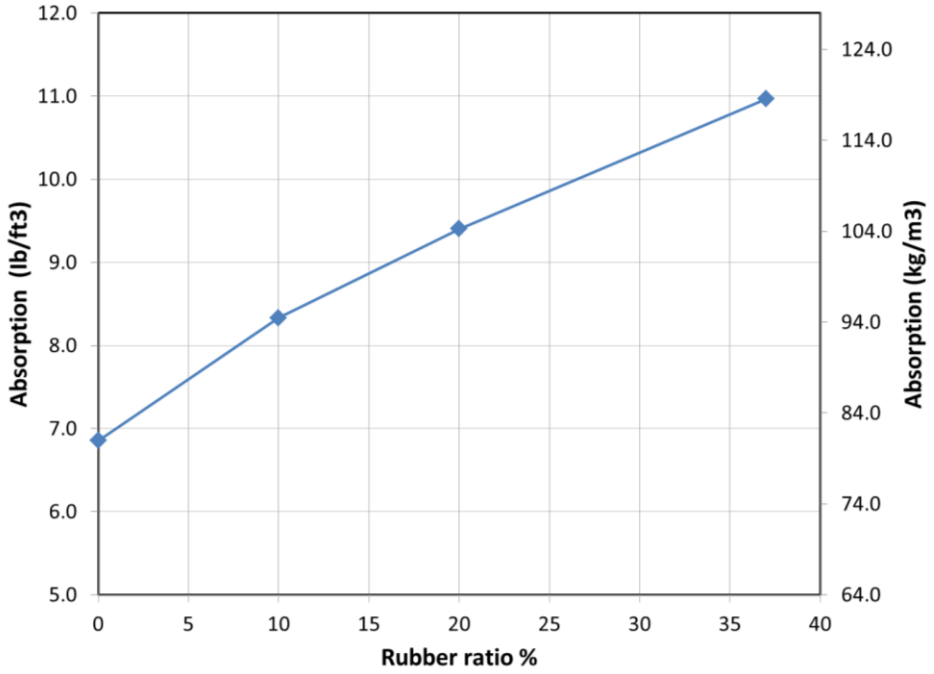

Figure 14. Effects of different rubber replacement ratios on the water absorption.

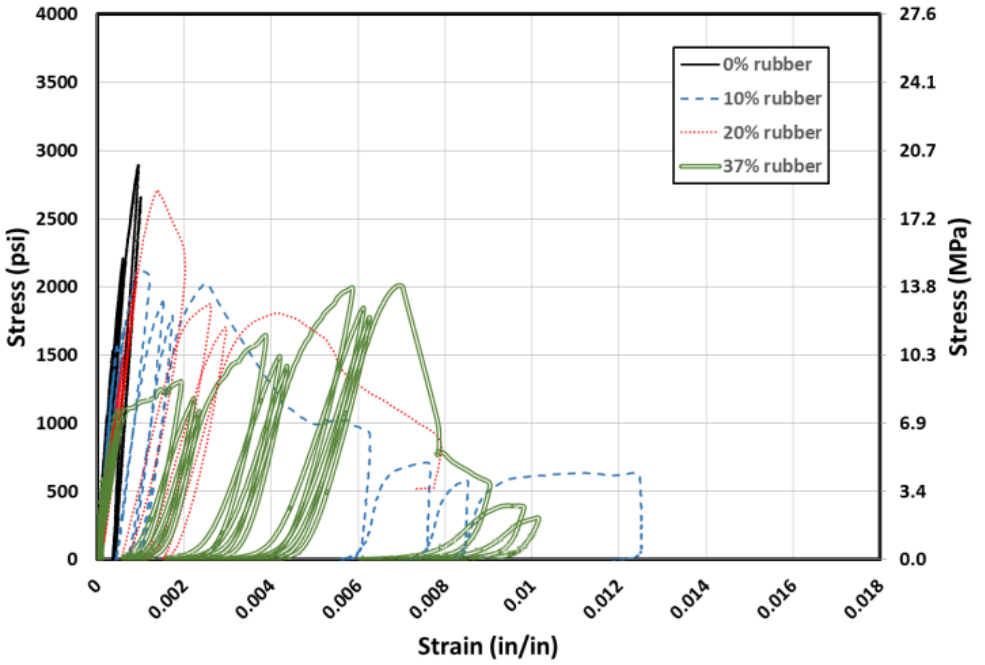

(a)

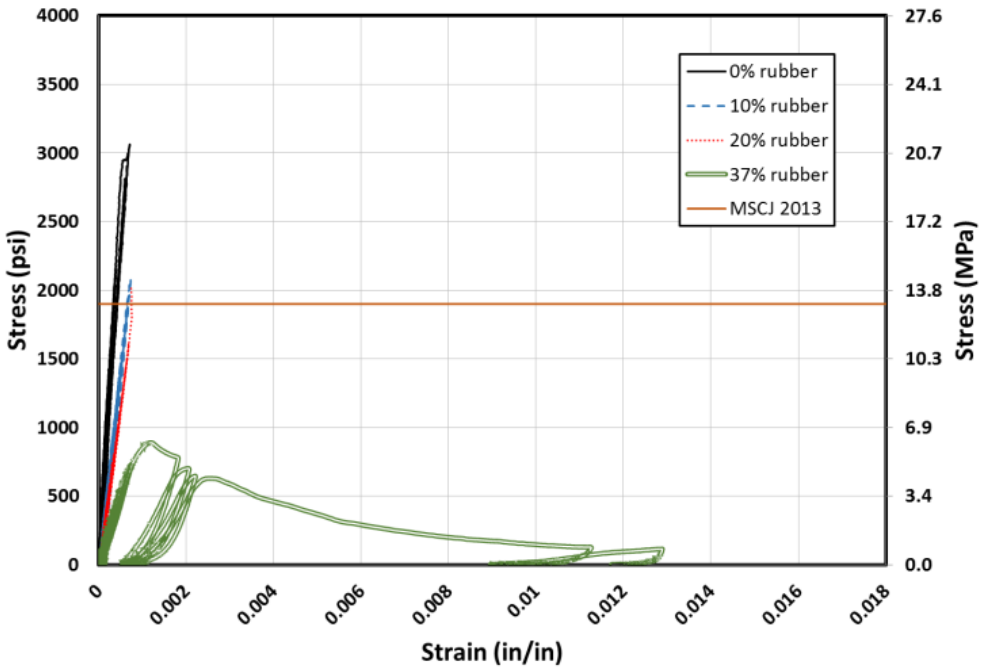

(b)

Figure 15. Stress vs. strain curves for four-block prisms with different rubber content. (a) fully grouted prisms and (b) ungrouted prisms.

(a) (b) (c)

Figure 16. Failure mechanism of four-blocks CMUs prisms (no rubber): (a) rupture of webs, (b) rupture of face shells, (c) grout after failure (note the minor cracking in the grout in the different pictures).

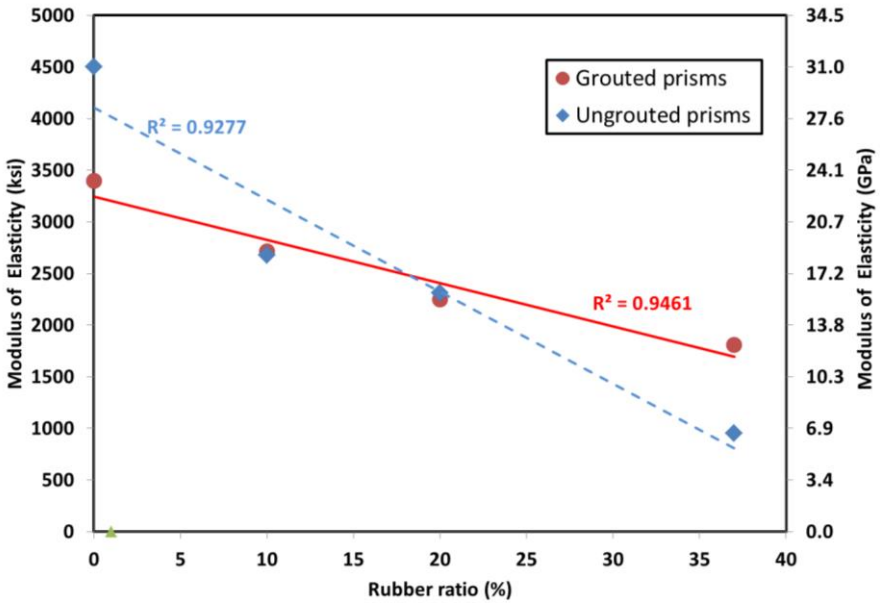

Figure 17. Modules of elasticity of masonry prisms with different rubber content.

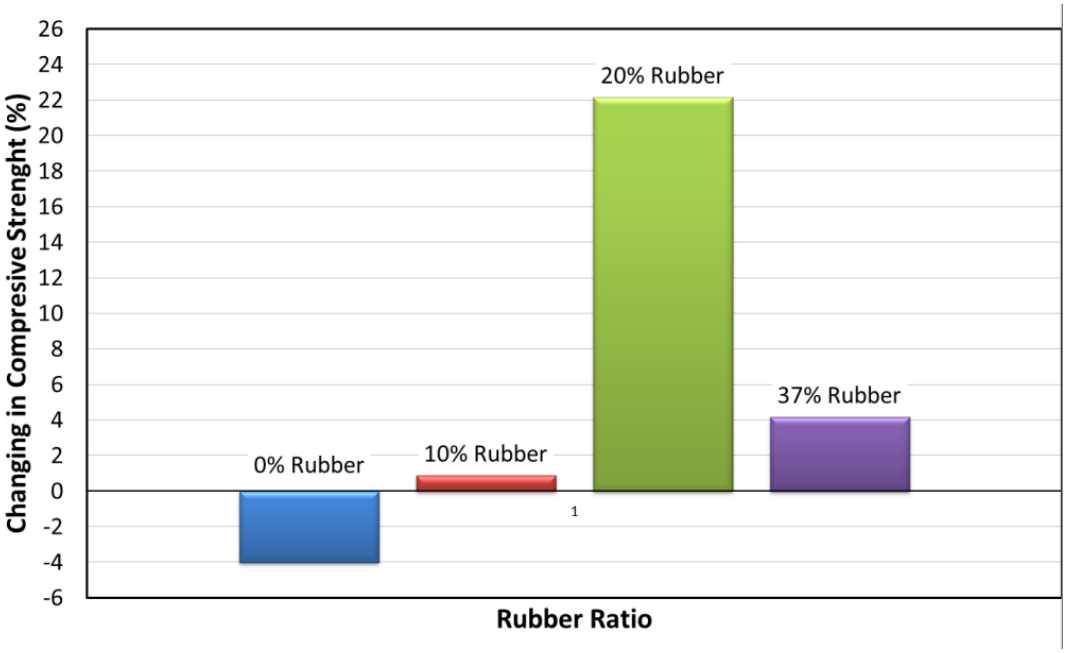

Figure 18. Effect of extreme environmental conditions on the compressive strength for different rubber replacement ratios.

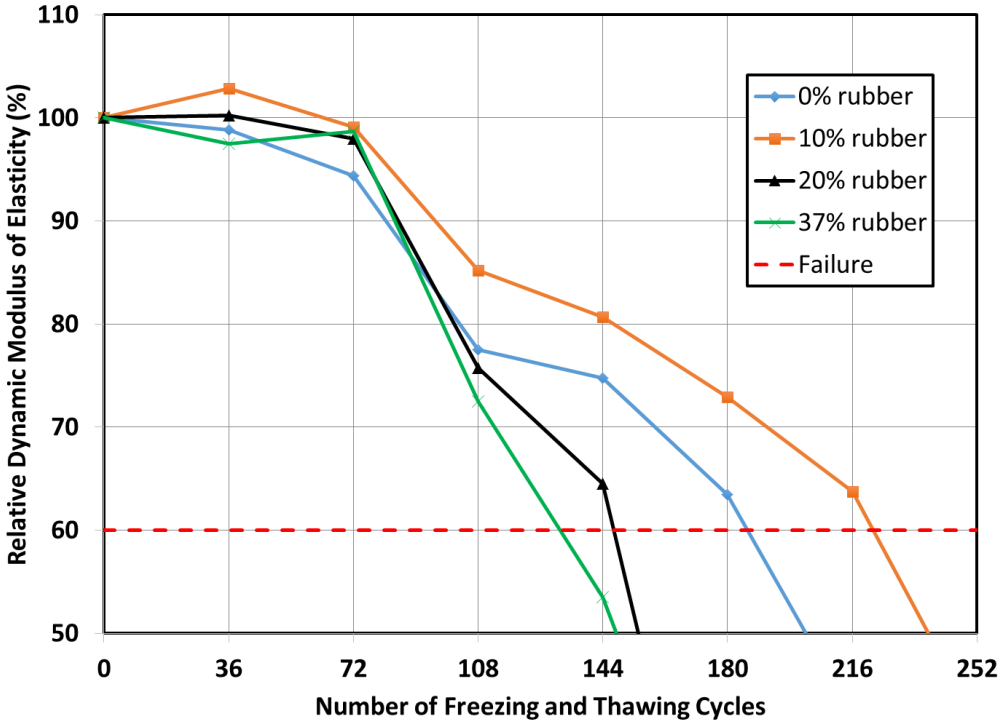

Figure 19. The relative dynamic modulus of elasticity vs. number of freezing and thawing cycles.

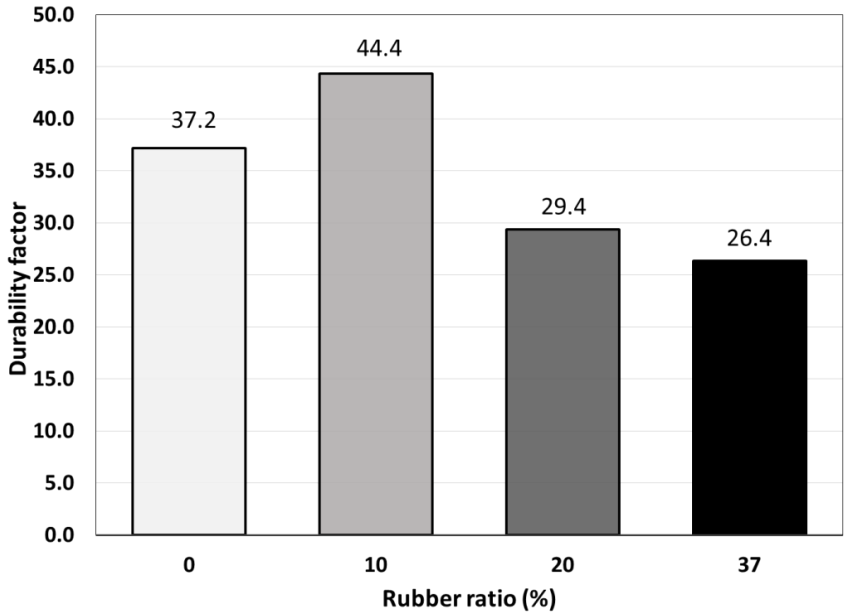

Figure 20. The durability factor of masonry blocks with different rubber ratios.

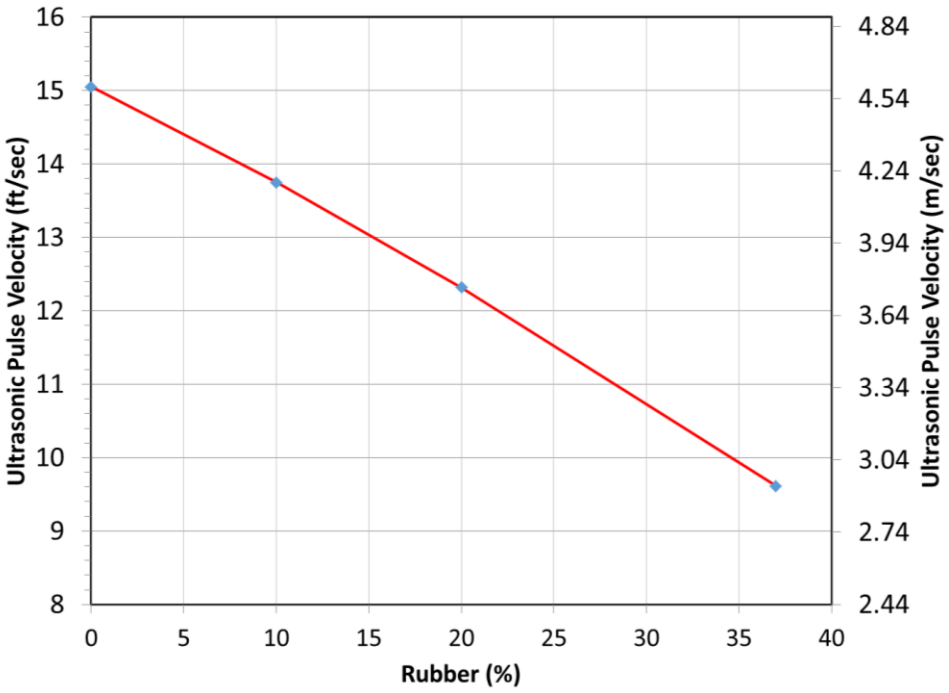

Figure 21. Effect of rubber content on ultrasonic pulse velocity.

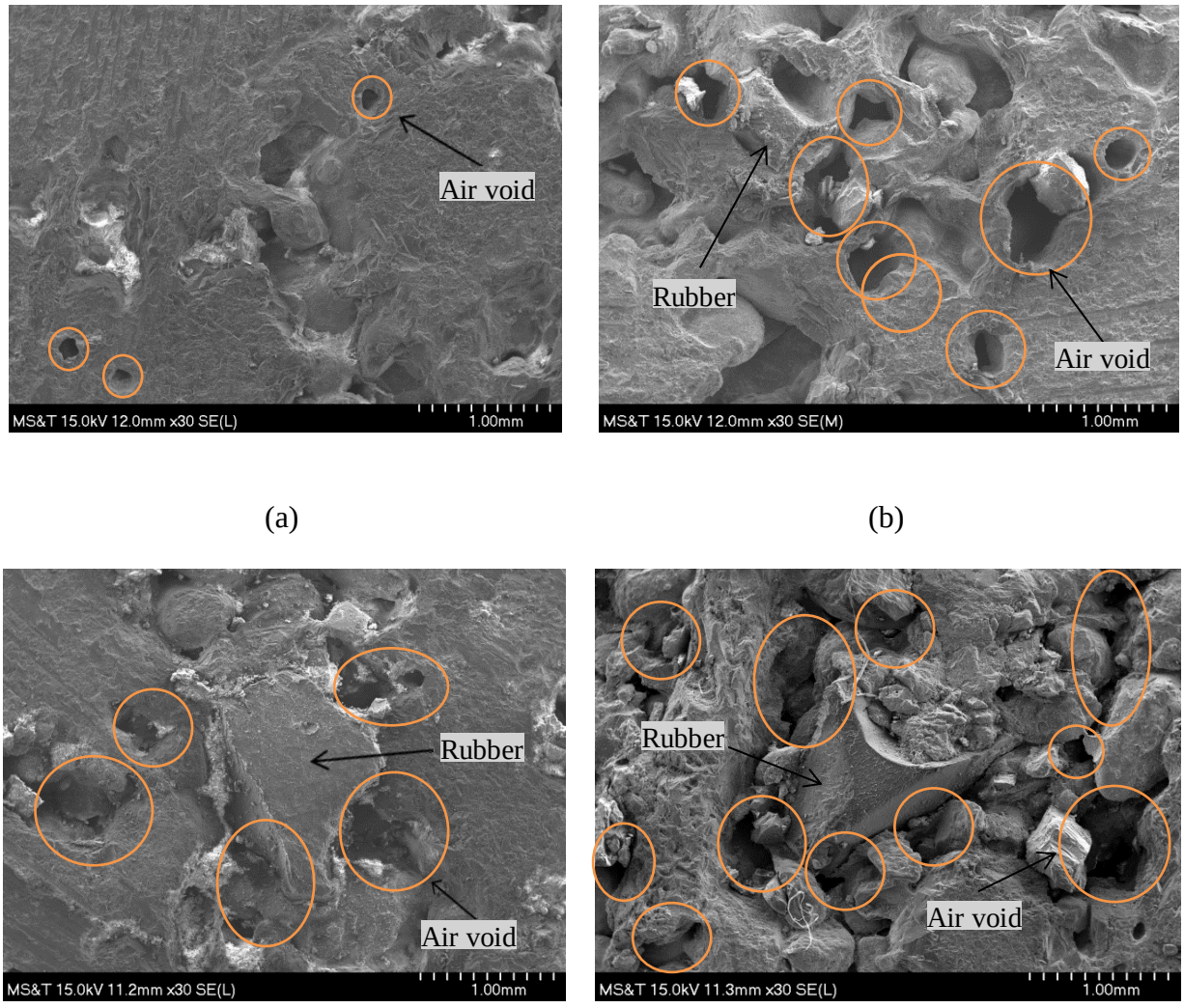

Figure 22. Air voids for block units with different rubber content: (a) 0% rubber, (b) 10% rubber, (c) 20% rubber, and (d) 37% rubber.

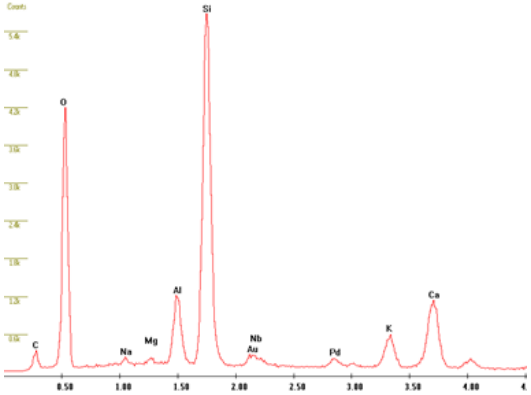

(a)

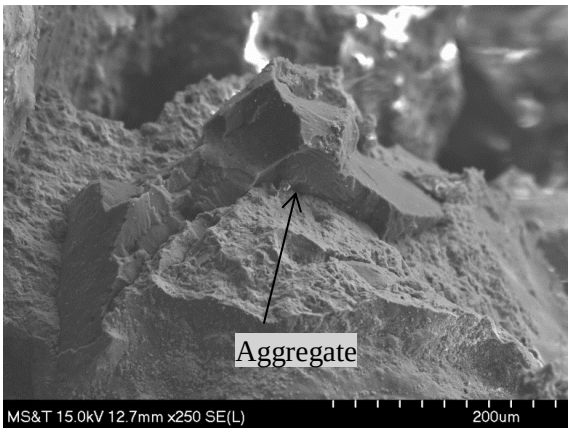

(b)

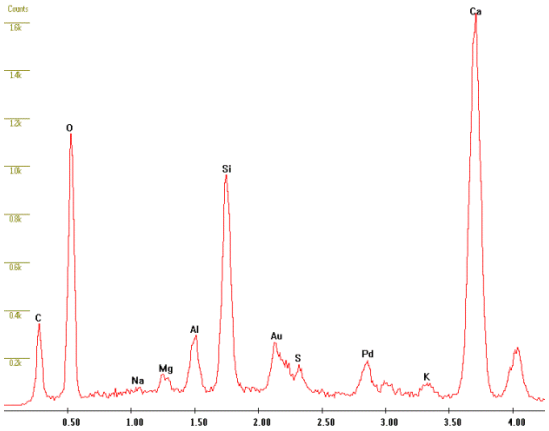

(c)

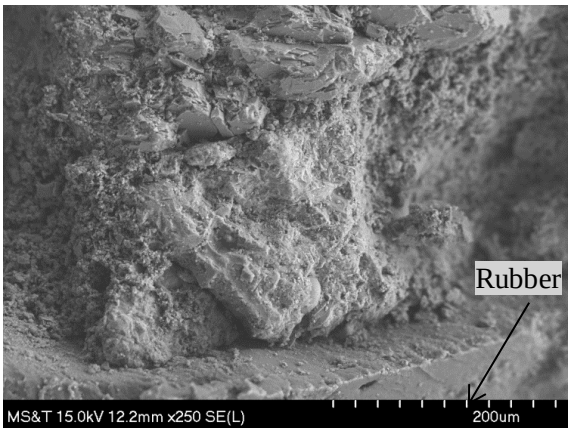

(d)

Figure 23. The ITZ:(a) Chemical analysis for the ITZ between natural aggregate and cement paste, (b) The ITZ between natural aggregate and cement paste, (c) Chemical analysis for the ITZ between crumb rubber and cement paste, and (d) The ITZ between rubber and cement paste.

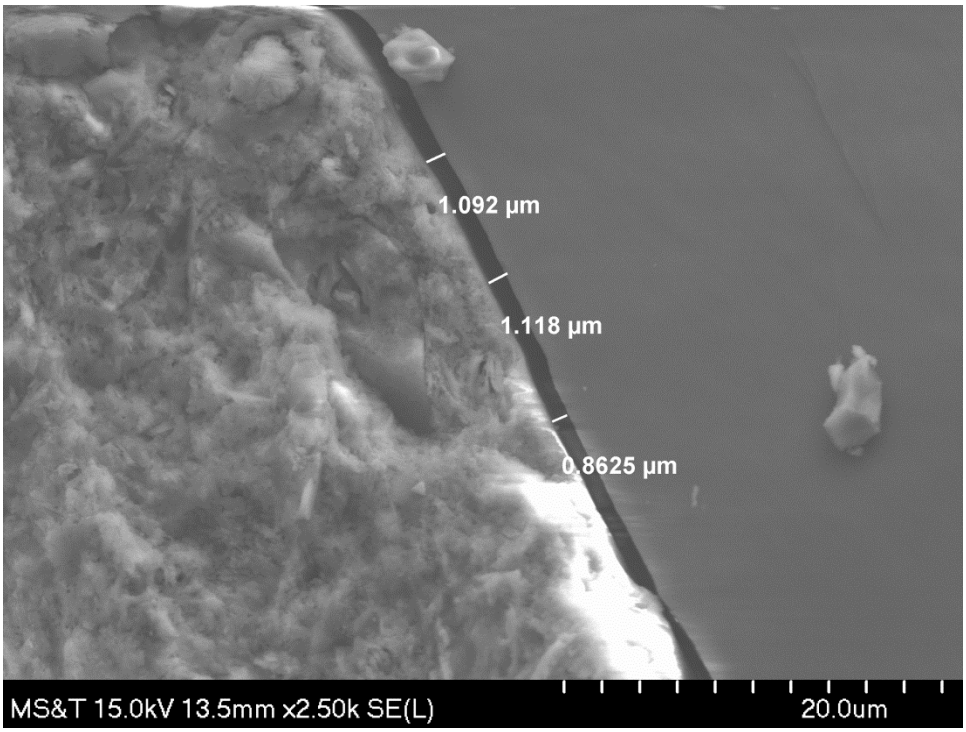

Figure 24. A gap between the rubber particle and cement paste after failure.

REFERENCES

1. Mohammed BS, Hossain KMA, Swee JTE, Wong G, Abdullahi M, "*Properties of crumb rubber hollow concrete block,*" Journal of Cleaner Production, V. 23, No. 1. 2012, pp. 57-67.

2. Thiyagarajan SV, Doddurani M, Thenmozhi R, "*Experimental Study On Crumb Rubber Hollow Concrete Block,*" i-Manager's Journal on Civil Engineering, V. 3, No. 4. 2013, pp. 16.

3. Robisson A, Maheshwari S, Musso S, Thomas JJ, Auzerais FM, Han D, et al., "*Reactive elastomeric composites: When rubber meets cement,*" Composites Science and Technology, V. 75. 2013, pp. 77-83.

4. Gou M, Liu X, "*Effect of rubber particle modification on properties of rubberized concrete,*" Journal of Wuhan University of Technology-Mater Sci Ed, V. 29, No. 4. 2014, pp. 763-8.

5. Siddique R, Naik TR, "*Properties of concrete containing scrap-tire rubber–an overview,*" Waste management, V. 24, No. 6. 2004, pp. 563-9.

6. Sukontasukkul P, Chaikaew C, "*Properties of concrete pedestrian block mixed with crumb rubber,*" Construction and Building Materials, V. 20, No. 7. 2006, pp. 450-7.

7. Najim K, Hall M, "*A review of the fresh/hardened properties and applications for plain-(PRC) and self-compacting rubberised concrete (SCRC),*" Construction and Building Materials, V. 24, No. 11. 2010, pp. 2043-51.

8. Batayneh MK, Marie I, Asi I, "*Promoting the use of crumb rubber concrete in developing countries,*" Waste Management, V. 28, No. 11. 2008, pp. 2171-6.

9. Thomas BS, Gupta RC, "*Mechanical properties and durability characteristics of concrete containing solid waste materials,*" Journal of Cleaner Production. 2013.

10. Youssf O, ElGawady MA, Mills JE, Ma X, "*An experimental investigation of crumb rubber concrete confined by fibre reinforced polymer tubes,*" Construction and Building Materials, V. 53. 2014, pp. 522-32.

11. Zheng L, Huo XS, Yuan Y, "*Experimental investigation on dynamic properties of rubberized concrete,*" Construction and building materials, V. 22, No. 5. 2008, pp. 939-47.

12. Xue J, Shinozuka M, "*Rubberized concrete: A green structural material with enhanced energy-dissipation capability,*" Construction and Building Materials, V. 42. 2013, pp. 196-204.

13. Atahan AO, Yücel AÖ, "*Crumb rubber in concrete: static and dynamic evaluation,*" Construction and Building Materials, V. 36. 2012, pp. 617-22.

14. Moustafa A, ElGawady MA, "*Mechanical properties of high strength concrete with scrap tire rubber,*" Construction and Building Materials, V. 93, 9/15/. 2015, pp. 249-56.

15. Sukontasukkul P, "*Use of crumb rubber to improve thermal and sound properties of pre-cast concrete panel,*" Construction and Building Materials, V. 23, No. 2. 2009, pp. 1084-92.

16. Turgut P, Yesilata B, "*Physico-mechanical and thermal performances of newly developed rubber-added bricks,*" Energy and Buildings, V. 40, No. 5. 2008, pp. 679-88.

17. Hall MR, Najim KB, Hopfe CJ, "*Transient thermal behaviour of crumb rubber-modified concrete and implications for thermal response and energy efficiency in buildings,*" Applied thermal engineering, V. 33. 2012, pp. 77-85.

18. Pacheco-Torgal F, Lourenço PB, Labrincha J, Kumar S, "*Eco-efficient masonry bricks and blocks: design, properties and durability.*" Woodhead Publishing; 2014.

19. Isler JW, "*Assessment of concrete masonry units containing aggregate replacements of waste glass and rubber tire particles,*" Book Assessment of concrete masonry units containing aggregate replacements of waste glass and rubber tire particles, Editor, ed.^eds., University of Colorado Denver, City, 2012, pp.

20. Micelli F, Myers J, "*Durability of FRP-confined concrete,*" Proceedings of the ICE-Construction Materials, V. 161, No. 4. 2008, pp. 173-85.

21. Tuwair H, Volz J, ElGawady M, Mohamed M, Chandrashekhara K, Birman V, "*Behavior of GFRP bridge deck panels infilled with polyurethane foam under various environmental exposure,*" Structures, V. 5, 2//. 2016, pp. 141-51.

22. Fuller K, Gough J, Thomas A, "*The effect of low-temperature crystallization on the mechanical behavior of rubber,*" Journal of Polymer Science Part B: Polymer Physics, V. 42, No. 11. 2004, pp. 2181-90.

23. Nehdi M, Khan A, "*Cementitious composites containing recycled tire rubber: an overview of engineering properties and potential applications,*" Cement, concrete and aggregates, V. 23, No. 1. 2001, pp. 3-10.

24. Xincheng P, "*Super-High-Strength High Performance Concrete.*" CRC Press; 2012.

II. THERMAL CHARACTERIZATION OF CLEANER AND ECO-EFFICIENT MASONRY UNITS USING SUSTAINABLE AGGREGATES

Ahmed Gheni , Mohamed A. ElGawady and John J. Myers

ABSTRACT

With 4.5 billion structural concrete masonry units (CMU) been produced in the U.S during 2014 alone, CMU is one of the most important and widely used construction materials. CMUs are still produced using non-renewable natural aggregate which creates pressure on the natural resources and resulted in unsustainable production. Moreover, one of the drawbacks of using CMUs is its relatively high thermal conductivity and low thermal insulation capacity compared to other options such as lumber and dry walls. Motivated by the reasons above, an experimental investigation was undertaken where the mineral aggregate in CMUs was partially replaced by recycled rubber aggregate, manufactured from scrap tires, producing what is called rubberized concrete masonry units (RCMUs). This paper presents the results of the thermal conductivity and the energy efficiency of RCMUs having replacement ratios of 0%, 10%, 20%, and 37%. The thermal properties, including thermal conductivity, time to reach the thermal steady state and energy efficiency, were investigated at the material and unit levels using four different approaches. RCMUs with 10%, 20%, 37% rubber replacement ratio exhibited a reduction in thermal conductivity of 9.5%, 20%, 45% at the material level and 22%, 26%, and 34% at the unit level, respectively. Furthermore, RCMUs with 37% rubber replacement ratio cut the energy consumption by 41% compared to conventional CMUs. Results indicated that the RCMUs are more efficient by cutting both embodied and operation energy as well as it has lower thermal conductivity.

Keywords: Masonry, crumb rubber, rubberized concrete, sustainable product development, thermal conductivity, cleaner construction.

1. INTRODUCTION

Concrete masonry unit (CMU) is one of the broadly used construction materials with 4.5 billion structural masonry units been produced in the U.S during the year of 2014 (Pacheco-Torgal et al. 2015). However, the natural aggregate is still the major component of CMU matrix which put more pressure on the depleted natural resources. Furthermore, the cradle-to-gate energy processing of natural aggregate, including the extraction, manufacturing, and transporting, makes the embodied energy of the CMUs is the highest compared to other construction materials such as timber and stone which increase the environmental devastations (Milne and Reardon 2005, Hammond and Jones 2008). The high operating energy of masonry buildings also shows a pressing need to develop energy-efficient masonry units to reduce such energy (Cabeza et al. 2013). This paper reports on a study where crumb rubber, obtained from scrap tires, is used as an aggregate in CMUs producing rubberized concrete masonry units (RCMUs), which addresses all the above-mentioned challenges.

Large volumes of scrap tires are readily available in the U.S. For example, the Rubber Manufacturer's Association reported that 242.8 million scrap tires were generated in the U.S. during the year of 2015 alone (RMA 2018). Tires are bulky, and 75% of the space a tire occupies is void, so landfilling requires a large amount of space. At the same time, tires are not biodegradable, so they serve as a home for mosquitoes, rats, and snakes and they represent a tremendous fire hazard. Once a tire pile catches fire, it is very difficult, to extinguish. Burning waste tires emits dangerous toxic gasses, such as CO, NO_2, and

SO_2. Burned tires will also produce runoff oils that could result in severe soil and water pollution problems. For example, in 1983, a scrap tire bone yard near Winchester, Virginia caught fire. More than 7 million tires burned for almost 9 months (Poole Jr 1998). Visibility impairment accrued due to a dense black smoke plume that spread downwind distance for up to 80 km (Fadiel 2013). In addition, 7.6 liters of oil could be produced from each burned tire which creates a pressing challenge to deal with the disposing of scrap tires properly. Most states in the U.S. have enacted legislation that either restricts or bans dumping scrap tires in landfills.

Crumb rubber has been mainly used in pavement within the construction field (Carder and Construction 2004). Comprehensive research has been devoted to characterize the fresh and hardened properties of rubberized concrete where crumb rubber replaced cement and/or natural aggregates. A reduction was noted in the unit weight of rubberized concrete because of the rubber particle's low specific gravity and increased entrapped air contents. Researchers reported also that there is a rubber content threshold; before that threshold adding rubber will increase slump values due to the hydrophobic nature of rubber which causes a water film coating on the rubber particles that reduce the friction with other particles. Beyond the threshold, the low unit weight of the rubber causes a reduction in slump (Siddique and Naik 2004, Sukontasukkul and Chaikaew 2006, Gou and Liu 2014).

Both the compressive and flexural strengths were negatively affected when crumb rubber was used as one of the constituent of concrete mixture due to rubber's relatively low stiffness and the poor bond between the rubber particles and cement paste (Siddique and Naik 2004, Batayneh et al. 2008, Najim and Hall 2010, Thomas and Gupta 2013, Gou and Liu 2014, Moustafa and ElGawady 2016, Youssf et al. 2017). However, rubberized

concrete displayed higher energy dissipation, viscous damping and hysteric damping compared with the corresponding conventional concrete (Hernandez-Olivares et al. 2002, Zheng et al. 2008, Xue and Shinozuka 2013, Moustafa and ElGawady 2015, Youssf et al. 2015, Youssf et al. 2016, Moustafa and ElGawady 2017, Moustafa et al. 2017). Compared with conventional concrete, rubberized concrete provides higher sound and heat insulation, sound absorption, and noise reduction coefficient as well as lower heat transfer properties (Turgut and Yesilata 2008, Sukontasukkul 2009, Hall et al. 2012).

(Yesilata et al. 2011) reported that composite concrete-scrap-tire-pieces walls increased the thermal insulation of a model room by 11%. Using granulated rubber in the concrete of flooring and foundations was enough to have low-rise dwellings meet the UK Building Regulations in term of thermal insulations without the need to any additional insulating layers (Paine and Dhir 2010). Both the amount of rubber and particles sizes has an impact on the thermal conductivity of rubberized concrete (Abu-Lebdeh et al. 2014). Using larger size of rubber particle in the production of rubberized gypsum board resulted in a better reduction in the thermal conductivity and the same trend was reported with cement mortar as well (Fadiel et al. 2014).

Very few researchers produced both load-bearing and non-load-bearing rubberized masonry hollow blocks (Isler 2012, Mohammed et al. 2012, Sadek and El-Attar 2015, Gheni et al. 2017)) and rubberized brick (Isler 2012, Mohammed et al. 2012, Sadek and El-Attar 2015, Gheni et al. 2017) where mineral aggregates were partially replaced with crumb rubber. It was reported an improvement in thermal, acoustic, and electrical properties of rubberized masonry compared to conventional masonry.

2. CONTRIBUTIONS OF CRUMB RUBBER IN THE PRODUCTION OF CLEANER CONCRETE MASONRY UNITS

Construction activities were the largest consumer of natural materials in U.S. during the last century. By 1998, mineral fine and coarse aggregate production reached 1.12 Gigaton representing 73% of all used natural materials (Horvath 2004). Therefore, construction activities are responsible for exhausting the environment and natural resources. However, there is an opportunity for reducing the impact of the construction industry on the environment by replacing a small portion of the mineral aggregate with a recycled one. For example, replacing only 10% of the mineral aggregate with recycled materials resulting in cutting of the annual total production of the natural aggregate by 112 million ton. Furthermore, concrete products have the highest embodied energy in buildings, compared to other construction materials such as timber and stone, due to the extraction process of its constituents, manufacturing, and transporting. For example, the embodied energy of concrete is 1.6 to 14.4 times that of steel, aluminum, copper, timber, plastic, brick, glass, plaster, stone, and ceramic which put another burden on the environment by increasing carbon dioxide emissions (Sajwani and Nielsen 2017).

Using recycled crumb rubber as a mineral aggregate replacement is one of the alternatives toward a cleaner production of masonry units. Replacing mineral aggregate with recycled rubber potentially will cut both the embodied and operation energy of masonry buildings constructed out of rubberized masonry. Rubberized masonry will reduce the extraction and transportation energy due to its lightweight. Furthermore, it is anticipated that rubberized masonry will reduce the heating and cooling energy use in buildings, which represent 20–24% of the total energy consumed in the world (Papadopoulos and Giama 2007, Yesilata et al. 2011).

This study focuses on the thermal characterization of RCMUs having rubber contents of 0, 10, 20, and 37% as a partial replacement of natural aggregate. As a preliminary investigation, cement paste mixtures with the same rubber ratios of 0%, 10%, 20%, and 37% were prepared and tested for their thermal performance. The differential scanning calorimetry (DSC), differential thermal analysis (DTA), and thermogravimetric analysis (TGA) tests were conducted to determine the specific heat, the change in the mass under elevated temperature, and the phase transition point. Then, another four tests were conducted to study the effects of rubber content on the thermal conductivity of RCMUs (ASTM C1363) or its material (ASTM D5334) and (CRD-C 45-65), energy consumption (ASTM.C1363), and the time needed to reach steady-state (ASTM C136) Figure 1 illustrates a schematic overview of the whole paper.

3. EXPERIMENTAL PROGRAM

Crumb rubber from scrap tires was used as a mineral aggregate replacement to produce rubberized concrete masonry blocks (RCMUs) with four different ratios of rubber content namely 0%, 10%, 20%, and 37%. The manufacturing was carried out using a standard masonry manufacturing process at masonry plant in Jefferson City, Missouri. The lower replacement ratios of 10% and 20% were selected to produce structural RCMUS while a high replacement ratio of 40% was targeted to produce nonstructural RCMUs (Gheni et al., 2017). However, during the mixing process in the masonry planet, the back calculations showed that the final replacement ratio was only 37%.

3.1. MATERIAL PROPERTIES

All materials used in this research were sampled and tested according to standard test methods (Table 1). Figure 2 shows the sieve analysis results for the used rubber mix and mineral fine aggregate. Three different sizes of crumb rubber namely ≤0.595 mm, 0.595-1.41 mm, and 2.83-3.36 mm (Figure 3) were used to create the aggregate particle distribution that had the closest distribution to the replaced fine aggregate.

Three masonry units for each rubber replacement were placed in an oven at 113 ℃ for 25 hours. Following heat treatment, each unit was then soaked in a large water container for 24 hours. The absorption rate of each unit with a different amount of rubber replacement, according to ASTM C140/C140M−14b was measured. As shown in Table 1, increasing the rubber replacement ratio in RCMUs increased the water absorption. This increase was related to the increase of the air voids because of the rubber particles' tendency to entrap more air at their rough surface due to the particles' non-polar nature (Dhir et al., 2001; Eldin and Senouci, 1993; Fedroff et al., 1996; Topcu, 1995). The compressive strength results showed that RCMUs with both 10% and 20% rubber replacement ratios met the ASTM C90-12 for concrete masonry bearing units while the 37% replacement met ASTM C129-14a for non-loadbearing units.

The TA Instruments DSC 2010 was used to determine the transition glass point. The instrument works under a temperature range of -180 to 725 ℃ and heat flow associated with thermal transitions in a material. In the term of low temperature, as shown in Figure 4, the glass transition point was at -65 ℃, which is far from the lowest expected temperature in the United State.

3.2. THERMAL CHARACTERIZATION OF RUBBERIZED CEMENT PASTE

Mixes of cement and rubber powder were prepared using rubber replacement ratios of 0%, 10%, 20%, and 37% of Portland cement by weight. The mixtures were used to preliminarily investigate the thermal characteristics of rubber-modified paste using differential scanning calorimetry (DSC), differential thermal analysis (DTA), thermogravimetric analysis (TGA), and specific heat tests. These tests can help to determine the potential of using rubber to improve the thermal efficiency of masonry units.

For mixtures preparation, the rubber powder was added to cement in stainless steel mixer and mixed for two minutes. Then, the required amount of water was added to the mix and mixed for two minutes. The water to cement ratio in all investigated specimens was kept at 0.35. The paste was poured then into aluminum circular pan molds with a typical diameter of 8mm and depth of 5mm (Figure 5). The specimens were cured at an ambient temperature in the lab for 28 days.

Both the TGA and DTA analyses were run simultaneously using Netzsch Simultaneous TGA/DTA which is a thermal analysis instrument that can provide information such as phase changes, melting and glass transition temperatures, and weight loss as a function of temperature that varied from room temperature to 1500 °C under a controlled environment. The TGA analysis investigates the thermal stability and composition of the rubberized paste. The DTA studies the difference in temperature between the tested rubberized paste and a thermally inert reference under varied temperatures. As a result, the transition temperatures of the rubberized paste can be determined.

As shown in Figure 6, up to 300 °C all rubberized and reference mixtures behaved similarly. During the 0 °C – 300 °C range, each specimen lost about 2 - 3% of its weight due to dehydration of hydrated paste. The TGA curves for rubberized paste mixtures show a noticeable mass loss in the 300 – 450 °C interval with the 37% rubber content paste mixture displaying the highest mass loss with mass loss of 15%.

DTA curve (Figure 7) shows an intense peak centered at 350 °C for samples with 37% rubber. This peak is followed by a less intense range, due to the presence of liquid oil. The same trend was reported for testing scrap tire rubber only (Berrueco et al. 2005, Rada et al. 2012).

However, reference sample without rubber had a smooth curve without any point of inflection due to the absences of any organic liquid oil component. Samples with 10 and 20% rubber had a transition behavior between the samples with 0 and 37% rubber.

The last test to characterize thermal characteristics of rubberized paste is the specific heat. The specific heat represents the heat required to raise the temperature of the unit mass by one degree. Therefore, samples with relatively high specific heat represent better thermal insulation. The specific heat was measured for five samples with varied rubber content, namely 0%, 10%, 20%, 37%, and 100% (rubber only). Samples similar to those used for thermal characterization of rubberized paste mixtures (Figure 5) were used during this test.

Figure 8a shows the heat flow vs. temperatures for different rubberized paste mixtures. Figure 8b represents the specific heat of different mixes at 30° C, 45° C, and 60° C. The specific heat was calculated using the following equation:

$$C_p = \left[\frac{60E}{H_r}\right]\frac{\Delta H * 10^9}{m} \quad (1)$$

where:

E= cell calibration at the temperature of interest (dimensionless)

Hr= heating rate (℃ /min)

ΔH= difference in y-axis deflection between sample and blank curve at the temperature of interest

m= sample mass (kg)

Cp= specific heat (J /kg K)

As shown in Figure 8b, the relation between the rubber content and specific heat is approximately linear, which represents the impact of having rubber on the thermal insulation. The figure also shows that the effects of rubber on specific heat at high temperature, i.e., 60 ℃ is less pronounced compared to its effects at lower temperature, i.e., 30 ℃ and 45 ℃. The specific heat for rubberize paste mixtures at 30 ℃, 45 ℃, and 60 ℃ can be determined using Equations 2 through 4, respectively.

$$C_p = 5.3110R + 922.04 \quad (2)$$

$$C_p = 5.5196R + 950.30 \quad (3)$$

$$C_p = 3.5353R + 1045.8 \quad (4)$$

where:

Cp= specific heat (J/kg. K)

R= rubber ratio (%)

The preliminary results presented from this set of tests indicate that the rubberized paste thermally behaved similarly to a conventional paste up to 300 ℃ and has the ability to sustain extreme hot and cold weathers and hence can be used for building envelopes.

Therefore, it was encouraging to proceed with the second part of this research where the thermal characterization of RCMUs was determined.

3.3. THERMAL CONDUCTIVITY OF RCMUS

During this experimental work, the thermal characteristics of RCMUs were determined using four different approaches namely the thermal needle probe, the two controlled sides guarded hot box, the guarded hot box, and the guarded hot plate assembly.

3.3.1. Thermal Needle Probe. A portable thermal analyzer that has a metal probe with high aspect ratio can be used to measure the thermal conductivity of various kinds of materials per ASTM D5334−14. This method is originally designed to measure the thermal conductivity of soil where the needle probe can be inserted with a small amount of pressure without the need to create a hole prior to inserting the probe for the test. In this case, a full contact is assured between the testing probe and the tested material. However, measurements in stiff materials such as masonry using needle probe has some challenges compared to measurements in soil medium. As the standard probe has a diameter of 3.9 mm, a drill bit was used to create a 4-mm diameter hole in an RCMU where the probe can be inserted. The probe was covered with a thermal grease to assure a full contact between the probe and surrounding tested materials and eliminating any entrapped air that leads to inaccurate results. The metal probe contained a heater element and a temperature sensor. Once the probe is inserted into the sample, current is passed through the heater, which raises the temperature, and the temperature sensor records the change with time. After cycles of heating and cooling, the temperature degradation will be recorded with time to calculate the ability of the material to absorb and dissipate heat which leads to determining the thermal conductivity using KD2 Pro portable thermal properties analyzer (Figure 9a).

The test was conducted in five different spots within the masonry unit namely face shell, end shell, web, the intersection between the face and web shells, and the intersection between the web and face shell (Figure 9b). The thermal conductivity was calculated for each RCMU.

3.3.2. Guarded Hot Plate Assembly Method. This test was conducted following the Whole Building Design Guide CRD-C 45-65 on 100 mm X 100 mm X 25 mm masonry plate specimens. As shown in Figs. 10 and 11, the apparatus used in this test consisted of a guarded hot plate, controlled heat source, temperature measurement system and energy consumption meter. The guarded hot plate apparatus was fabricated using double layers of 50 mm thick corkboard surrounded by 20 mm thick plywood. The corkboard was preferred on Styrofoam because of its high insulation value even with full contact with the hot plate. As shown in Figure 10, the layers of corkboard were arranged around the tested specimen in a way that blocks the path of any possible leaks through the joints. Therefore, all the heat transferred vertically through the tested sample only without significant dissipation through the walls or the joints in the other directions.

A 100 mm X 100 mm X 3mm aluminum plate with a slim heat sheet was used as a heat source that kept the temperature at 60 ℃ ± 2 ℃ using a proportional integral derivative (PID) digital temperature controller that was connected to the slim heat sheet. A similar aluminum plate was also placed atop of each test specimen to measure the temperature of the collected heat at the top side. To achieve full contact between the aluminum plates and the tested sample, thermal grease was used to cover the contact areas.

The temperatures of the aluminum plates above and below each test specimen were measured using a set of thermocouples that were connected to a data acquisition system.

Once a specimen is placed inside the Guarded Hot Plate apparatus, the upper box door (that made out of 50-mm thick layer of corkboard) was tightened and sealed to eliminate heat leaks. The heating plate was then turned on for 24 hours to get a temperature of 60 °C ± 2 °C measured at the bottom side. The temperature data were collected at the top side with a rate of 10 readings/min using a data acquisition system (Figure 11b) and the consumed energy was recorded for the whole testing time using a digital power meter. The thermal conductivity of each specimen was then calculated using Fourier's heat conduction equation as follows:

$$k = \frac{qL}{A(t_1 - t_2)} \quad (5)$$

where:

k: thermal conductivity factor, (W/m K).

L: thickness of the tested specimen, (m).

A: area of the tested specimen, (m^2).

t_1: the temperature of bottom aluminum (hot) plate face in contact with the specimen, K.

t_2: the temperature at the top aluminum (heat collecting) plate on the top face of the sample, K.

q: heat flow rate within the tested specimen, W/m^2. (q = 3.41 times the rate of electrical energy input to the hot plate, Watts).

3.3.3. Two Controlled Sides Guarded Hot Box Apparatus. The heat transfer across a CMU was determined, per the ASTM C1363−11, by placing a CMU in the middle of a well-insulated box (Figure12) where one face shell of the CMU was subjected to a constant temperature of 49.5±0.5 °C while the other face shell was not subjected to any heat. The heat was emitted from an aluminum plate and controlled by a PID controller as

explained earlier (Figure 12a). The testing apparatus was fabricated using an exterior 12.5 mm thick plywood and interior 50 mm thick Styrofoam with a thermal resistance value (R) equal to 10 on the inner face. The Styrofoam inner faces were engraved as shown in Figure 12a to assure a tight fit for the masonry unit to eliminate any masonry manufacturing tolerance that may cause a heat leak within any possible gaps between the tested masonry block and the Styrofoam layer.

The testing apparatus was first calibrated using A Styrofoam masonry unit (Figure 12c) with an R value equal to 31 m^2.K/W. The results of the calibration were used to ensure that the flanking loss around the metered specimen was negligible.

Twenty thermocouples were used to monitor the heat transfer through each masonry block and across the two controlled rooms in the apparatus itself. The heat transfer was monitored by collecting the temperature in five separate locations on each side of the masonry unit and at the middle of the web (Figure 12d). As the inside of the hotbox was under full monitoring for the temperature at different locations, the temperature outside the hotbox was also monitored and recorded. Once a specimen is placed inside the hotbox apparatus, the upper box door (that had a 50-mm thick layer of Styrofoam) was tightened and sealed to eliminate heat leaks. The heating plate was then turned on for 24 hours to get a temperature of 49.5 °C ± 0.5 °C measured at 25 mm from the middle of the face shell of the masonry unit at the metering chamber. The temperature data were collected with a rate of 10 readings/min using a data acquisition system (Figure 12b). The time required for each specimen to reach its thermal steady state (i.e. the temperature recorded on both sides of the masonry unit remained constant) with a variation of temperature within 5% for each sensor was collected. This indicated the time needed

for heat to fully penetrate the materials since the material with good insulation required more time to reach the steady-state case. Furthermore, the differences in temperatures between both sides of the tested masonry unit at the thermal steady state were calculated for each tested specimen. These differences can be used to quantify the amount of insulation provided by masonry unit. A large difference between the temperatures on both sides indicated a higher capacity of transferring heat.

3.3.4. The Hot Box Apparatus. A well-insulated thermal box was fabricated (Figure 13), following ASTM C1363, in order to calculate the thermal conductivity of a masonry unit at the thermal steady state that occurred after exposing a tested unit to a constant and continues heat source for 24 hours. The box was fabricated as explained in the previous section with one exception. Instead of having the masonry unit placed in the middle of the hot box it was placed at one end of the hot box (Figure 13a).

This testing apparatus simulate a well-insulated room with one exposed side, which is the test subject. Thermal images and videos (Figure 14) proved that there was no heat leak from the testing apparatus and the heat transferred through the tested blocks only.

The Styrofoam faces were engraved, and a masonry test specimen was placed in the testing apparatus with the interior side was subjected to a constant temperature of 47.5±2.5 °C representing an extreme outdoor summer temperature. An aluminum plate and PID controller were used for emitting and controlling the heat as explained earlier (Figure 13a). The exterior masonry specimen face was subjected to a constant temperature of 18.5±1.5 °C using AC system simulating a temperature inside a residential building. The effects of masonry units having different rubber content were determined by

measuring the consumed energy to maintain an average temperature inside the hot box apparatus at 47.5 °C.

Since only one of the six sides of the testing apparatus is the tested masonry unit while the other five sides are made from plywood and Styrofoam, it was required to subtract the energy consumed by the other five walls and then determine and the energy consumption of the tested masonry unit only. This was achieved by using the Styrofoam unit (Figure 12c) as explained earlier. The test then was run to calculate the consumed energy by the testing apparatus itself without the masonry unit to be subtracted later from the total consumed energy by the same apparatus with masonry unit on one side. Fourier's heat conduction equation, Equation 5, was used to compute the thermal conductivity of the tested masonry units where t_1: temperature of the face shell inside the hot box (the heated face), t_2: the temperature at the outside face (the cold face), and A: area of the tested masonry unit that facing the heat source.

A digital power meter was connected to the heating source to record the consumed energy during this test (Figure 13b). A data acquisition system and two thermocouples were used to monitor the temperatures inside and outside the testing apparatus (Figure 13a). The testing apparatus in the procedure described above were calibrated using six different materials having well known thermal conductivity (Figure 15).

4. RESULTS AND DISCUSSION

In general, rubberized masonry units displayed higher thermal insulation, which was measured using four different approaches. While the general trend was similar for all used methods, the measured insulation improvement was a function for the method of measurement. The hot box and the two controlled sides guarded hot box methods measure

the thermal insulation of a masonry unit (as a structure), while the thermal probe and guarded hot plate assembly methods measure the thermal insulation at the material level through examining either a plate of material or inserting the thermal probe in various locations within the masonry unit.

4.1. THE THERMAL NEEDLE PROBE METHOD

The relationship between the rubber replacement ratio and the thermal conductivity factor was approximately linear and consistent (Figure 16). Replacing 10%, 20%, and 37% of the mineral aggregate with crumb rubber reduced the thermal conductivity factor by 9.5%, 20% and 45% from 1.99 w/m. k to 1.8, 1.6, and 1.1 W/m.K. In addition, the results of lightweight of concrete masonry unit (LWCMU) is shown in the figure for comparison. As shown in the figure, the thermal conductivity of the LWCMUs is 60% of that of the CMU. Furthermore, the thermal conductivity of RCMU approached that of the LWCMU at a crumb rubber ratio of 33%.

4.2. THE GUARDED HOT PLATE ASSEMBLY METHOD

Figure 16 shows the thermal conductivity measured on masonry plate specimens. Replacing 10%, 20%, and 37% of the mineral aggregate with crumb rubber reduced the thermal conductivity factor by 8.75%, 17.5% and 42.5% from 1.6 W/m.K to 1.46, 1.32, and 0.92 W/m.K, respectively. As shown in the figure, the thermal conductivity of the LWCMUs is 60% of that of the CMU. Furthermore, the thermal conductivity of RCMU approached that of the LWCMU at a crumb rubber ratio of 32%. These results are similar to those obtained using the thermal needle probe procedure as both methods deal with the thermal conductivity at the material level, not the masonry unit. It is of interest that the

thermal conductivity values measured using the needle probe method are 20% to 25% higher than those obtained using the guarded hot plate assembly method. This difference is attributed to the difference in the specimen exposure as the specimen in the needle probe procedure is fully exposed to the ambient temperature which helps to dissipate the heat easier than that in the guarded hot plate assembly where the specimen is fully insulated.

4.3. THE TWO CONTROLLED SIDES GUARDED HOT BOX METHOD

This test quantified the thermal effects of rubber content using two different measures, namely the difference in temperature and time to reach steady state. The heat flow through a tested masonry unit became steady after 24 hours. The difference between the temperatures on both sides of the apparatus (ΔT) was measured for each test specimen as an indication of the thermal insulation (Figure 17). The higher content of rubber led to a higher ΔT. RCMU with a 37% rubber ratio had a ΔT of 24 °C after 24 hours, while the unit with 0% rubber had a ΔT of 14.3 °C.

Another measure of the thermal efficiency of RCMUs was noticed through monitoring the rate of increase of interior temperature (Figure 18). The interior temperature recorded for units with 0% rubber reached a steady state faster than the units with rubber. Units with 37% rubber took 8.2 hours to reach the steady state, compared to 5.5 hours for the conventional CMU. This proved that rubberized units do not lose heat as quickly as a conventional CMU due to the relatively low thermal conductivity of the rubberized blocks.

4.4. THE HOT BOX APPARATUS METHOD

Before running the test, the hotbox apparatus was calibrated by using it to compute the thermal conductivity of well-known thermal materials (Figure 15). Second-degree approach (Equation 3) was able to predict the manufacturer provided thermal conductivity with an R^2 value of 0.971.

$$K_{actual} = -0.1269\left(K_{exp}\right)^2 + 2.0155\,K_{exp} - 0.1584 \quad (6)$$

Where:

K_{actual} = the actual thermal conductivity (W/m K).

K_{exp} = the calculated thermal conductivity using the hotbox apparatus method (W/m K).

The impact of having crumb rubber on the coefficient of thermal conductivity is shown in Figure 16. Replacing 10%, 20%, and 37% of the mineral aggregate with crumb rubber reduced the thermal conductivity factor by 22%, 26%, and 34% from 1.0 W/m.K to 0.78, 0.74, and 0.66 W/m.K, respectively. These values are smaller than those obtained using the needle probe and guarded hot plate assembly. Both the needle probe and guarded hot plate assembly measure the thermal conductivity at the material level which is different from the hot box apparatus where the thermal conductivity is measured at the block level. Therefore, the shape of the block including thermal bridging and empty cells with low thermal conductivity plays an essential role in determining the thermal conductivity using the hotbox apparatus. Furthermore, the relationship of the crumb rubber and reduction of thermal conductivity at the material level was linear. However, a large drop was noticed in the thermal conductivity factor when 10% rubber was used. The reason behind that was the significant difference between the thermal conductivity of concrete and rubber. The average thermal conductivity of masonry material at the ambient temperature was 8.4

times that of the rubber, i.e., 1.01 (W/m.K) for masonry (Figure 16) and 0.12 (W/m.K) for rubber. The specific heat for masonry material was also 0.47 times that of the rubber, i.e., 950 J/kg.K for masonry and 2010 J/kg.K for rubber. Therefore, the thermal diffusivity of masonry is about 5.6 times that of rubber. The thermal diffusivity, calculated as the thermal conductivity divided by density and specific heat capacity, measures the rate of transfer of heat of a material from the hot side to the cold side. Using a small amount of rubber content will cause a significant drop in the thermal diffusivity of rubberized masonry units. The thermal conductivity of LWCMU measured using the hot box apparatus is also presented in Figure 16. As shown in the figure, the thermal conductivity of the LWCMU was equivalent to RCMU having 12% rubber content.

Another measure of the thermal efficiency of RCMUs is the amount of the consumed energy to maintain an average temperature inside the testing apparatus at 50°C for 24 hours with an average outside temperature of 18.5 °C. This energy was computed for each RMCU and then compared with that of the conventional CMU and LWCMU (Figure 19). Reductions of 26%, 32%, and 41% were achieved for RCMUs with 10%, 20%, and 37% rubber content ratios, respectively while using the LWCMU cut the energy consumption by 28% only.

5. FINDINGS, CONCLUSIONS, AND FURTHER WORK

Crumb rubber was used as a replacement of mineral fine aggregates to manufacture rubberized concrete masonry units (RCMUs). The thermal characteristics thermal conductivity of RCMUs having rubber replacement ratio of 0%, 10%, 20%, 37% were examined at the material and masonry block levels using four methods namely, thermal needle probe procedure, guarded hot plate assembly method, guarded hot box method, and

two controlled sides guarded hot box. The thermal performance of lightweight CMU was also investigated as a reference specimen. The thermal characteristics are highly affected by the measuring method and the sample geometry (masonry unit vs. masonry plate). However, the general trends of the data were similar. Based on the experimental investigation, the following conclusions can be drawn:

1. The specific heat increased linearly with increasing the rubber content. Increasing the rubber content from 0% to 37% increased the specific heat by an average of 19% depending on the experiment temperature. For example, at 45 °C, the specific heat increased from 950 J/kg.K to 1150 J/kg.K with increasing rubber content in cement paste from 0% to 37%. A similar trend was measured at 30 °C and 60 °C.
2. The thermal conductivity measured at the material level for rubberized masonry linearly decreased with increasing the rubber content. While the absolute values of the measured thermal conductivity varied depending on the used measuring method, both the thermal needle probe and guarded hot plate showed a reduction of 44.9% and 42.5% in the thermal conductivity, respectively, when the rubber content increased from 0% to 37%.
3. The thermal conductivity measured at the masonry unit level showed a nonlinear decrease with increasing the rubber content. Adding small rubber content of 10% reduce the thermal diffusivity of the block resulted in a significant drop of 22% in the thermal conductivity. Beyond that adding more rubber decreased the thermal conductivity at a smaller rate. Increasing the rubber content from 10% to 37% decreased the thermal conductivity by 16%.

4. A reduction in energy consumption was measured when RCMU was used in lieu of CMU. Replacing the fine aggregate with 10%, 20%, and 37% crumb rubber reduced the energy consumption that is needed to keep the temperature constant inside the hot box by 9.4%, 20%, and 45% respectively.
5. At the steady state, RCMUs had higher differences between the inner and outer temperatures compared to that of the CMUs. While the differences in inner and outer temperatures were 14.3 ℃ for CMU it increased to 24 ℃ for RCMU having 37% rubber content. Furthermore, the time to reach steady state heat flow was higher in the case of RCMUs compared to that of CMU. Increasing the rubber content from 0% to 37% increased the time required to reach steady state by 49%.

While the work presented in this paper comprehensively addressed the thermal characteristics of RCMU, the effect of rubber particle size on the thermal characterization of RCMUs need to be addressed in future studies. Furthermore, the effects of these measured characteristics on the overall energy consumption of RCMU buildings need to be addressed.

ACKNOWLEDGEMENTS

This research was supported by Missouri Department of Natural Resources. Manufacturing the RCMUs took place at Midwest Block & Brick Inc. Their support is gratefully appreciated. However, any opinions, findings, conclusions, and recommendations presented in this paper are those of the authors and do not necessarily reflect the views of the sponsors.

Table 1. Material properties.

Items	Tests type	Results	ASTM limits
RCMU	Compressive strength ASTM C90−12	0% rubber 29.8 MPa 10% rubber 25.3 MPa 20% rubber 15.4 MPa 37% rubber 6.7 MPa	Min. of 13.1 MPa and 4.14 MPa for structural and non-structural, respectively
RCMU	Absorption Testing ASTM C90−12	0% rubber 109 kg/m^3 10% rubber 133 kg/m^3 20% rubber 151 kg/m^3 37% rubber 176 kg/m^3	Max. of 208 kg/m^3
RCMU	Density Classification ASTM C90−12	0% rubber 2206 kg/m^3 10% rubber 2122 kg/m^3 20% rubber 2050 kg/m^3 37% rubber 1913 kg/m^3	Lightweight less than 1680 kg/m^3 Medium weight 1680–2000 kg/m^3 Normal weight 2000 kg/m^3 or more
Rubber	Unit weight	641 kg/m^3	----------

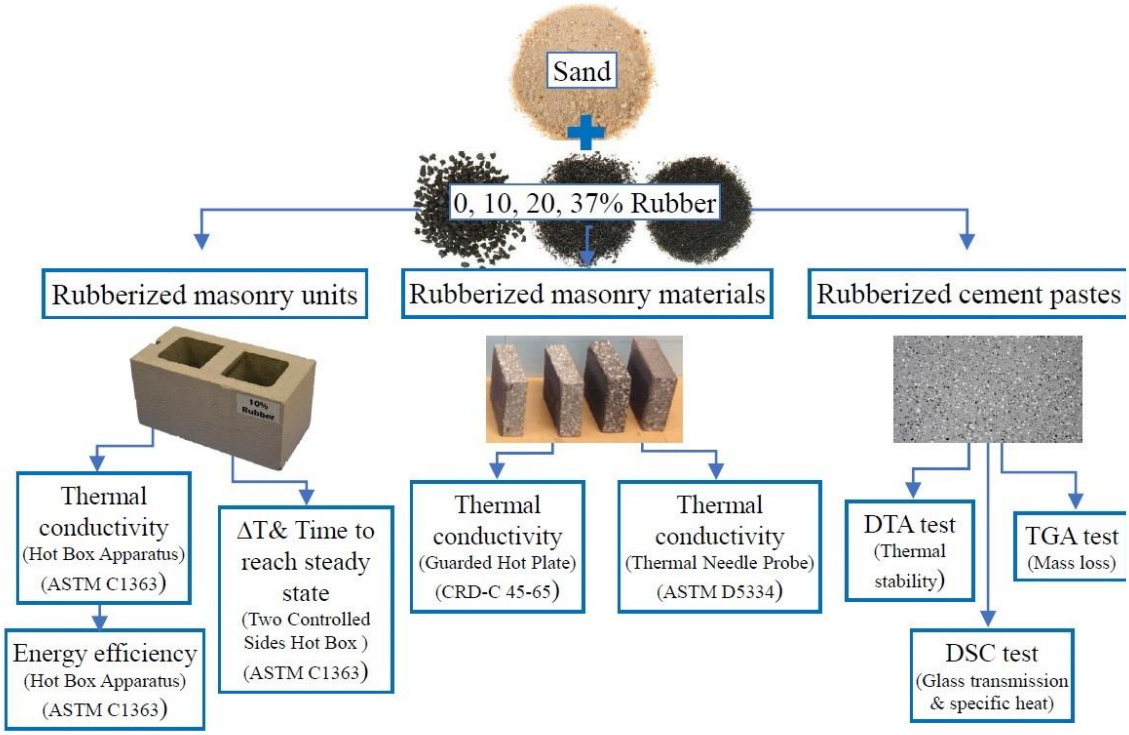

Figure 1. Schematic overview of the work.

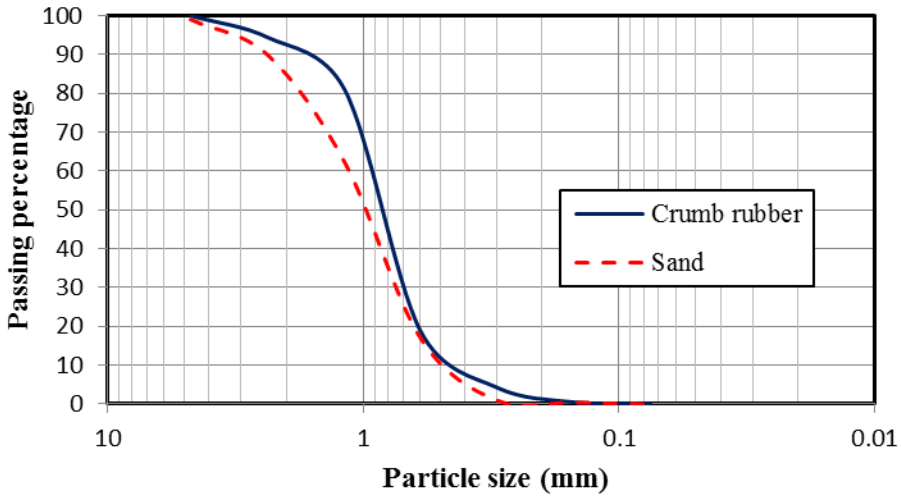

Figure 2. Sieve analysis of the used mix of crumb rubber.

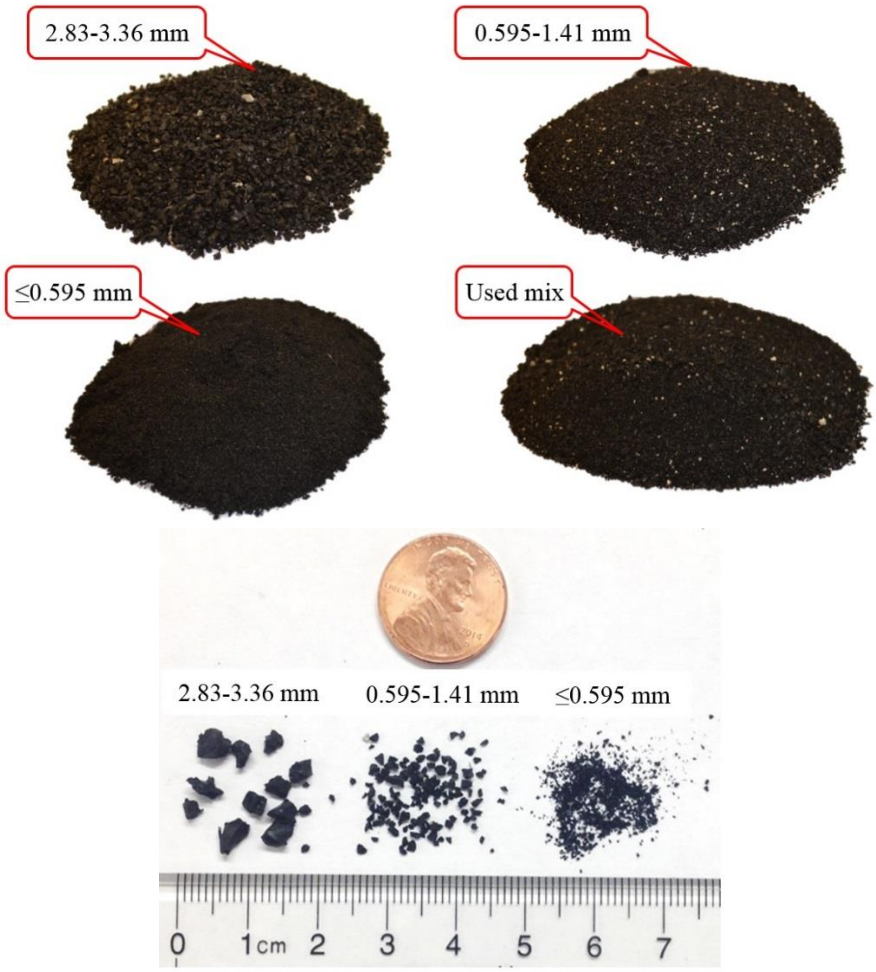

Figure 3. The different sizes of crumb rubber that used in RCMU's production.

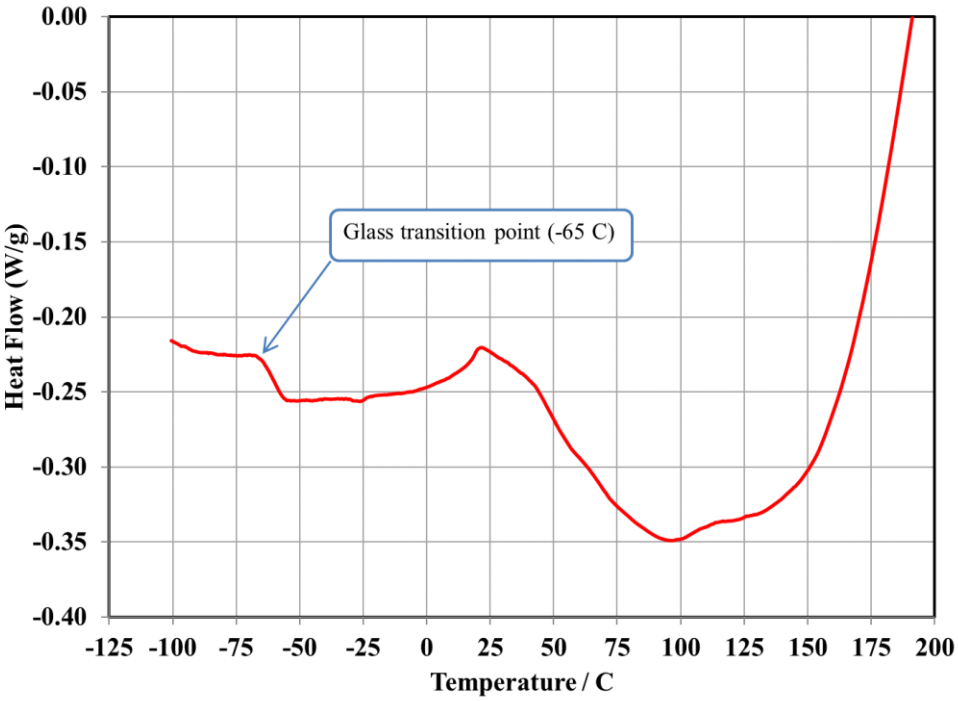

Figure 4. Differential scanning calorimetry (DSC) for scrap tire rubber.

Figure 5. Standard molds for samples to test the thermal characterization of rubberized paste.

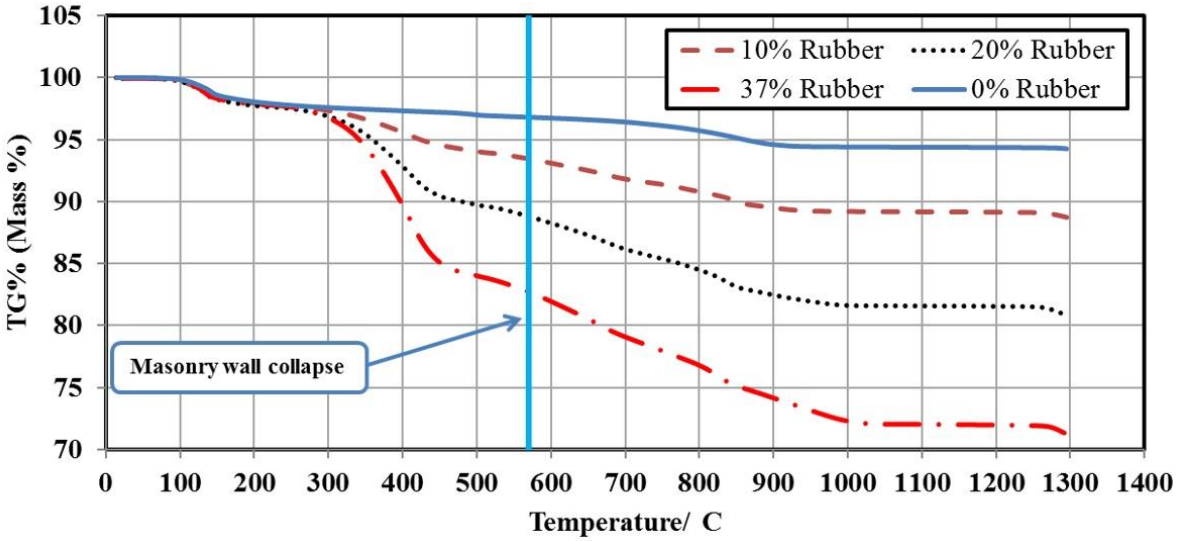

Figure 6. Thermogravimetric analysis (TGA) for cement mixes with varying rubber content.

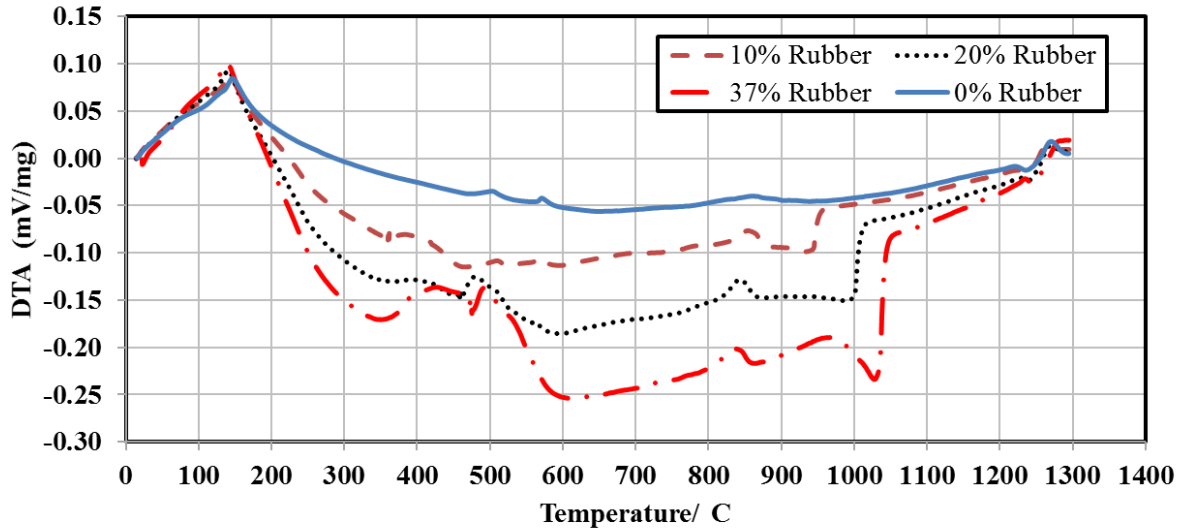

Figure 7. Differential thermal analysis (DTA) for cement mixes with varying rubber content.

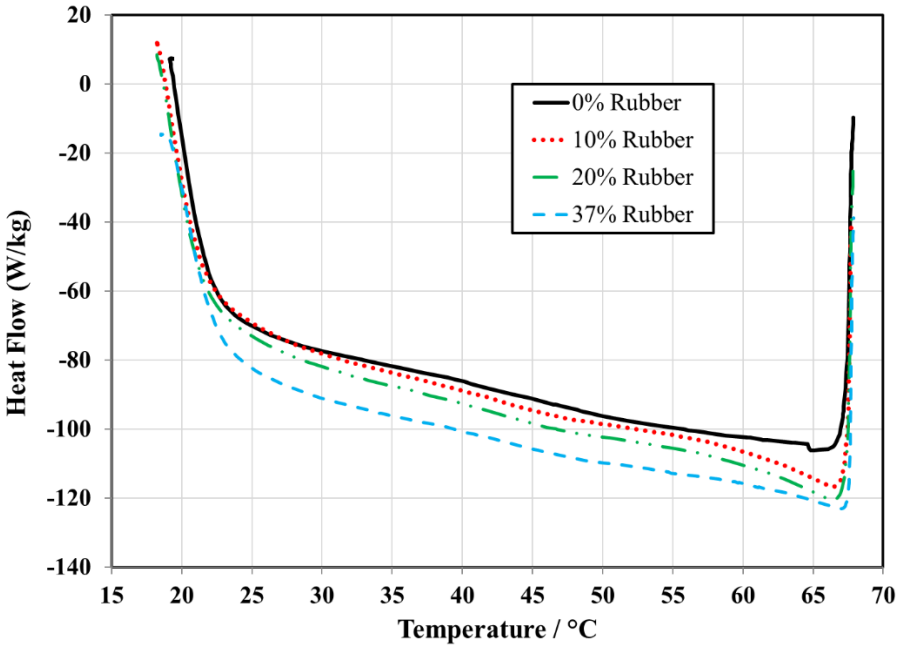

a

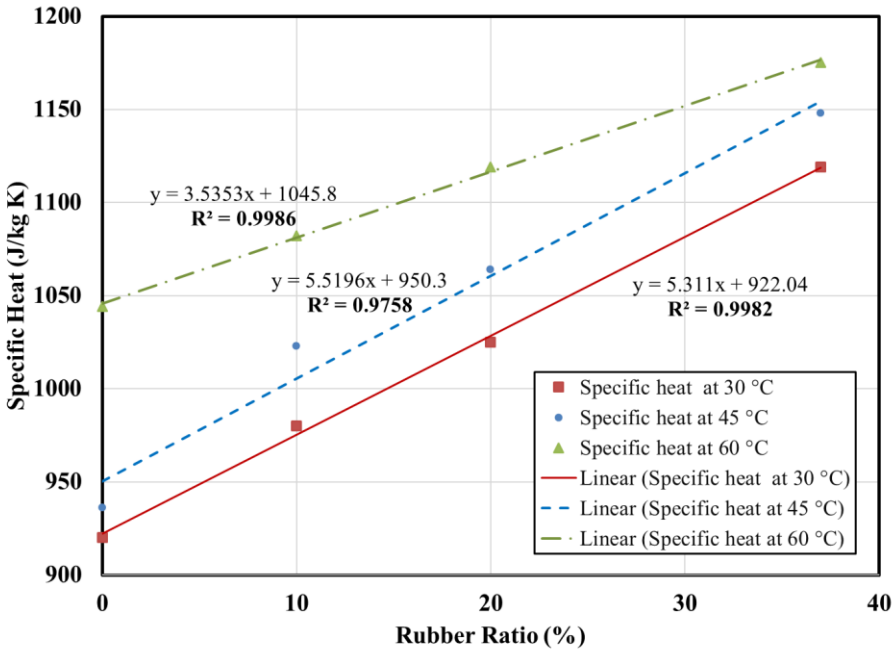

b

Figure 8. Specific heat test of rubberized cement paste (a) Heat flow vs. temp. (b) Specific heat vs. rubber content.

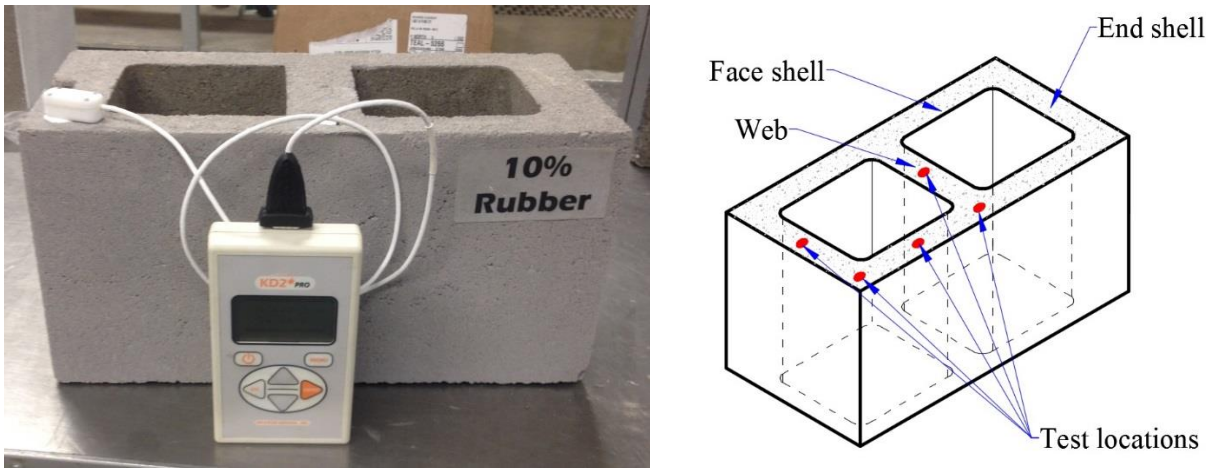

(a) (b)

Figure 9. Thermal needle probe test using (a) Testing RMCU with KD2 PRO portable thermal properties analyzer. (b) CMU's components with test locations.

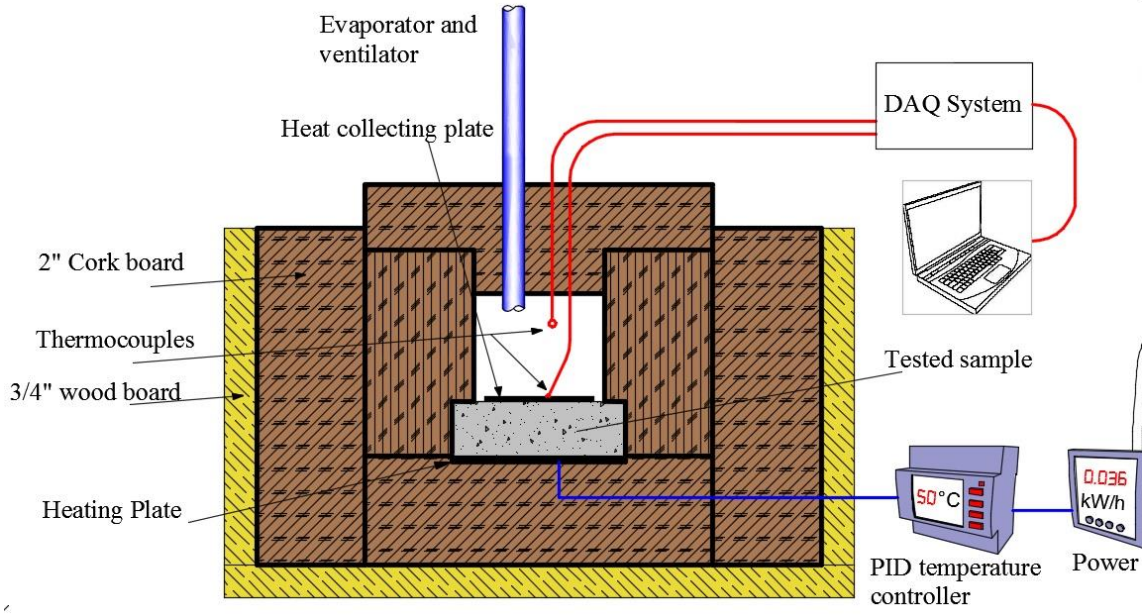

Figure 10. Thermal conductivity apparatus general layout.

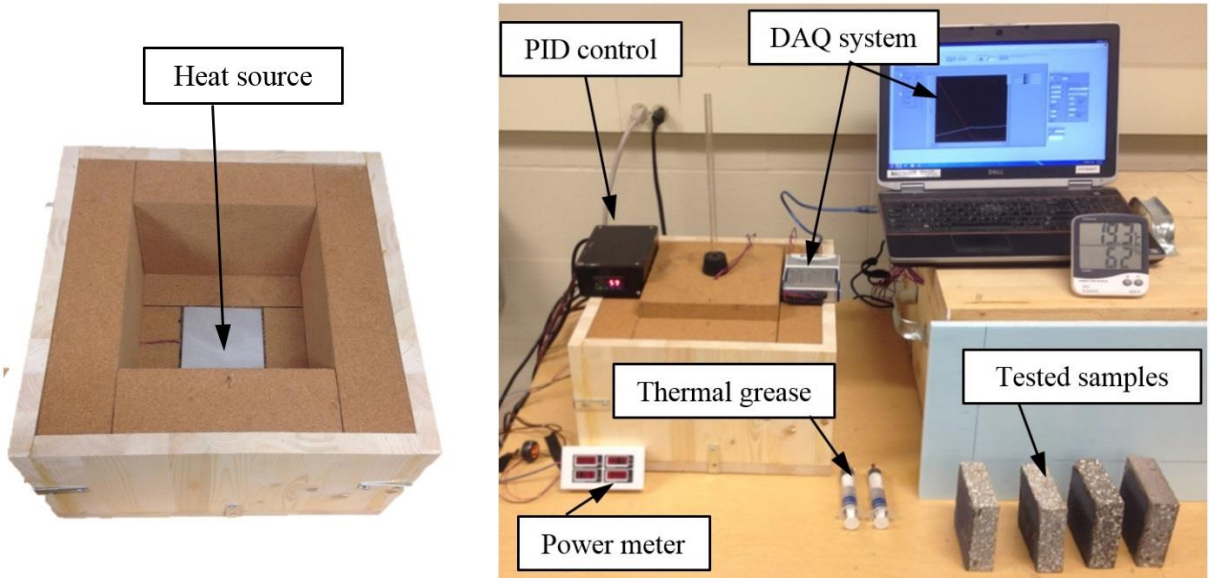

(a) (b)

Figure 11. Thermal conductivity measuring system: (a) Testing box (b) The whole system.

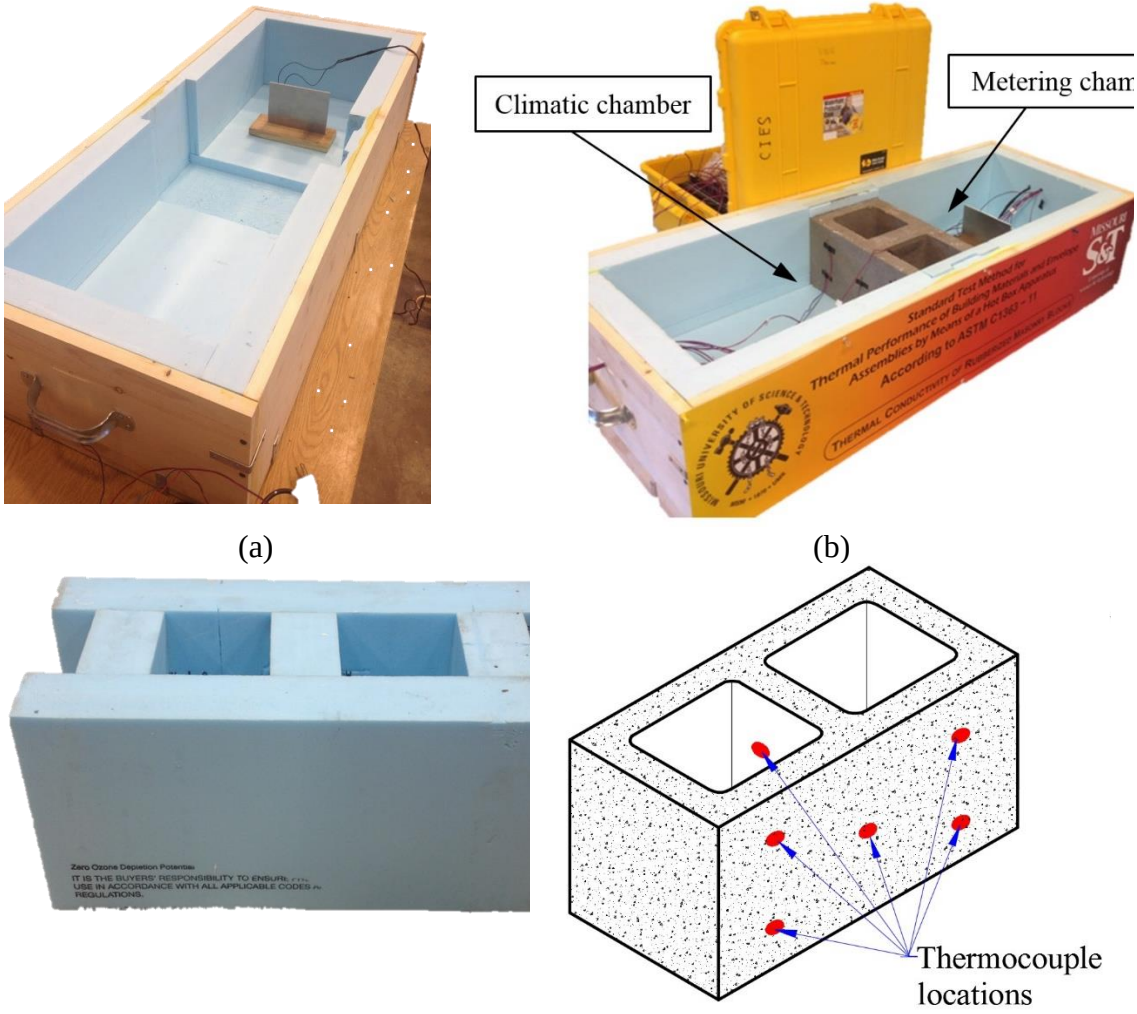

Figure 12. Two Controlled Sides Apparatus (a) The controlled heat source in the apparatus. (b) Testing specimen and data acquisition system (c) Calibration block (d) Measuring the transferred heat with thermocouples.

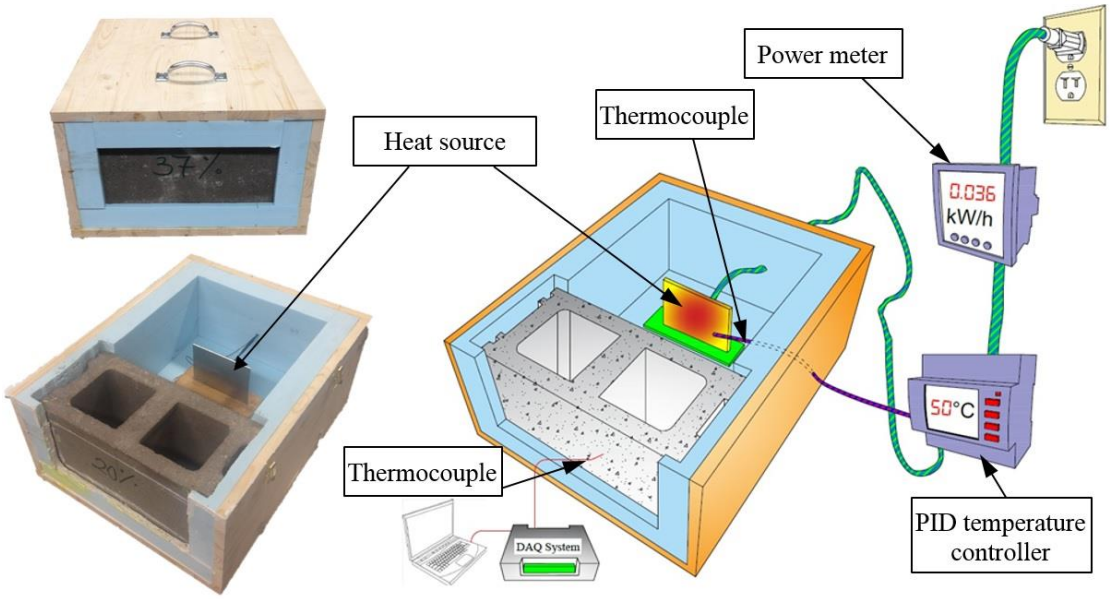

(a)

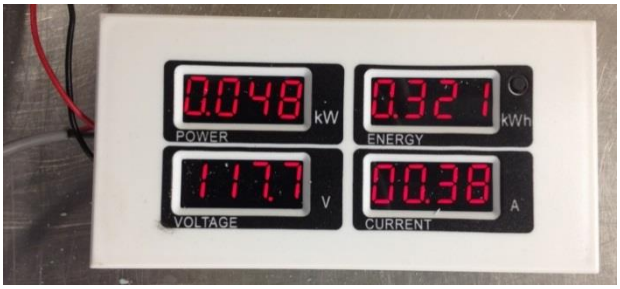

(b)

Figure 13. The hot box apparatus: (a) Hotbox (b) Power monitoring meter.

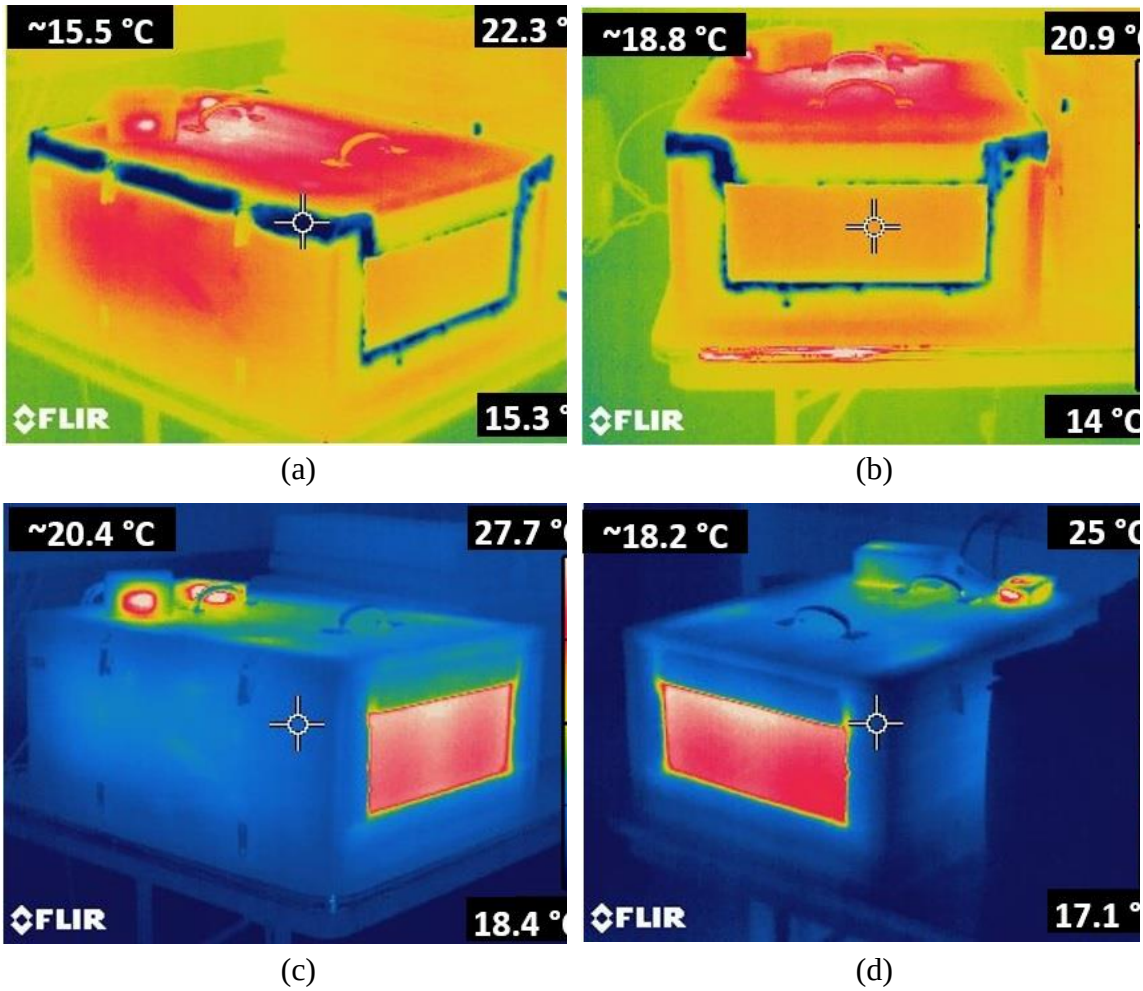

(a) (b)

(c) (d)

Figure 14. Thermal images of the Guarded Hot box (a) Side view image before testing, (b) front view image before, (c) side view image during testing, and (d) front view image during testing.

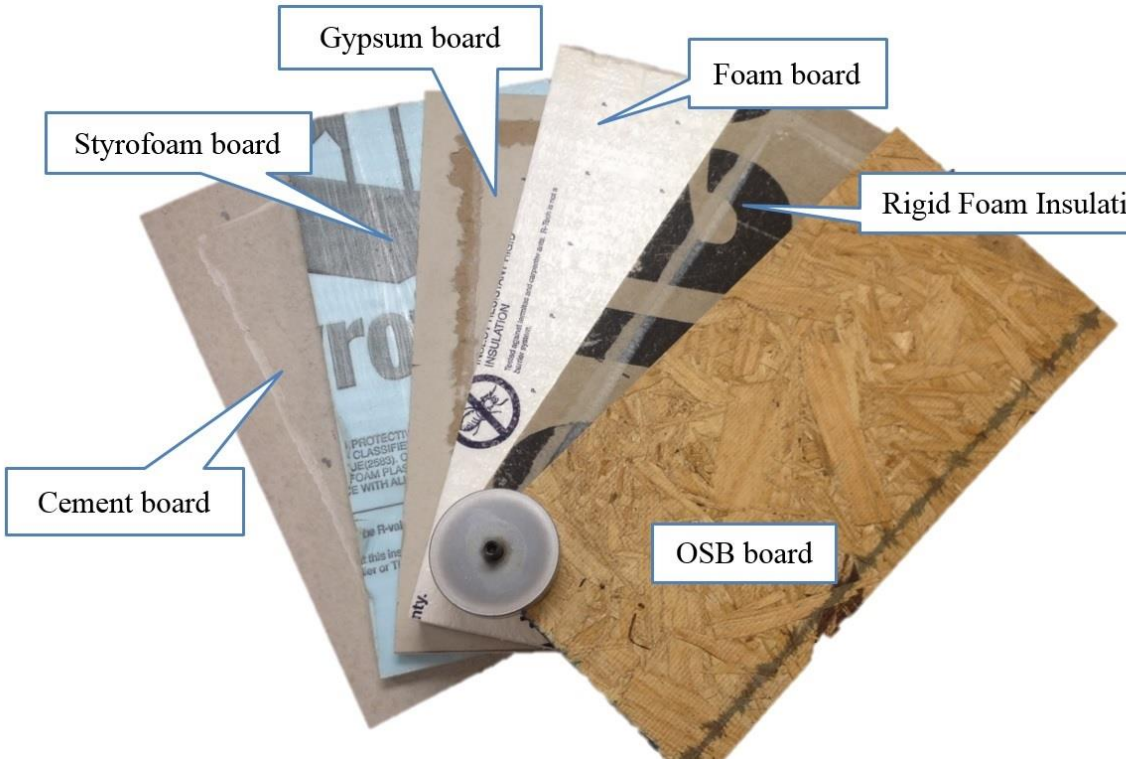

Figure 15. The materials that used for calibration.

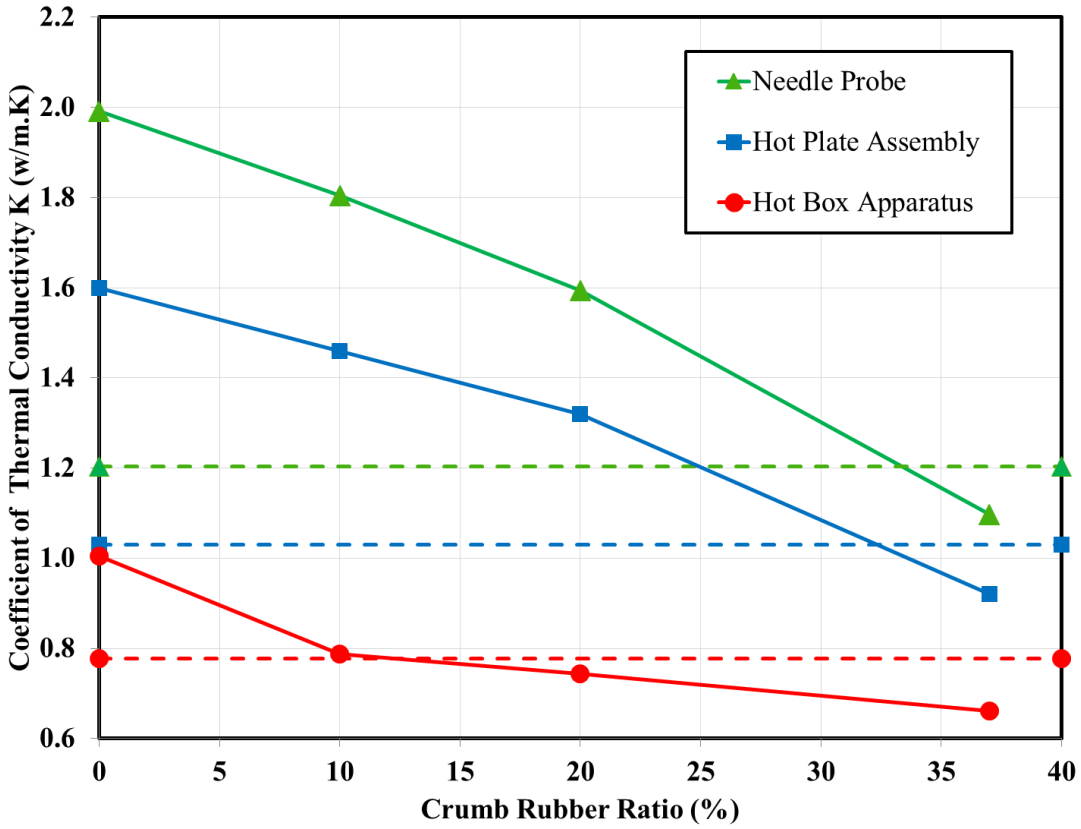

Figure16. Thermal conductivity factor for RCMUs (solid lines) and LWCMUs (dotted lines) using different approaches.

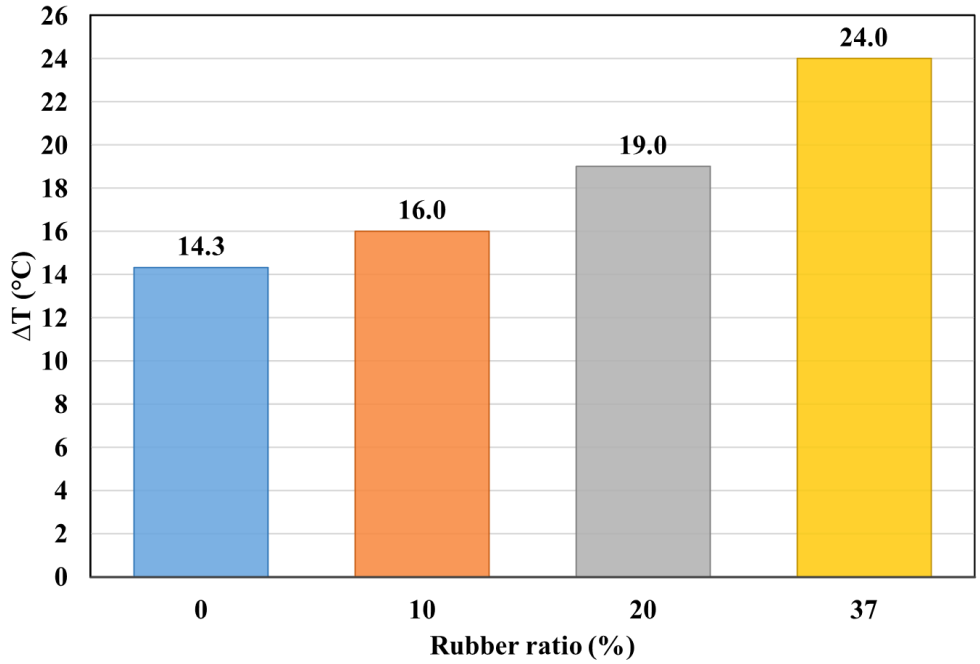

Figure 17. ΔT between the inner and outer faces of blocks at steady state case.

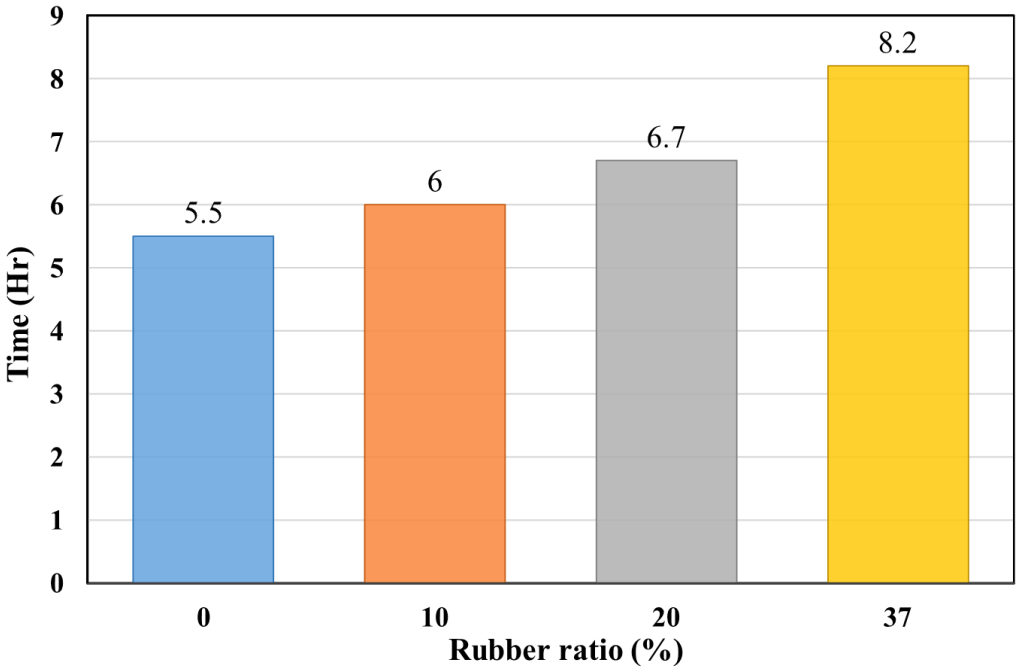

Figure18. Time to reach steady state.

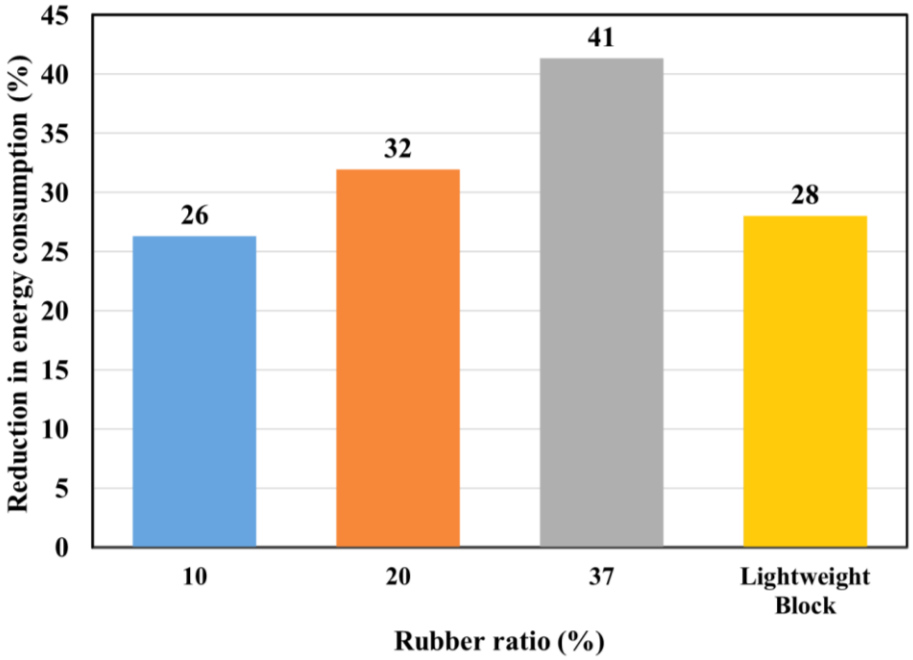

Figure19. Reduction in energy consumption for rubberized and lightweight masonry units.

REFERENCES

Abu-Lebdeh, T., Fini, E., Fadiel, A., 2014. Thermal conductivity of rubberized gypsum board. Am. J. Eng. Applied Sci 7, 12-22.

Batayneh, M.K., Marie, I., Asi, I., 2008. Promoting the use of crumb rubber concrete in developing countries. Waste Management 28, 2171-2176.

Berrueco, C., Esperanza, E., Mastral, F., Ceamanos, J., García-Bacaicoa, P., 2005. Pyrolysis of waste tyres in an atmospheric static-bed batch reactor: Analysis of the gases obtained. Journal of Analytical and Applied Pyrolysis 74, 245-253.

Cabeza, L.F., Barreneche, C., Miró, L., Morera, J.M., Bartolí, E., Fernández, A.I., 2013. Low carbon and low embodied energy materials in buildings: A review. Renewable and Sustainable Energy Reviews 23, 536-542.

Carder, C., Construction, R.M., 2004. Rubberized concrete. Colorado: Rocky Mountain Construction.

Dhir, R.K., Limbachiya, M.C., Paine, K.A., 2001. Recycling and Reuse of Used Tyres: Proceedings of the International Symposium Organised by the Concrete Technology Unit, University of Dundee and Held at the University of Dundee, UK on 19-20 March 2001. Thomas Telford.

Eldin, N.N., Senouci, A.B., 1993. Rubber-tire particles as concrete aggregate. Journal of materials in civil engineering 5, 478-496.

Fadiel, A., 2013. Use of Crumb Rubber to Improve Thermal Efficiency of Construction Materials. North Carolina Agricultural and Technical State University.

Fadiel, A., Al Rifaie, F., Abu-Lebdeh, T., Fini, E., 2014. Use of crumb rubber to improve thermal efficiency of cement-based materials. American Journal of Engineering and Applied Sciences 7, 1-11.

Fedroff, D., Ahmad, S., Savas, B., 1996. Mechanical properties of concrete with ground waste tire rubber. Transportation Research Record: Journal of the Transportation Research Board, 66-72.

Gheni, A.A., ElGawady, M.A., Myers, J.J., 2017. Mechanical Characterization of Concrete Masonry Units Manufactured with Crumb Rubber Aggregate. ACI Materials Journal 114.

Gou, M., Liu, X., 2014. Effect of rubber particle modification on properties of rubberized concrete. Journal of Wuhan University of Technology-Mater. Sci. Ed. 29, 763-768.

Hall, M.R., Najim, K.B., Hopfe, C.J., 2012. Transient thermal behaviour of crumb rubber-modified concrete and implications for thermal response and energy efficiency in buildings. Applied thermal engineering 33, 77-85.

Hammond, G.P., Jones, C.I., 2008. Embodied energy and carbon in construction materials. Proceedings of the Institution of Civil Engineers-Energy 161, 87-98.

Hernandez-Olivares, F., Barluenga, G., Bollati, M., Witoszek, B., 2002. Static and dynamic behaviour of recycled tyre rubber-filled concrete. Cement and concrete research 32, 1587-1596.

Horvath, A., 2004. Construction materials and the environment. Annu. Rev. Environ. Resour. 29, 181-204.

Isler, J.W., 2012. Assessment of concrete masonry units containing aggregate replacements of waste glass and rubber tire particles. University of Colorado Denver.

Milne, G., Reardon, C., 2005. Embodied energy. Your Home Technical Manual: Australia's guide to environmentally sustainable homes. Commonwealth of Australia.

Mohammed, B.S., Hossain, K.M.A., Swee, J.T.E., Wong, G., Abdullahi, M., 2012. Properties of crumb rubber hollow concrete block. Journal of Cleaner Production 23, 57-67.

Moustafa, A., ElGawady, M.A., 2015. Mechanical properties of high strength concrete with scrap tire rubber. Construction and Building Materials 93, 249-256.

Moustafa, A., ElGawady, M.A., 2016. Strain rate effect on properties of rubberized concrete confined with glass fiber–reinforced polymers. Journal of Composites for Construction 20, 04016014.

Moustafa, A., ElGawady, M.A., 2017. Dynamic properties of high strength rubberized concrete. ACI Spec. Publ 314, 1-22.

Moustafa, A., Gheni, A., ElGawady, M.A., 2017. Shaking-Table Testing of High Energy–Dissipating Rubberized Concrete Columns. Journal of Bridge Engineering 22, 04017042.

Najim, K., Hall, M., 2010. A review of the fresh/hardened properties and applications for plain-(PRC) and self-compacting rubberised concrete (SCRC). Construction and building materials 24, 2043-2051.

Pacheco-Torgal, F., Lourenço, P.B., Labrincha, J., Kumar, S., 2015. Eco-efficient masonry bricks and blocks: design, properties and durability. Woodhead Publishing.

Paine, K.A., Dhir, R.K., 2010. Research on new applications for granulated rubber in concrete. Proceedings of the institution of civil engineers: construction materials 163, 7-17.

Papadopoulos, A.M., Giama, E., 2007. Environmental performance evaluation of thermal insulation materials and its impact on the building. Building and environment 42, 2178-2187.

Poole Jr, S., 1998. Scrap and Shredded Tire Fires Special Report.

Rada, E.C., Ragazzi, M., Dal Maschio, R., Ischia, M., Panaitescu, V.N., 2012. Energy recovery from tyres waste through thermal option. Scientific Bulletin, Politehnica University of Bucharest, Series D, Mechanical Engineering 74, 201-210.

RMA, R.M.A., 2016. 2015 U.S. Scrap Tire Management Summary, Wasington, DC.

Sadek, D.M., El-Attar, M.M., 2015. Structural behavior of rubberized masonry walls. Journal of Cleaner Production 89, 174-186.

Sajwani, A., Nielsen, Y., 2017. THE APPLICATION OF THE ENVIRONMENTAL MANAGEMENT SYSTEM AT THE ALUMINUM INDUSTRY IN UAE. International Journal 12, 1-10.

Siddique, R., Naik, T.R., 2004. Properties of concrete containing scrap-tire rubber–an overview. Waste management 24, 563-569.

Sukontasukkul, P., 2009. Use of crumb rubber to improve thermal and sound properties of pre-cast concrete panel. Construction and Building Materials 23, 1084-1092.

Sukontasukkul, P., Chaikaew, C., 2006. Properties of concrete pedestrian block mixed with crumb rubber. Construction and Building Materials 20, 450-457.

Thomas, B.S., Gupta, R.C., 2013. Mechanical properties and durability characteristics of concrete containing solid waste materials. Journal of Cleaner Production.

Topcu, I.B., 1995. The properties of rubberized concretes. Cement and Concrete Research 25, 304-310.

Turgut, P., Yesilata, B., 2008. Physico-mechanical and thermal performances of newly developed rubber-added bricks. Energy and Buildings 40, 679-688.

Xue, J., Shinozuka, M., 2013. Rubberized concrete: A green structural material with enhanced energy-dissipation capability. Construction and Building Materials 42, 196-204.

Yesilata, B., Bulut, H., Turgut, P., 2011. Experimental study on thermal behavior of a building structure using rubberized exterior-walls. Energy and Buildings 43, 393-399.

Youssf, O., ElGawady, M.A., Mills, J.E., 2015. Experimental investigation of crumb rubber concrete columns under seismic loading, Structures. Elsevier, pp. 13-27.

Youssf, O., ElGawady, M.A., Mills, J.E., 2016. Static cyclic behaviour of FRP-confined crumb rubber concrete columns. Engineering Structures 113, 371-387.

Youssf, O., ElGawady, M.A., Mills, J.E., Ma, X., 2017. Analytical modeling of the main characteristics of crumb rubber concrete. Special Publication 314, 1-18.

Zheng, L., Huo, X.S., Yuan, Y., 2008. Experimental investigation on dynamic properties of rubberized concrete. Construction and building materials 22, 939-947.

III. RETENTION BEHAVIOR OF CRUMB RUBBER AS AN AGGREGATE IN INNOVATIVE CHIP SEAL SURFACING

Ahmed A. Gheni; Steven M. Lusher, Ph.D.; Mohamed A. ElGawady, Ph.D.

ABSTRACT

Statistics show that the world's transportation infrastructures are a primary backer to greenhouse gas emissions within the globe. This paper introduces an innovative chip seal pavement surfacing that uses chopped scrap tires as aggregates. A broad investigation on aggregate retention was performed. Eighty chip seal specimens with varied aggregate and binder parameters were examined for aggregate retention under five tests namely, the standard sweep test, a modified sweep test, the Vialit test, a modified Vialit test, and the Pennsylvania test. Four asphalt-based binders were examined in this study including different types of emulsions and asphalt cement. Two different mineral aggregates were examined in the tested specimens in addition to the crumb rubber. Results showed that the crumb rubber performed well in terms of aggregate retention. The Vialit and Pennsylvania tests indicated that the crumb rubber chip seal exceeded the performance of the mineral aggregate chip seals in terms of aggregate retention. The enhanced performance was primarily due to the low unit weight of the recycled rubber and its scratchy surface, that strengthened the adhesion of the crumb rubber to the binder. The sweep test results show that the mineral aggregate in chip seal surfacing can be replaced up to 100% with crumb rubber but it is recommended to increase the curing time before opening the roads for traffic due to the negligible water absorption capacity of crumb rubber.

Keywords: Chip Sealing, Eco-Friendly, Road maintenance, Crumb Rubber, Aggregate Retention, Green pavement

1. INTRODUCTION

Chip seal has been widely used as a pavement maintenance surface treatment. Chip seal is constructed by spreading binder on an existing pavement, followed by application of uniformly-graded aggregates. Rollers are used after spreading the aggregates for compaction in order to achieve the required embedment of the aggregates into the layer of binder. Chip seal surfacing is usually used on roads with traffic volumes in a range of 500-2400 vehicles per day. With certain techniques such as increasing the embedment depth, traffic control at an early age using a pilot vehicle, and/or using a push or vacuum sweeper instead of the traditional sweep methods, the chip seal can be used as a protecting layer and crack sealant for conventional pavements with traffic volumes higher than 7,500 vehicles per day per lane (Shuler 1998). By sealing existing fine cracks, chip seal protects the asphalt pavement layers by preventing water penetration to the subbase (Brown 1988, O'Brien 1989). Also, chip seal is effective in resisting tire-damage actions and creates a macrotexture that provides a good skid-resistant surface to ensure a safe driving atmosphere. One important feature that makes chip seal competitive with other maintenance techniques is its affordability (Gransberg and James 2005, Karasahin et al. 2014).

The effects of construction procedure and requirements, binder types, and mineral aggregate types on performance of chip seal pavement have been widely investigated to determine the optimum time to place the chips after spraying the seals and the

recommended time before opening the road to full-speed traffic, and how that is related to ambient temperature (Gransberg 2006, Banerjee et al. 2012).

One of the essential aspects in evaluating the behavior of chip seal is the aggregate retention, which is a key parameter of the design. Many factors affect the relationship between the aggregate and the binder, such as porosity, texture, mineralogy, and surface chemistry of the aggregate (Howard and Baumgardner 2009, Islam and Hossain 2011). The net electrical charge on the surface of the aggregate dictates the selection of the appropriate binder emulsion to use. Emulsions are classified as anionic, cationic, or non-ionic based on the ionic charge at the surface of the emulsifier-dispersed binder droplets. For example, if the net charge on an aggregate is positive (e.g. limestone), a negatively-charged (anionic) emulsion should be used, if possible, to promote maximum attraction (adhesion) of the binder droplets to the aggregate. In general, asphalt cement or emulsion modified with polymer content has better performance in aggregate retention than the non-polymer-modified due to the elastic membrane effect that holds the asphalt particles (Rahman et al. 2012). There are a number of standard tests that measure aggregate retention, such as the sweep test (ASTM 2011), Vialit test (Caltrans 2006), and Pennsylvania test (Kandhal and Motter 1991). However, some researchers modified these standard tests or developed new tests to evaluate the aggregate retention with the recent increase of research studies on chip seal (Kandhal and Motter 1991, Jordan III and Howard 2011, Rahman et al. 2012).

To achieve high skid resistance in chip seal, it is preferred to use uniformly graded (one size) aggregates, which improves the waterproofing as well (Wood et al. 2006). Using well-graded aggregates results in each aggregate having a different embedment depth which leads to dislodging of the aggregate and might cause vehicle damage and human

injury. Furthermore, the macrotexture and microtexture of aggregates affect the friction resistance of a chip seal's surface. The macrotexture refers to the aggregate size, shape, and uniformity, while the microtexture refers to the properties of the individual aggregate particles (Flintsch et al. 2003, Gheni et al. 2017).

Transportation infrastructure is a primary contributor to global carbon dioxide (CO_2) emissions (Ang and Marchal 2013). Using mineral aggregate instead of sustainable alternatives is one of the reasons for high global (CO_2) emissions. As the natural resources are depleted, the construction industry is forced to find replacements for virgin construction materials, and using recycled material is one of the main options. Furthermore, dealing with the world's scrap tires is an ongoing issue; the United States generated 246.43 million scrap tires during 2015 alone (RMA 2018). One of the common approaches to recycle these tires is to use them as an aggregate to completely or partially replace mineral aggregates, producing more environment-friendly materials such as rubberized concrete. Many researchers proposed using the crumb rubber in concrete and hot asphalt mixes to improve the sustainability and durability (Papagiannakis and Lougheed 1995, Hanson et al. 1996, Amirkhanian 2001, Shuler 2011, Rangaraju and Gadkar 2012, Moustafa and ElGawady 2015, Moustafa and ElGawady 2016, Youssf et al. 2016, Gheni et al. 2017, Gheni et al. 2017, Gheni et al. 2017, Moustafa et al. 2017, Gheni et al. 2018). Previous studies were also conducted using crumb rubber as a binder modifier, improving the overall performance of the binders in terms of temperature susceptibility and rutting resistance of pavement (Jensen and Abdelrahman 2006, Lee et al. 2008, Elseifi et al. 2011, Mohammad et al. 2011, Presti 2013).

In terms of chip seal surfacing, recycled rubber was used as a binder modifier to limit reflection cracking and increase the life cycle of asphalt pavement (LaForce 1983, LaForce 1986). The riding surface was smoother compared to conventional chip seal when rubberized asphalt binder was used (Way 2012). However, there has been no published research on using crumb rubber as aggregate in chip seal. Replacing the natural aggregate with recycled crumb rubber has potential positive impacts on the economy, environment, and the performance of chip seal pavement. First, by eliminating the safety issue, and the cost related to it, which is associated with the dislodged aggregate that affects the pedestrian and windshield of passerby vehicles. The dark black color of crumb rubber eliminates the cost and the need for applying a fog seal coating over chip seal with natural aggregate to cover its rocky color. In addition, this paper studied the improvement in aggregate retention which will cause a longer life cycle and less damage due to the snow plow action which was reported as one of the challenges that faces chip seal surfacing.

This paper investigates the feasibility of using recycled rubber in chip seal surfacing in term of aggregate retention. Different aggregate replacement ratios were examined and compared with reference specimens. The resulting chip seal is eco-friendlier than the conventional one. The aggregate retention of chip seal specimens with four different types of binder including two emulsions and two asphalt cement binders were investigated during this study under three standard tests namely standard sweep test, Vialit test, and Pennsylvania test. In addition, this paper proposes a modification to two of the aggregate retention tests (i.e., sweep and Vialit tests) in order to be more representative of the in-service conditions of chip seal.

2. MATERIAL CHARACTERIZATION AND PROPERTIES

Two asphalt cement binders (asphalt cement 1 and 2) and two emulsions (emulsion 1 and 2) were used during this study. The major difference between the two emulsions is that one is high-float and the other is not, while the two asphalt cement binders are performance graded (PG) binders with different levels of polymer-modification affecting the high-temperature performance. While the asphalt cement has no water in it, the emulsion has about 30-35% water content and emulsifiers to give it the required flowability under lower temperature (i.e., 35 ˚C) than the asphalt cement binders. However, the needed temperature for an asphalt cement binder to be flowable is significantly high at about 165 ˚C. Both emulsion 1 (trade name CRS-2P) and emulsion 2 (trade name CHFRS-2P) are cationic, which means that the emulsion has a positive charge that causes a migration towards the cathode (Mertens and Wright 1959). The emulsions and asphalt cement binders were supplied to the research team by a local distributor of these products with specification sheets. To estimate the required curing time, the water breakout development for both emulsions was determined under a temperature of 35 ˚C, (Figure 1). The figure shows that 81% of the water in both emulsion 1 and 2 evaporated during the first 6 hours, while the water breakout action reached the steady state after almost 24 hours of exposing the emulsion samples to a temperature of 35 ˚C.

In addition to the crumb rubber, two different mineral aggregates were evaluated (Table 1). Aggregate 1 was a creek/river gravel, while aggregate 2 was crushed traprock (i.e fine-grained igneous rock). These aggregate types are the most commonly used aggregates in chip seal in Missouri. In addition, the production process and the chemical

composition are different for each one of the aggregates. Figure 2 illustrates the sieve analysis of the two mineral aggregates and the recycled tire aggregate.

The three aggregate types had a similar median size ranging from 6.1 to 6.5 mm. The dry bulk specific gravity of crumb rubber was very low (0.87) which represents 37% of aggregate 1 and 33% of aggregate 2. Crumb rubber has a negligible water absorption compared to aggregates 1 and 2. Aggregates 1 and 2 had higher levels of very fine materials than the crumb rubber. Since they were cut or crushed, both recycled rubber and aggregate 2 had high fractured faces, while aggregate 1 had less fractured faces due to the water polishing action in creeks or rivers where the aggregate 1 came from. The flakiness index, which represents the Percentage of the aggregates' particles that have a thickness smaller than three-fifths of the mean dimension of the whole aggregate, was higher in the case of aggregate 2 than that in the other mineral aggregate and recycled rubber.

From the durability perspective, the National Cooperative Highway Research Program (NCHRP) (Shuler 2011) and many other agencies and DOTs (Caltrans 2003, Wood et al. 2006, Testa and Hossain 2014, Transportation 2016) are evaluating the durability and toughness of chip seal aggregates through their crushing and abrasion resistance using the Los Angeles (L.A.) abrasion test (AASHTO T 96) for dry conditions, but more recently the Micro-Deval test (AASHTO T 327) to test the aggregate under wet condition. Based on the expected traffic level, the maximum L.A. abrasion loss and Micro-Deval loss is between 12 and 15% by weight of the tested aggregate. As shown in Table 1, the recycled crumb rubber has a negligible loss in mass under the dry L.A. abrasion test while both aggregates 1 and 2 have a mass loss of 18.7% and 8.2%, respectively. Under the wet condition using the Micro-Deval test, there was no mass loss in the case of crumb

rubber versus 6% and 2.1% for aggregates 1 and 2, respectively. These numbers are logical since all the crumb rubber comes originally from tires that pass high manufacturing strength and durability standards. This high durability is reported as a concern by the U.S. Environmental Protection Agency (EPA) which gives a very long age to the used tires in the landfills (USEPA 2010).

Crumb rubber is commonly manufactured by either ambient or cryogenic grinding. The ambient recycled rubber is processed by leaving scrap tires at room temperature as they enter the shearing mill. The cryogenic recycled rubber is processed by freezing the recycled tires in a bath of liquid nitrogen followed by cracking them to the required sizes. Hence, cryogenic crumb rubber uses an excessive amount of energy and is less eco-friendly competitive compared to ambient crumb rubber. Furthermore, another difference between the two types of crumb rubber is the surface microtexture. Figure 3 shows the surface microtexture conditions of both types of rubber examined under a digital 3D microscope KH-8700. The figure also shows the surface of the mineral aggregates and presents the cross-sectional profiles of the aggregates in a range of 250 µm. The ambient crumb rubber had a coarse texture that incorporates various valleys and peaks (Figure 3a) which enhance its bond with the asphalt emulsions and asphalt cement, while the cryogenic recycled rubber had a relatively smooth texture (Figure 3b). As shown in Figure 3e, with a simple calculation, a projection of 1-mm width x 1-mm length of the aggregates resulted in a surface area of 1.222, 1.028, 1.042 and 1.032 mm^2/mm^2 for the ambient, cryogenic, crushed traprock, and creek/river gravel, respectively. Crushed traprock had a rougher surface than creek/river gravel but smoother than the ambient crumb rubber. Since the cryogenic process produces glass-like rubber particles with a relatively smooth surface, the ambient

crumb rubber was used in the remainder of this study and the cryogenic crumb rubber was excluded.

3. EXPERIMENTAL PROGRAM

Eighty chip seal specimens were examined over the span of this investigation using five aggregate retention evaluation test methods: the sweep test (ASTM 2011), a modified sweep test, the Vialit test (Caltrans 2006), a modified Vialit test, and the Pennsylvania test (Kandhal and Motter 1991). Tables 2 to 4 summarize the variables for the Vialit tests, sweep tests, and Pennsylvania tests, respectively.

For both sweep and modified sweep tests, specimens with 0%, 50%, and 100% rubber replacement by volume were prepared and tested. The rubber aggregate was used in conjunction with aggregates 1 and 2 and emulsions 1 and 2. For the other tests, specimens with 100% rubber and 0% rubber (100% mineral aggregate) were prepared and tested with emulsion 1, emulsion 2, asphalt cement 1, and asphalt cement 2.

3.1. STANDARD AND MODIFIED SWEEP TESTS

Soon after the construction of a chip seal, the surface, normally, is swept to remove any loose aggregates or dust before opening the road to traffic. A standard sweep test was conducted according to ASTM D7000-11 on chip seal specimens with ten different chip seal combinations to investigate the retention of the aggregate after the specified standard 1-hour curing. Since this test measures the curing performance of emulsion and aggregates and their curing time development which influences the aggregate retention, this paper presents a modified sweep test by conducting the standard test on another 40 chip seal specimens at curing times of 3, 6, 24, and 72 hours. Besides the crumb rubber aggregate,

two types of mineral aggregate with a combination of two types of asphalt emulsion were examined under the standard and modified sweep tests as listed in Table 2. A combination of each emulsion with crumb rubber only, aggregate 1 only, aggregate 2 only, or a combination of 50% crumb rubber and 50% of either aggregate 1 or 2. The purpose of this matrix is to explore the effects of the aggregate absorption and dry bulk specific gravity on the performance of chip seal. Since they need an elevated temperature (around 165 ˚C) to make them flowable, neither of the two asphalt cements were used during the sweep tests.

The sweep test started by applying 83 ± 5 gm of asphalt emulsion on a standard asphalt felt disk followed by spreading the aggregates uniformly (Figure 4a). For each type of aggregate, two grades of 9.5 - 6.3 mm (grade 1) and 6.3 - 4.75 mm (grade 2) were used for this test with a combination of 50% from each grade. Both types of mineral aggregate were replaced by rubber with volume replacement ratios of 0%, 50%, and 100% to be used in preparing the sweep test samples. The volume of each mix of aggregate was constant regardless of the rubber replacement ratio. This volume was calculated according to ASTM D7000-11 (Eq. 1) to provide one layer of aggregate on the asphalt felt with the least amount of voids.

$$Aggregate\ weight\ (gm) = \frac{A\ (202.1\ X - 15.8)}{100} + \frac{B\ (146.4\ X - 4.7)}{100} \quad (1)$$

Where:

A is the ratio of the grade 1 (from 9.5 to 6.3 mm), B is the ratio of the grade 2 (from 6.3 to 4.75 mm), and X is dry bulk specific gravity.

A mathematical model was proposed by Praticò et al. (Praticò et al. 2015) to predict the aggregate application rate as shown in Eq. 2

$$aggregate\ application\ rate\ (gm/cm^2) = \pi\ \frac{r.\gamma_A.\beta}{3.\alpha} \quad (2)$$

Where:

r is the radius of quasi-spherical particles (cm)

γ_A is the average specific gravity of the single aggregate particle

α is defined in the range (30.5/4, 1), while β is defined in the range (0.5 to 1).

For comparison, while equ.1 from ASTM D7000-11 resulted in an aggregate application rate of 0.65 and 0.72 gm/cm2 for aggregate 1 and 2 respectively, Equation 2 resulted in a range of (0.38 to 1.76) and (0.42 to 1.93) for aggregate 1 and 2 respectively based on the value of α and β.

To assure good aggregate embedment into the emulsion, the chip seal specimens were compacted with a standard compactor with a minimum curved surface radius of 550 ± 30 mm (Figure 4b). The specimens then were put in the oven to be cured at 35 °C for the required curing times. After curing, the asphalt felt was rotated 90° and the loose aggregates were removed (Figure 4c). Then, each specimen was weighed (W_{S1}) followed by setting for 3 minutes in the sweep test mixer. Thereafter, the test mixer ran for one minute of abrasion (Figure 4d). Any loose aggregates were removed, and the specimen was weighed (W_{S2}). The percentage of the weight loss was calculated using Equation 2 to represent the performance of the chip seal during the sweep test:

$$Sweeping\ weight\ loss = \frac{W_{S1} - W_{S2}}{W_{S1}} \times 100 \quad (3)$$

Figures 5 and 6 illustrate a sample of the investigated specimens before and after the sweep test.

3.2. STANDARD AND MODIFIED VIALIT TESTS

The Vialit test is used to evaluate the retention of binder/aggregate in chip seal pavement subjected to dynamic loads at low temperatures. The standard Vialit test was performed on 12 chip seal specimens (Figure 7) based on the British Standard 12272–3 (EN 2003), and shown in Table 4. The Vialit test began by applying the asphalt emulsion (at 60 °C) or asphalt cement (at 165 °C) to the standard square steel pan (200 mm × 200 mm). Next, 100 aggregate particles with a homogeneous particle size of 9.5 mm were distributed in 10 × 10 grid prior to curing the specimens in the oven at 60 °C for 48 hours.

After curing, the specimens were allowed to rest and cool outside the oven for 30 minutes at 25 ±5 °C. later one, the steel pans were put in a freezer at a temperature less than 0 °C for 30 minutes and then tested within 10 seconds after being removed from the freezer. The test involved dropping a stainless-steel ball weighing 500 ± 5g three times from a height of 500 mm onto the steel pan of each inverted specimen (Figure 8).

The detached particles were counted after each ball impact, and the retained aggregates were counted and recorded to represent the percentage of retention. However, the standard test required only three drops of the ball on the specimen which was insufficient to evaluate the differences between the different specimens made with emulsions. Therefore, a modified Vialit test was performed by increasing the number of drops to 30 and 40. The total number of drops in each test, i.e., the 30 or 40 drops, were carried out within 60 seconds after removing the specimen from the freezer to assure performing the test on frozen specimens. A total of 24 specimens were investigated for the standard and modified Vialit tests, as listed in Table 4. The three aggregates and the two emulsions were examined under the standard and modified Vialit tests. The standard Vialit

test was sufficient for the specimens made with asphalt cement, therefore, they were not examined under the modified Vialit test. Figs. 8b to 8e illustrate samples of the specimens and the conditions of the detached aggregates after conducting the Vialit test.

3.2. PENNSYLVANIA TEST

Pennsylvania aggregate retention test was developed by Kandhal and Motter (1991) in order to evaluate the initial adhesion loss and knock-off loss and how that will affect the aggregate retention in the asphalt emulsion. Specimens having 100% crumb rubber, 100% aggregate 1, and 100% aggregate 2 in combination with emulsions 1 or 2 were examined under the Pennsylvania test, as shown in Table 4.

The test requires six sieves and two pans with a diameter of 200 mm and depth of 50 mm, a sieve shaker, and rubber pads to prepare the specimens. The test procedure started by pouring the asphalt emulsion into a clean pan with an application rate of 1.13 liter/m^2 (0.25 gallon/yd^2) at 60 °C. The aggregate specimen weight (W_{P1}) was 300 gm. For each type of aggregate, two grades of 9.5-6.3 mm and 6.3-4.75 mm were used to prepare the test specimen for this test with a combination of 50% from each grade. A column of 12.5 mm sieves was set above the pan of the emulsion and the whole assembly was inserted into the sieve shaker. The sieve shaker was inclined at 60^o and run for 5 minutes. While running the sieve shaker, the aggregates were dropped from the top of the sieve column, passing through the sieves until they reached the bottom pan of the emulsion (Figure 9a).

The bottom pan now contained the chip seal specimen of emulsion covered with the aggregates. The previous sequence mixed and distributed the aggregates above the emulsion. Within 15 minutes, the chip seal specimen was covered with a neoprene bearing pad with a diameter of 190 mm and placed under a compressive load of 8.9 kN for about 5

seconds (Figure 9b). After embedding the aggregates, the bearing pad was removed, and the pan was cured at 35 ˚C for 24 hours. The pan was then inverted to allow the excess aggregates to fall away, and then they were weighed (W_{P2}). The pan was then placed upside down at the top of the same system of sieves that was used during the specimen preparation, and another clean pan was placed at the bottom of the sieve column. The whole column was inserted into the sieve shaker and it was turned on for 5 minutes (Figure 9c). The weight of the knocked-off aggregates (W_{P3}) in the bottom pan was measured. The knock-off percent loss was determined using Equation 3 and used as a representative of aggregate retention:

$$Percentage\ of\ Knock-off\ loss = \frac{W_{P3}}{W_{P1} - W_{P2}} \times 100 \qquad (4)$$

Specimens with recycled rubber and two types of mineral aggregates were prepared in combination with two types of asphalt emulsions to be examined in this test (Figure10). However, specimens with asphalt cement were not examined in this test because they need a high temperature (around 165 ˚C) to make the asphalt cement flowable.

4. RESULTS AND DISCUSSION

4.1. STANDARD AND MODIFIED SWEEP TESTS RESULTS

The percentage weight loss from the sweep tests was used for the comparisons between the specimens. Table 2 gives a summary of results for all the examined specimens under the standard and modified sweep tests. Figs. 11a and 11b illustrate the weight loss versus the percentage of the crumb rubber contribution in the specimens made of aggregates 1 and 2, respectively, for the sweep test.

As shown in Figure 11, the trend of the performance of the specimens is similar regardless of the aggregate type. The weight loss linearly increased with increasing crumb rubber percentage. The lost aggregate included both rubber and mineral aggregates proportional to their existence in the tested specimens, i.e., for specimens having 50% rubber replacement, the lost aggregate due to the sweep test would include 50% rubber. Furthermore, although the crumb rubber had a higher surface area in the microtexture than the other two aggregates, it did not show better performance under the sweep test. This behavior was likely due to the insignificant water absorption of the crumb rubber relative to the other two types of aggregate, leading to later hardening of the asphalt emulsion. In addition, the crumb rubber had a low relative density approximately 34-36% of that of the other two aggregates, likely causing the crumb rubber to be swept easily. Specimens made with emulsion 2 had better performance than those made with emulsion 1 in terms of weight loss. The reason for this behavior most likely was the high flowability of emulsion 2 which gave the emulsion a better mechanical bond and helped the emulsion to encapsulate the aggregate particles and be in contact with troughs and crests of all types of aggregate. The weight loss increased by approximately 33% when the crumb rubber increased from 0% to 100%. Furthermore, aggregate 1 showed slightly better performance than aggregate 2 at 0% rubber replacement. After one hour curing, the weight loss of aggregate 1 was 40% compared to 44% for aggregate 2 likely due to the high absorption of aggregate 1 over aggregate 2 which helps in breaking out the emulsion's water.

During the modified sweep test, the weight loss of the aggregates was determined at curing times ranging from 1 to 72 hours, as shown in Figs. 12 and 13 for emulsion 1 and 2, respectively. The weight loss decreased significantly during the first 6 hours of curing,

reaching a range between 5% and 20% for all specimens, while it decreased slightly beyond 6 hours. The rapid decrease in the weight losses in the first 6 hours is due to early water breakout leading to emulsion hardening.

As shown in Figure 1, 73% of the water breakout occurred for both emulsions in the first 6 hours of exposure. Beyond that, the water breakout is very slow. The figures also show that rubberized chip seal will require more curing time compared to mineral aggregate to achieve a given weight loss. For example, the weight loss in chip seal with 50% rubber replacement will achieve the same weight loss as that in the chip seal with mineral aggregate when the curing time increases from 1.00 hour to 1.75 hours for both emulsion 1 and 2. For chip seal with 100% rubber, a mass loss equal to or less than that in conventional chip seal can be achieved when the curing time is increased from 1 hour to 2.5-3.0 hours. Furthermore, Figs. 14 and 15 show the weight losses for different crumb rubber replacements at different curing times for emulsion 1 and emulsion 2, respectively. As shown in the figures, a minimum curing time of 6 hours is required for 100% mineral aggregates to keep the weight losses below 20%. For crumb rubber replacement up to 40%, a curing time of 6 hours seems appropriate as well. At 100% rubber replacement, a curing time of 24 hours is required to keep the weight losses below approximately 12%. Finally, for a given curing time, specimens having aggregate 1 with crumb rubber showed better performance than those having aggregate 2 with crumb rubber due to the higher water absorption of aggregate 1 leading to faster hardening of the emulsion.

4.2. STANDARD AND MODIFIED VIALIT TESTS RESULTS

The number of aggregate particles retained in the asphalt binder was recorded for each specimen (Table 4). The performance of the three aggregates in combination with

each type of binder was compared under the standard Vialit test (Figure 16). The recycled rubber exhibited an exceptional performance where 100% of rubber particles retained with all four binders. This compatibility between the rubber and the asphalt binders contributed to high adhesion capacity between the rubber's external surface and the asphalt binders.

The Differential Scanning Calorimeter (DSC) test was conducted according to ASTM D1519–95 to determine the melting range of rubber. As shown in Figure 17, the melting point for scrap tire rubber Tp was 97 ℃. According to these results and the high temperature of binder (165 ℃) during the aggregate application, part of the crumb rubber, especially the surface, melted in the embedment depth inside the binder, which creates a stronger bond. However, this effect did not appear with the other two aggregates. Also, the crumb rubber did not easily detach during the test because of its low unit weight. As shown in Figure 16, aggregates 1 and 2 exhibited a better performance with the emulsions than with the asphalt cements during the standard test. This behavior was likely a result of the asphalt cements becoming brittle after freezing the specimens at -25 ˚C as required by the test procedure.

The three types of aggregate did not show any difference in performance with the two emulsions during the standard test of three drops of the steel ball. Therefore, the modified Vialit test was conducted for such types of specimens with 30 and 40 drops of the ball. Figure 18 illustrates the number of drops versus the number of the retained aggregates during the modified Vialit test for the two emulsions. The crumb rubber continued showing its superior performance with 100% retained aggregates. Aggregate 1 had slightly better performance than aggregate 2 because of its lower unit weight. The aggregates' surface area did not affect their performance during this test because dislodging

of the aggregates was due to rupture in the asphalt cement/emulsion and not at the interfaces between the asphalt cement/emulsion and aggregates, as shown in Figure 8e. Also, the aggregate's absorption and the emulsion water breakout did not affect the chip seal performance because the Vialit test was conducted after 24 hours of curing.

4.3. PENNSYLVANIA TEST RESULTS

The knock-off weight losses of the aggregates were determined for all of the specimens of the Pennsylvania test. Table 5 summarizes the Pennsylvania test results. Figs. 19a and 19b illustrate the knock-off weight loss of the aggregates for the different emulsions and aggregates, respectively. The Pennsylvania test examined the aggregate retention based mainly on the aggregate self-weight and surface area because each specimen was subjected to high compression forces to achieve good embedment depth. Therefore, the crumb rubber showed superior performance with knock-off loss of about 1% and 2% for emulsion 1 and emulsion 2, respectively. This behavior was likely due to the low unit weight and the relatively rough surface of the crumb rubber. Aggregate 2 had better performance compared to aggregate 1 because of its rougher surface. The aggregate's absorption and the emulsion water breakout did not affect the performance of the chip seal specimens because the Pennsylvania test was conducted after 24 hours of curing. As shown in Figure 19b, emulsion 1 had better performance than emulsion 2 during the Pennsylvania test, which contradicted the results from the other tests (sweep and Vialit). This behavior was likely because of the compaction load that was applied to each specimen. Emulsion 1 was more viscous than emulsion 2. Therefore, the applied load achieved greater embedment depth in the case of emulsion 1 than in the case of emulsion 2, which was

considerably flowable. However, this effect did not appear in the other tests because there was no applied compaction force.

In both Vialit test and Pennsylvania test results, aggregate 2 with higher flakiness index than that in the other mineral aggregate and recycled rubber has the least aggregate retention among the three tested aggregates. This trend was reported before by Liu, Li et al. (Liu et al. 2018) when he concluded throw a finite element model that the aggregate with a higher ratio of length to height (around 4.66) has a lower aggregate retention compared to ones with length to height ratios of 2.33 and 1.55 respectively.

5. CONCLUSIONS

Presented is a study on chip seal pavement constructed using crumb rubber that was produced from scrap tires as an eco-friendly aggregate. Using recycled crumb rubber in chip seal instead of mineral aggregate consumes up to 2500 scrap tire/km with 100% replacement ratio. Furthermore, crumb rubber has a loose unit weight that is approximately 35% of the mineral aggregate. Hence, for a given aggregate volume, the freight cost should be much cheaper. However, until it is produced in a massive quantity that meets the construction sector need, it is not easy to compare the life cycle costs between standard and the eco-friendly chip seals.

During this study, eighty chip seal specimens were prepared using four types of binders, including emulsions and asphalt cement, two reference mineral aggregates, and the crumb rubber aggregate. Standard and modified sweep tests, standard and modified Vialit tests, and the Pennsylvania test were used to investigate the retention of the different types of aggregates in chip seal. This investigation showed that the recycled rubber has the

potential to be used as coarse aggregates in the chip seal with good aggregate retention performance. The findings and conclusions are as follows:

1- The crumb rubber can be used as a mineral aggregate replacement; however, it is recommended to increase the curing time based on the crumb rubber replacement percentage. For a crumb rubber replacement percentage of 50% and above, curing time of six hours is required before sweeping.

2- For mineral aggregate, a minimum curing time of five hours is required before sweeping the chip seal.

3- Based on the microtexture analysis and the environmental impact, the ambient crumb rubber is recommended over the cryogenic crumb rubber because it has a much rougher surface and lower energy consumption during the production process. For example, the ambiently processed rubber tested in this study had a surface area 1.19 times that of the cryogenic rubber.

4- The standard sweep test, which specifies only one hour of curing time, does not give enough data to estimate the time to open the road. Therefore, the test should be performed with a range of curing times to decide the best time of curing that causes less aggregate loss.

5- Chip seals with 100% crumb rubber aggregate, aggregate 1, or aggregate 2 passed the standard Vialit test with 100% aggregate retention. However, when the number of drops was increased to 40, the crumb rubber aggregate had 100% retention versus 65% to 90% for the mineral aggregates when emulsions were used, and 40% to 50% for the mineral aggregates when asphalt cements were used.

6- The Pennsylvania test showed that the crumb rubber had better retention than the mineral aggregates. The knock-off weight loss was between 1% to 3% for crumb rubber versus 7% to 12% for mineral aggregates for both emulsions 1 and 2.

Although this investigation shows the feasibility of utilizing recycled rubber in chip seal treatment, additional examinations are still required to evaluate the aggregate retention at the micro level and under different environments and driving speed as well as the effect of snow plowing. In addition, it is recommended to measure the long-term aggregate retention with different types of binders.

ACKNOWLEDGEMENTS

The authors would like to acknowledge Missouri University of Science and Technology, Missouri Department of Natural Resources, and Pettis County for their support for this work. The authors would like to thank Vance Brothers for their support with the asphalt materials.

Table 1. Properties of crumb rubber and mineral aggregates.

Type of Aggregate		Rubber	Aggregate 1	Aggregate 2
Dry bulk specific gravity		0.87	2.35	2.62
Absorption, %		0.1%	4.7%	0.8%
Coefficient of Uniformity		1.9	1.9	1.3
Fractured faces	% of non-fractured faces	0.00%	4.60%	0.00%
	% of aggregates with one face	100 %	95.4%	100%
	% of aggregates with two or more faces	88.7%	93.1%	100%
Loose dry unit weight, kg/m^3		423	1180	1249
Voids in loose aggregates, %		15.4	49.8	52.8
Abrasion loss by Los Angeles test, %		0.30%	18.7%	8.20%
Weight loss by Micro-Deval test, %		0.0%	6.0%	2.1%
Materials passing No. 200 sieve, %		0.20%	0.50%	0.52%
Median particle size, mm		6.5	6.2	6.1
Flakiness index, %		31.3%	37.6%	42.0%

Table 2. Specimen variables for the standard and modified Vialit tests.

Groups	Specimen label	Type of test	No. of drops	Binder type	Aggregate type	Percentage of retained aggregates
Group C	CS-51	Standard Vialit Test	3	Emulsion 1	Rubber	100.0%
	CS-52				Aggregate 1	100.0%
	CS-53				Aggregate 2	100.0%
	CS-54			Emulsion 2	Rubber	100.0%
	CS-55				Aggregate 1	100.0%
	CS-56				Aggregate 2	100.0%
	CS-57			Asphalt cement 1	Rubber	100.0%
	CS-58				Aggregate 1	60.0%
	CS-59				Aggregate 2	41.0%
	CS-60			Asphalt cement 2	Rubber	100.0%
	CS-61				Aggregate 1	71.0%
	CS-62				Aggregate 2	52.0%
Group D	CS-63	Modified Vialit Test	30	Emulsion 1	Rubber	100.0%
	CS-64				Aggregate 1	88.0%
	CS-65				Aggregate 2	75.0%
	CS-66			Emulsion 2	Rubber	100.0%
	CS-67				Aggregate 1	96.0%
	CS-68				Aggregate 2	89.0%
Group E	CS-69		40	Emulsion 1	Rubber	100.0%
	CS-70				Aggregate 1	80.0%
	CS-71				Aggregate 2	68.0%
	CS-72			Emulsion 2	Rubber	100.0%
	CS-73				Aggregate 1	92.0%
	CS-74				Aggregate 2	75.0%

Table 3. Specimens details for the standard and modified sweep tests.

Groups	Specimen label	Type of test	Curing time (hours)	Emulsion type	Percentage of the Aggregate type (by volume)			Weight loss (%)
					Rubber	Aggregate 1	Aggregate 2	
Group A	CS-1	Standard sweep test	1	Emulsion 1	100%	0%	0%	58.9%
	CS-2				50%	50%	0%	50.0%
	CS-3				50%	0%	50%	49.9%
	CS-4				0%	100%	0%	39.9%
	CS-5				0%	0%	100%	43.7%
	CS-6			Emulsion 2	100%	0%	0%	54.9%
	CS-7				50%	50%	0%	44.5%
	CS-8				50%	0%	50%	43.5%
	CS-9				0%	100%	0%	34.4%
	CS-10				0%	0%	100%	35.8%
Group B	CS-11	Modified sweep test	3	Emulsion 1	100%	0%	0%	32.4%
	CS-12				50%	50%	0%	22.5%
	CS-13				50%	0%	50%	28.2%
	CS-14				0%	100%	0%	10.2%
	CS-15				0%	0%	100%	23.1%
	CS-16		6		100%	0%	0%	20.6%
	CS-17				50%	50%	0%	11.1%
	CS-18				50%	0%	50%	10.7%
	CS-19				0%	100%	0%	6.6%
	CS-20				0%	0%	100%	8.1%
	CS-21		24		100%	0%	0%	13.4%
	CS-22				50%	50%	0%	9.6%
	CS-23				50%	0%	50%	7.7%
	CS-24				0%	100%	0%	5.0%
	CS-25				0%	0%	100%	4.9%
	CS-26		72		100%	0%	0%	10.7%
	CS-27				50%	50%	0%	7.3%
	CS-28				50%	0%	50%	6.9%
	CS-29				0%	100%	0%	3.4%
	CS-30				0%	0%	100%	3.3%
	CS-31		3	Emulsion 2	100%	0%	0%	35.4%
	CS-32				50%	50%	0%	20.7%
	CS-33				50%	0%	50%	28.8%
	CS-34				0%	100%	0%	13.3%
	CS-35				0%	0%	100%	19.3%
	CS-36		6		100%	0%	0%	22.3%
	CS-37				50%	50%	0%	9.9%
	CS-38				50%	0%	50%	12.2%
	CS-39				0%	100%	0%	4.6%
	CS-40				0%	0%	100%	6.4%
	CS-41		24		100%	0%	0%	11.3%
	CS-42				50%	50%	0%	6.3%
	CS-43				50%	0%	50%	6.9%
	CS-44				0%	100%	0%	3.3%
	CS-45				0%	0%	100%	3.3%
	CS-46		72		100%	0%	0%	8.6%
	CS-47				50%	50%	0%	5.2%
	CS-48				50%	0%	50%	5.5%
	CS-49				0%	100%	0%	3.2%
	CS-50				0%	0%	100%	3.2%

Table 4. Specimen variables for the standard Pennsylvania tests.

Groups	Specimen label	Type of test	Emulsion type	Aggregate type	Knock-off Weight loss (%)
Group F	CS-75	Pennsylvania Test	Emulsion 1	Rubber	1.3%
	CS-76			Aggregate-1	8.8%
	CS-77			Aggregate-2	6.8%
	CS-78		Emulsion 2	Rubber	2.8%
	CS-79			Aggregate-1	12.0%
	CS-80			Aggregate-2	8.5%

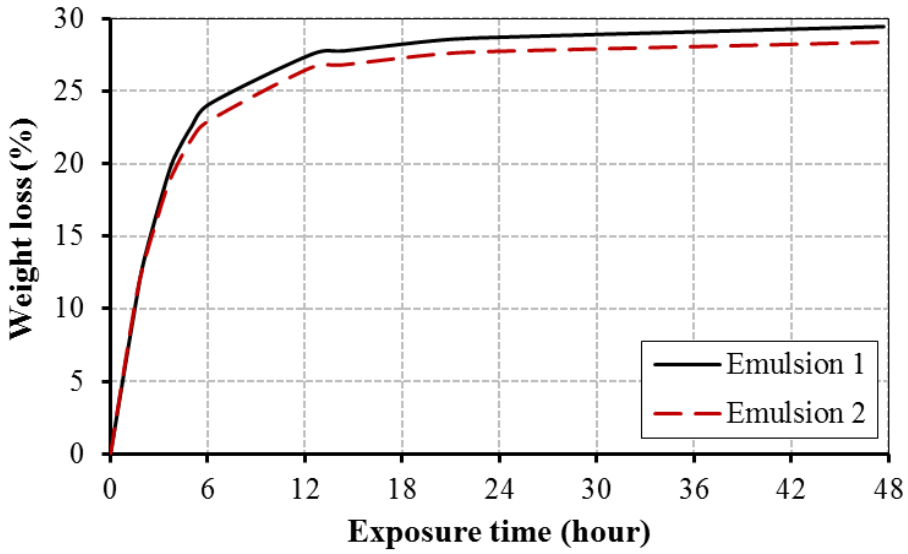

Figure 1. Water breakout under varied exposure time for emulsion 1and 2.

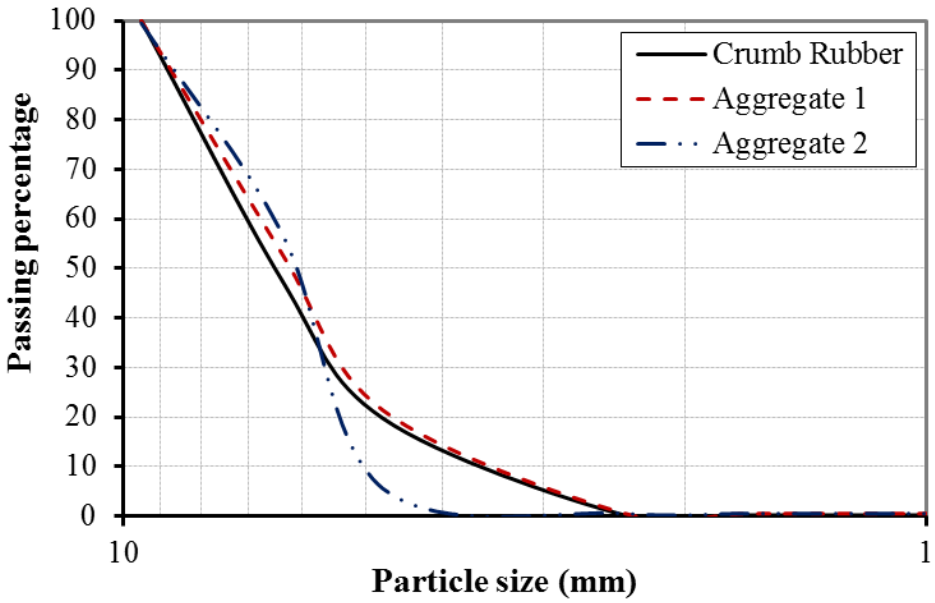

Figure 2. Sieve analysis of the aggregates.

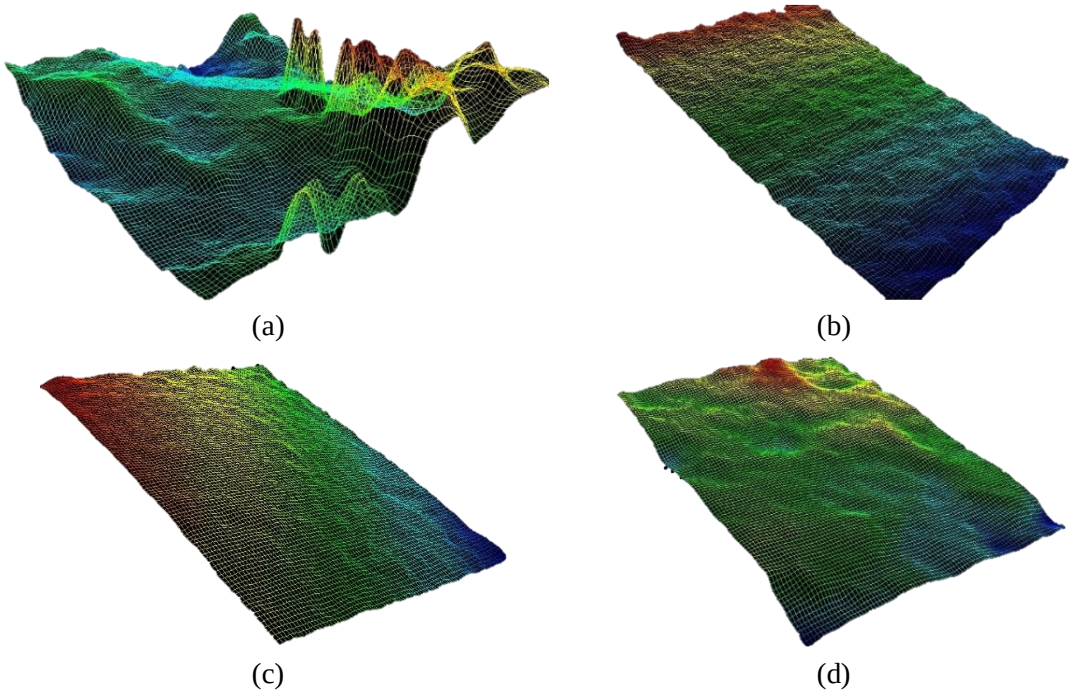

(a) (b)

(c) (d)

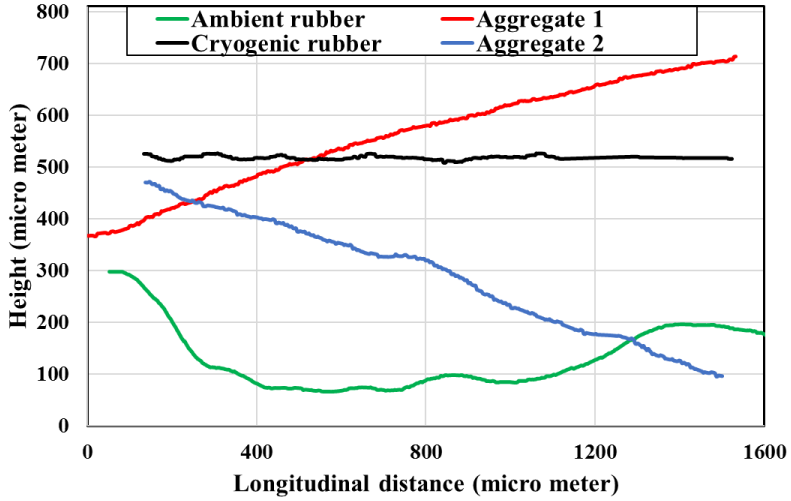

(e)

Figure 3. 3D Microscope surface texture analysis a range of 250 µm: (a) 3D texture view of ambient crumb rubber, (b) 3D texture view of cryogenic recycled rubber, (c) 3D texture view of aggregate 1, (d) 3D texture view of aggregate 2, and (e) cross-sectional profiles of all tested aggregate.

(a) (b)

(c) (d)

Figure 4. Sweep test: (a) spreading aggregate on the leveled emulsion, (b) chip seal specimen's compaction, (c) removing the unattached aggregates, and (d) running the test.

CS-1

CS-2

CS-3

CS-4

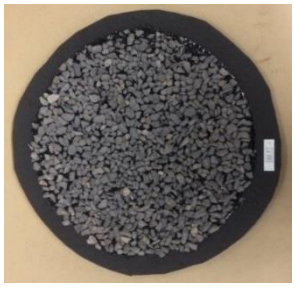

CS-5

Figure 5. Sample of specimens before sweep test.

CS-1

CS-2

CS-3

CS-4

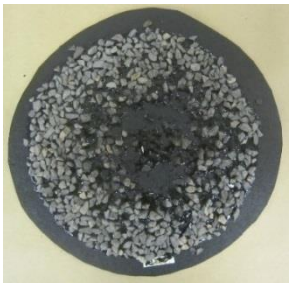

CS-5

Figure 6. Sample of specimens after sweep test.

(a) (b) (c)

Figure 7. Vialit test specimens with different aggregate types: (a) rubber (i.e., CS-49), (b) aggregate 1 (i.e., CS-50), and (c) aggregate 2 (i.e., CS-51).

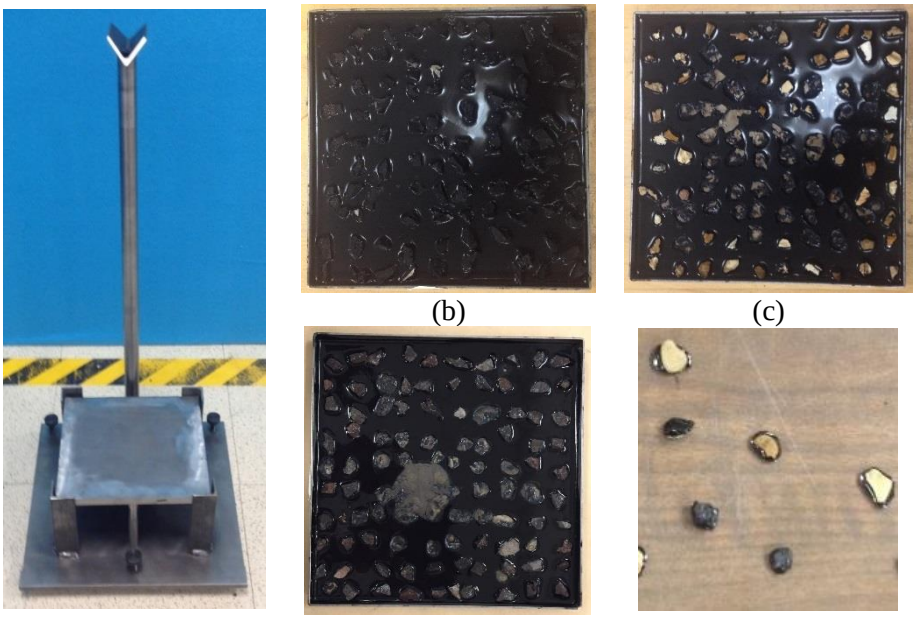

(a) (b) (c) (d) (e)

Figure 8. Vialit test: (a) test setup during the test, (b) specimen CS-63 after testing, (c) specimen CS-64 after testing, (d) specimen CS-65 after testing, and (e) dislodged aggregates.

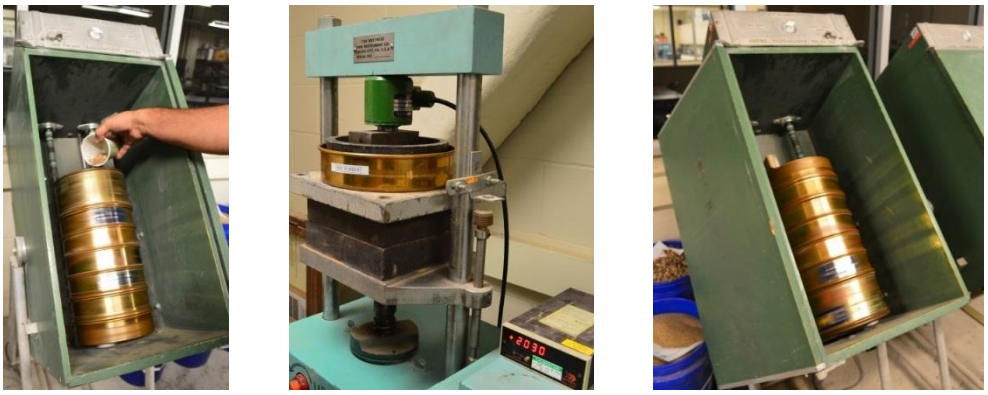

(a) (b) (c)

Figure 9. Pennsylvania test preparation: (a) spreading the aggregate during running the sieve shaker, (b) Compacting the specimen at 8.9 kN, (c) running the sieve shaker with the upside-down specimen.

(a) (b) (c)

Figure 10. Sample of Pennsylvania test specimens with different aggregates: (a) recycled rubber, (b) aggregate 1, and (c) aggregate 2.

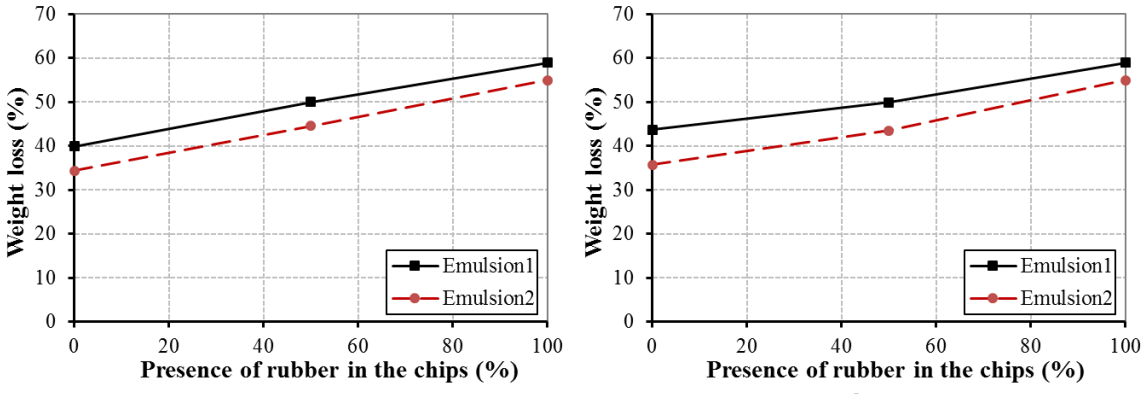

(a) (b)

Figure 11. Weight loss versus the percentage of crumb rubber presence in the chip seal: (a) with aggregate-1 and (b) with aggregate-2, in the two emulsions.

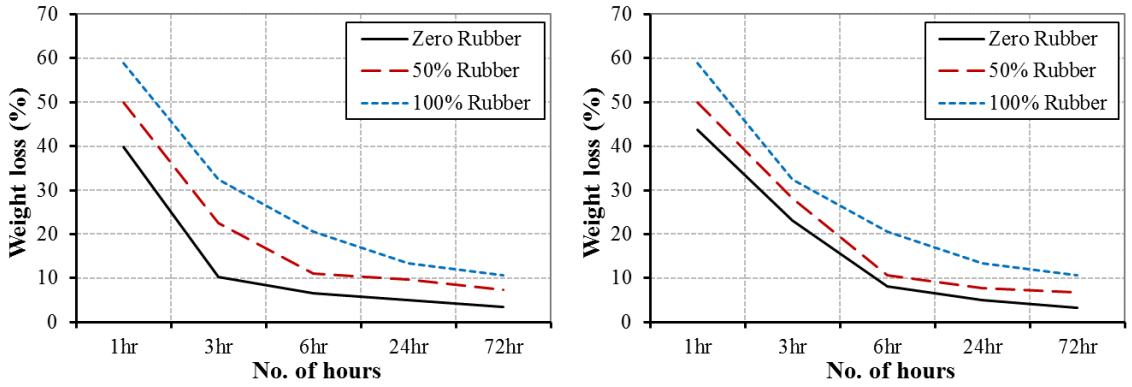

(a) (b)

Figure 12. Sweep test Weight loss versus the curing time for different rubber percentages in the chip seal: (a) with aggregate-1 and (b) with aggregate-2, in emulsion-1.

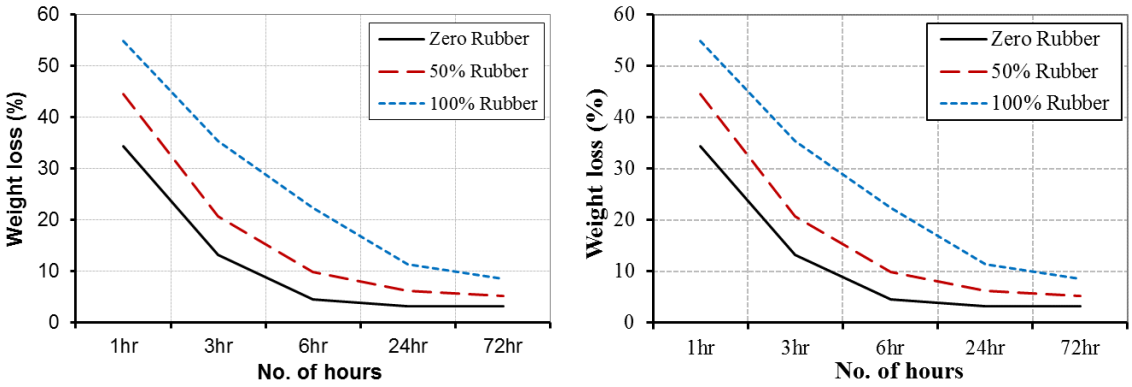

(a) (b)

Figure 13. Sweep test weight loss versus the curing time for different rubber percentages in the chip seal: (a) with aggregate-1 and (b) with aggregate-2, in emulsion-2.

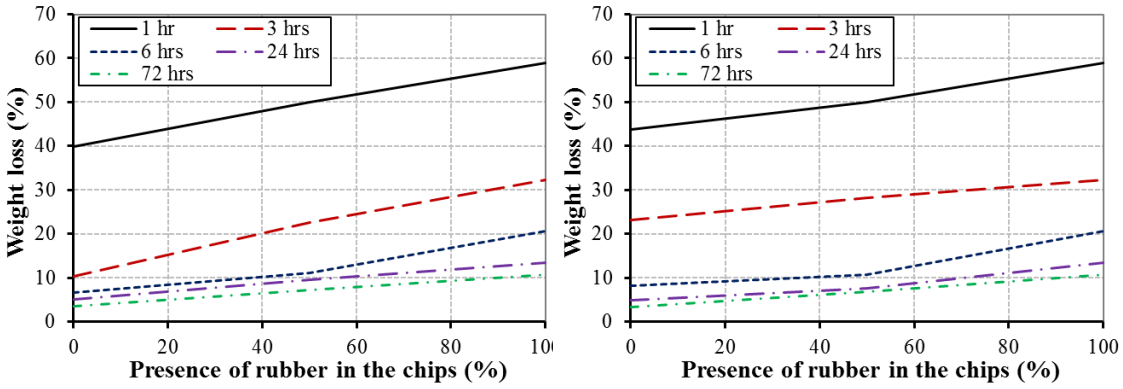

(a) (b)

Figure 14. Sweep test weight loss at different curing times versus the percentage of rubber presence in the chip seal: (a) with aggregate-1 and (b) with aggregate-2, in emulsion-1.

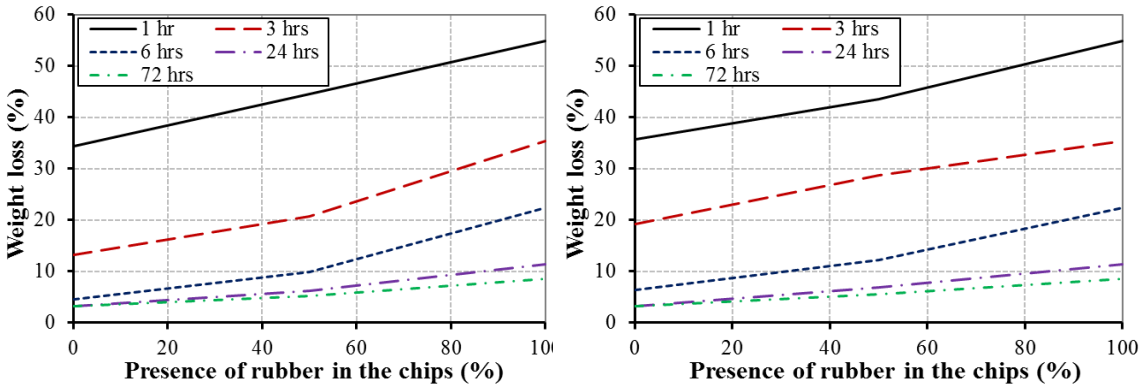

(a) (b)

Figure15. Sweep test weight loss at different curing times versus the percentage of rubber presence in the chip seal: (a) with aggregate-1 and (b) with aggregate-2, in emulsion-2.

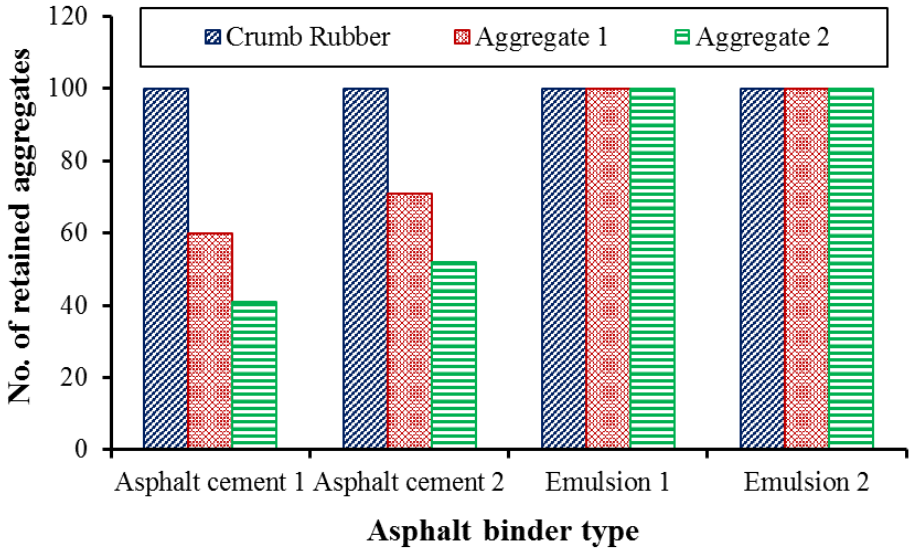

Figure 16. Number of retained aggregates per binder type for the three aggregates.

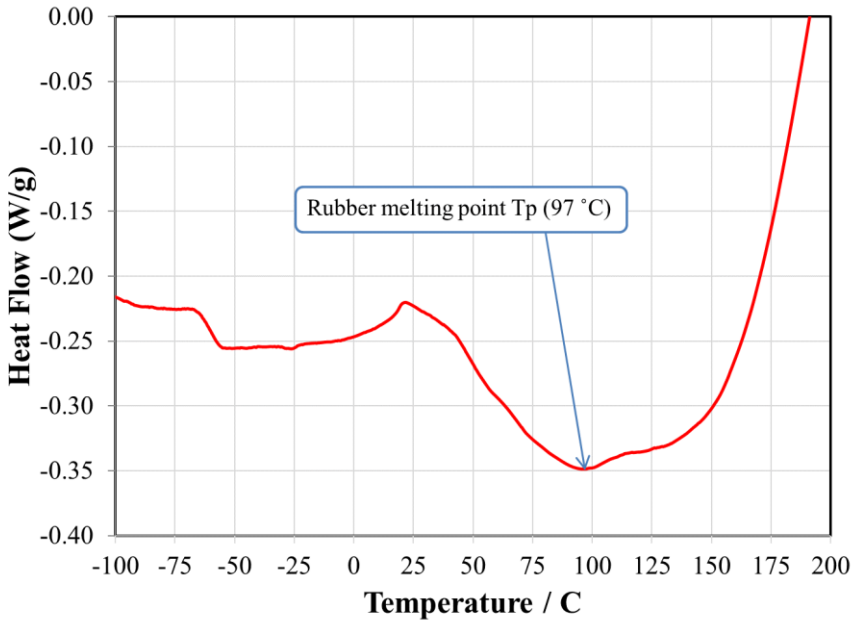

Figure 17. Differential scanning calorimetry (DSC) for scrap tire rubber.

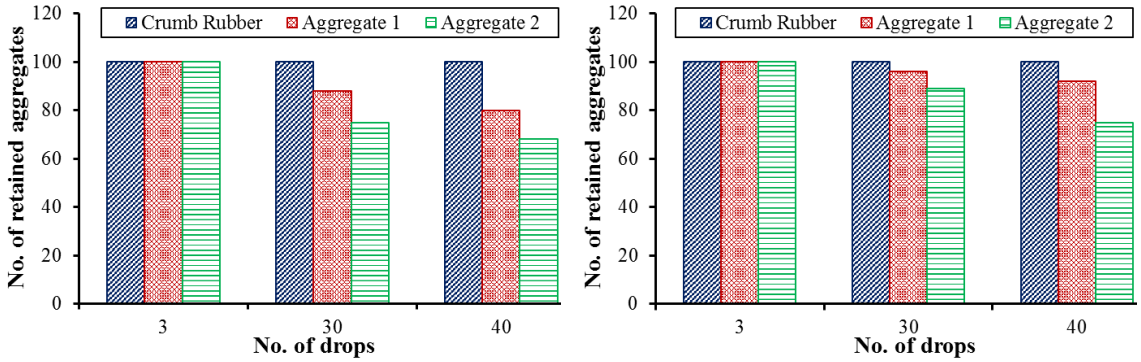

(a) (b)

Figure 18. Number of retained aggregates versus the number of drops: (a) emulsion 1 and (b) emulsion 2.

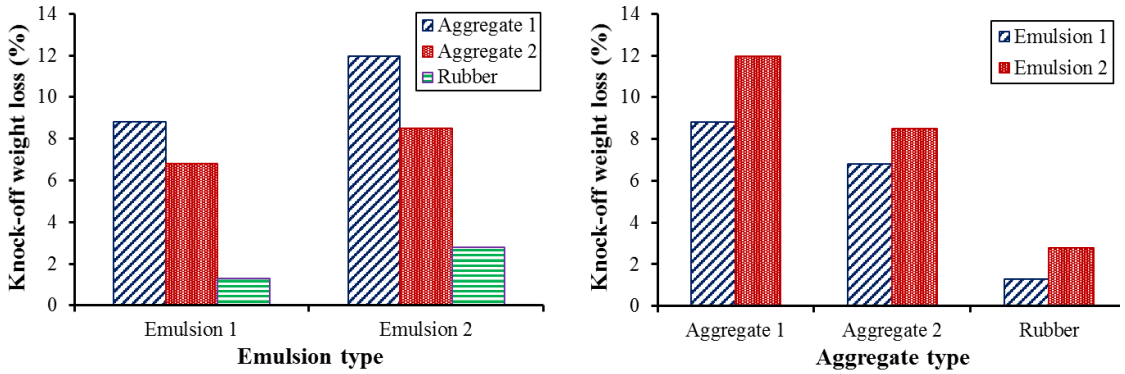

(a) (b)

Figure 19. (a) Knock-off weight loss for different chip seal types for the aggregates and (b) Knock-off weight loss for different chip seal types for emulsions 1 and 2.

REFERENCES

1. Shuler, S., DESIGN AND CONSTRUCTION OF CHIP SEALS FOR HIGH TRAFFIC. Flexible Pavement Rehabilitation and Maintenance, 1998. 1348: p. 96.

2. Brown, E.R., Preventative maintenance of asphalt concrete pavements. National Center for Asphalt Technology, Auburn, AL, 1988.

3. O'Brien, L.G., Evolution and benefits of preventive maintenance strategies. 1989.

4. Gransberg, D.D. and D.M. James, Chip seal best practices. Vol. 342. 2005: Transportation Research Board.

5. Karasahin, M., et al., Laboratory and In Situ Investigation of Chip Seal Surface Condition Improvement. Journal of Performance of Constructed Facilities, 2014. 29(2): p. 04014047.

6. Banerjee, A., A. de Fortier Smit, and J.A. Prozzi, Modeling the effect of environmental factors on evaporative water loss in asphalt emulsions for chip seal applications. Construction and Building Materials, 2012. 27(1): p. 158-164.

7. Gransberg, D., Correlating chip seal performance and construction methods. Transportation Research Record: Journal of the Transportation Research Board, 2006(1958): p. 54-58.

8. Howard, I.L. and G. Baumgardner, US Highway 84 Chip Seal Field Trials and Laboratory Test Results. 2009, Mississippi Department of Transportation.

9. Islam, S. and M. Hossain, Chip seal with lightweight aggregates for low-volume roads. Transportation Research Record: Journal of the Transportation Research Board, 2011(2205): p. 58-66.

10. Rahman, F., et al., Aggregate retention in chip seal. Transportation Research Record: Journal of the Transportation Research Board, 2012(2267): p. 56-64.

11. ASTM, ASTM D7000 Standard Test Method for Sweep Test of Bituminous Emulsion Surface Treatment Samples,. 2011: ASTM International, West Conshohocken, PA.

12. Caltrans, Method of Test for Vialit Test for Aggregate Retention in Chip Seals: “French Chip”. 2006, California Department of Transportation.

13. Kandhal, P.S. and J.B. Motter, Criteria for accepting precoated aggregates for seal coats and surface treatments. 1991.

14. Jordan III, W.S. and I.L. Howard, Applicability of Modified Vialit Adhesion Test for Seal Treatment Specifications. Journal of Civil Engineering and Architecture, 2011. 5(3).

15. Wood, T.J., D.W. Janisch, and F.S. Gaillard, Minnesota seal coat handbook 2006. 2006.

16. Flintsch, G., et al., Pavement surface macrotexture measurement and applications. Transportation Research Record: Journal of the Transportation Research Board, 2003(1860): p. 168-177.

17. Gheni, A.A., et al., Texture and design of green chip seal using recycled crumb rubber aggregate. Journal of Cleaner Production, 2017. 166: p. 1084-1101.

18. Ang, G. and V. Marchal, Mobilising private investment in sustainable transport: The case of land-based passenger transport infrastructure. OECD Environment Working Papers, 2013(56): p. 0_1.

19. RMA, R.M.A., 2015 U.S. Scrap Tire Management Summary, in Wasington, DC. 2016.

20. Rangaraju, P. and S. Gadkar, Durability evaluation of crumb rubber addition rate on Portland cement concrete. Department of Civil Engineering, Clemson University, Clemson, 2012: p. 1-126.

21. Shuler, S., Use of Waste Tires, Crumb Rubber, on Colorado Highways. 2011: Colorado Department of Transportation, DTD Applied Research and Innovation Branch.

22. Amirkhanian, S.N., Utilization of crumb rubber in asphaltic concrete mixtures–South Carolina's Experience. See ref, 2001. 3: p. 163-174.

23. Papagiannakis, A. and T. Lougheed, A REVIEW OF CRUMB-RUBBER MODIFIED ASPHALT CONCRETE TECHNOLOGY. RESEARCH REPORT. 1995.

24. Hanson, D., J. Epps, and R. Hicks, Construction Guidelines for Crumb Rubber Modified Hot Mix Asphalt. Federal Highway Administration Report DTFH61-94-C-00035, 1996.

25. Moustafa, A. and M.A. ElGawady, Mechanical properties of high strength concrete with scrap tire rubber. Construction and Building Materials, 2015. 93: p. 249-256.

26. Youssf, O., M.A. ElGawady, and J.E. Mills, Static cyclic behaviour of FRP-confined crumb rubber concrete columns. Engineering Structures, 2016. 113: p. 371-387.

27. Moustafa, A., A. Gheni, and M.A. ElGawady, Shaking-Table Testing of High Energy–Dissipating Rubberized Concrete Columns. Journal of Bridge Engineering, 2017. 22(8): p. 04017042.

28. Gheni, A., M.A. ElGawady, and J.J. Myers, Thermal Characterization of Cleaner and Eco-Efficient Masonry Units Using Sustainable Aggregates. Journal of Cleaner Production, 2017.

29. Gheni, A.A., M.A. ElGawady, and J.J. Myers, Mechanical Characterization of Concrete Masonry Units Manufactured with Crumb Rubber Aggregate. ACI Materials Journal, 2017. 114(01).

30. Moustafa, A. and M.A. ElGawady, Strain rate effect on properties of rubberized concrete confined with glass fiber–reinforced polymers. Journal of Composites for Construction, 2016. 20(5): p. 04016014.

31. Gheni, A., et al., Leaching Assessment of Eco-Friendly Rubberized Chip Seal Pavement. Transportation Research Record, 2018: p. 0361198118758688.

32. Lee, S.-J., C.K. Akisetty, and S.N. Amirkhanian, The effect of crumb rubber modifier (CRM) on the performance properties of rubberized binders in HMA pavements. Construction and Building Materials, 2008. 22(7): p. 1368-1376.

33. Presti, D.L., Recycled tyre rubber modified bitumens for road asphalt mixtures: a literature review. Construction and Building Materials, 2013. 49: p. 863-881.

34. Jensen, W. and M. Abdelrahman, Use of crumb rubber in performance graded binder. 2006.

35. Mohammad, L.N., S.B. Cooper Jr, and M.A. Elseifi, Characterization of HMA mixtures containing high reclaimed asphalt pavement content with crumb rubber additives. Journal of Materials in Civil Engineering, 2011. 23(11): p. 1560-1568.

36. Elseifi, M.A., L.N. Mohammad, and S.B. Cooper III, Laboratory evaluation of asphalt mixtures containing sustainable technologies. Journal of the Association of Asphalt Paving Technologists, 2011. 80.

37. LaForce, R.F., Squeegee Seal and Crumb Rubber Chip Seal Sapinero-East. Colorado Department of Transportation, CDH-DTP, 1983.

38. LaForce, R.F., Crumb rubber chip seal east of Punkin Center. 1986.

39. Way, J.R.S.G.B., Asphalt-Rubber Chip Seal and Polymer Modified Asphalt-Rubber Two Layer System, Case Studies, in Asphalt Rubber Conference 2012, Rubberized Asphalt Foundation: Munich.

40. Mertens, E. and J. Wright. Cationic asphalt emulsions: How they differ from conventional emulsions in theory and practice. in Highway Research Board Proceedings. 1959.

41. Shuler, S., Manual for emulsion-based chip seals for pavement preservation. Vol. 680. 2011: Transportation Research Board.

42. Transportation, M.D.o., Missouri Standard Specifications for Highway Construction in AGGREGATE FOR SEAL COATS. 2016, Missouri Highway and Transportaion Commission.

43. Testa, D.M. and M. Hossain, Kansas Department of Transportation 2014 Chip Seal Manual. 2014, Kansas Department of Transportation.

44. Caltrans, O.o.P.P., Maintenance Technical Advisory Guide (TAG), in Division of Maintenance. 2003, Caltrans.

45. USEPA, Scrap Tires: Handbook on Recycling Applications and Management for the U.S. and Mexico, O.o.R.C.a. Recovery, Editor. 2010, United States Environmental Protection Agency: Washington DC.

46. ASTM, A., D7000-08 Standard test method for sweep test of bituminous emulsion surface treatment samples. American Society for Testing and Materials, West Conshohocken, PA, 2011.

47. Praticò, F.G., R. Vaiana, and T. Iuele, Macrotexture modeling and experimental validation for pavement surface treatments. Construction and Building Materials, 2015. 95: p. 658-666.

48. EN, B., 12272-3. Surface dressing. Test methods-determination of binder aggregate adhesivity by the vialit plate shock test method, 2003.

49. Liu, L., et al., Evaluation of significant factors for aggregate retention in chip seals based on mesostructured finite element model. International Journal of Pavement Research and Technology, 2018.

IV. TEXTURE AND DESIGN OF GREEN CHIP SEAL PAVEMENT USING RECYCLED CRUMB RUBBER AGGREGATE

Ahmed Gheni ; Omar I. Abdelkarim , Ph.D.; Mohanad Abdulazeez ; Mohamed A. ElGawady , Ph.D.

ABSTRACT

The depletion of natural resources forces the construction industry to explore using cleaner recycled material as replacements of virgin construction materials. A new eco-friendly chip seal pavement, in which the mineral aggregate was replaced by crumb rubber obtained from scrap tires, was investigated in this study. A total of 142 chip seal specimens were prepared and tested to investigate the impact of using recycled rubber aggregate on the chip seal's micro and macro texture and their impacts on the skid resistance. The microtexture of the new proposed recycled aggregate was examined using a high-resolution 3D digital microscope. The macrotexture of the new chip seal pavement was examined using image processing and sand patch methods. The skid resistance of the new chip seal under both ambient and elevated temperatures was then explored. Two types of emulsions, two types of asphalt cement binders, two types of mineral aggregate as well as two types of recycled crumb rubber were involved in the examined test matrix. This study concluded that the crumb rubber can be used in the chip seal as partial or full replacement of mineral aggregates. Using crumb rubber has a significant impact on improving both macrotexture and microtexture of chip seal. In addition, the low thermal conductivity of crumb rubber helped the chip seal resist elevated temperature without significant loss in skid resistance.

A 3D geometrical model was then proposed to simulate the aggregate embedment, so it can be used to design the required binder application rate that provides adequate embedment depth and skid resistance.

Keywords: Chip Seal, Road Sealing, Crumb Rubber, Skid Resistance, Eco-Friendly, Macrotexture, Microtexture, Rubberized Chip Seal, Green Construction

1. INTRODUCTION

Chip seal is a type of pavement coating treatment that is carried out by spraying binder on subbase, followed by a layer of coarse aggregate that is compacted into the sprayed binder. Chip seal is used as a maintenance treatment to protect asphalt layers from severe weather by sealing the fine crack which blocks water permeation to the subbase (Brown 1988, O'Brien 1989). Chip seal layer is, also, used to improve the macrotexture of existing pavement, which provides a good skid-resistant and high friction surface leading to increased driving safety (Gransberg and James 2005). In addition, the affordable cost of chip seal makes it a competitive alternative maintenance technique to extend pavement's life cycle (Gransberg and James 2005, Karasahin et al. 2014). Furthermore, chip seal is used as the main pavement in roads with low traffic volumes ranging from 500-2400 vehicles per day. The predominant chip seal practice in the United States is carried out using an emulsion binder; however, few states use both emulsion and asphalt cement binders (Gransberg and James 2005).

Chip seal's aggregates are typically uniformly-graded to provide high surface friction and better waterproofing (Wood et al. 2006). Well-graded aggregates perform poorly because of the difference in the embedment depth of each aggregate size; small aggregates will have too much embedment depth leading to less friction values while large

aggregates will have small embedment depth leading to potential aggregate dislodging (McHattie 2001, Islam and Hossain 2011).

Depletion of natural aggregates forces the construction industry to explore using recycled material as an aggregate. Crumb rubber aggregate obtained from scrap tires was successfully used in concrete and masonry construction (Papagiannakis and Lougheed 1995, Hanson et al. 1996, Amirkhanian 2001, Shuler 2011, Rangaraju and Gadkar 2012, Youssf et al. 2014, Moustafa and ElGawady 2015, Youssf et al. 2015, Youssf et al. 2016, Gheni et al. 2017, Moustafa et al. 2017). However, crumb rubber aggregate has not been used in chip seal pavement. Scrap tires are widely available resource in the United States with four million tons of scrap tires were dumped in landfills during 2015 alone (RMA 2018). Using crumb rubber aggregate will reduce the CO2 emission linked to the construction industry. Currently, transportation infrastructure contributes to global greenhouse gas emissions with 23% of global carbon dioxide (CO2) emissions, which makes it the second largest contributor, only behind electricity generation (Ang and Marchal 2013).

Scrap tires has a successful track record as an additive in the construction of hot mix asphalt roadway. Crumb rubber was used as an asphalt binder additive to produce polymer modified asphalt binder. Generally, adding crumb rubber to asphalt binder enhances the temperature susceptibility, viscosity, and stiffness of asphalt binder (Lee et al. 2008, Presti 2013). Modifying asphalt binder with crumb rubber increased the asphalt film thickness, binder resiliency, viscosity, and shear strength (Page 1992).

After five to seven years of service life rubber, a modified asphalt binder performed better than conventional asphalt binder in term of rut depth, fatigue cracks, and international roughness index (IRI) numbers (Huang et al. 2002).

Rubber modified binder was also used in chip seal pavement and showed a better ability, than conventional binders, to prevent the reflection cracking and keep the badly cracked roads from falling apart (LaForce 1983, LaForce 1986). Furthermore, rubber modified asphalt binders displayed a smoother riding while maintaining the required surface skid resistance under varied weather conditions (Way 2012).

Using crumb rubber as an additive for asphalt binder consumes small amount of available scrap tires. Replacing 15% of asphalt binder with crumb rubber consumes 0.45 lb. of crumb rubber per yd^2 corresponding to 317 tires per mile assuming two-lane road and binder application rate of 0.35 gal/yd^2. This paper proposes using crumb rubber as an aggregate, not a binder additive. Full replacement of mineral aggregate in chip seal with crumb rubber consumes about 5.75 lb. of crumb rubber per yd^2 corresponding to 4000 tires per mile assuming two-lane road. Furthermore, using mineral aggregate in chip seal faces several challenges. Mineral aggregates may dislodge and fly causing a serious safety issue for pedestrian, motorcyclist, bicyclist, and windshield of passerby vehicles. Chip seal features also noisy driving. Moreover, it is a common practice in the United States to apply a fog seal layer on top of chip seal to hide its rocky color and display a dark color for better perception by the local community at the chip seal site. The applied fog seal increases the cost and reduces the pavement friction. Using crumb rubber aggregate may address these challenges. Preliminary studies showed that crumb rubber aggregates have a better retention with both asphalt cement binder and asphalt emulsion (Gheni et al. 2017). The

enhancement in the aggregate retention has a protentional capacity to reduce the snow plow damage which is one of the challenges for chip seal pavement (Beck 2006). However, there remain questions about the effect of using crumb aggregate on skid and friction resistance of chip seal.

This paper presents an investigation of the texture and friction resistance of a new green system of rubberized chip seal having different rubber aggregate contents. The paper starts with a detailed discussion of the micro and macro texture of chip seal. This is followed by investigating the microtexture of the new chip seal using a high-resolution 3D digital microscope to study the surface texture at a fine-scale. The macrotexture, which is the coarse-scale texture of chip seal pavement, was also studied using image processing and sand patch procedures. The impact of the two levels of textures on the skid resistance of chip seal was then concluded at both ambient and elevated temperatures. In addition, the paper presents an extensive study on the design of chip seal and finding the optimum embedment depth.

2. FRICTION RESISTANCE OF CHIP SEAL

The surface texture of chip seal is an important feature linked to traffic safety, ride quality, and noise control (Yandell 1971, Forster 1981, Yandell and Sawyer 1994, Do et al. 2000). The surface texture can be categorized into unevenness, megatexture, macrotexture, and microtexture for surface indentations wavelengths of 500-50000 mm, 50-500 mm, 0.5-50 mm, and 0.001-0.5 mm respectively(Figure1). The friction and skid resistance of pavement are strongly connected with both the macrotexture and microtexture of the pavement surface (Yandell 1971, Forster 1981, Yandell and Sawyer 1994, Do et al. 2000). Megatexture and unevenness, however, do not significantly affect the skid

resistance. Microtexture is fine-scale texture created by the roughness of small prominences of grains on the stone particles' surface. Microtexture is affected by the type, component, and the manufacturing process of an aggregate. As shown in Figure1, microtexture has a direct impact on adhesion component of the friction because it influences the tire chip seal contact area. Microtexture has a major impact on skid resistance for vehicles with having speed up to 40 km/h.

Macrotexture, a coarse-scale texture, is caused by the organization of the aggregate particles on the chip seal surface and can be defined by the roughness of the road surface instead of the aggregate particle itself. Macrotexture is affected by aggregate gradation, size, and shape among other parameters. Macrotexture affects the hysteretic component of the skid resistance of vehicles which is related to the stored and dissipated energy due to the compression and decompression in vehicles' tires. As macrotexture affects the drainage of chip seal surface, it indirectly affects the adhesion components by improving the contact between the tires and chip seal particles (Henry 2000, Flintsch et al. 2003, Choubane et al. 2004). Macrotexture controls the skid resistance for vehicles with speed exceeding 40 km/h (Kotek and Kováč 2015). Macrotexture is quantified by measuring the mean texture depth (MTD) using volumetric methods such as sand patch method (ASTM E965), the Outflow Meter Test (OFT), or advanced laser technology methods such as the mini texture meter, the Selcom laser system, and circular texture meter (CT Meter).

3. EXPERIMENTAL PROGRAM

3.1. MATERIAL PROPERTIES

Two types of asphalt cement, PG 64-28 and PG 70-28, and two types of emulsions, CRS-2P and CHFRS-2P, were used during this study. Hereinafter, these two asphalt cement and two emulsions will be referred to as asphalt cement 1, asphalt cement 2, emulsion 1, and emulsion 2, respectively. Tables 1 and 2 summarize the properties of these emulsions and asphalt cement. Both emulsion 1 and emulsion 2 are Cationic, which is defined as the migration of asphalt particles under an electric field towards the cathode (negative electrode). Emulsion 1 is a rapid-setting and high-viscous type, while emulsion 2 is a high-float, rapid-setting, high-viscous type. The main difference between the two asphalt cement types is the softening temperature. The main difference between asphalt cement and emulsion is the water content and other admixtures such as emulsifiers that keep the emulsions flowable and workable at a low temperature of 35 °C compared to 165 °C for asphalt cement.

The water breakout of the emulsions was examined for weight loss during exposure time at a temperature of 35 °C (Figure 2). As shown in the figure, approximately 81% of the water breakout occurred after 6 hours for both types of emulsions, while there was almost no evaporation after 24 hours of exposure.

Crumb rubber aggregate and other two types of mineral aggregates, namely creek gravel, and trap rock were used during this study (Figure3). Hereinafter these aggregates will be referred to as crumb rubber aggregate, aggregate 1, and aggregate 2, respectively.

Crumb rubber can be produced at ambient temperature by tearing and shredding the scrap tires in the cutting mills. Another approach to produce crumb rubber is to freeze

the scrap tires to -80 ºC using liquid nitrogen, followed by grounding the glass-like frozen tires to the required sizes using a hammer mill. Therefore, the energy cost of processing and producing the ambient crumb rubber is much lower than that of the cryogenic crumb rubber. During this research, both types were investigated.

Two grades for each aggregate type were used during this study with a contribution of 50% of each grade. The first grade was aggregate passing the 9.5 mm (0.37 in.) sieve and retained on the 6.3 mm (0.25 in.) sieve. The second grade was aggregate passing the 6.3 mm (0.25 in.) sieve and retained on the 4.75 mm (0.19 in.) sieve. Figure 4 presents the sieve analysis for the used aggregates. All the used aggregates had approximately the same median size of approximately 6.3 mm with maximum aggregate size of 9.5 mm (3/8”). The dust, materials passing No. 200 sieve, in the three aggregate types ranged from 0.20% to 0.52% with the crumb rubber having the lowest percentage of dust followed by aggregate 1, aggregate 2, respectively (Table 3).

Table 3 presents the properties of the three types of aggregates. The crumb rubber had a low bulk specific gravity of 0.87, which is 37% and 33% of that of aggregates 1 and 2, respectively. Furthermore, the crumb rubber had a dry unit weight of 423 kg/m^3 that is approximately 36% and 34% of that of aggregates 1 and 2, respectively. Aggregate 1 had a water-absorption of 4.7% which is 488% higher than that of aggregate 2. The water absorption of the crumb rubber was negligible. The crumb rubber and aggregate 2 had higher fractured faces than aggregate 1 because they went through cutting process during the production while aggregate 1 had the smoothest face due to the continuous flow of water during its formation in the creek.

In term of durability, the crumb rubber has almost zero loss in mass due to abrasion and impact during Los Angeles test compared to 18.7% and 8.2% for aggregate 1 and 2 respectively. The same trend was noticed with the Micro-Deval test with mass losses of 6% and 2.1% for aggregate 1 and 2 respectively. In addition, since the source of the crumb rubber is the tire industry only, it should have passed all of the durability and appropriate mechanical tests before it was used in tires' manufacturing and those tests are including abrasion test, static and dynamic tensile strength, tear strength, elongation at break, low and high temperatures, resistance to liquids, accelerated static ozone exposure and staining of light colored surface (Lewis 1980). The high durability and non-biodegradability of the scrap tires are already one of the main problems that facing the U.S. Environmental Protection Agency (EPA) while they are dealing with the solid waste management (USEPA 2010). Table 4 shows the physical properties of crumb rubber.

The flakiness index, defined as the percentage by weight of the used aggregates whose least dimension is less than three-fifths of its mean dimension, is another key factor in the design of chip seal. The lower the flakiness index is, the better the aggregate. The flakiness indices of the aggregates ranged from 31.3% to 42% with aggregate 2 having the highest index followed by aggregate 1 and crumb rubber, respectively.

3.2. DESIGN AND PREPARATION OF CHIP SEAL SPECIMENS

There is no consensus in the United States on how to design chip seal. A recent survey including 54 states and cities in the United States showed that only 18% of respondents use McLeod et al. (1969), Kearby (1953), and modified Kearby (Stockton and Epps 1975) methods to design chip seal while 26% of the respondents do not use a formal design method. The remaining 56% of the respondents use their local, empirical, or past

experience design approach (Gransberg and James 2005). The goal of all these design approaches is to determine the aggregate application rate to form a blanket of one stone in depth and determine the corresponding asphalt binder application rate to satisfy a given aggregate embedment depth ranging from 50% to 80% of the median aggregate size.

The test specimens during the course of this study were first designed using different approaches. McLeod method resulted in aggregate application rates of 7.4 kg/m^2 (13.7 lb/yd^2), 7.8 kg/m^2 (14.4 lb/yd^2), 3.0 kg/m^2 (5.5 lb/yd^2) for aggregate 1, aggregate 2, and crumb rubber, respectively. Kearby and modified Kearby methods resulted in aggregate application rates of 7.05 kg/m^2 (13 lb/yd^2), 7.65 kg/m^2 (14.1 lb/yd^2), 2.71 kg/m^2 (5.0 lb/yd^2) for aggregate 1, aggregate 2, and crumb rubber, respectively. Furthermore, the ASTM D7000-11 (ASTM 2011) provides Equation 1 for determining the aggregate application rate for sweep test.

$$Aggregate\ weight\ \left(\frac{kg}{m^2}\right) = \left(\frac{A\ (202.1\ X - 15.8)}{100} + \frac{B\ (146.4\ X - 4.7)}{100}\right) * \frac{1}{61.6} \quad (1)$$

where A is the percentage of the aggregate with grade 1 from 9.5 to 6.3 mm, B is the percentage of the aggregate grade 2 from 6.3 to 4.75 mm, and X is bulk specific gravity. Equation 1 resulted in application rates of 7.4 kg/m^2 (13.6 lb/yd^2), 8.2 kg/m^2 (15.1 lb/yd^2), 2.7 kg/m^2 (5.0 lb/yd^2) for aggregate 1, aggregate 2, and crumb rubber, respectively. Since the results of Equation 1 were more conservative than the other two approaches, except for the rubber case compared to the McLeod method, it was decided to use the aggregate application rate resulting from Equation 1 throughout this research.

Determining the binder application rate is more challenging, as there are more discrepancies between the different approaches. The main reason for this discrepancy is the time considered to achieve the design aggregate embedment depth. For example,

McLeod assumed that the design aggregate embedment depth would be satisfied after two years of service. This will generally result in a smaller binder application rate compared to the Kearby and modified Kearby approaches. McLeod, Kearby, and modified Kearby design approaches resulted in emulsion application rates of 1.0 liter/m^2 (0.22 gal/yd^2), 2.22 liter/m^2 (0.49 gal/yd^2), and 2.22 liter/m^2 (0.49 gal/yd^2), respectively.

To validate the application rate results, a trial and error approach was adopted during the experimental work. A rectangular mold having a height equal to the aggregate average least dimension (ADL) was prepared and chip seal samples were prepared using this mold. The required binder application rate that exactly fills the mold after spreading and compacting the aggregate was recorded. After several trials, a binder application rate of 2.13 liter/m^2 (0.47 gal/yd^2) was found to fill the mold with emulsion after placing and compacting the aggregate. Assuming the emulsion had 30 to 35% water content the selected emulsion application rate will result in 70% to 65% aggregate embedment ratio after emulsion's water broke out (McLeod et al. 1969, Wood et al. 2006). The experimentally calculated emulsion rate was in a good agreement with that calculated using the Kearby's approach and hence, the empirical value of the emulsion application rate was used throughout this experimental work. For specimens where asphalt cement binders were used, the binder application rate was adjusted to address the water content of the emulsion, which equals to 30%, and then was used.

Once the binder and aggregate application rates were determined, the required specimens were prepared using aggregate having median sizes of 6.2 mm (0.244 in), 6.1 mm (0.24 in), 6.5 mm (0.256 in) for aggregate 1, aggregate 2, and crumb rubber, respectively.

3.3. MEASURING THE MICROTEXTURE OF CHIP SEAL

Measurement of the surface's microtexture deals with very small dimensions and demands a high-resolution reading resulting in either high cost to do or inaccurate measurements (Masad 2007). This study used a 3D digital microscope KH-8700 to study the aggregates' microtexture. The technique can provide quantitative data for aggregates' microtexture such as aggregates' profile lines and surface area measurements. Such measurements can be linked to the adhesion, friction, and skid resistance. During this task, the surfaces' microtexture of ambient and cryogenic crumb rubber as well as mineral aggregates, were investigated using KH-8700 3D digital microscope.

3.4. MEASURING THE MACROTEXTURE OF CHIP SEAL

During the course of this study, two different methods were used to measure the MTD. The first method is a new approach where an image processing and analysis software, ImageJ™, was used to process sections of chip seals with different types of aggregate and different binder application rate. A second approach is to use the sand patch test which is simple, economical, and reliable (Abe et al. 2001, Flintsch et al. 2003, Hanson and Prowell 2004).

3.4.1. Image Processing Analysis Method. Specimens of chip seal with two types of aggregate, creek gravel and crumb rubber were prepared using different binder application rates. However, to have a better image processing, a transparent epoxy having a specific weight of 1.106 gm/cm^3 (69 lb/ft^3) was used to prepare these specimens instead of the emulsions (Figure 5). The specimens were then sectioned using a high-pressure highly precise waterjet cutting machine (Figure 6). The sections were scanned using high-resolution scanner and then examined using the ImageJ™ image processing program to

determine the MTD and aggregate embedment depth per binder application rate. To determine the aggregate embedment depth, the area of the binder that enclosed by the upper level of the binder and the base of the specimen was measured using the ImageJ™ (Figure 7a). The calculated area was then divided by the length of the specimen to find the average depth of the binder and then the embedment depth. Once the aggregate embedment depth was determined, the MTD was calculated by subtracting the aggregate embedment depth from the total chip seal depth.

3.4.2. Sand Patch Method. The sand patch specimens were prepared by applying asphalt emulsion of 150 gm (0.331lb) corresponding to binder application rate of 2.13 liter/m^2 (0.47 gal/yd2) on asphalt felt disk with a diameter of 300 mm (11.8 in.). Then, the designed aggregate quantities being 516 gm (1.14 lb), 530 gm (1.17 lb), and 191 gm (0.42 lb) corresponding to aggregate application rates of 7.4 kg/m^2 (13.6 lb/yd^2), 8.2 kg/m^2 (15.1 lb/yd^2), 2.7 kg/m^2 (5.0 lb/yd^2) for aggregate 1, aggregate 2, and crumb rubber, respectively, were uniformly distributed on the surface of each test specimen. The aggregates were embedded into the emulsion using a standard compactor with a weight of 7500 gm (16.5 lb) and a minimum curved surface radius of 550 ± 30 mm (21.65 ± 1.18 inches). After compacting the aggregates, the asphalt felt was rotated 90° so that the loose aggregates fell down. The specimens were then cured at 35 °C (95 °F) for 5 days followed by ambient curing for 2 days to break out all the water in the emulsion.

The standard sand patch method was used to determine the MTD of 14 specimens manufactured using the three types of aggregate and the two types of emulsions. Each emulsion was covered with either a single aggregate type or a combination of different aggregate types per Table 5. The two cement asphalt binders were not examined during

these tests because of the difficulty of dealing with them at the ambient temperature as they harden very quickly.

The procedure to carry out the sand patch test was as follows. Four hundred ml (24.41 in^3) of fine sand, passing a No. 60 sieve and retained on a No. 80 sieve, was spread uniformly on the surface of each of the investigated specimens using an ice hockey puck with its bottom surface covered with a stiff rubber material. The diameter of the spread sand on each investigated specimen was measured at least four times in different orientations (Figure 8d).

The average diameter, D, was determined and implemented in Equation 2 to determine the MTD which is an indication of the aggregate embedment depth.

$$MTD = \frac{4\,V}{\pi\,D^2} \tag{2}$$

where V is the sand volume which equals 400 ml (24.41 in^3).

3.5. SKID FRICTION RESISTANCE TESTS

In this study, the British Pendulum tester (BPT) was used to measure the friction values of different chip seal surfaces per ASTM E-303. For each specimen preparation, the required emulsion at 60 °C (140 °F) or asphalt cement at 160 °C (320 °F) was applied to an 88.9 mm (3.5 in.) x 152.4 mm (6.0 in.) aluminum plate per ASTM E303 (Figure 9a). Then, the appropriate aggregate quantity being 100 gm (0.22 lb), 110 gm (0.24 lb), and 37 gm (0.08 lb), representing aggregate spread rates of 7.4 kg/m^2 (13.6 lb/yd^2), 8.2 kg/m^2 (15.1 lb/yd^2), 2.7 kg/m^2 (5.0 lb/yd^2) for aggregate 1, aggregate 2, and crumb rubber respectively was uniformly spread on the asphalt cement or emulsion (Figure 9b). The aggregate was then compacted for three passes using rubber roller compactor (Figure 9c) with a weight

of 2 kg (4.4 lb), diameter of 127 mm (5 in.), and length of 152 mm (6 in.). The rubber used in the compactor had hardness type 75A. The specimens were cured at 35 °C (95 °F) for 5 days followed by ambient curing for 2 days to break out all water. Figure 10 shows different specimens ready for testing. Twenty-eight specimens with different aggregates and asphalt combinations (Table 6) were tested.

Each specimen was screwed into a plywood table and the pendulum was positioned to barely contact the specimen surface (Figure 11). The pendulum was vertically adjusted in order to achieve a slider contact path on the chip seal surface of 125 ± 1.6 mm (5 ± 1/16 in.). The distance between the center of gravity of the pendulum and the center of oscillation was 411 ± 5 mm (16.2 ± 0.2 in.). Water was sprinkled on the specimen surface before running the test per the ASTM E-303. After releasing the pendulum, the British Pendulum number (BPN) was recorded and used to represent the friction resistance of the surface. The test was repeated four times after one trial test to get the average BPN for each specimen.

In addition to the standard procedure, two independent modifications were carried out on the standard test. A set of tests was conducted on specimens with dry surfaces to investigate the effects of moisture content on the performance of chip seal. Another set of specimens was carried out where the temperature of the aluminum plate of each specimen was increased to 65 °C (149 °F) (Figure11c) which represents the worst-case scenario for asphalt pavements in the United States (Mohseni 1998). A controlled heat coil was connected to each aluminum plate underneath the chip seal specimens to increase the temperature of the plate and hence the chip seal specimens as shown in Fig 11b.

Then, the BPT was used to run the skid friction resistance test. Thirty-two specimens were tested during the modified tests (Tables 7 and 8).

4. RESULTS AND DISCUSSION

4.1. THE MICROTEXTURE OF CHIP SEAL

Figure 12 illustrates the surface images and elevation profiles in the range of 250 μm of the aggregates. The ambient processed crumb rubber had a rough surface with numerous troughs and crests that would improve its retention with the binders as shown in Figure 12a, while the cryogenically processed crumb rubber had a smooth surface as shown in Figure 12b. For example, the surface area of a projection of 1x1 in. length of the aggregates shown in Figure 12 were 1.028, 1.222, 1.032 and 1.042 $in.^2/in.^2$ for the cryogenically processed rubber, ambient processed rubber, aggregate 1, and aggregate 2 respectively. The surfaces were rougher in the case of ambient crumb rubber due to the cutting process. Therefore, the ambient crumb rubber had a surface area 19%, 18%, and 17% higher than that of cryogenic, aggregate 1, and aggregate 2 respectively. The surface of aggregate 1 was slightly smoother than aggregate 2 because it was subjected to continuous water flow and rolling of the aggregate particles during its formation in creeks. This test was carried out early during this project and hence the ambient processed crumb rubber was used during this study and the cryogenically processed crumb rubber was discarded. The larger surface area of ambient processed crumb rubber will provide about 20% extra contact area with tires which increase the adhesion component by about 20% as well.

4.2. THE MACROTEXTURE OF CHIP SEAL

4.2.1. Image Processing Method. Seventy-two specimens with nine different epoxy binder application rates were examined for both creek gravel and crumb rubber (Figure 13). The binder application rate versus MTD curve was then calculated (Figure 14). For the same binder application rate, the crumb rubber specimens had 1.2 to 1.0 mm larger MTD than that of the creek gravel specimens which is equivalent to an increase from 16% to 100% based on the binder application rate. This increase is equal to 16% to 19% of the median aggregate size. Considering that the crumb rubber had 0.3 mm larger median aggregate size than that of the creek gravel, the increase in the MTD values of the crumb rubber specimens was not only due to this small difference in particle size but mainly due to the rough surface of crumb rubber particle as shown by the microtexture measurements.

4.2.2. Sand Patch Method. Chip seal specimens with different aggregates and emulsions were prepared and tested (Table 5 and Figure 15). Figure 16 shows the MTD vs. the percentage of rubber for emulsion 1 and 2 for both types of aggregate. As the rubber percentage increased, the MTD value increased. An increase of 25% in MTD was observed when 100% of the trap rock was replaced with crumb rubber. Similarly, an increase of 33% was measured in the MTD when 100% of the creek gravel was replaced with crumb rubber. The difference in the increase percentage between the creek gravel and trap rock was due to the smoother surface of the creek gravel. As the test was conducted after the samples were cured causing complete water break, there was not a significant difference in the values of MTD when using emulsion 2 or emulsion 1.

A strong correlation between the image processing method and the sand patch method was noticed. The MTD was 5.2 mm and 5.0 mm for the sand patch and image

processing method respectively with 100% rubberized chip seal. In the case of 100% creek gravel chip seal, MTD values of 4.00 mm and 4.15 mm were calculated for the sand patch and image processing method respectively.

4.3. SKID FRICTION RESISTANCE

Figure 17 shows the measured BPN vs rubber content for the different binders and aggregates. While the sand patch and image processing indicated that the micro and macro texture of the crumb rubber were better than those of the mineral aggregates, the skid friction tests showed that the BPNs decreased with increasing the rubber replacement ratio regardless of the binder or mineral aggregate types (Figure 17). A decrease in the BPNs ranging from 7% to 20% and 0% to 13% were measured for specimens with aggregate 1 having rubber content ratios ranging from 25% to 100% with emulsion-based and asphalt cement-based chip seals, respectively. Similarly, a decrease in the BPNs ranging from 4% to 20% and 8% to 23% were measured for specimens with aggregate 1 having rubber content ratios ranging from 25% to 100% with emulsion-based and asphalt cement-based chip seals, respectively.

The contradiction between the skid resistance test and the texture characterization results are attributed to three main reasons. First, the adhesion component which is part of the skid friction resistance cannot be fully captured by the British Pendulum tester (BPT) as the contact area between the BPT slider and specimen is infinitesimal. Mataei et al. (2016) reported that BPT displayed unreliable behavior when used on coarse-textured pavement, which is the case for chip seal, due to the infinitesimal contact area. Second, the BPT measures the friction at low speed where microstructure of the pavement is controlling the behavior. Third, the hysteresis part of the friction is related to the energy loss that occurs

as rubber layers in tires are alternately compressed and decompressed; since crumb rubber aggregate is less rigid than mineral aggregate, the hysteretic component should be less in the case of rubberized chip seal. The hysteresis effect can't be captured during the surface characterization process.

For the skid resistance tests at an elevated temperature of 65 °C, Figure 18 shows that all specimens made with 100% crumb rubber did not display any loss in BPN compared to those measured at ambient temperature (~20 °C). Conventional chip seal with 100% mineral aggregates showed an average loss of 10% in BPNs for samples made with emulsion and 2% in BPNs for samples made with asphalt cement indicating degradation in the friction skid resistance. This occurred because the crumb rubber has low thermal conductivity. At the ambient temperature, the average thermal conductivity of mineral aggregate is between 1.83 and 2.90 (w/m.k) while the average thermal conductivity of rubber is 0.12 (w/m.k). The very low thermal conductivity of rubber compared to that of mineral aggregates significantly reduced the heat propagation into the binder; hot binders display stiffness degradation compared to binders at ambient temperature. However, such reduction was not severe for the asphalt cement as the 65 °C was not enough to trigger severe stiffness reduction.

4.4. BINDER APPLICATION RATE

To examine the ability of the existing design approaches to determine the correct binder application rate for a given aggregate embedment depth, chip seal specimens with ten different binder application rates varying from 0 to 0.96 gal/yd^2 were prepared for aggregate 1 and the crumb rubber aggregate. The embedment depth of each specimen was determined using the image processing procedure explained earlier in this report. Figure

19 shows the binder application rate versus the aggregate embedment depth as a percentage of aggregate least dimensions.

As shown in Figure 19, using McLeod application rate resulted in embedment ratio of 32% and 28.5% of the least aggregate dimension for aggregate 1 and crumb rubber aggregate, respectively. McLeod design approach assumes that the embedment ratio would reach 70% after two years in service. However, it is not anticipated that particles rearrangement and consolidation that take place, during the service life of a chip seal, due to traffic loads will double the aggregate embedment depth ratio. Furthermore, for low-volume traffic roads, the compaction due to passing traffic would be quite low for such dramatic increase in embedment. For high-volume roads with high speeds, the initial higher embedment ratio would be required to avoid dislodge of aggregates at high speeds.

The Kearby method produced chip seal with embedment ratios of 67% and 55% for aggregate 1 and crumb rubber, respectively. However, the Kearby design approach was developed based on 50% embedment. The modified Kearby method produced chip seal with embedment ratios of 72% and 66% for aggregate 1 and crumb rubber, respectively, while it was developed assuming 40% embedment depth. Hence, neither of the existing methods could provide the required application rate for the design embedment ratio. Hence, there is a need for a simple method to determine the required application rate for a given embedment ratio.

This study proposed a simple method to determine the binder application rate for a given embedment ratio of the median aggregate size. In this approach, aggregate was simulated considering three different regular geometrical shapes: a sphere having a diameter equal to the median aggregate size (Figure 20), a square pyramid with a base leg

and height equal to the median aggregate size (Figure 21), and an inverted square pyramid with the same dimensions for the regular pyramids (Figure 22).

Using each of these shapes, the volume of voids and hence the required binder application rate for a given embedment ratio was mathematically determined and plotted in Figure 23. Furthermore, the results obtained from the experimental work corresponding to embedment ratios of 50%, 66%, and 80% for aggregate 1 and crumb rubber aggregate were plotted on the same figures. As shown in the figure, the assumption for the regular pyramid was able to predict the required application rate for the considered embedment ratios with an error ranging from 2% to 19% for aggregate 1 and 0% to 30% for crumb rubber. For 66% embedment ratio, the model was able to predict the application rate with an accuracy of 93.52% and 98.04% for crumb rubber and creek gravel respectively as shown in Figure 23 and Table. 9. For the other models the errors in predicting the application rates ranged from 2% to 22% and 18 to 32% for the case of aggregate 1 and crumb rubber assuming sphere aggregates while it ranged from 31% to 63% and 21% to 57% for the case of aggregate 1 and crumb rubber assuming inverted pyramid aggregates.

5. FINDINGS AND RECOMMENDATIONS

In this study, a new eco-friendly chip seal was developed using crumb rubber as a partial or complete replacement for mineral aggregates. The crumb rubber was obtained from scrap tires. A total of 142 chip seal specimens were prepared and tested to investigate five different aspects: the microtexture, macrotexture, skid resistance, skid resistance under high temperature, and the required binder application rate for a given aggregate embedment depth. The performance of chip seal specimens manufactured using the crumb rubber was compared with that of specimens manufactured using two different mineral aggregate

namely, creek gravel and trap rock. Two types of emulsions and two types of binders were also used to manufacture the test specimens. A 3D geometrical model was proposed to simulate the shape of the aggregate which can be used to predict the required binder application rate for a given embedment ratio.

This study revealed that the crumb rubber from recycled tires could be used in the chip seal as aggregates. The crumb rubber improved both the macrotexture and microtexture of chip seal. In addition, the crumb rubber helped the chip seal to resist high temperature without significant loss in friction resistance. In particular, the following conclusions, findings, and recommendations can be drawn from the current study:

1- Ambient processed crumb rubber displayed 20% higher surface area compared to that of cryogenically processed crumb rubber. This resulted in significant improvement in the microtexture of crumb rubber aggregates with higher contact area with tires which increases the adhesion component in skid resistance by 20%. Hence, it is recommended to use ambient processed rubber as aggregate.

2- Sand patch and section image processing showed that replacing mineral aggregates with crumb rubber improves the macrotexture of chip seal. An Increase of 25% and 33% in mean texture depth (MTD) was observed when 100% of the trap rock and creek gravel was replaced with crumb rubber, respectively.

3- While both micro and macrotexture showed significant improvements when crumb rubber was used as aggregate, a reduction ranging from 1.5% to 20% in the British Pendulum number (BPN) for specimens with rubber replacement ratios ranging from 25% to 100% was recorded. It should be noted that the BPN is not reliable for a rough surface such as chip seal. Hence, more advanced techniques are required to

measure the skid resistance of crumb rubber-based chip seal. Furthermore, under high temperatures, crumb rubber-based chip seal outperformed mineral aggregate-based chip seal. Specimens with 100% rubber did not show any loss in BPN under elevated temperature of 65 °C while 10% loss was recorded in mineral aggregate-based chip seal.

4- A virtual 3D pyramid shape can be used to simulate aggregate particles to find the required binder application rate that produces chip seal with an embedment depth ranging from 50% to 80% of the average aggregate least dimension.

While this study showed the feasibility of using crumb rubber in chip seal, further studies are still required to fine-tune this application niche. Further studies to measure the different components of the surface friction resistance instead of the gross skid resistance (e.g. hysteresis forces and adhesion) as some of the standard tests such as British Pendulum tester does not simulate the real case scenario when tires have been in contact with chip seal surface. Also, it is recommended to measure the frictional property of chip seal at a varied speed. Finally, examining the applicability of the proposed pyramid shape model for different aggregate sizes and types is necessary.

ACKNOWLEDGEMENTS

This research was conducted at the Missouri University of Science and Technology and supported by the Missouri Department of Natural Resources, and Pettis County. Donations of the asphalt cement and emulsions by Vance Brothers are appreciated. However, any opinions, findings, conclusions, and recommendations presented in this paper are those of the authors and do not necessarily reflect the views of the sponsors. The authors would like to thank the many undergraduate and graduate students that contributed

to this project including Nicholas B. Colbert, Andrew Chapko, Ashley Crannick, Yasser Darwish, Eslam Gomaa, Monika Nain, and Janine Williams of Missouri S&T as well as Mr. Florian Lang of Karlsruhe Institute of Technology, Germany.

Table 1. Emulsions properties.

Properties	**Test Method**	CRS-2P		CHFRS-2P	
		Min	**Max**	**Min**	**Max**
Viscosity, SFS @ 122 °F	ASTM D-7496	100	300	100	400
Sieve Test, %	ASTM D-6933		0.3		0.1
Demulsibility, % 35 mls 0.8% sodium dioctyl sulfosuccinate	ASTM D-6936	40		60	
Storage Stability, 1 day, %	ASTM D-6930		1		1
Particle Charge	ASTM D-7402	Positive		Positive	
Distillation Test:					
Residue by distillation, % by weight	ASTM D-244	65		65	
Oil Distillate, % by volume of emulsion	ASTM D-6997		3		0.5
Tests on Residue from Distillation:					
Polymer content, wt. % (solids basis)		3		3	
Penetration, 77 °F, 100g., 5 secs.	ASTM D-5	100	150	80	130
Viscosity, 140 °F, poise	ASTM D-2171	NA	NA	1300	
Solubility in TCE, %	ASTM D-2042	NA	NA	95	
Elastic Recovery, 50 °F., %	ASTM D-6084	60		65	
Softening Point, °C,	ASTM D-36			54	
Float Test, 60 °C, secs.	ASTM D-139			1800	
Ductility, 39.2 °F., 5 cm/min, cms	ASTM D-113	30			

Table 2. Asphalt cement properties.

Properties		Test Method	Spec.	Results	
				PG 64-28	PG 70-28
Flash Point, °C		AASHTO T 48	230 min.	307	311
Rotational Viscosity, Pa·s	@ 135°C	AASHTO T 316	3.0 max.	0.718	0.829
	@ 165°C		Report	0.217	0.245
Specific Gravity			Report	1.027	1.034
Density, lbs/gal	@ 15.6°C	AASHTO T 228		8.55	8.61
Dynamic Shear kPa	@ 64°C	AASHTO T 315	1.0 min.	1.40	1.26
Separation Test, 163 °C, 48 hrs,			---	---	---
Top Softening Point, °C		ASTM D 5976	Report	52.2	62.2
Bottom Softening Point, °C			Report	52.2	62.2
Difference, °C			2 max	0.0	0.0
After RTFOT					
Mass Loss, %		AASHTO T 240	1.0 max.	0.476	0.572
Dynamic Shear kPa	@ 64°C	AASHTO T 315	2.2 min.	3.12	3.15
Elastic Recovery, 10 cm %	@ 25°C	ASTM D 6084	45 min.	81.0	81.0
Pressure Aging Residue (100 °C, 300 psi, 20 hr.)		AASHTO R 28			
Dynamic Shear kPa	@ 22°C	AASHTO T 315	5,000 max.	2,510	2163
Creep Stiffness, Stiffness, MPa (60 sec.)	@ -18°C	AASHTO T 313	300 max.	166	243
m Value			0.300 min.	0.345	0.308

Table 3. Aggregates properties.

Type of Aggregate		**Rubber**	**Aggregate 1 (creek gravel)**	**Aggregate 2 (crushed trap rock)**
Bulk specific gravity		0.87	2.35	2.62
Absorption, %		0.1%	4.7%	0.8%
Coefficient of Uniformity		1.9	1.9	1.3
Fractured faces	Percent of non-fractured faces	0.0%	4.6%	0.0%
	Percent of faces with one or more faces	100.0%	95.4%	100.0%
	Percent of faces with two or more faces	88.7%	93.1%	100.0%
Loose dry unit weight, kg/m^3		423	1,180	1,249
Voids in loose aggregates, %		15.4	49.8	52.8
Los Angeles loss by abrasion and impact, %		0.3%	18.7%	8.2%
Micro-Deval weight loss, %		0.0%	6.0%	2.1%
Materials passing No. 200 sieve, %		0.20%	0.50%	0.52%
Median particle size, mm		6.5	6.2	6.1
Flakiness index, %		31.3%	37.6%	42.0%

Table 4. Physical properties of crumb rubber.

Properties	**Value**
Elongation (Bekhiti et al. 2014)	420%
Thermal Stability using thermos gravimetric analysis (TGA) test	200 ℃
Glass transitions point using Differential scanning calorimetry (DSC) test	-65 ℃
Specific heat using Differential scanning calorimetry (DSC) test	2.01 J/gc
Thermal Conductivity	0.12 W/m.k
Tensile strength (Pusca et al. 2010)	16.3 MPa
Tensile impact strength (Pusca et al. 2010)	461 kJ/m2
Surface area of 1mm X 1mm segment using 3D digital microscope	1.22 mm^2
Los Angeles loss by abrasion and impact, %	0.3%
Micro-Deval weight loss, %	0.0%
Dust, %	0.2%

Table 5. Sand patch test specimens' details and results.

Specimen label	Emulsion type	Percentage of the Aggregate type			MTD mm	Range	Variance	STD	CV (%)
		Rubber	Agg 1	Agg 2					
CS-57		100	0	0	5.21	0.54	0.0921	0.30	5.82
CS-58		50	50	0	4.71	0.22	0.0121	0.11	2.34
CS-59		25	75	0	4.17	0.33	0.0276	0.17	3.98
CS-60	Emulsion 1	0	100	0	3.87	0.11	0.0031	0.06	1.44
CS-61		50	0	50	4.78	0.35	0.0308	0.18	3.67
CS-62		25	0	75	4.34	0.39	0.0384	0.20	4.51
CS-63		0	0	100	4.19	0.38	0.0361	0.19	4.53
CS-64		100	0	0	5.45	0.57	0.0819	0.29	5.25
CS-65		50	50	0	4.87	0.60	0.1033	0.32	6.61
CS-66		25	75	0	4.21	0.26	0.0217	0.15	3.50
CS-67	Emulsion 2	0	100	0	3.83	0.12	0.0037	0.06	1.59
CS-68		50	0	50	4.43	0.50	0.0646	0.25	5.74
CS-69		25	0	75	4.25	0.24	0.0171	0.13	3.08
CS-70		0	0	100	4.06	0.56	0.0796	0.28	6.95

Table 6. Standard skid test specimens' details and results.

Specimen label	Binder type	Percentage of the aggregate types			BPN	Range	Variance	STD	CV (%)
		Rubber	Agg 1	Agg 2					
CS-1	Emulsion 1	100	0	0	59.5	2.6	1.85	1.36	2.29
CS-2		50	50	0	61.0	1.4	0.52	0.72	1.18
CS-3		25	75	0	64.0	2.0	1.05	1.03	1.60
CS-4		0	100	0	69.0	2.0	1.00	1.00	1.45
CS-5		50	0	50	64.2	1.6	0.76	0.87	1.36
CS-6		25	0	75	66.4	4.0	5.08	2.25	3.39
CS-7		0	0	100	67.4	1.2	0.36	0.60	0.89
CS-8	Emulsion 2	100	0	0	51.8	1.6	0.64	0.80	1.54
CS-9		50	50	0	55.4	5.8	8.68	2.95	5.32
CS-10		25	75	0	60.0	4.0	4.00	2.00	3.33
CS-11		0	100	0	64.8	2.0	1.12	1.06	1.63
CS-12		50	0	50	61.6	5.8	8.44	2.91	4.72
CS-13		25	0	75	62.8	4.8	7.68	2.77	4.41
CS-14		0	0	100	63.2	4.0	4.12	2.03	3.21
CS-15	Asphalt cement 1	100	0	0	59.0	5.0	7.00	2.65	4.48
CS-16		50	50	0	65.2	5.0	7.00	2.65	4.06
CS-17		25	75	0	66.0	4.5	5.25	2.29	3.47
CS-18		0	100	0	68.0	5.6	8.92	2.99	4.39
CS-19		50	0	50	64.0	4.2	4.44	2.11	3.29
CS-20		25	0	75	70.0	5.0	6.52	2.55	3.65
CS-21		0	0	100	76.6	3.8	3.88	1.97	2.57
CS-22	Asphalt cement 2	100	0	0	56.5	3.8	4.01	2.00	3.55
CS-23		50	50	0	64.0	5.0	6.52	2.55	3.99
CS-24		25	75	0	64.0	4.0	4.00	2.00	3.13
CS-25		0	100	0	65.0	5.6	7.96	2.82	4.34
CS-26		50	0	50	62.0	4.0	4.00	2.00	3.23
CS-27		25	0	75	67.5	1.6	0.69	0.83	1.23
CS-28		0	0	100	75.2	5.8	8.68	2.95	3.92

Table 7. Skid test specimens' details and results of the BPN for dry surface at 20 ℃.

Specimen label	Binder type	Percentage of the aggregate types			BPN	Range	Variance	STD	CV (%)
		Rubber	Agg 1	Agg 2					
CS-29	Emulsion 1	100	0	0	77.8	4.8	7.68	2.77	3.56
CS-30		50	50	0	90.0	4.8	6.24	2.50	2.78
CS-31		25	75	0	91.3	5.2	6.81	2.61	2.86
CS-32		0	100	0	94.5	5.0	6.65	2.58	2.73
CS-33		50	0	50	83.2	3.8	3.64	1.91	2.29
CS-34		25	0	75	85.0	5.6	9.76	3.12	3.68
CS-35		0	0	100	87.8	5.4	7.32	2.71	3.09
CS-36	Emulsion 2	100	0	0	69.0	4.0	5.08	2.25	3.27
CS-37		50	50	0	84.0	4.6	6.04	2.46	2.93
CS-38		25	75	0	85.5	5.0	8.33	2.89	3.38
CS-39		0	100	0	90.0	4.0	4.48	2.12	2.35
CS-40		50	0	50	82.2	5.6	8.32	2.88	3.51
CS-41		25	0	75	83.4	2.2	1.48	1.22	1.46
CS-42		0	0	100	87.0	4.0	4.48	2.12	2.43
CS-43	Asphalt cement 1	100	0	0	80.0	6.4	10.2	3.20	4.00
CS-44		50	50	0	84.2	6.0	9.00	3.00	3.56
CS-45		25	75	0	85.0	6.2	11.1	3.33	3.92
CS-46		0	100	0	86.8	5.4	8.76	2.96	3.41
CS-47		50	0	50	85.0	4.2	5.16	2.27	2.67
CS-48		25	0	75	90.0	3.2	3.04	1.74	1.94
CS-49		0	0	100	99.0	5.0	7.00	2.65	2.67
CS-50	Asphalt cement 2	100	0	0	65.0	6.0	9.12	3.02	4.65
CS-51		50	50	0	74.0	6.2	11.1	3.33	4.50
CS-52		25	75	0	75.0	4.2	5.16	2.27	3.03
CS-53		0	100	0	75.0	3.6	4.32	2.08	2.77
CS-54		50	0	50	70.0	3.6	3.36	1.83	2.62
CS-55		25	0	75	75.0	2.4	1.56	1.25	1.67
CS-56		0	0	100	85.0	5.2	6.88	2.62	3.09

Table 8. Skid test specimens' details and results of the loss in BPN for dry surface at 65 ℃.

Specimen label	Binder type	Percentage of the aggregate types			BPN	Loss in BPN	Range	Variance	STD	CV (%)
		Rubber	Agg 1	Agg 2						
CS-57	Emulsion 1	100	0	0	78.0	0.0	0.0	0.00	0.00	0.00
CS-58		50	50	0	83.0	7.8	0.4	0.04	0.20	2.56
CS-59		25	75	0	83.3	8.8	0.4	0.04	0.20	2.27
CS-60		0	100	0	85.0	10	1.0	0.25	0.50	5.00
CS-61		50	0	50	79.0	5.0	0.4	0.04	0.20	4.00
CS-62		25	0	75	79.5	6.5	0.2	0.01	0.12	1.79
CS-63		0	0	100	80.0	8.8	0.4	0.04	0.20	2.27
CS-64	Emulsion 2	100	0	0	69.0	0.0	0.0	0.00	0.00	0.00
CS-65		50	50	0	83.0	1.2	0.0	0.00	0.00	0.00
CS-66		25	75	0	83.5	1.3	0.2	0.01	0.12	9.12
CS-67		0	100	0	86.3	4.2	0.4	0.04	0.20	4.76
CS-68		50	0	50	81.5	0.9	0.2	0.01	0.12	12.4
CS-69		25	0	75	82.0	1.7	0.2	0.01	0.12	6.93
CS-70		0	0	100	85.0	2.3	0.2	0.01	0.12	5.09
CS-71	Asphalt cement 1	100	0	0	80.0	0.0	0.0	0.00	0.00	0.00
CS-72		50	50	0	84.2	0.0	0.0	0.00	0.00	0.00
CS-73		25	75	0	84.0	1.2	0.2	0.01	0.10	8.33
CS-74		0	100	0	84.8	2.3	0.2	0.01	0.10	4.35
CS-75		50	0	50	85.0	0.0	0.0	0.00	0.00	0.00
CS-76		25	0	75	89.0	1.1	0.2	0.01	0.08	6.84
CS-77		0	0	100	97.0	2.0	0.4	0.04	0.21	10.2
CS-78	Asphalt cement 2	100	0	0	65.0	0.0	0.0	0.00	0.00	0.00
CS-79		50	50	0	74.0	0.0	0.0	0.00	0.00	0.00
CS-80		25	75	0	74.5	0.7	0.0	0.00	0.02	2.17
CS-81		0	100	0	74.0	1.3	0.1	0.00	0.04	2.67
CS-82		50	0	50	70.0	0.0	0.0	0.00	0.00	0.00
CS-83		25	0	75	74.3	0.9	0.1	0.00	0.03	2.79
CS-84		0	0	100	84.0	1.2	0.2	0.01	0.08	6.65

Table 9. Accuracy of evaluating binder application rates using different aggregate models.

Model's shape and agg. type	Median particle size (mm)	Embedment ratio for models	Binder application rate from models (gal/yd^2)	Targeted embedment depth from models (mm)	Actual embedment depth (mm)	Accuracy of the models (%)
Sphere Rubber	6.5	50%	0.365	3.25	2.66	81.85
		66%	0.425	4.29	2.92	67.97
		80%	0.505	5.2	3.85	74.00
Sphere Creek gravel	6.2	50%	0.32	3.1	3.04	97.92
		66%	0.37	4.09	3.46	84.59
		80%	0.44	4.96	3.89	78.33
Pyramid Rubber	6.5	50%	0.32	3.25	2.26	69.68
		66%	0.52	4.29	4.01	93.52
		80%	0.72	5.2	5.22	100.29
Pyramid Creek gravel	6.2	50%	0.28	3.1	2.50	80.72
		66%	0.45	4.09	4.01	98.04
		80%	0.622	4.96	5.20	104.84
Inv. Pyramid Rubber	6.5	50%	0.7	3.25	5.11	157.23
		66%	0.86	4.29	6.10	142.18
		80%	0.96	5.2	6.31	121.28
Inv. Pyramid Creek gravel	6.2	50%	0.605	3.1	5.05	162.90
		66%	0.75	4.09	6.12	149.61
		80%	0.835	4.96	6.51	131.35

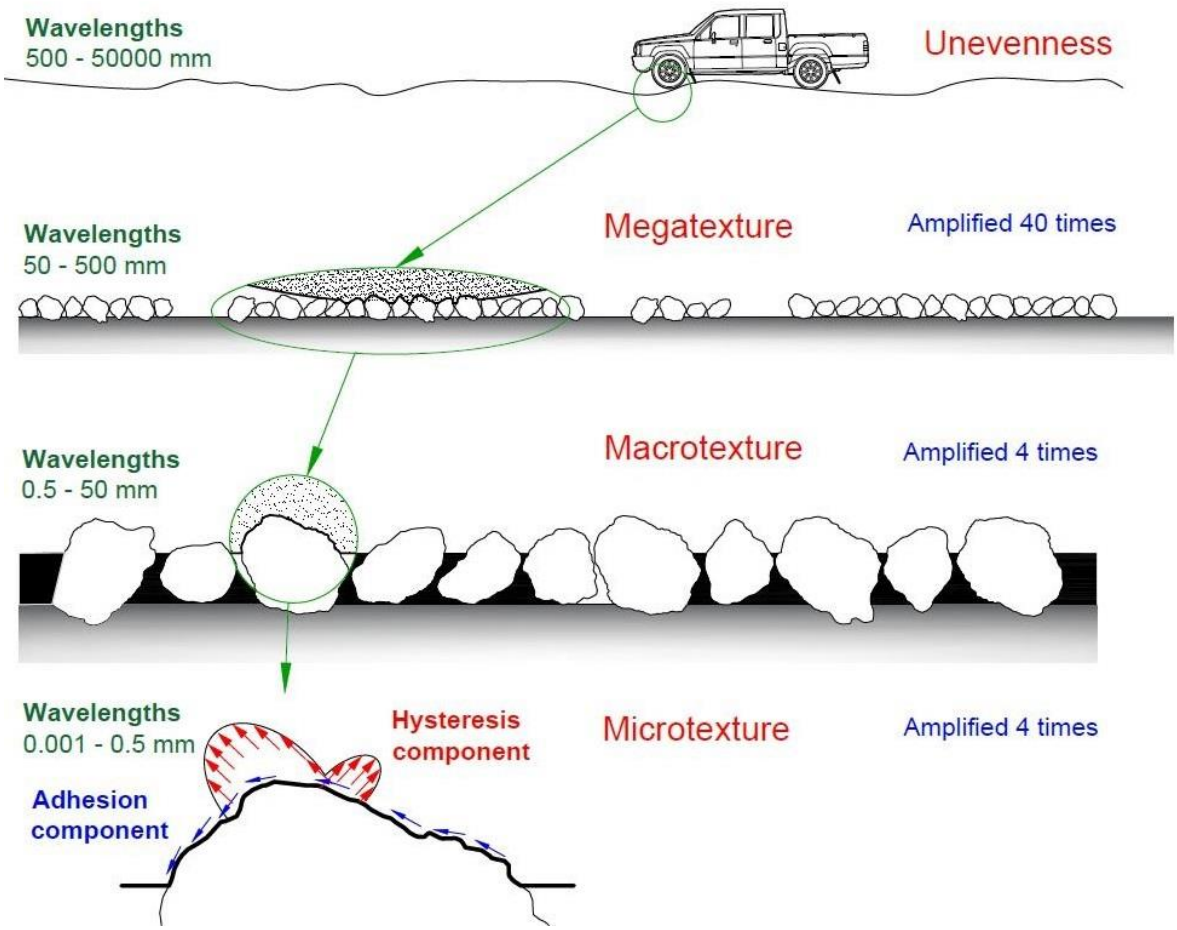

Figure 1. Schematic of surface textures.

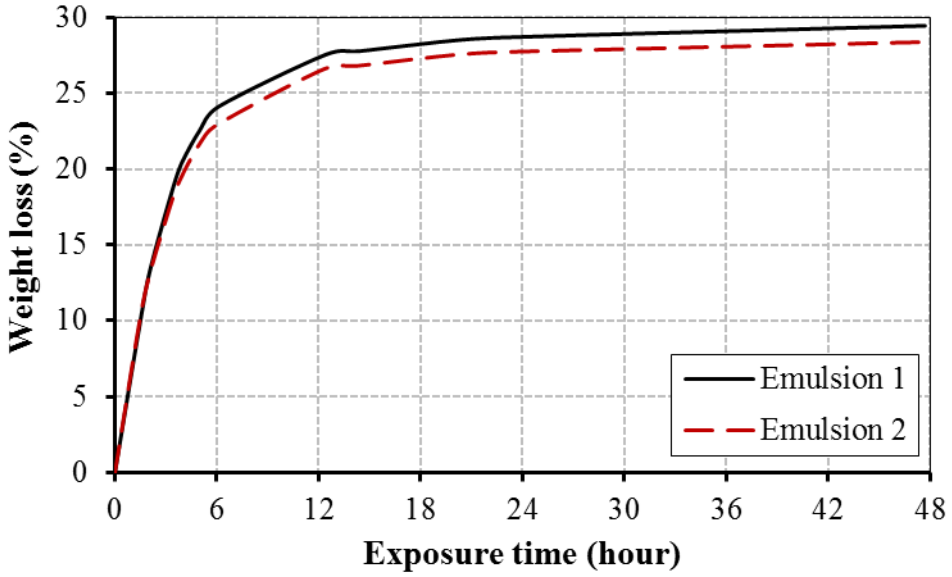

Figure 2. Emulsion weight loss due to water breakout.

(a) (b) (c)

Figure 3. Aggregates used throughout this study (a) crumb rubber, (b) creek gravel, and (c) trap rock.

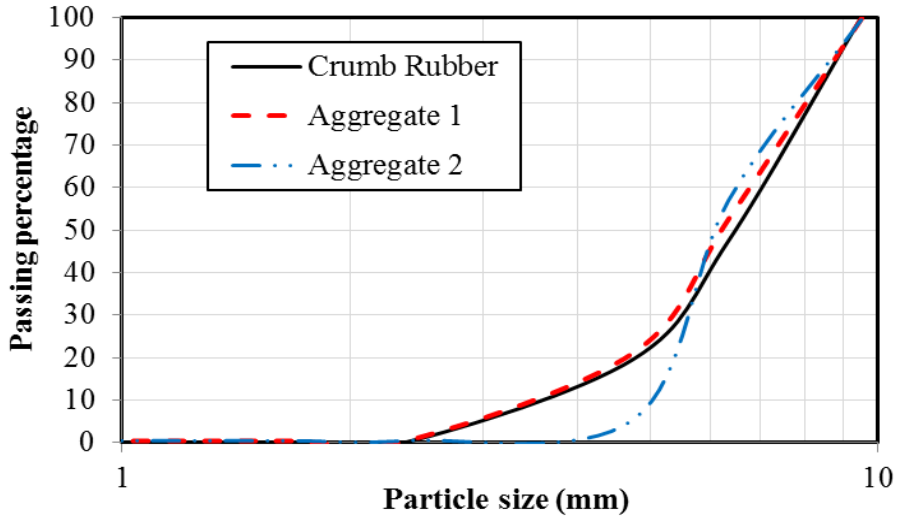

Figure 4. Sieve analysis of the aggregates.

Figure 5. Chip seal specimens for image processing test.

Figure 6. Sectioning the chip seal specimens using water jet cutter.

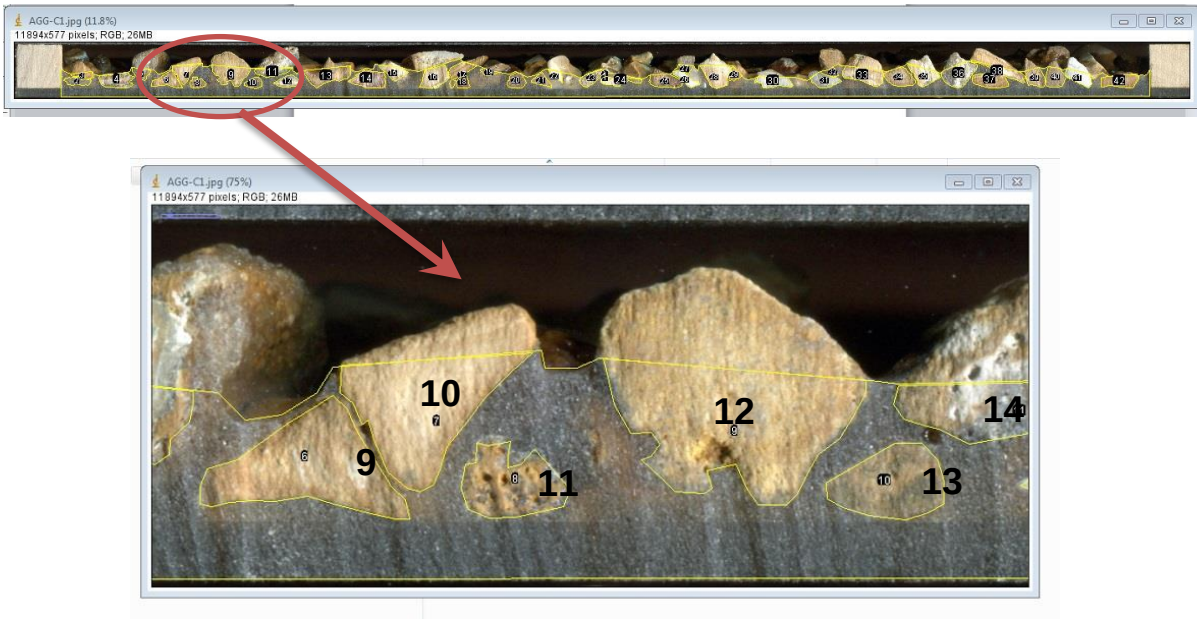

(a)

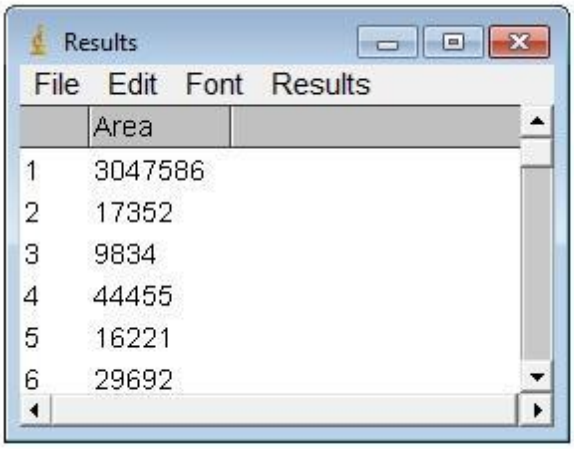

(b)

Figure 7. An example of using image processing ImageJ™ program to find the mean depth of binder (a) chip seal cross-section, and (b) surface areas of binder and embedded particles.

(a) (b) (c)

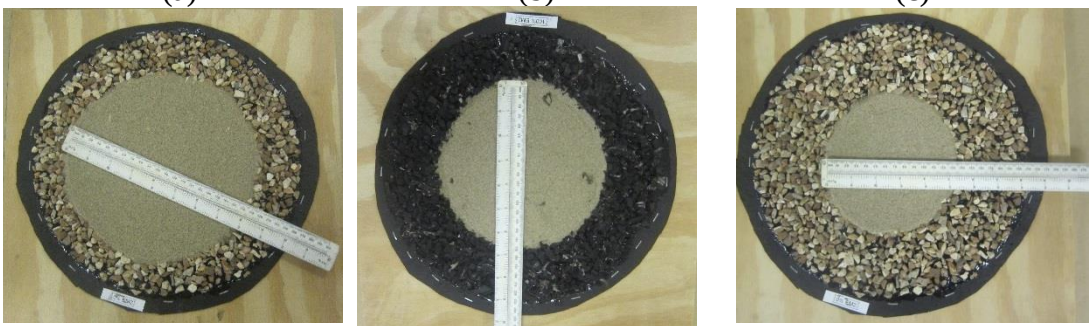

(d)

Figure 8. Procedure of sand patch test: (a) weigh the sand, (b) applying sand, (c) distributing the sand, and (d) measuring the diameter of sand in several directions.

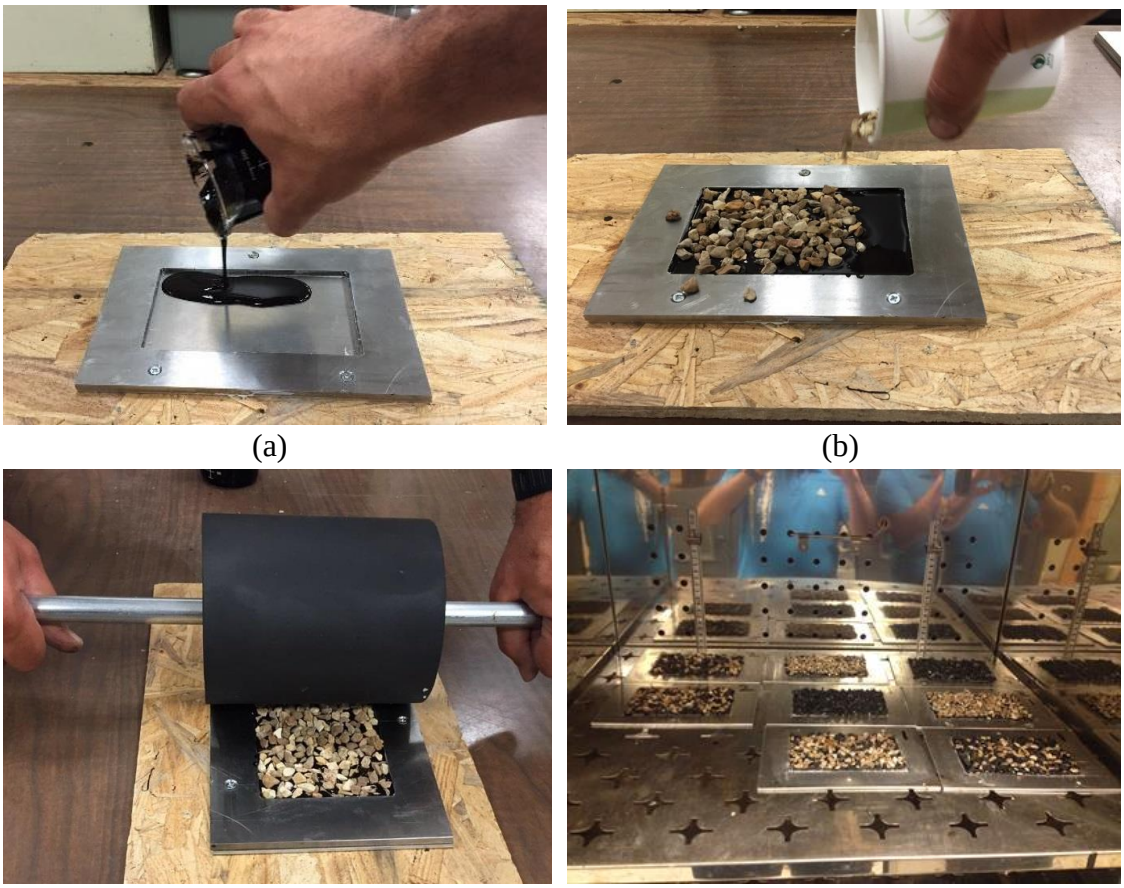

(a) (b)

(c) (d)

Figure 9. Skid test specimen preparation (a) apply emulsion, (b) adding aggregates on the emulsion, (c) compacting the aggregates, and (d) curing the test specimens.

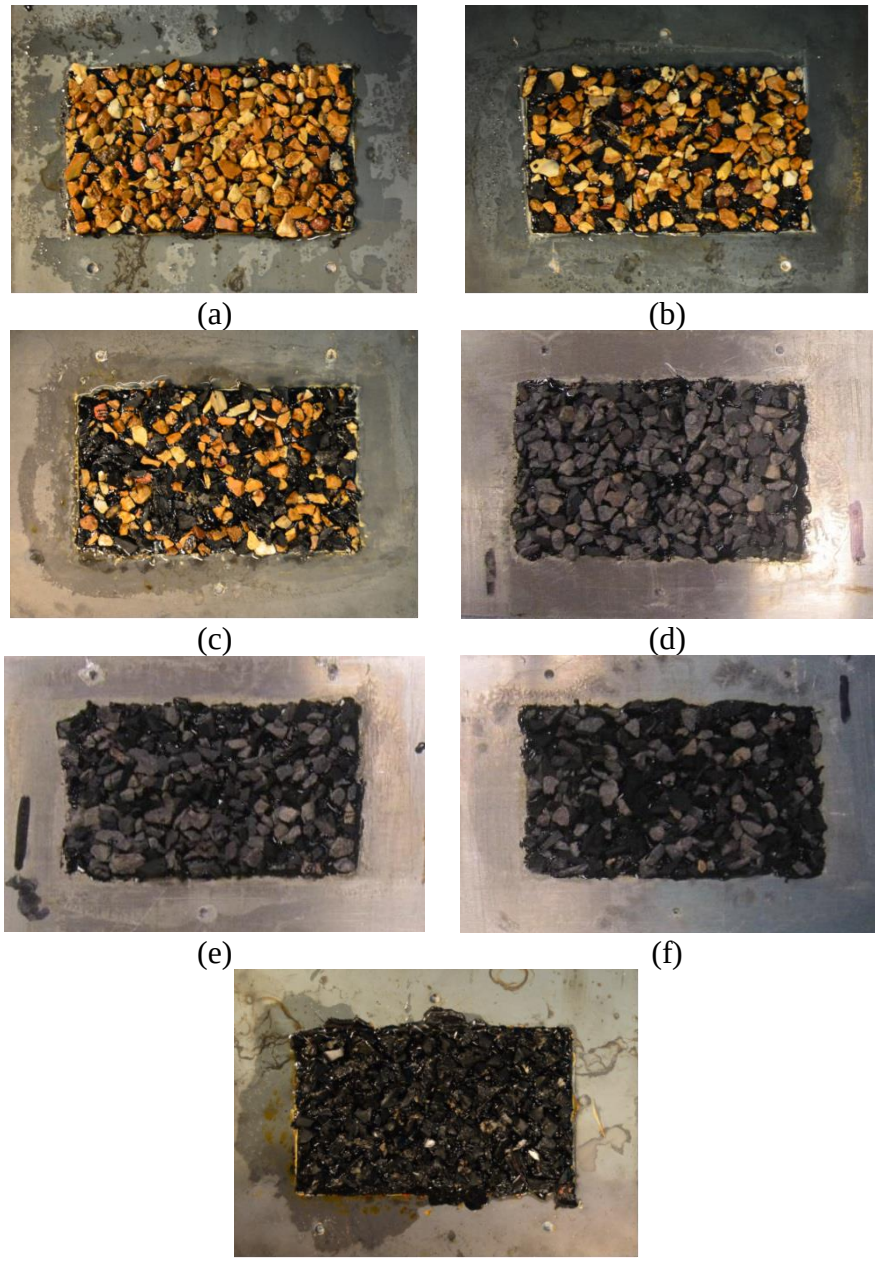

(a) (b) (c) (d) (e) (f) (g)

Figure 10. Skid test specimens ready for testing (a) 100% aggregate 1, (b) 75% aggregate 1 -25% crumb rubber, (c) 50% aggregate 1 - 50% crumb rubber, (d) 100% aggregate 2, (e) 75% aggregate 2 - 25% crumb rubber, (f) 50% aggregate 2 - 50% crumb rubber, and (g) 100% crumb rubber.

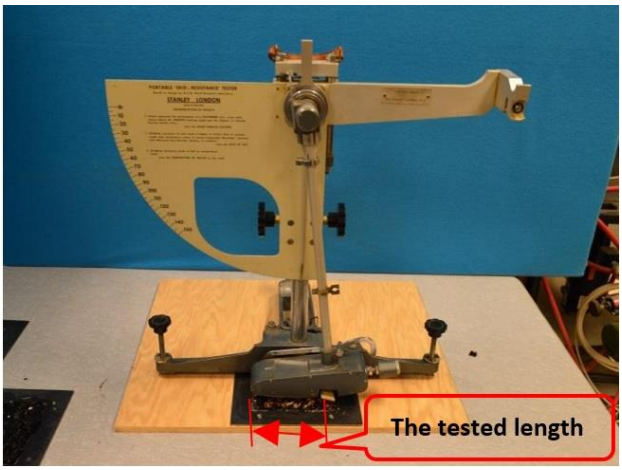

(a)

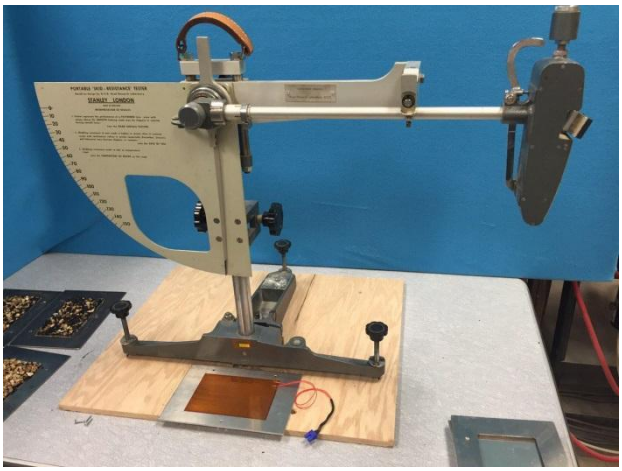

(b)

(c)

Figure 11. Skid test procedure: (a) adding aggregates on the emulsion, (b) compacting the aggregates, (c) applying the test, (d) heating chips, and (e) temperature measurement of the specimen.

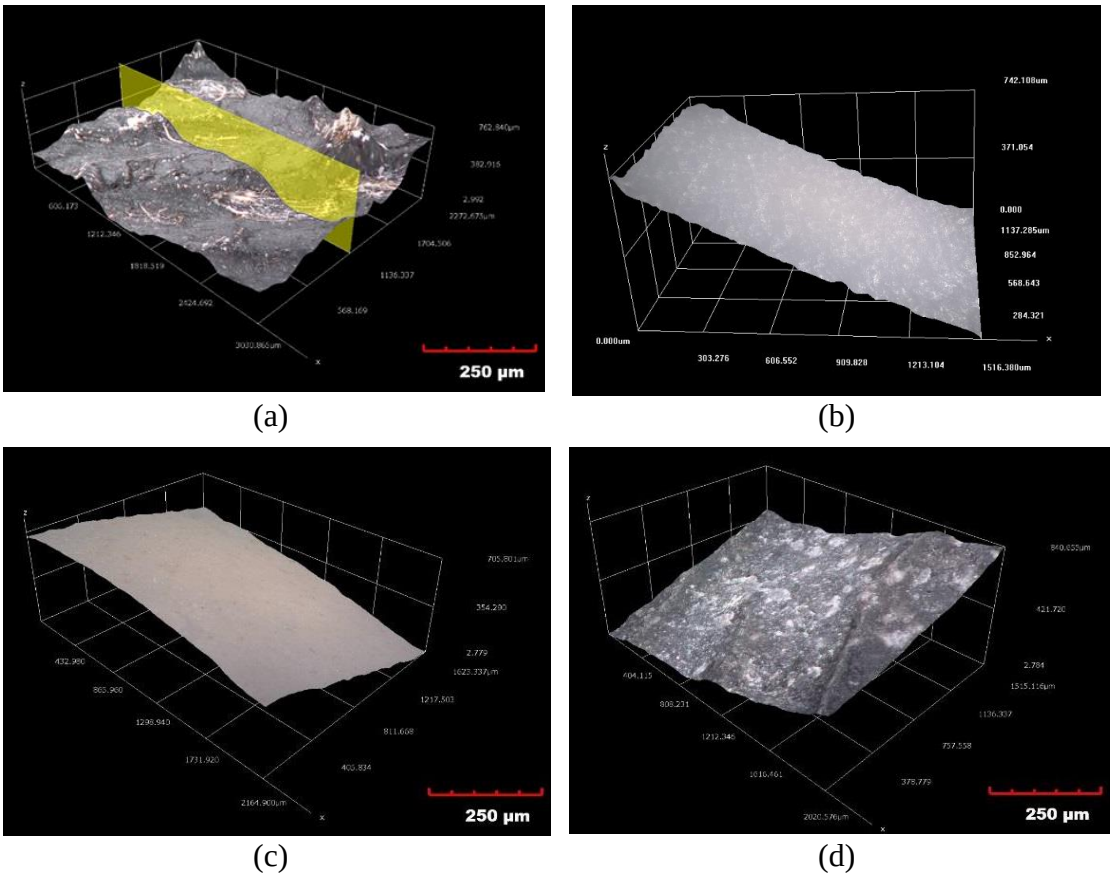

(a) (b)

(c) (d)

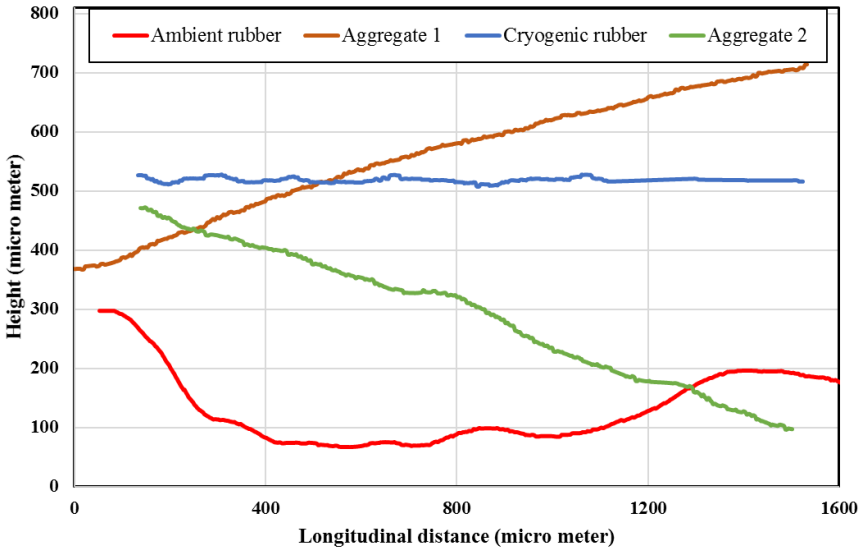

(e)

Figure 12. Microscopic results of the surface of the aggregates in range of 250 µm (a) image of crumb rubber, (b) image of cryogenic crumb rubber, (c) image of aggregate 1, (d) image of aggregate 2, and (e) surfaces' profiles of the aggregates.

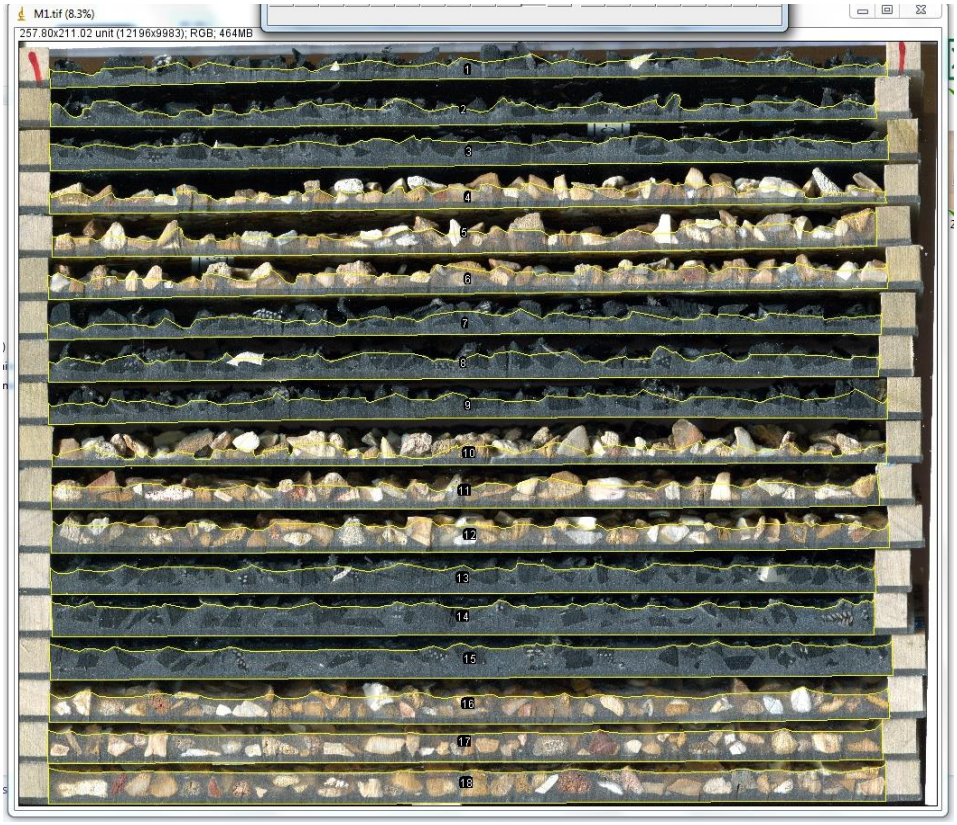

Figure 13. Different chip seal sections for image processing.

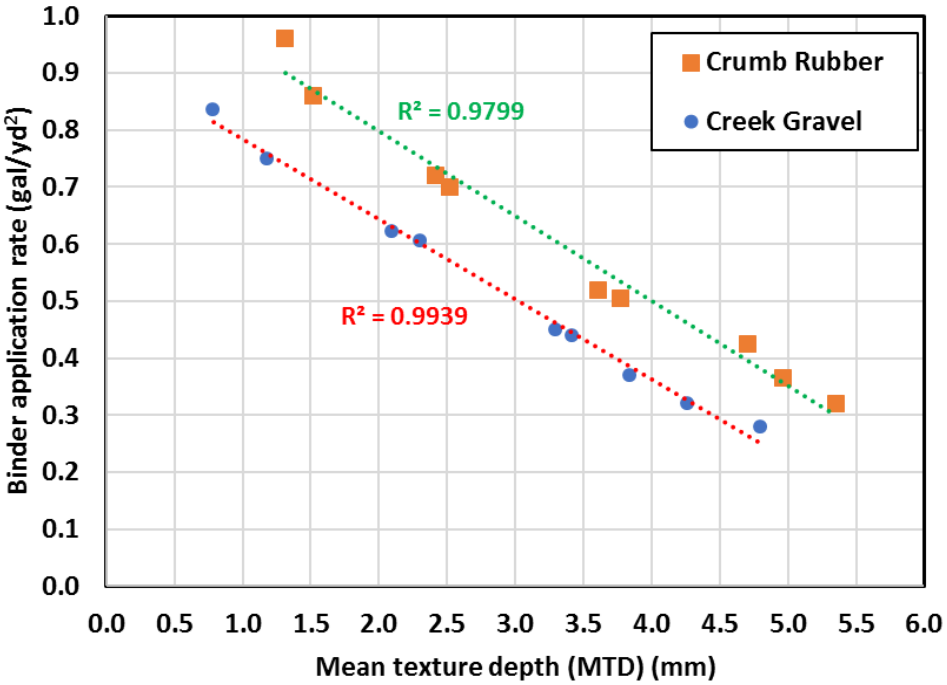

Figure 14. Binder application rate versus mean texture depth (MTD).

(a)

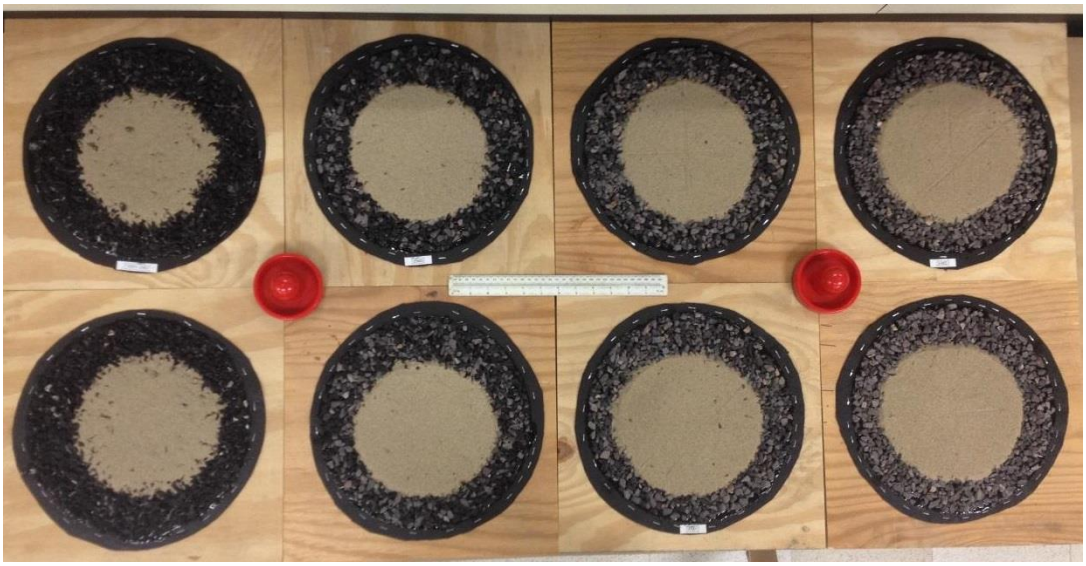

(b)

Figure 15. Sand patch test specimens with different aggregate combinations for specimens with: (a) creek gravel, and (b) trap rock in combination with crumb rubber.

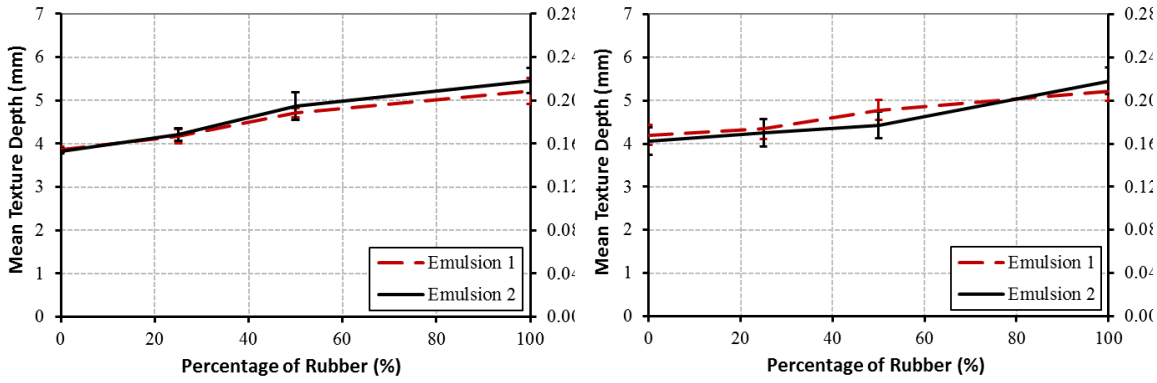

Figure 16. Percentage of crumb rubber versus the macrotexture depth from sand patch test for (a) specimens with aggregate 1, and (b) specimens with aggregate 2.

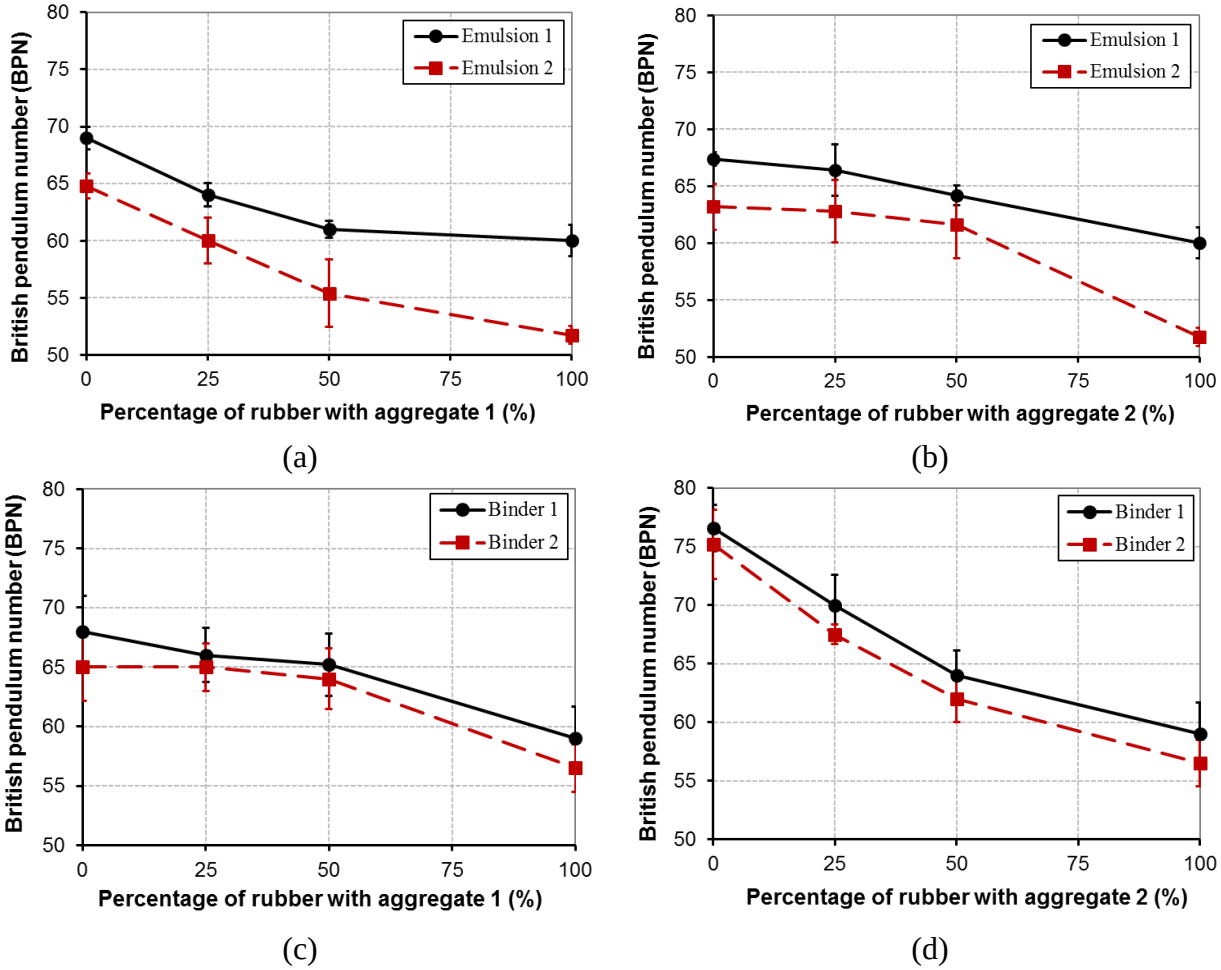

Figure 17. Standard skid test BPN versus percentage of rubber with: (a) aggregate 1, (b) aggregate 2, (c) aggregate 1, and (d) aggregate 2.

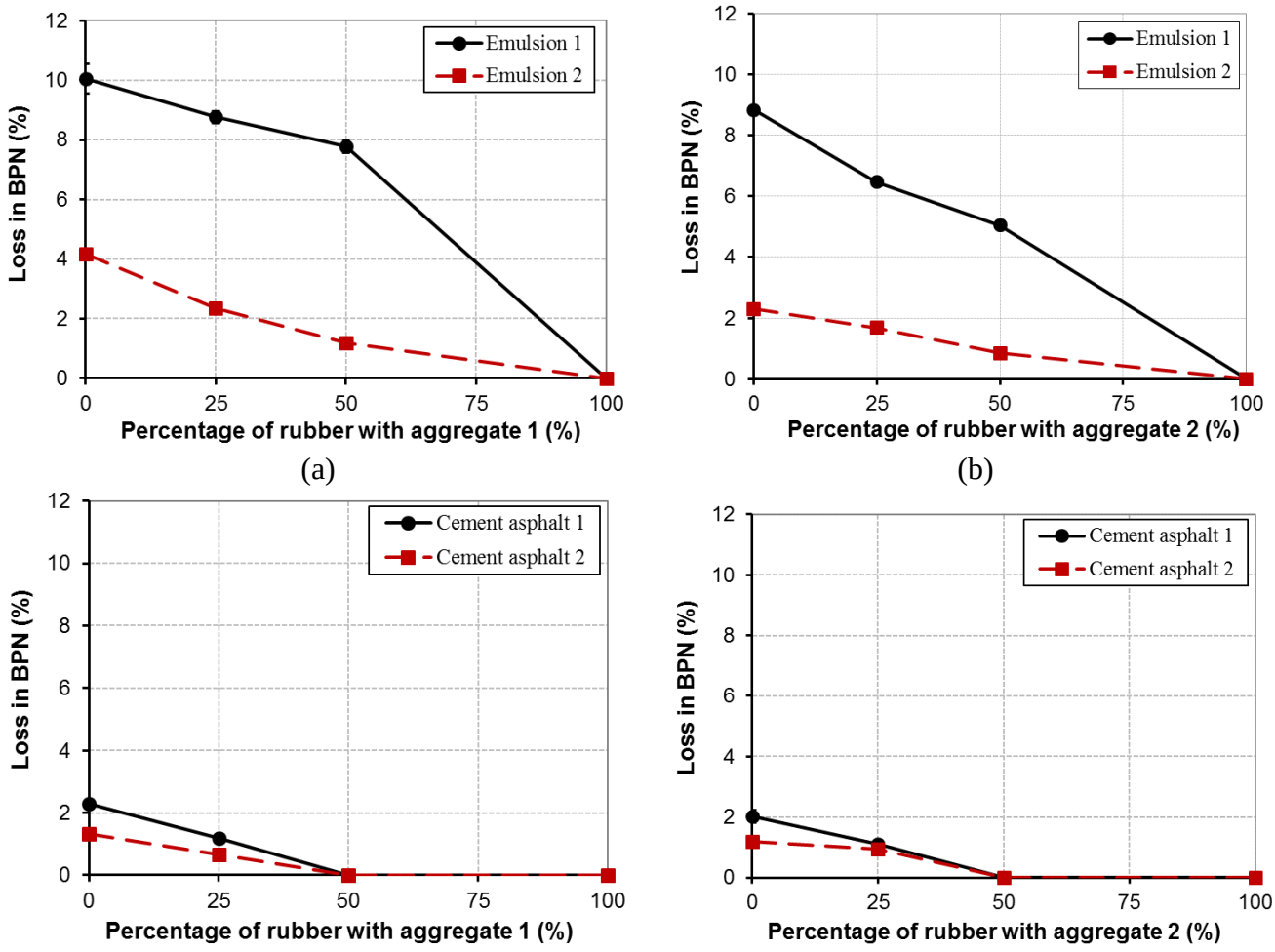

Figure 18. Modified skid test loss in BPN versus percentage of rubber with: (a) aggregate 1 in emulsions, (b) aggregate 2 in emulsions, (c) aggregate 1 in cement asphalt, and (d) aggregate 2 in cement asphalt.

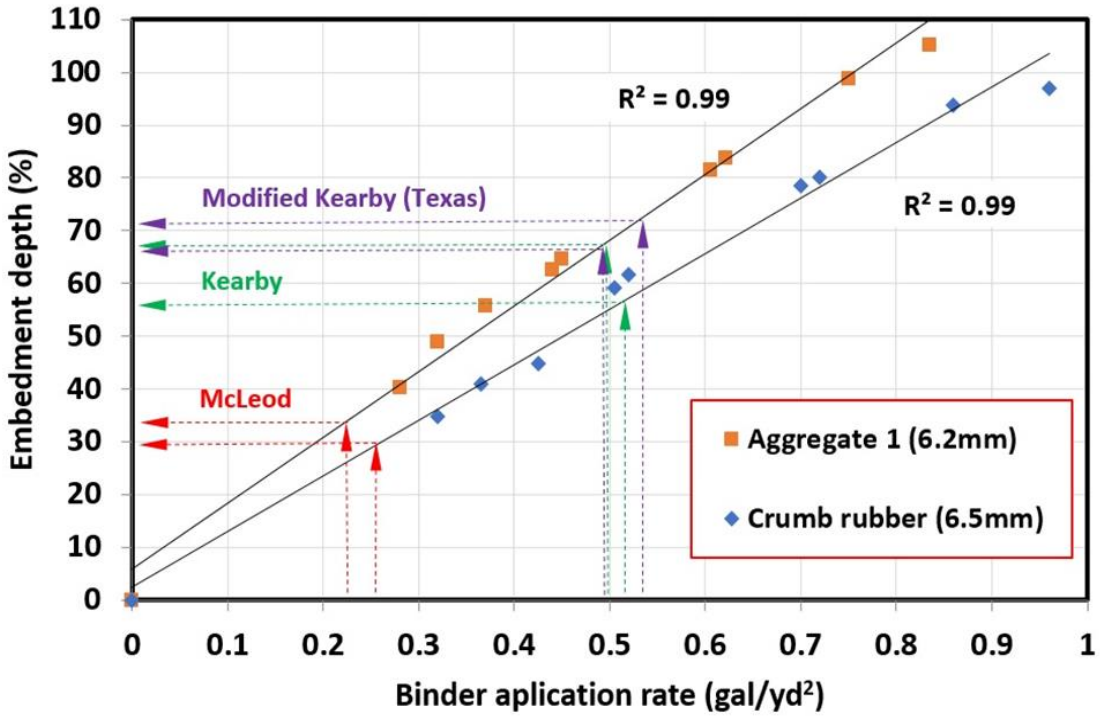

Figure 19. Binder application rate versus embedment depth for aggregate 1 and crumb rubber.

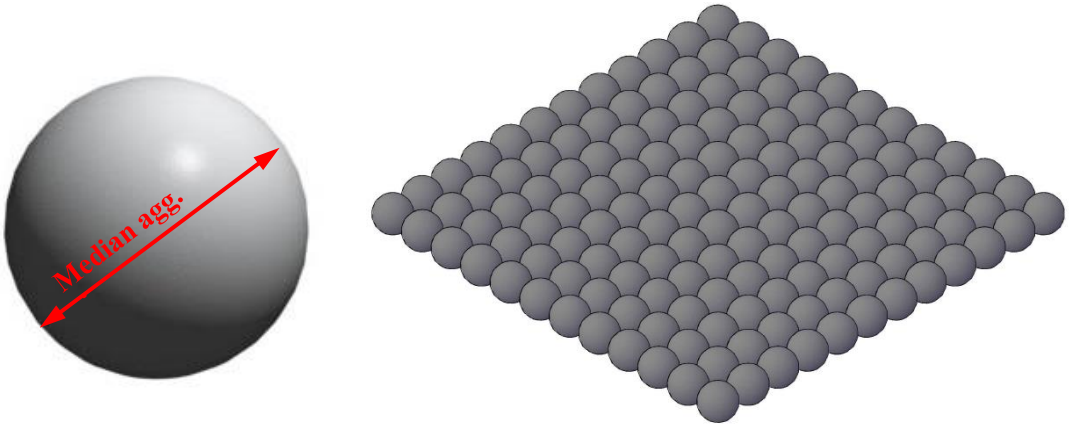

(a) (b)

Figure 20. Modeling aggregate particle (a) particle shape, and (b) chip seal aggregate model.

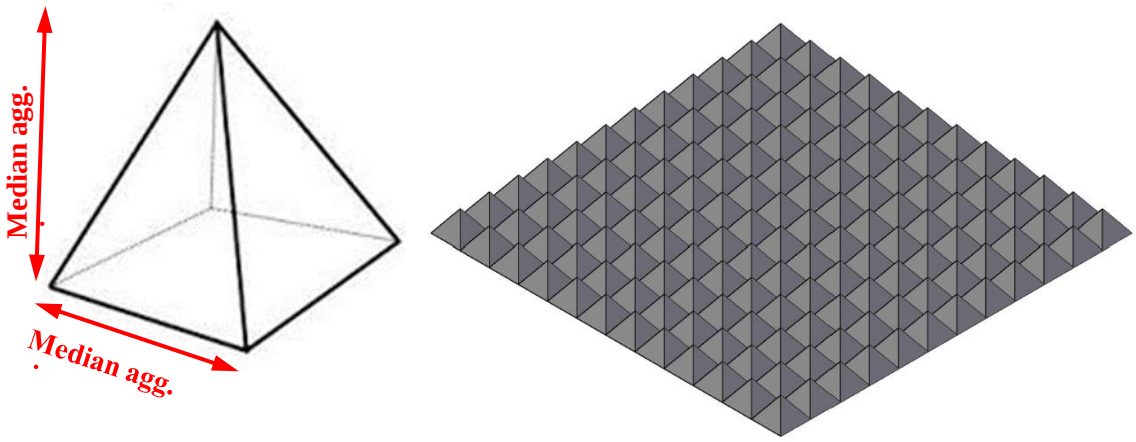

(a) (b)

Figure 21. Modeling aggregate particle (a) particle shape, and (b) chip seal aggregate model.

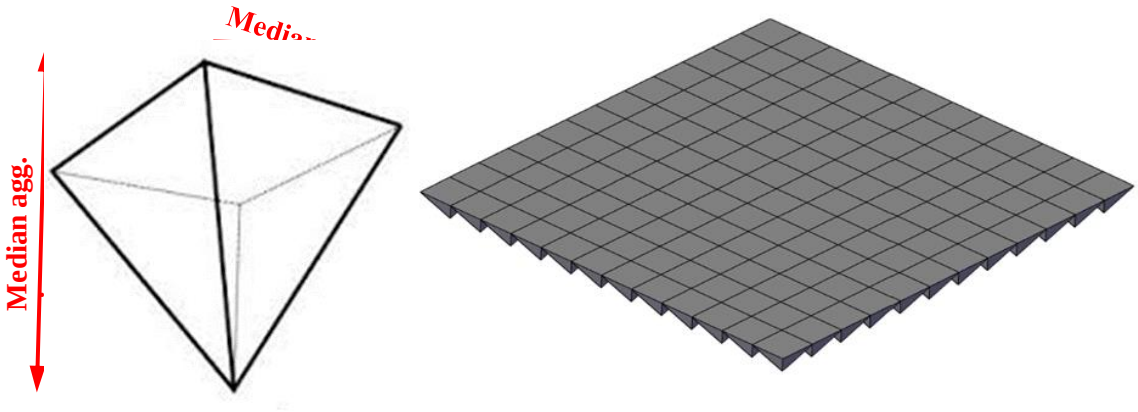

(a) (b)

Figure 22. Modeling aggregate particle (a) particle shape, and (b) chip seal aggregate model.

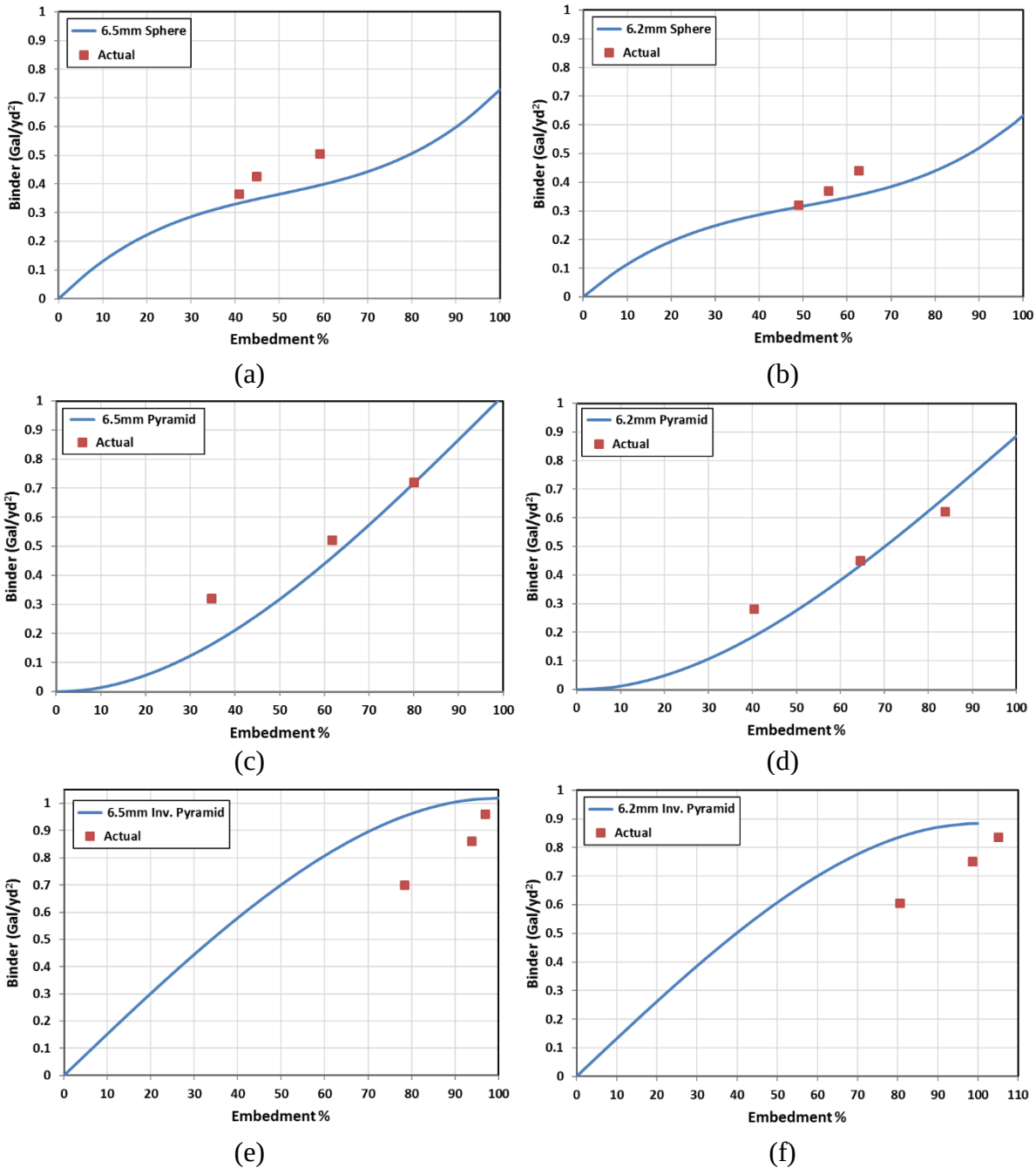

Figure 23. Analytical and experimental binder application rates versus aggregate embedment ratios (a) 6.5mm sphere model, (b) 6.2mm sphere model, (c) 6.5mm pyramid model, (d) 6.2mm pyramid model, (e) 6.5mm inverted pyramid model, and (d) 6.2mm inverted pyramid model.

REFERENCES

1. Brown, E.R., *Preventative maintenance of asphalt concrete pavements.* National Center for Asphalt Technology, Auburn, AL, 1988.

2. O'Brien, L.G., *Evolution and benefits of preventive maintenance strategies*. 1989.

3. Gransberg, D. and D. James, *Chip Seal Best Practices, National Cooperative Highway Research Program Synthesis 342.* Transportation Research Board, National Academies, Washington, DC, 2005.

4. Karasahin, M., et al., *Laboratory and In Situ Investigation of Chip Seal Surface Condition Improvement.* Journal of Performance of Constructed Facilities, 2014. 29(2): p. 04014047.

5. Wood, T.J., D.W. Janisch, and F.S. Gaillard, *Minnesota seal coat handbook 2006*. 2006.

6. Islam, S. and M. Hossain, *Chip seal with lightweight aggregates for low-volume roads.* Transportation Research Record: Journal of the Transportation Research Board, 2011(2205): p. 58-66.

7. McHattie, R.L., *Asphalt surface treatment guide*. 2001: Alaska Department of Transportation and Public Facilities.

8. Amirkhanian, S.N., *Utilization of crumb rubber in asphaltic concrete mixtures–South Carolina's Experience.* See ref, 2001. 3: p. 163-174.

9. Gheni, A.A., M.A. ElGawady, and J.J. Myers, *Mechanical Characterization of Concrete Masonry Units Manufactured with Crumb Rubber Aggregate.* ACI Materials Journal, 2017. 114(01).

10. Hanson, D.I., J. Epps, and R.G. Hicks, *Construction Guidelines for Crumb Rubber Modified Hot Mix Asphalt: Interim Report*. 1996: National Center for Asphalt Technology.

11. Moustafa, A. and M.A. ElGawady, *Mechanical properties of high strength concrete with scrap tire rubber.* Construction and Building Materials, 2015. 93: p. 249-256.

12. Papagiannakis, A. and T. Lougheed, *Review of Crumb-Rubber Modified Asphalt Concrete Technology.* 1995.

13. Rangaraju, P. and S. Gadkar, *Durability evaluation of crumb rubber addition rate on Portland cement concrete.* Department of Civil Engineering, Clemson University, Clemson, 2012: p. 1-126.

14. Shuler, S., *Use of Waste Tires, Crumb Rubber, on Colorado Highways*. 2011: Colorado Department of Transportation, DTD Applied Research and Innovation Branch.

15. Youssf, O., M.A. ElGawady, and J.E. Mills, *Static cyclic behaviour of FRP-confined crumb rubber concrete columns.* Engineering Structures, 2016. 113: p. 371-387.

16. Youssf, O., et al., *Prediction of crumb rubber concrete strength.* 2014.

17. Youssf, O., M.A. ElGawady, and J.E. Mills. *Experimental investigation of crumb rubber concrete columns under seismic loading*. in *Structures*. 2015. Elsevier.

18. Moustafa, A., A. Gheni, and M.A. ElGawady, *Shaking-Table Testing of High Energy–Dissipating Rubberized Concrete Columns.* Journal of Bridge Engineering, 2017. 22(8): p. 04017042.

19. RMA, R.M.A., *Scrap tire markets in the United States.* 2016.

20. Ang, G. and V. Marchal, *Mobilising private investment in sustainable transport: The case of land-based passenger transport infrastructure.* OECD Environment Working Papers, 2013(56): p. 0_1.

21. Lee, S.-J., C.K. Akisetty, and S.N. Amirkhanian, *The effect of crumb rubber modifier (CRM) on the performance properties of rubberized binders in HMA pavements.* Construction and Building Materials, 2008. 22(7): p. 1368-1376.

22. Presti, D.L., *Recycled tyre rubber modified bitumens for road asphalt mixtures: a literature review.* Construction and Building Materials, 2013. 49: p. 863-881.

23. Page, G.C., *Florida's initial experience utilizing ground tire rubber in asphalt concrete mixes.* Journal of the Association of Asphalt Paving Technologists, 1992. 61.

24. Huang, B., et al., *Louisiana experience with crumb rubber-modified hot-mix asphalt pavement.* Transportation Research Record: Journal of the Transportation Research Board, 2002(1789): p. 1-13.

25. LaForce, R.F., *Squeegee Seal and Crumb Rubber Chip Seal Sapinero-East.* Colorado Department of Transportation, CDH-DTP, 1983.

26. LaForce, R.F., *Crumb rubber chip seal east of Punkin Center.* 1986.

27. Way, J.R.S.G.B., *Asphalt-Rubber Chip Seal and Polymer Modified Asphalt-Rubber Two Layer System, Case Studies*, in *Asphalt Rubber Conference* 2012, Rubberized Asphalt Foundation: Munich.

28. Gheni, A., et al., *Mechanical and Environmental Performance of Eco-Friendly Chip Seal with Recycled Crumb Rubber*. 2017.

29. Beck, P.E., Robert, *A Basic Emulsion Manual*, in *Asphalt Institute Manual Series MS-19*. 2006, Colorado Department of Transportation: Salida, Colorado.

30. Do, M.-T., H. Zahouani, and R. Vargiolu, *Angular parameter for characterizing road surface microtexture.* Transportation Research Record: Journal of the Transportation Research Board, 2000(1723): p. 66-72.

31. Forster, S.W., *Aggregate microtexture: Profile measurement and related frictional levels*. 1981.

32. Yandell, W., *A new theory of hysteretic sliding friction.* Wear, 1971. 17(4): p. 229-244.

33. Yandell, W. and S. Sawyer, *Prediction of tire-road friction from texture measurements.* Transportation Research Record, 1994(1435).

34. Choubane, B., C. Holzschuher, and S. Gokhale, *Precision of locked-wheel testers for measurement of roadway surface friction characteristics.* Transportation Research Record: Journal of the Transportation Research Board, 2004(1869): p. 145-151.

35. Flintsch, G., et al., *Pavement surface macrotexture measurement and applications.* Transportation Research Record: Journal of the Transportation Research Board, 2003(1860): p. 168-177.

36. Henry, J.J., *Evaluation of pavement friction characteristics*. Vol. 291. 2000: Transportation Research Board.

37. Kotek, P. and M. Kováč, *Comparison of Valuation of Skid Resistance of Pavements by two Device with Standard Methods.* Procedia Engineering, 2015. 111: p. 436-443.

38. Lewis, P., *Laboratory testing of rubber durability.* Polymer Testing, 1980. 1(3): p. 167-189.

39. USEPA, *Scrap Tires: Handbook on Recycling Applications and Management for the U.S. and Mexico*, O.o.R.C.a. Recovery, Editor. 2010, United States Environmental Protection Agency: Washington DC.

40. Bekhiti, M., H. Trouzine, and A. Asroun, *Properties of Waste Tire Rubber Powder.* Engineering, Technology & Applied Science Research, 2014. 4(4): p. pp. 669-672.

41. Pusca, A., S. Bobancu, and A. Duta, *MECHANICAL PROPERTIES OF RUBBER- AN OVERVIEW.* Bulletin of the Transilvania University of Brasov., 2010. 3(107): p. 2010.

42. McLeod, N.W., et al. *A general method of design for seal coats and surface treatments*. in *Association of Asphalt Paving Technologists Proc*. 1969.

43. Kearby, J. *Tests and theories on penetration surfaces*. in *Highway Research Board Proceedings*. 1953.

44. Stockton, W.R. and J.A. Epps, *ENGINEERING ECONOMY AND ENERGY CONSIDERATIONS. SEAL COAT ECONOMICS AND DESIGN*. 1975.

45. ASTM, *ASTM D7000 Standard Test Method for Sweep Test of Bituminous Emulsion Surface Treatment Samples,*. 2011: ASTM International, West Conshohocken, PA.

46. Masad, E., *Test methods for characterizing aggregate shape, texture, and angularity*. Vol. 555. 2007: Transportation Research Board.

47. Hanson, D.I. and B.D. Prowell, *Evaluation of circular texture meter for measuring surface texture of pavements*. 2004, the Center.

48. Abe, H., et al., *Measurement of pavement macrotexture with circular texture meter.* Transportation Research Record: Journal of the Transportation Research Board, 2001(1764): p. 201-209.

49. Mohseni, A., *LTPP seasonal asphalt concrete (AC) pavement temperature models*. 1998.

50. Mataei, B., et al., *Pavement Friction and Skid Resistance Measurement Methods: A Literature Review.* Open Journal of Civil Engineering, 2016. 6(04): p. 537.

V. LEACHING ASSESSMENT OF ECO-FRIENDLY RUBBERIZED CHIP SEAL PAVEMENT

Ahmed Gheni1, Xuesong Liu, Mohamed A. ElGawady, Honglan Shi, and Jianmin Wang

ABSTRACT

Companies in the United States need to mine billions of tons of raw natural aggregate each year. At the same time, billions of scrap tires are stockpiled every year. As a result, replacing the natural aggregate with recycled aggregate is beneficial to the construction industry and the environment. This paper is part of a comprehensive project that developed, and field implemented a new eco-friendly rubberized chip seal where the mineral aggregate in chip seal is partially or totally replaced with crumb rubber made of recycled tires. This paper presents an extensive study of the environmental impact of using rubber aggregate in chip seal pavement in terms of leaching under different pH conditions including simulated acid rain. The results are compared with those of conventional chip seal. Leaching from the constituents of chip seal, i.e., rubber aggregate and emulsion was investigated. Two types of rubber and two types of asphalt emulsions were studied. The leaching performance of rubberized chip seal was also investigated. This study revealed that the toxic heavy metals leached from the rubberized chip seal, for pH ranging from 4 to 10, were below that of the EPA drinking water standards. In addition, a significant reduction of heavy metal leaching was recorded when rubber was used with emulsion in the form of chip seal pavement under different pH conditions. Finally, the metal leaching in all types of samples (including rubber, asphalt emulsion, and chip seal) decreased with the increase in pH value.

Keywords: Crumb rubber, Chip seal, Rubber leaching, Rubberized pavement, Eco-friendly, Sustainable construction

1. INTRODUCTION

As the natural resources are depleting, the construction industry is forced to find replacements for the virgin construction materials and using recycled material is one of the main options. At the same time, the world is facing a severe problem dealing with scrap tires. More than four million tons of scrap tires were dumped in the United States during 2015 alone, taking up valuable space in landfills and wasting valuable resources in the form of the rubber material and textile and metal cord (RMA 2018). Crumb rubber obtained from scrap tires can be used to replace mineral aggregate, leading to an eco-friendly construction industry (Moustafa and ElGawady 2016, Gheni et al. 2017, Gheni et al. 2017). Recycled crumb rubber has been widely used in concrete to improve durability, seismic behavior, sustainability, sound absorption, noise reduction coefficient, and heat transfer properties (Siddique and Naik 2004, Turgut and Yesilata 2008, Gheni et al. 2017, Moustafa et al. 2017).

Transportation infrastructure contributes 23% of global carbon dioxide (CO_2) emissions, making it the second largest contributor, only behind electricity generation (Ang and Marchal 2013). As a result, using recycled material in the construction of the transportation infrastructure will reduce CO_2 emission significantly. One application is using scrap tire material in roadway construction. Previous studies have shown that using crumb rubber as an asphalt binder modifier can improve the overall performance of the binders in terms of temperature susceptibility, viscosity, and stiffness (Presti 2013). However, this application does not consume a significant amount of scrap rubber.

Chip seal is a type of pavement treatment that consists of a single application of asphalt binder directly on existing pavement, followed by an application of aggregate chips that are rolled with a pneumatic roller. In this process, the aggregate chip layer is typically one stone thick. Chip seal with two layers of aggregate has been used (Figure 1b). Recycled rubber has been used with chip seal before as an asphalt binder modifier. According to the authors' best knowledge, there has been no research on using crumb rubber aggregate in chip seal.

This research aims to investigate the potential use of crumb rubber aggregate in chip seal, producing what is called rubberized chip seal, which would significantly increase the sustainability of chip seal. This project studied the overall performance of rubberized chip seal pavement (Figure 2). The aggregate retention was investigated using three standard tests. Furthermore, the micro and macro texture have been investigated, as well as the skid resistance under ambient and elevated temperatures. The results were compared with conventional chip seal using two types of asphalt emulsion and two types of mineral aggregate (Gheni et al. 2017).

In addition to the comprehensive laboratory testing and assessment, two different locations in the State of Missouri were selected for field-testing of rubberized chip seal. The main objective of the first location was to ensure the feasibility of constructing rubberized chip seal using the same set of equipment, tools, and procedures that are currently used by an average contractor to apply a conventional chip seal while the performance of the rubberized chip seal in the second location will be monitored for one year. The first location consisted of two chip seal sections with different crumb rubber volume-replacement ratios of 50% and 100%. Each section was about 350 ft long. The

second location consisted of five chip seal sections with different crumb rubber volume-replacement ratios of 0%, 25%, 50%, 75%, and 100%. Without any modification, the traditional chip seal procedure was used to apply the rubberized chip seal (Figure 5). An ambient processed crumb rubber with a size of 2.3–6.0 mm and 6.0–12.5 mm was used in location 1 and 2, respectively. This was similar in size to the creek gravel aggregate and trap rock used in the blend, respectively. Emulsion type CRS2P with a temperature of 54 °C was used at an air temperature of 26 °C in both locations. During the compaction, it was noticed that rubber particles were adherent to the tires of the rubber tires compactors (Figure 5) due to the flexibility of the rubber particles that allowed the rubber tires to penetrate and squeeze the crumb rubber layer and reach to the emulsion. As a result, the rubber tire compactors were replaced by steel roller compactors which compacted the material appropriately.

While the laboratory work and field implementation showed the high performance of rubberized chip seal, the leaching of toxic metals in rubberized chip seal could be a concern due to the absence of any research on this issue. This paper presents a comprehensive study to determine the metal leaching behavior of rubberized chip seal under various conditions.

2. EXPERIMENTAL PROGRAM

3.1. MATERIAL CHARACTERIZATION AND PROPERTIES

Two types of emulsions, CRS-2P and CHFRS-2P, were used during this study. Both emulsions were rapid-setting, high-viscous, and cationic, which is defined as the migration of asphalt particles under an electric field towards the cathode (negative electrode).

Emulsion 2, CHFRS-2P, was a high-float type while emulsion 1, CRS-2P, was a conventional type. The water break-out of the emulsions was examined through weight loss measurements after exposing the emulsion to different temperatures for different periods (Figure 3). Approximately 81% of the water breakout occurred after 6 hours for both types of emulsion, while there was almost no evaporation after 24 hours of exposure.

Two types of recycled rubber, ambient and cryogenic, were used during this study. The former type was produced by tearing and shredding the scrap tires in the cutting mills at ambient temperature. The later type was produced by reducing the temperature of the scrap tires to -80 ºC using liquid nitrogen, followed by grounding the glass-like frozen tires to the required sizes using a hammer mill.

The microtexture surface conditions of the mineral and crumb rubber aggregates were examined using a digital 3D microscope KH-8700. The ambient crumb rubber had a very rough surface with many crests and troughs, which improved its retention with the asphalt emulsions and binders, whereas the cryogenic crumb rubber had a smooth surface (Figure 4).

3. ENVIRONMENTAL ASSESSMENT

The first step in the environmental assessment was to perform an X-ray diffraction test to determine the chemical composition of the rubber aggregate. Zinc (Zn) and zinc oxide (ZnO) had the highest concentration compared to other elements (Figure 6).

The leaching of heavy metals was studied for bare rubber particles and for chip seal (rubber and emulsion). The specimens were exposed to drinking water, acid, and simulated acid rain. The effect of pH in a pH range between 4 and 10 on metal leaching was also investigated. This part of the study consisted of the following four tasks:

1. Leaching behavior of heavy metals from bare crumb rubber under different pH conditions;
2. Acid-extractable metal contents from chip seal samples. This was to determine the maximum leachable heavy metals from these materials;
3. Leaching behavior of heavy metals from chip seal samples under a simulated acid rain condition in Missouri (west of Mississippi river);
4. Leaching behavior of heavy metals of different chip seal specimens with pH ranging between 4 and 10.

3.1. CHIP SEAL SPECIMENS' PREPARATION

The amount of aggregate and asphalt emulsion in chip seal specimens should be calculated properly. There is no consensus in the United States on how to design a chip seal. A recent survey covering 54 cities and entire states showed that only 18% of respondents use the McLeod, Kearby, and modified Kearby methods to design chip seal, while 26% of the respondents do not use a formal design method. The remaining 56% of the respondents use their local, empirical, or past experience design approach (Gransberg and James 2005). The ASTM D7000-11 provides Equation 1 for determining the aggregate application rate for sweep test:

$$\text{Aggregate weight } (\frac{kg}{m^2}) = \left(\frac{A(202.1X - 15.8)}{100} + \frac{B(146.4X - 4.7)}{100} \right) * \frac{1}{61.6} \qquad (1)$$

where A is the percentage of aggregate grade 1 from 9.5 to 6.3 mm, B is the percentage of aggregate grade 2 from 6.3 to 4.75 mm, and X is the bulk specific gravity.

Equation 1 resulted in an application rate of 2.7 kg/m^2 (5.0 lb/yd^2) which was used throughout this research.

To avoid cross-contamination, special tools and cleaning procedures were used. The cutting tool used to prepare the specimens was a ceramic knife instead of a metal knife. Before cutting each specimen, the ceramic knife was cleaned with gasoline to dissolve asphalt residual, followed by deionized (DI) water rinsing. Then, the knife was cleaned again with acetone to remove gasoline residual, and then rinsed with DI water. This procedure was followed exactly for each specimen during the experiment.

Task 1: Leaching Behavior of Heavy Metals from Bare Crumb Rubber

It was found through the particle size distribution that the cryogenic crumb rubber had a representative particle size between 2.0–4.75 mm, and the ambient crumb rubber had a representative particle size between 4.75–9.52 mm. As a result, these two samples were collected and used for the leaching experiment. The leaching experiments were conducted under different pH conditions by following EPA method 1313. A solid-to-liquid ratio of 1:10 was used. Pure water (MQ water) was used as the leaching liquid. The pH of different leaching bottles was adjusted by adding different volumes of stock nitric acid or sodium hydroxide solution at the beginning of the leaching experiment. Several types of control experiments were also performed. Even though EPA 1313 recommends 2 N/M HNO3 and 1 N/M KOH/NaOH for the test, 6 M HNO3 and 10 M NaOH were used to control the pH because the solution is N.I.S.T traceable, so we did not dilute to make it to a lower concentration (2 M HNO3 or 1 M NaOH). Besides this, use of a high concentration acid/base can also minimize the sample volume change caused by acid/base addition. The experimental matrix is shown in Table 1.

The experimental procedure started with adding 5 g of the sample into each of the 125 mL pre-acid cleaned plastic leaching bottles (except the blanks) and then adding 50

mL of MQ water into each of the leaching bottles. After that, different volumes of nitric acid or sodium hydroxide solution were added into different bottles to adjust pH; then, all bottles were sealed tightly. All bottles were then shaken for 24 hours at 180 rpm under room temperature. After shaking, all bottles were settled for 1 hour. The supernatant was then filtered through 0.22 μm nylon membrane filter. A partial filtrate was then used to measure pH and TDS. The remaining filtrate was acidified with trace metal grade nitric acid to a pH<2. Finally, thirteen elements were analyzed using ICP-MS, GFAA, or flame AA after appropriate dilution with 1% HNO_3 solution if needed.

Task 2: Acid-Extractable Metal Contents from Chip Seal Samples

In this task, chip seal specimens made of ambient crumb rubber and two asphalt emulsions were digested with acid for heavy-metal availability testing. The digestion experiment was conducted in a microwave digester (ETHOS E, MILESTONE) using EPA method 3051A with slight modifications. The mixture of concentrated trace metal grade hydrochloric acid and nitric acid was used as the digestion solution. Several types of control experiments, spike recovery, and blank were also performed (Table 2).

The digestion procedure started with weighing 0.2 g sample into a digestion vessel and then adding 3 mL of trace metal grade hydrochloric acid and 9 mL of nitric acid. Sample duplicate, sample spike, and blank were included using different vessels. The digestion vessels were sealed and loaded into the microwave digester. The digestion program included a 10-min ramp to 180 °C with a 10-min hold, followed by a 10-min cooling time. The digestion vessels were then removed from the digester and cooled for one hour. The solution was then transferred to pre-acid cleaned 50 mL centrifuge tubes to dilute to 50 mL with MQ water. Finally, 13 selected elements in the digestion solution were

measured using ICP-MS or flame AA after appropriate dilutions with 1% HNO_3 (if needed) and filtration through 0.22 μm nylon membrane filter.

Task 3: Leaching of Chip Seal Samples Under a Simulated Acid Rain Condition

In this task, the leaching behavior of different chip seal samples was tested at a pH of 5 following EPA method 1312. The tests were performed by adding extraction fluid with a pH of 5 (containing sulfuric acid and nitric acid at a ratio of 60:40) to the chip seal at a solid-to-liquid ratio of 1:20 followed by mixing at a rate of 180 rpm on a mechanical shaker for 24 h. Several control bottles were also included. The sample information is shown in Table 3.

The test procedure started by preparing the chip seal specimens according to the aggregate and emulsion amounts mentioned before in the Chip Seal Specimens' Preparation section. Chip seal specimens contained ambient crumb rubber were mixed with each type of asphalt emulsion. Other specimens were prepared using mineral aggregate with each type of asphalt emulsion. A control group included each of the asphalt emulsions, crumb rubber, and mineral aggregates. The sample size was reduced by cutting the specimens with a ceramic knife and putting them through standard size sieves:- 3/8", 1/4", and No.4. The retained portion of the sample on No.4 sieve was used for this experiment (size range 4.75–6.30 mm). The pH 5 extraction fluid was then prepared by adding 16.5 μL acid mixture (acid mixture prepared by adding 0.15 g H_2SO_4 and 0.10 g HNO_3 in 20 mL MQ water) into 100 mL MQ water in a 125 mL pre-acid cleaned plastic bottles. After that, five grams of sample was added to each leaching bottles (except the blanks). Bottles were sealed tightly after the addition of extraction fluid and sample. The leaching bottles were then shaken for 24 hours at 180 rpm under room temperature and then settled for 1

hour. The supernatant was then filtered through a 0.22 μm nylon membrane filter. The partial filtrate was then used to measure pH and TDS. The remaining filtrate was acidified with trace metal grade nitric acid to a pH < 2. Finally, the heavy metal concentrations in the acidified filtrate samples were determined using ICP-MS or flame AA. Appropriate dilution with 1% HNO_3 was needed before ICP-MS measurement.

Task 4: Effect of pH on Metal Leaching of Chip Seal Samples

In this task, the effect of pH on the leaching behavior of different specimens was tested with pH ranging between 4 and 10 following EPA method 1313. A solid-to-liquid ratio of 1:10 was used in this experiment. Several control experiments were also performed. The experiment procedures were similar to the acid rain leaching experiment, except the pH of the leaching bottles was adjusted individually. The detailed experimental information is shown in Table 4.

Quality Assurance/Quality Control

To ensure high-quality data, most of the recommended QA/QC by the EPA was followed. For analysis using ICP-MS, US EPA method 200.8 QC guidelines were closely followed. ICP-MS was calibrated with standard solutions diluted from a calibration standard mixture. The linear ranges of the calibration were determined and used for the quantitative analysis of the samples. Detailed control samples are listed in Table 1, 2, 3, and 4. Laboratory reagent blank was tested to check any procedural contamination. The blank sample was prepared and measured using the same procedures as for the samples except no solid sample was used. The method detection limits (MDLs) for the leaching test were determined by instrumentation detection limits (IDLs) where MDLs were 10 times the IDLs. The MDLs for the screening test and digestion test were 20 times the IDLs. To

ensure good reproducibility, duplicated samples were performed for some samples. The precision of the duplication was expressed as the relative percentage difference (RPD) and was calculated using the equation 2 below.

$$RPD\ (\%) = 100 \times (C_h - C_1) / C_{av} \quad (2)$$

where

C_h is detected high concentration of duplicated sample,

C_l is detected low concentration of duplicated sample, and

C_{av} is the average of the C_h and C_l

Sample spike was tested by adding known concentration standards into the leached sample solution before performing the analysis. The spike recoveries (%) were calculated by the following equation:

Spike recovery (%) = 100 x (detected conc. of spiked sample–control sample)/Spiked concentration

4. RESULTS AND DISCUSSION

Task 1: Leaching Behavior of Heavy Metals from Bare Crumb Rubber

The metal leaching concentration from the rubber particle specimens as a function of pH is shown in Figure7 where most of the rubber specimens were tested in very high or low pH conditions to determine which rubber, i.e., ambient or cryogenic had more leachable metal. The major heavy metal leached out from the bare rubber is zinc (Zn), followed by copper (Cu), and barium (Ba). Note that Zn has the highest concentration in rubber (Figure 6). In the leaching solution, Zn concentration is in parts per million which is significantly higher than any other metals. The leaching of most metals from both the cryogenic crumb rubber (2–4.75 mm) and the ambient crumb rubber (4.75–9.32 mm) was

consistent, although the sizes were different. Furthermore, generally the ambient crumb rubber heavy metal leaching was significantly less than that of the cryogenic rubber and hence was selected for further research in this project.

Task 2: Acid-Extractable Metal Contents from Chip Seal Specimens

The acid extractable metal content in chip seal specimens was converted from metal concentration in digestion solution based on the final volume of digestion solution and mass of the sample. Table 5 shows the metal contents of chip seal specimens. The results show the major metal content in the rubber was Zn, which was about 1.6% of the total rubber weight. The major metal content in both types of asphalt was Ni, but generally, the content of all metals was very low (some of them were below the method's detection limit). The reproducibility and spike recovery of the rubber sample were not good through the microwave digestion method, probably because of the incomplete digestion of rubber sample. After microwave digestion, there were some solids found in the rubber digestion vessel, but not in the asphalt digestion vessel.

Task 3: Leaching Under Simulated Acid Rain Condition

The experimental results using simulated acid rain as the leaching solution are shown in Table 6. From the test results, trace amount heavy metal was leached from the sample after 24 hours and all the concentrations are below EPA drinking water standard.

Task 4: Effect of pH on Metal Leaching from Chip Seal

The soluble metal concentration as a function of pH for Task 4 (pH effect) is shown in Figure 8. It indicated that when rubber was encapsulated in emulsion for the chip seal, there was a significant reduction of heavy metal, especially Zn, leaching under different pH conditions. Approximately 50% reduction of Zn leaching was found when compared to

the bare rubber. The leaching values of Co, Cu, and Ba were also reduced when rubber was used in asphalt emulsion. The leached concentrations of Be, Cr, As, Cd, Sb, Tl, and Pb were very low, i.e., below or close to the method's detection limit in the cases of crumb rubber, emulsion, and chip seal samples. Besides the effect of using asphalt emulsion to cover the rubber particles' surface, the elevated pH condition also reduced the metal leaching in all types of samples. From the comparison between the control group and chip seal, the rubber contributed to most of the metal leaching, except Ni, which is the major metal element in asphalt emulsion.

5. CONCLUSIONS

This study revealed the following findings and conclusions:

1. Using the crumb rubber that comes from scrap tires as a mineral aggregate replacement in chip seal pavement does not have a negative environmental impact in terms of heavy metal leaching. The toxic heavy metals leached from the recycle rubber or rubberized chip seal are below EPA drinking water standards.
2. The major leached heavy metal from the recycled bare rubber particles is Zn, which is consistent with the tire component. However, Zn is not regulated in primary drinking water regulations.
3. Under different pH conditions, a significant reduction of heavy metal leaching was recorded when rubber is used with emulsion in the form of chip seal pavement because asphalt is hydrophobic and prohibited the contact of tire and solution. About a 50% reduction of Zn leaching was recorded with chip seal specimens compared with the leaching from bare crumb rubber.

4. The metal leaching in all types of samples including rubber, asphalt emulsion, and chip seal decreased with the increase in pH value.
5. The cryogenic crumb rubber has a different metal leaching behavior than the ambient crumb rubber, depending on the pH value.

ACKNOWLEDGEMENTS

This research was conducted at the Missouri University of Science and Technology and supported by the Missouri Department of Natural Resources and Missouri Department of Transportation. Donations of the asphalt cement and emulsions by Vance Brothers are appreciated. However, any opinions, findings, conclusions, and recommendations presented in this paper are those of the authors and do not necessarily reflect the views of the sponsors.

Table 1. Sample Matrix for Leaching Behavior from Bare Crumb Rubber.

Sample ID	**Rubber (5 g)**	**Acid/Base**
F+5	Cryogenic	1.0 mL 6M HNO3
F+4	Cryogenic	0.8 mL 6M HNO3
F+3	Cryogenic	0.6 mL 6M HNO3
F+2	Cryogenic	0.4 mL 6M HNO3
F+2D*	Cryogenic	0.4 mL 6M HNO3
F+1	Cryogenic	0.2 mL 6M HNO3
F	Cryogenic	0
F-1	Cryogenic	0.2 mL 10M NaOH
F-2	Cryogenic	0.4 mL 10M NaOH
F-3	Cryogenic	0.6 mL 10M NaOH
F-4	Cryogenic	0.8 mL 10M NaOH
F-5	Cryogenic	1.0 mL 10M NaOH
MQ	0	0
MQ+HNO3	0	1.0 mL 6M HNO3
MQ+NaOH	0	1.0 mL 10M NaOH
UF+5	Ambient	0.6 mL 1M HNO3
UF+4	Ambient	0.4 mL 1M HNO3
UF+3	Ambient	0.2 mL 1M HNO3
UF+2	Ambient	0.1 mL 1M HNO3
UF+1	Ambient	0.2 mL 0.1M HNO3
UF	Ambient	0
UF-1	Ambient	0.2 mL 0.1M NaOH
UF-2	Ambient	0.1 mL 1M NaOH
UF-2D*	Ambient	0.1 mL 1M NaOH
UF-3	Ambient	0.2 mL 1M NaOH
UF-4	Ambient	0.4 mL 1M NaOH
UF-5	Ambient	0.6 mL 1M NaOH
MQ	0	0

Note: * "D" represents sample duplication
"F" represents cryogenic rubber
"UF" represents ambient rubber

Table 2. Sample Matrix for Acid Digestion Experiment.

Sample ID	**Sample Component (0.2 g)**
T	Ambient rubber
T(D)*	Ambient rubber
Tspike	Ambient rubber with spike
A1	Emulsion 1
A2	Emulsion 2
A2(D)	Emulsion 2
A2spike	Emulsion 2 with spike
Blank	N.A.

Table 3. Sample Matrix for Simulated Acid Rain Experiment.

Sample ID	**Sample (5 g)**	**Liquid Volume**
T+A1	Rubberized chip seal with emulsion 1	100 mL extraction fluid
T+A2	Rubberized chip seal with emulsion 2	100 mL extraction fluid
T+A2(D)*	Rubberized chip seal with emulsion 2	100 mL extraction fluid
A+A1	Conventional chip seal with emulsion 1	100 mL extraction fluid
A+A2	Conventional chip seal with emulsion 2	100 mL extraction fluid
A1	Emulsion 1	100 mL extraction fluid
A2	Emulsion 2	100 mL extraction fluid
T	Ambient rubber	100 mL extraction fluid
A	Mineral aggregate	100 mL extraction fluid
Acid	0	100 mL extraction fluid
MQ	0	100 mL MQ water

Table 4. Sample Matrix for Effect of pH on Metal Leaching Experiment.

Sample ID	**Sample Component (5 g in 50 mL MQ)**	**Acid/Base**
TA1-1	Chip seal with emulsion 1	0.20 mL 0.1 M HNO_3
TA1-2	Chip seal with emulsion 1	0.14 mL 0.1 M HNO_3
TA1-2(D)*	Chip seal with emulsion 1	0.14 mL 0.1 M HNO_3
TA1-3	Chip seal with emulsion 1	0.07 mL 0.1 M HNO_3
TA1-4	Chip seal with emulsion 1	0
TA1-5	Chip seal with emulsion 1	0.05 mL 0.1 M NaOH
TA1-6	Chip seal with emulsion 1	0.14 mL 0.1 M NaOH
TA1-7	Chip seal with emulsion 1	0.20 mL 0.1 M NaOH
TA2-1	Chip seal with emulsion 2	0.20 mL 0.1 M HNO_3
TA2-1(D)	Chip seal with emulsion 2	0.20 mL 0.1 M HNO_3
TA2-2	Chip seal with emulsion 2	0.14 mL 0.1 M HNO_3
TA2-3	Chip seal with emulsion 2	0.08 mL 0.1 M HNO_3
TA2-4	Chip seal with emulsion 2	0
TA2-5	Chip seal with emulsion 2	0.06 mL 0.1 M NaOH
TA2-6	Chip seal with emulsion 2	0.14 mL 0.1 M NaOH
TA2-7	Chip seal with emulsion 2	0.20 mL 0.1 M NaOH
T1	Ambient crumb rubber	0.40 mL 0.1 M HNO_3
T2	Ambient crumb rubber	0.30 mL 0.1 M HNO_3
T3	Ambient crumb rubber	0.20 mL 0.1 M HNO_3
T3(D)	Ambient crumb rubber	0.20 mL 0.1 M HNO_3
T4	Ambient crumb rubber	0.08 mL 0.1 M HNO_3
T5	Ambient crumb rubber	0.06 mL 0.1 M NaOH
T6	Ambient crumb rubber	0.14 mL 0.1 M NaOH
T7	Ambient crumb rubber	0.20 mL 0.1 M NaOH
A1-1	Emulsion 1	0.05 mL 0.1 M HNO_3
A1-1(D)	Emulsion 1	0.05 mL 0.1 M HNO_3
A1-2	Emulsion 1	0
A1-3	Emulsion 1	0.03 mL 0.1 M NaOH
A1-4	Emulsion 1	0.06 mL 0.1 M NaOH
A1-5	Emulsion 1	0.09 mL 0.1 M NaOH
A1-6	Emulsion 1	0.12 mL 0.1 M NaOH
A1-7	Emulsion 1	0.30 mL 0.1 M NaOH
A2-1	Emulsion 2	0.08 mL 0.1 M HNO_3
A2-2	Emulsion 2	0.05 mL 0.1 M HNO_3
A2-3	Emulsion 2	0.02 mL 0.1 M HNO_3
A2-4	Emulsion 2	0.03 mL 0.1 M NaOH
A2-5	emulsion 2	0.06 mL 0.1 M NaOH
A2-5(D)	emulsion 2	0.06 mL 0.1 M NaOH
A2-6	emulsion 2	0.15 mL 0.1 M NaOH
A2-7	emulsion 2	0.30 mL 0.1 M NaOH
Acid	N.A.	0.4 mL HNO_3
Base	N.A.	0.3 mL NaOH
MQ	Blank	N.A.

Table 5. Metal Concentration in Leaching Solution of rubber and emulsions.

Sample ID	Be (µg/g)	Cr (µg/g)	Co (µg/g)	Ni (µg/g)	Cu (µg/g)	As (µg/g)	Se (µg/g)	Cd (µg/g)	Sb (µg/g)	Ba (µg/g)	Tl (µg/g)	Pb (µg/g)	Zn* (mg/g)
T	<MDL	4.97	286	3.28	244.9	24.78	2.68	0.73	2.22	4.42	<MDL	1.73	17.06
T(D)	<MDL	5.52	227.7	3.16	59.63	26.65	6.58	0.96	2.44	4.97	<MDL	2.95	15.94
T spike	2.54	6.13	30.41	31.48	78.29	24.05	7.11	2.81	3.73	5.88	1.74	20.47	21.5
Spiked Conc.	2.5	2.5	10	25	50	2.5	5	2.5	2.5	2.5	2.5	10	5
T recovery (%)	101.8	35.11	-209.6	113	-147.9	-66.79	49.55	78.33	55.95	47.49	69.54	181.2	100
A1	<MDL	4.4	<MDL	65	4.73	21.72	0.87	<MDL	0.98	1.58	<MDL	0.57	0.09
A2	<MDL	5.91	<MDL	72.96	<MDL	26.57	0.96	<MDL	1.2	1.28	<MDL	<MDL	0.12
A2(D)	<MDL	5.21	<MDL	67.05	<MDL	23.62	0.7	<MDL	0.78	1.28	<MDL	<MDL	0.11
A2spike	2.62	8.19	1.94	125	30.65	29.6	4.93	2.64	3.41	3.88	1.7	5.85	7.05
Spiked Conc.	2.5	2.5	2.5	50	25	2.5	5	2.5	2.5	2.5	2.5	5	10
A2 recovery (%)	104.7	105.1	77.62	110	122.6	180.2	82.01	105.4	96.92	103.8	68.00	117	70.5
Blank	<MDL	2.61	<MDL	<MDL	<MDL	19.57	1.05	<MDL	0.8	0.44	<MDL	<MDL	<MDL
MDL	0.125	0.25	0.625	2.5	2.5	0.125	0.5	0.125	0.125	0.125	0.125	0.5	0.005
T RPD (%)	N.A.	10.49	22.73	3.88	121.7	7.28	84.22	27.09	9.33	11.82	N.A.	52.12	6.73
A2 RPD (%)	N.A.	12.67	N.A.	8.44	N.A.	11.77	31.67	N.A.	42.12	0.34	N.A.	N.A.	6.56

Table 6. Metal Concentration in Leaching Solution Under Simulate Acid Rain of Rubberized Chip Seal.

Sample ID	pH	TDS (mg/L	Be (µg/L)	Cr (µg/L)	Co (µg/L)	Ni (µg/L)	Cu (µg/L)	As (µg/L)	Se (µg/L)	Cd (µg/L)	Sb (µg/L)	Ba (µg/L)	Pb (µg/L)	Tl (µg/L)	Zn** (mg/L)
T+A1	7.10	21.20	<MDL	<MDL	3.25	<MDL	37.52	<MDL	<MDL	<MDL	<MDL	11.94	<MDL	<MDL	0.46
T+A2	6.51	16.10	<MDL	<MDL	4.22	<MDL	<MDL	<MDL	9.72	<MDL	<MDL	11.89	<MDL	<MDL	0.51
T+A2(D)	7.35	17.90	<MDL	<MDL	3.54	<MDL	<MDL	<MDL	<MDL	<MDL	0.61	12.41	<MDL	<MDL	0.29
A+A1	7.59	17.40	<MDL	<MDL	0.64	<MDL	28.16	<MDL	<MDL	<MDL	<MDL	5.83	<MDL	<MDL	<MDL
A+A2	6.95	16.90	<MDL	<MDL	0.72	<MDL	17.29	<MDL	<MDL	<MDL	<MDL	5.17	<MDL	<MDL	<MDL
A1	4.40	24.00	<MDL	<MDL	0.97	10.73	49.75	<MDL	<MDL	<MDL	<MDL	<MDL	<MDL	<MDL	0.24
A2	4.28	26.20	<MDL	<MDL	1.00	<MDL	<MDL	<MDL	8.34	<MDL	<MDL	<MDL	<MDL	<MDL	0.18
T	7.10	12.60	<MDL	<MDL	9.50	<MDL	16.08	<MDL	<MDL	<MDL	3.13	30.68	2.11	<MDL	0.40
A	7.26	5.48	<MDL	<MDL	<MDL	<MDL	<MDL	<MDL	<MDL	<MDL	<MDL	0.74	<MDL	<MDL	<MDL
Acid	4.60	N.A.	<MDL	<MDL	<MDL	<MDL	<MDL	<MDL	<MDL	<MDL	<MDL	<MDL	<MDL	<MDL	<MDL
MQ	N.A.	N.A.	<MDL	<MDL	<MDL	<MDL	<MDL	<MDL	<MDL	<MDL	<MDL	<MDL	<MDL	<MDL	<MDL
MDL			0.50	1.00	0.50	10.00	10.00	0.50	2.00	0.50	0.50	0.50	2.00	0.50	0.10
EPA limits	6.5-8.5	500	4	100	N.A.	N.A.	1300	10	50	5	6	2000	15	2	5
T+A1 Spike recovery (%)			104.00	94.79	99.34	85.25	8.94	103.88	104.79	99.60	104.64	102.08	95.95	104.41	N.A.
T+A2 RPD (%)	12.12	10.59	N.A.	N.A.	17.63	N.A.	N.A.	N.A.	N.A.	N.A.	N.A.	4.27	N.A.	N.A.	54.95

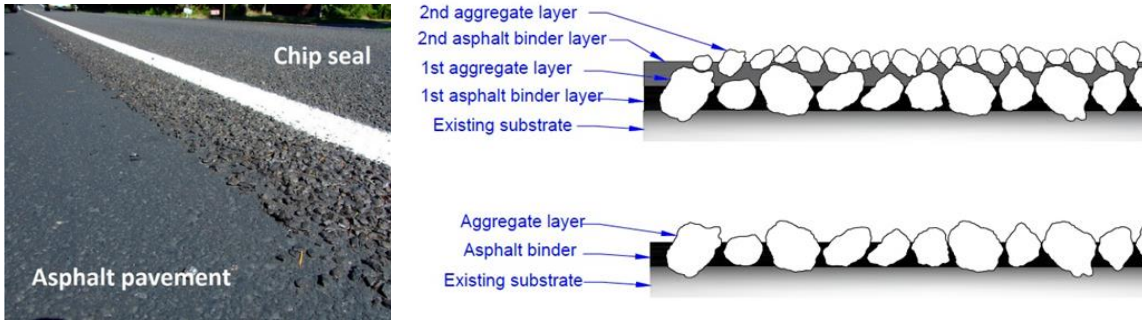

(a) (b)

Figure 1. (a) Chip seal vs asphalt pavement, and (b) Types of chip seal.

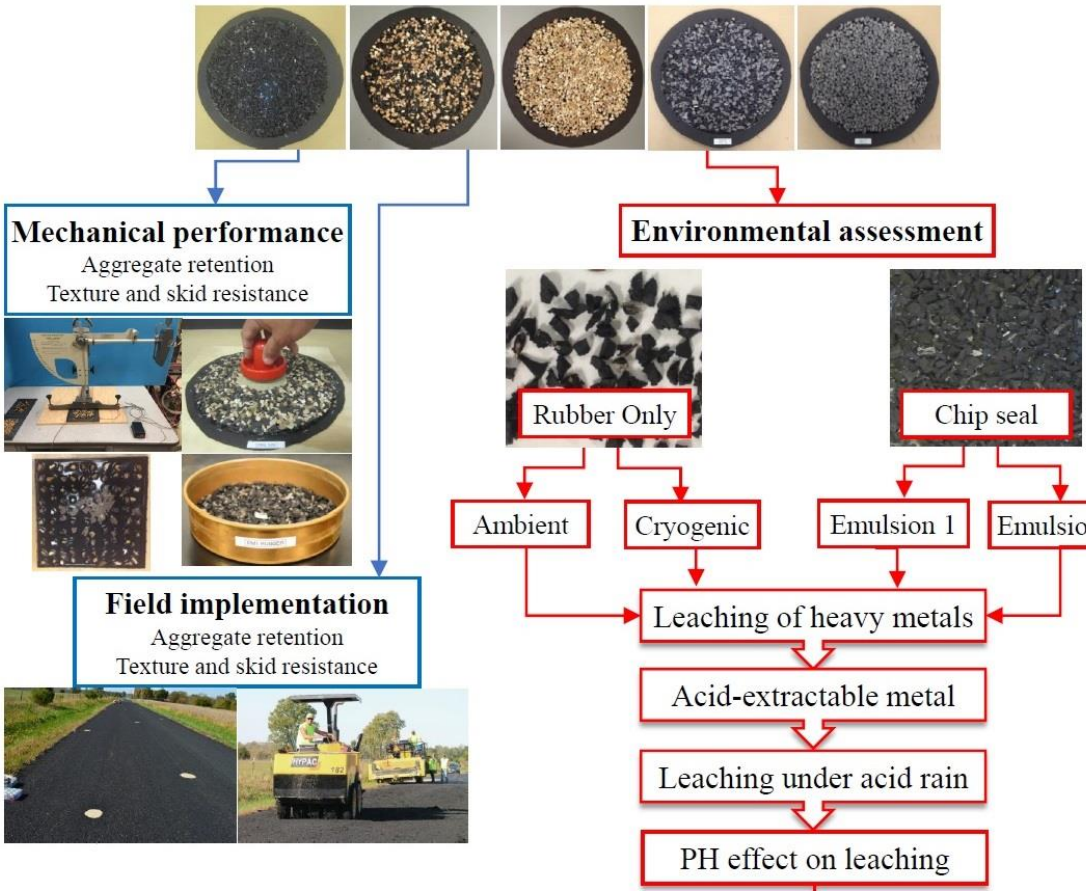

Figure 2. Schematic overview of the project.

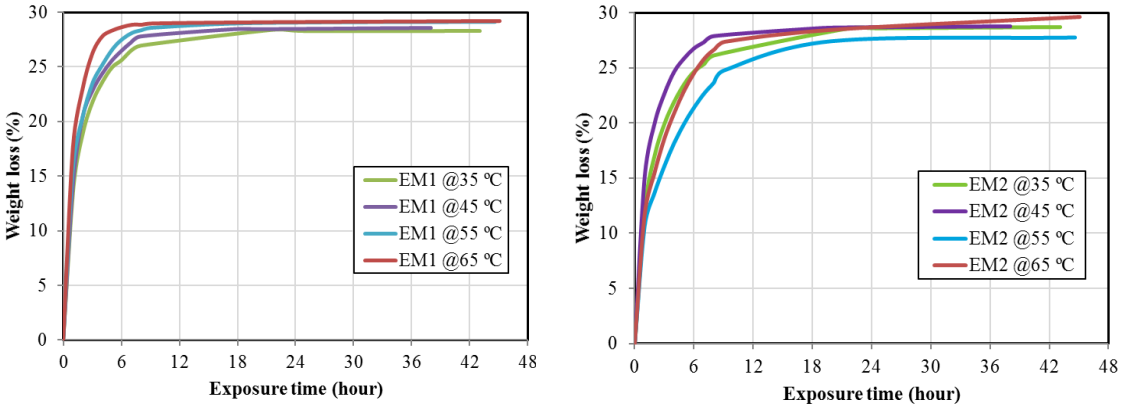

(a) (b)

Figure 3. Emulsion weight loss due to water break out, (a) Emulsion 1, and (b) Emulsion-2.

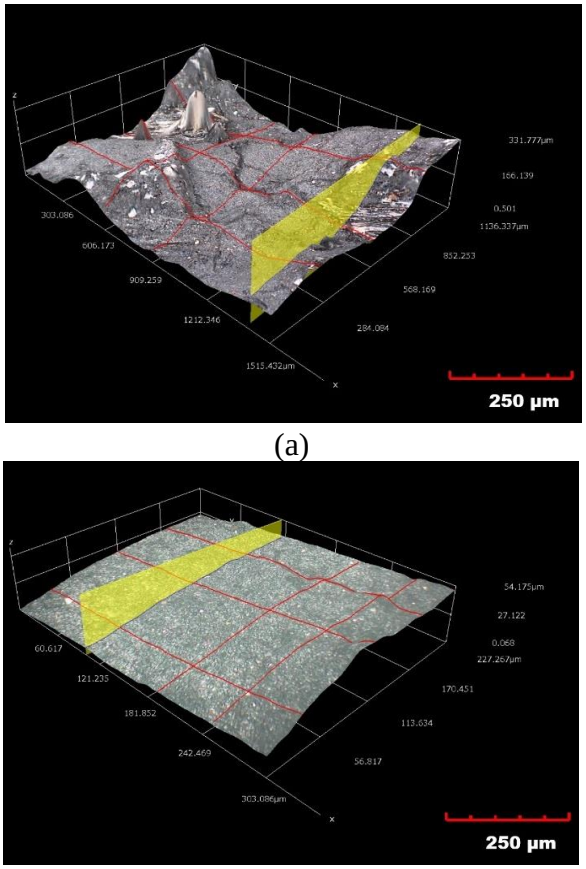

(a)

(b)

Figure 4. Microscopic results of the surface of the crumb rubber aggregates in range of 250 µm (a) Ambient, and (b) Cryogenic.

Figure 5. Field implementation of rubberized chip seal with 100% crumb rubber replacement ratio.

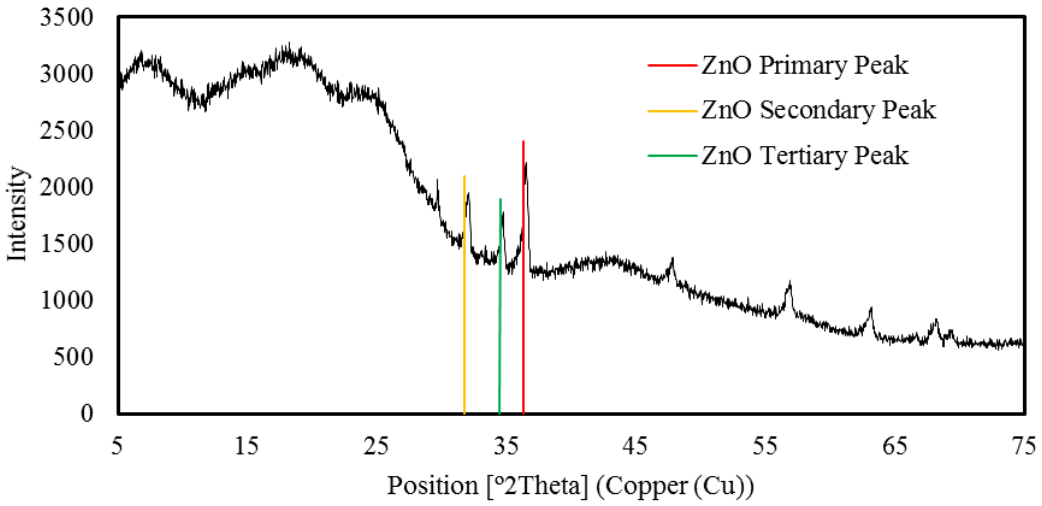

Figure 6. X-Ray diffraction of crumb rubber.

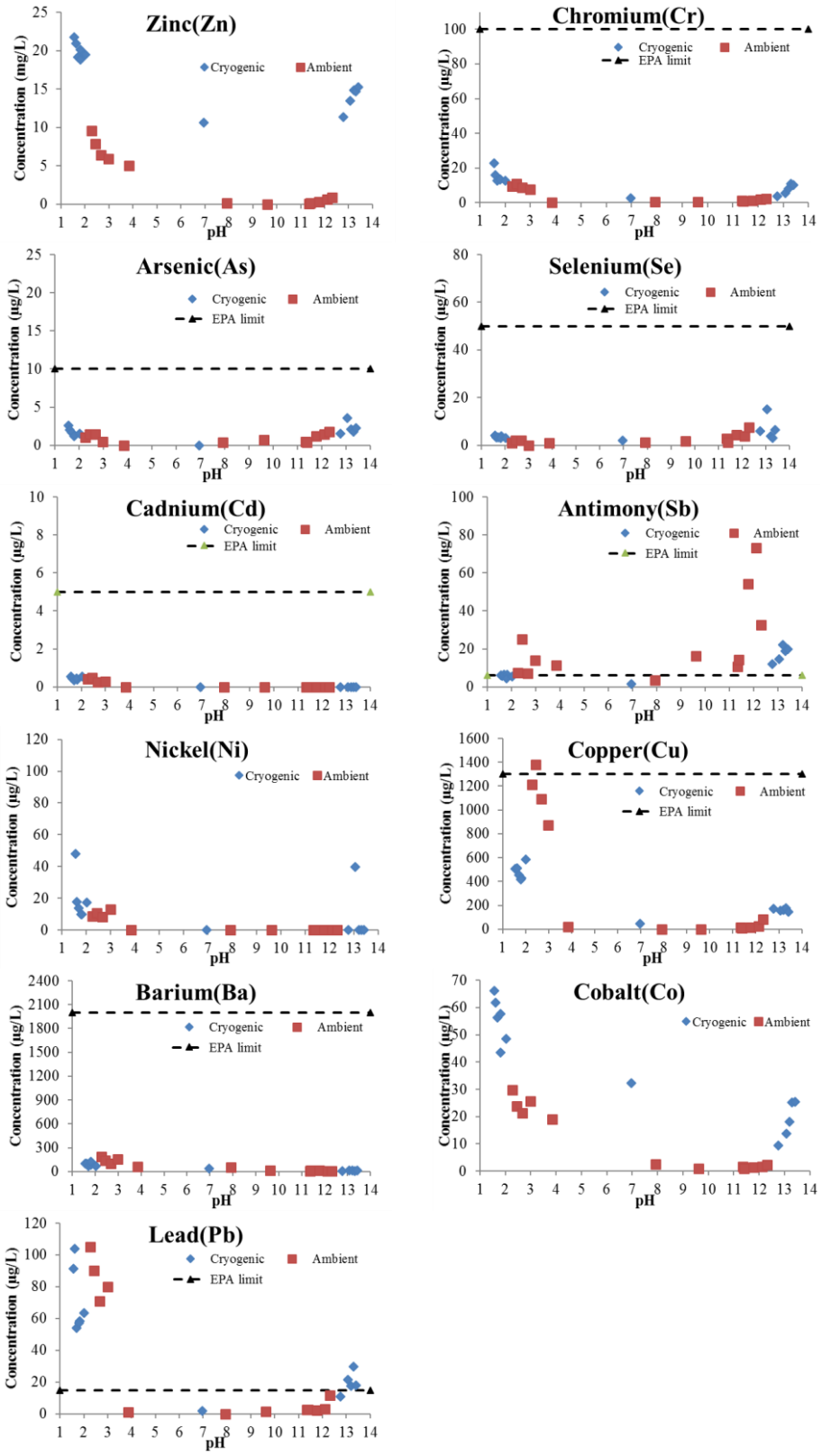

Figure 7. Metal concentration in leaching solution as function of pHs for rubber only.

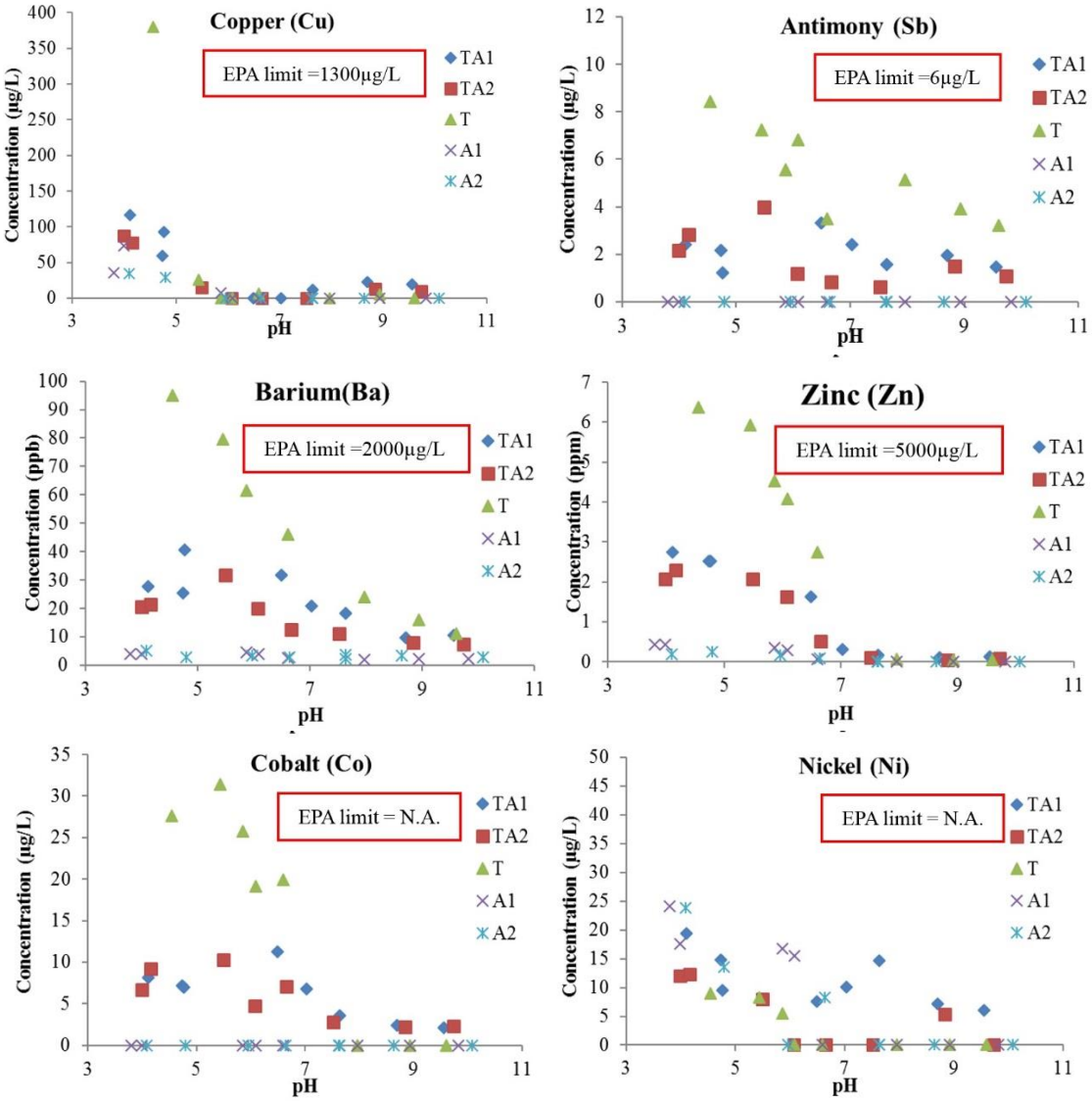

Figure 8. Metal concentration in leaching solution as a function of pHs for rubberized chip seal. Note: Other elements are close or below MDLs.

REFERENCES

1. RMA, R.M.A., 2015 U.S. Scrap Tire Management Summary, in Wasington, DC. 2016.

2. Gheni, A.A., et al., Texture and design of green chip seal using recycled crumb rubber aggregate. *Journal of Cleaner Production, 2017*. 166: p. 1084-1101.

3. Gheni, A.A., M.A. ElGawady, and J.J. Myers, Mechanical Characterization of Concrete Masonry Units Manufactured with Crumb Rubber Aggregate. *ACI Materials Journal, 2017*. 114(01).

4. Moustafa, A. and M.A. ElGawady, Strain rate effect on properties of rubberized concrete confined with glass fiber–reinforced polymers. *Journal of Composites for Construction, 2016*. 20(5): p. 04016014.

5. Siddique, R. and T.R. Naik, Properties of concrete containing scrap-tire rubber–an overview. *Waste management, 2004*. 24(6): p. 563-569.

6. Moustafa, A., A. Gheni, and M.A. ElGawady, Shaking-Table Testing of High Energy–Dissipating Rubberized Concrete Columns. *Journal of Bridge Engineering, 2017*. 22(8): p. 04017042.

7. Turgut, P. and B. Yesilata, Physico-mechanical and thermal performances of newly developed rubber-added bricks. *Energy and Buildings, 2008*. 40(5): p. 679-688.

8. Gheni, A., M.A. ElGawady, and J.J. Myers, Thermal Characterization of Cleaner and Eco-Efficient Masonry Units Using Sustainable Aggregates. *Journal of Cleaner Production, 2017*.

9. Ang, G. and V. Marchal, Mobilising private investment in sustainable transport: The case of land-based passenger transport infrastructure. *OECD Environment Working Papers, 2013*(56): p. 0_1.

10. Presti, D.L., Recycled tyre rubber modified bitumens for road asphalt mixtures: a literature review. *Construction and Building Materials, 2013*. 49: p. 863-881.

11. Gransberg, D. and D. James, Chip Seal Best Practices, National Cooperative Highway Research Program Synthesis 342. *Transportation Research Board, National Academies, Washington, DC, 2005*.

VI. DURABILITY PROPERTIES OF CLEANER CEMENT MORTAR WITH BY-PRODUCTS OF TIRE RECYCLING

Ahmed A. Gheni , Hayder Alghazali , Mohamed A. ElGawady, John J. Myers and Dimitri Feys

ABSTRACT

This study investigates using rubber-fiber powder (RFP), which is by-products of tire recycling, as an additive in a cement-based mortar. Five different RFP ratios of 5, 10, 15, 20, and 25% were used in this study as an additive filler side by side with reducing the cement content by the same amount. In addition to the fresh properties and the heat of hydration, the physical characterization of the rubberized mixtures including the compressive, and flexural strength the hardened density, absorption, and air voids were investigated. The results were compared to those where the cement content was reduced without adding the RFP as well as a reference mortar mixture having 0% RFP. To evaluate the new rubberized mortar as a reinforcement corrosion protector, the bulk and surface electrical resistivity, the accelerated carbon dioxide penetration, and the rapid chloride ion penetration tests were determined. Although there was a reduction in some of the mechanical characterizations, this study revealed that the recycled rubber-fiber powder could be used in the mortar as an additive to provide more corrosion resistance and less heat of hydration compared to the control mixture. Adding the RFP lowered and delayed the peak temperature for the heat of hydration compared to reducing the cement content only. From the durability side, mortar mixtures with up to 20% RFP showed an improved reinforcement corrosion resistance by increasing both bulk and surface electrical resistivity.

1. INTRODUCTION

The United States annually produces about 250 million scrap tires (RMA 2018); furthermore, it is expected that the number of vehicles will nearly double worldwide by 2040, which results in even larger environmental concerns of how to properly dispose or deal with scrap tires. Since scrap tires are not a biodegradable material, there is a major concern with fire hazards. Rubber tires burn very quickly and are very difficult to extinguish, which can lead to months of fire with a high rate of toxic gas emissions as well as surface and groundwater pollution due to the melted oily residue from the burned tires. It is very difficult to prevent or quench the oxygen supply of the donut-shaped tire since it contains 75% void space, which increases the fire exposure risk of scrap tires in landfills.

In addition, scrap tires serve as a fertile breeding ground for mosquitoes and other insects due to their ability to collect and retain water and heat. With the serious threat of the mosquito-borne Zika virus, the focus not only on dealing with the new generated scrap tires but also cleaning up old stockpiles of scrap tires.

Reusing scrap tires is the best practical way to deal with them due to the lack of both technical and economical disposal mechanisms of them. Current popular use of scrap tires includes using their recycled crumb rubber as mulch in farms or playgrounds and a binder modifier in asphalt; however, these applications do not consume a significant amount of the scrap tires annually created in the USA. Another widely used application for the scrap tires was using them as a fuel in cement production kilns; however, their use resulted in higher CO_2 and Sulphur dioxide emissions during the burning process affecting the chemical composition of cement, which resulted in delayed ettringite formation and potential cracking in concrete members (Olorunniwo 1994).

Seventy-three percent of all materials used in the United States, by weight, are construction materials (Horvath 2004). Therefore, there is a promising opportunity to find a new home for a large portion of scrap tires by using them as a partial replacement component within construction materials. For example, the behavior of rubberized concrete where crumb rubber partially replaced mineral aggregate have been extensively investigated. In terms of the fresh properties, the slump and workability decreased with the increase of rubber content (Khatib and Bayomy 1999, Moustafa and ElGawady 2015). The measured air content was higher in rubberized concrete than in reference mixtures without rubber (Fedroff et al. 1996, Khatib and Bayomy 1999, Siddique and Naik 2004). Rubber replacement also decreased the compressive, tensile, and flexural strength due to rubber's relatively low stiffness and the poor bond between the rubber particles and cement paste (Siddique and Naik 2004, Ghaly and Cahill IV 2005, Gou and Liu 2014, Youssf et al. 2014, Hesami et al. 2016, Thomas and Gupta 2016, Gheni et al. 2017). Using large rubber particles were also more influential in reducing the compressive strength of rubberized concrete than using small particles. This influence is due to the low stiffness of rubber particles which makes it act like air voids where their effect increase with increasing the volume of each void (Eldin and Senouci 1993, Fattuhi and Clark 1996, Batayneh et al. 2008). Furthermore, the elastic modulus of rubberized concrete decreased with the increase of rubber content since rubber has lower stiffness compared to aggregate. However, using lower stiffness materials, i.e., rubber increased the ultimate strain of rubberized concrete (Ganjian et al. 2009).

Many desirable improvements were achieved by using recycled rubber in concrete, such as lowering the unit weight, improving the ductility and toughness, and increasing the

crack resistance capacity. Rubberized concrete exhibited better freeze and thaw durability and sulfate resistance compared to conventional concrete mixtures (Savas et al. 1997, Benazzouk and Queneudec 2002, Yung et al. 2013, Thomas and Gupta 2015, Liu et al. 2016, Richardson et al. 2016, Thomas et al. 2016). The freeze and thaw of rubberized concrete can be further improved should a finer particle size, up to 20 μm, be used (Richardson et al. 2016), which is comparable to the size of cement particles. However, it is very expensive to produce recycled rubber with a particle size smaller than 1.5 mm (Yang et al. 2011, Shu and Huang 2014).

Processing the scrap tie results in about 65% crumb rubber in different sizes and 35% solid waste that includes steel cords and fibers, nylon fiber, contaminated rubber, and rubber-fiber powder (Granuband Macon 2017). About 25% of this solid waste, which equates to 8% of the total scrap tires volume, is rubber powder and nylon fiber (RFP), which is still going to landfills. In this study, as an Eco-friendly alternative to an expensive materials, rubber and nylon fiber powder (RFP) with a size smaller than 75 μm was collected, as a byproduct of tire recycling plants, and used as a powder filler side by side with reducing the cement content to improve the corrosion protection capacity of cement mortar.

This study used by-products of tire recycling as a sustainable alternative to produce rubberized mortar. The fresh properties of rubberized mortar with different RFP ratios were investigated, including workability and fresh mortar density. In addition to the heat of hydration, the mechanical characterization of the rubberized mortar including hardened density, water absorption, compressive strength, flexural strength, and tensile strength were tested. Finally, the bulk and surface electric resistivity, rapid chloride ion penetration

(RCIP), and the depth of carbonation were investigated to evaluate the durability of the new rubberized mortar mixtures. Fig 1 illustrates a schematic overview of the whole paper.

2. MATERIALS AND METHODS

2.1. MATERIAL PROPERTIES

Well-graded (Figure 2a) locally available river sand that meets the grain size distribution of ASTM C33 was used in this study. The waste RFP was obtained from a scrap tire processing factory in Macon, Missouri, USA. The RFP was sieved through a #200 sieve to remove any oversized particles. The particle size distribution of RFP and cement was determined using a laser diffraction analyzer (Figure 2b). Although both the RFP and cement passed #200 sieve (Figure2b), about 25% and 9% of the RFP and cement particles respectively are still shown as having a size larger than #200 sieve since laser diffraction analyzer considers the larger dimension for each particle. For example, fibers or flaky particles with a length larger than 75 μm can pass #200 sieve but it is still considered larger than #200 sieve in laser diffraction analysis. The densities of RFP, cement, and sand were measured (Table 1) per ASTM B923−16 using Ultrapyc 1200e density analysis by the ultimate gas pycnometers.

A 3D digital microscope KH-8700 was used to investigate the RFP particles' shape, and the results showed the existence of nylon fibers as well as the irregular non-spherical shape of rubber particles (Figure 3). The x-ray photoelectron spectroscopy (XPS), which is a surface-sensitive quantitative spectroscopic technique that measures the elemental composition, was used to measure the percentage of rubber vs. nylon fiber in RFP and it was found that the RFP consisted of 76% rubber and 24% nylon fiber by volume.

2.2. EXPERIMENTAL WORK

This study investigated 39 mixtures (Table 2) that were grouped into four groups. Three different groups each had 11 mixtures and having water-to-cement ratios (w/c) of either 0.42, 0.51, or 0.56. The minimum used W/C ratio of 0.42 was selected based on optimization process such that the reference mortar mixture would display a minimum increase in the flow of 40±20% using the mini-slump per ASTM C230/ C230M.

In each group, one reference mixture without rubber and with a cement to sand ratio equal to 1:3 by weight was prepared. Each group also included another ten mixtures either RPF or sand at five different volume ratios of 5, 10, 15, 20 and 25% was added side by side with reducing the cement at the same ratio. The fourth group had six mixtures with w/c ratio of 0.51. One reference mixture and five mixtures where RPF was used as a sand replacement at five different volume ratios of 5, 10, 15, 20, and 25%. This was a very comprehensive approach to decouple the effects decreasing the cement content and adding inactive material being sand or RFP; then, assess the effect of replacing sand with RFP.

A brass conical mold with a height of 50 mm, the diameter of the top opening of 70 mm and diameter of the bottom opening of 100 mm was used to carry out the mini-slump test per ASTM C1437−15 for each mixture right after mixing and 30 minutes later. The fresh density of each mortar mixture was measured using a standard cylinder having a volume of 400 ± 1 mL, packed with mortar, and consolidated by placing the molds on a micro-vibration table for 40 seconds. Using the measured weight of the infill mortar and knowing the volume of the cylinder, the density was calculated. The density, absorption, and voids in hardened mortar were tested according to ASTM C642−13. The heat of hydration was also monitored and recorded for each mixture according to both ASTM

C1679-17 and ASTM C1702-17. All specimens were demolded at the age of one day and were then moist-cured under a relative humidity of 95 ± 5% and a temperature of 23.0 ± 2.0º C until the testing day. Finally, both of the compressive strength and modulus of rupture (MOR) were tested at the age of 28 days according to ASTM C109-16a and ASTM C348–14 respectively, and the results are listed in Table 2.

2.2.1. Density, Absorption, And Air Voids in Hardened Mortar. Concrete cylinders, 100×200 mm, out of each mixture were used to measure the density and voids in hardened mortar according to ASTM C642-13 method which can be used to deduce concrete permeability attribute and it yields results similar to that of vacuum saturation method; however, the former approach is more versatile. The test procedure can be summarized as follows: the oven-dried masses of all specimens were determined followed by saturating them in water and determine their surface-dry masses after immersion for not less than 48 hrs. After boiling the specimens in water for 5 hours, the soaked, boiled, and surface-dried masses were determined. Finally, after suspending the specimens in water, the apparent masses in water after immersion and boiling were determined. Based on the results from this procedure, the following characteristics can be calculated:

$$\text{Absorption after immersion, \%} = [(B - A)/A] \times 100 \quad (1)$$

$$\text{Absorption after immersion and boiling, \%} = [(C - A)/A] \times 100 \quad (2)$$

$$\text{Bulk density, dry} = [A/(C - D)].\rho = g_1 \quad (3)$$

$$\text{Bulk density after immersion} = [B/(C - D)].\rho \quad (4)$$

$$\text{Bulk density after immersion and boiling} = [C/(C - D)].\rho \quad (5)$$

$$\text{Apparent density} = [A/(A - D)].\rho = g_2 \quad (6)$$

$$\text{Volume of permeable pore space (voids), \%} = (g_1 - g_2)/g_2 \times 100 \quad (7)$$

Where: A = mass of oven-dried sample in air, B = mass of surface-dry sample in air after immersion, C = mass of surface-dry sample in air after immersion and boiling, D = apparent mass of sample in water after immersion and boiling, g_1 = dry bulk density, g_2= apparent density, and ρ = density of water.

2.2.2. Heat of Hydration. An eight-receptacles I-Cal 8000 isothermal portable calorimeter was used in this study to evaluate the heat of hydration behavior of the different mortar mixtures. Each of the eight receptacles has a thermistor at the bottom, and all these receptacles were fixed inside a well-insulated box. The heat of hydration was recorded during the first 65 hours after adding the water to the mixture. Isothermal calorimeters, as opposed to semi-adiabatic calorimeters, allow for testing at a controlled temperature and thus enabling excellent repeatability.

A thermal hydration curve for each mixture was plotted while the ambient temperature around the sample remained constant at 20º C. The temperature was set via software interface with a feedback loop to ensure optimal control, while precision sensors measure the heat of hydration generated by the reaction of cementitious binders in the mixture. Embedded reference cells eliminate the need for duplicate test samples.

2.2.3. Accelerated Carbonation. After being cured in the moisture room for 28 days, three mortar cylinders with a diameter of 100 mm and height of 50 mm were prepared, out of each mortar mixture, for accelerated carbonation test according to RILEM CPC18. The perimeter of each cylinder was painted with protective epoxy resin to secure one-dimension diffusion of the carbon dioxide into the specimens through its two opposite faces. The rubberized cylinders were placed in the carbonation chamber under a condition of 23º C, 70% relative humidity, and a 20% carbon dioxide concentration for the duration

of 8 weeks. Then, the test cylinders were removed from the carbonation chamber and subjected to a splitting tension test. The freshly split surface was then cleaned and sprayed with a phenolphthalein pH indicator. After applying the indicator, the noncarbonated part would display a purple-red color due to the reduction in the alkalinity while the carbonated part remained gray. The depth of the carbonated area was measured at three various locations and averaged.

2.2.4. Electrical Resistivity. Solid materials have a relatively higher resistivity than air voids and capillary pores; hence, the electrical resistivity can evaluate the quality of the microstructure and porosity of a solid material such as mortar, which indicates mortar's permeability class and durability. After 28 days of moist curing, both bulk and surface electrical resistivity of two 100×200 mm mortar cylinders samples from each mixture were determined using a Proceq Resipod bulk and surface resistivity tester (Figure 4) per ASTM C1760-12 (Figure 4a), and AASHTO T 358 (AASHTO 2015), respectively. The Proceq Resipod resistivity meter uses the principle of the Wenner probe where four equally spaced, 38 mm spaced, co-linear electrodes put in contact with a mortar specimen where the outermost electrodes are subjected to oscillating current while the middle two electrodes read the voltage. The surface resistivity can be calculated using Eq. 8.

$$\rho = 2\pi aV/I \tag{8}$$

where ρ = surface resistivity (kΩcm), a = electrode spacing (25 mm), V = potential difference (V), and I = applied electric current.

2.2.5. Rapid Chloride Ion Penetration (RCIP). While the chloride ion penetration during the service life of concrete is a very slow process, ASTM International developed a rapid testing method (ASTM C1202-17) that can be used as an indication for

chloride penetration based on the electrical charge passed (Table 3). However, the values in Table 3 are for concrete not mortar which would have more paste compared to concrete. As a result, higher values are expected for mortar.

The test was conducted for each mixture using a 50 mm thick mortar disk test specimen, which was cut from a fully cured 100 mm diameter cement mortar cylinder. To assure a one-dimension flow of the chloride ions, the surface of the side of each test specimen was coated with a water-proof epoxy. The specimens then put in vacuum desiccator where both end uncoated faces of the mortar pieces were in contact with water. After that, the desiccator closed tightly before starting the vacuum pump to decrease the pressure to less than 50 mm Hg (6650 Pa) within a few minutes and continued for 3 hrs (Figure 5). The specimens then were placed in the test cells to be tested for chloride ion penetration with 3% NaCl solution on one side and 0.3 N NaOH solution on the other side.

3. RESULTS AND DISCUSSION

3.1. FRESH PROPERTIES

Reducing the cement content, and adding either the sand or RFP, decreased the mixture workability almost linearly (Figure 6) which was associated with the reduction in water content to keep w/c constant. It is worth noting that the decrease in the workability was slightly higher in the case of introducing the RFP compared to introducing more sand. Mixtures having low w/c ratio of 0.42 was very dry reaching zero flow by 15% reduction in cement content and there was a significant fluctuation in the results of the table flow, with some mixtures displaying flow table results higher than that in the reference mixture only because of a collapse in the slump cone due to the lack of fine binding materials. Based on these results, mixtures with 0.42 were not used for further tests or investigations.

All the investigated mixtures had a cement to sand (or sand and RFP) ratio of at most 1:3, to ensure that the same behavior would be observed in higher-cement content mixtures, an extra set of mixtures were prepared with a cement to sand ratio of 1:2, W/C ratio of 0.51, and different reductions in cement and additions of RFP as was done in the other sets. The performance of this set was similar to the corresponding set but with cement to sand ratio of 1:3 (Figure 7), The only slight difference was that adding sand or RFP had the same effect on flowability. This occurred since, for higher cementitious content, the effect of reducing cement and hence water was more dominant than in the other case. Therefore, it can be concluded that the reduction in the workability is due to the reduction of water within the mortar matrix, not due to the introduction of RFP. The influence of RFP on workability will thus only play a role when the paste volume is sufficiently low.

3.2. DENSITY, ABSORPTION, AND AIR VOIDS IN HARDENED MORTAR

Figure 8 shows the influence of using varied RFP, and sand ratios on each of the different types of densities. Adding RFP up to 15%, decreased the bulk densities of mixtures with w/c of 0.51 and 0.56. Replacing sand with RFP up to 5% also decreased the apparent density. Beyond these RFP content values, the bulk densities slightly increased then decreased again. Although it was anticipated to have a lower bulk density in the case of increasing the RFP content due to the relatively low density of RFP compared to sand or cement, adding RFP beyond a certain amount changed the mortar packing density as the present of RFP caused a decrease in the volume of permeable voids (Figure 9) leading to a more condense mixtures. However, there was no consistent trend since the workability is decreasing with both adding the RFP or sand to the mortar matrix side by side with reducing cement content. The lack of workability caused less compaction and higher air voids.

Optimizing the maximum particle packing density is another factor that affects the density. To optimize the particle packing density of mortar, the particles should be selected to fill up the voids between large particles with smaller particles and so on, to obtain a dense and stiff particle structure. A higher degree of particle packing leads to minimum voids, maximum density and requirement of cement and water will be less. However, optimizing the particle packing density require neutralizing the influence of the lack of compaction due to the lack of workability. As a result, mixtures with w/c ratio of 0.56, which resulted in the highest and the consistent workability (Figure 6), was used to evaluate the particle packing density. Taking the bulk density after immersion and boiling as an example since the immersion and boiling fill more air voids compared to the other densities. For example, the bulk density after immersion and boiling at RFP dosage of 20% decreased by 1.6% only (Figure8b), while mathematically the density should be decreased by 4.3% due the low density of RFP compared to the other component. The difference between the actual density deduction (1.6%) and the mathematical density reduction (4.3%) refer to a change in the particles arrangement that leads to more dense matrix.

This conclusion was consistent with the result of the permeable pore space (voids) in Figure 9b where the permeable air voids decreased with the increase of RFP dosage to 20%. Same consistency of results was noticed between the density and air void results. Mixture with w/c ratio of 0.51 has the highest volume of permeable voids at 25% RFP (Figure 9a) which caused the lowest density at the same ratio (Figure 8a). Same trend was noticed when the sand was added. Adding 15% sand resulted in the highest volume of permeable voids (Figure 9a) and lowest density (Figure 8a). When the RFP was used with

reducing the sand instead of cement (Figure 8c and Figure 9c), RFP ratio of 15% resulted in the least volume of permeable voids.

3.3. HEAT OF HYDRATION

Figure 10 shows the temporal variation of the heat of hydration per gram of cement over approximately three days for the different mortar mixtures. The higher the magnitude of the peak of temperature is the higher the rate of hydration of tricalcium silicate and paste hardening. In both cases, the w/c ratio was kept constant at 0.51 since we care only about the heat of hydration, not the workability.

As shown in Figure10a, adding extra sand to the mixture did not affect the normalized heat flow per gram of cement. However, adding RFP changed the temporal variation of the heat of hydration. This change due to the incorporation of the RFP which had a relatively high specific heat of 2010 J/kg.K, the amount of heat per unit mass required to raise the temperature by one degree, compared to 840 J/kg.K for cement. As a result, mixtures with RFP needs more heat and time to reach a certain temperature compared to the reference mixture. This extra heat was obtained from the heat of cement hydration.

Figure 11 shows the magnitude of the peak heat flow and induction time for the different mixtures. The induction time, the period of inactivity just before the peak of hydration, is linked to the setting time which would increase with increasing RFP ratio. Adding RFP significantly decreased the heat of hydration and increased the induction time. For example, compared to the reference mixture, the magnitude of the peak heat flow of mixtures with w/c of 0.51 and with 15, 20, and 35% RFP ratios decreased by 20.7, 25.5, and 29.4%, respectively. However, the time of induction increased by 24.3, 31.5, and

78.5% for mixtures with 15, 20, and 35% RFP respectively. Adding extra sand did not have a significant effect on either the peak heat flow nor the time of induction.

The areas under the time – heat flow curves representing the heat of hydration divided by the mass of cement were calculated (Figure12). The results indicate that increasing the RFP content lowers the peak heat flow of rubberized mortar.

3.4. ELECTRICAL RESISTIVITY

Adding RFP to the mortar matrix influenced both the surface and bulk resistivity significantly compared to adding sand (Figs. 13 and 14). For example, mixtures with w/c of 0.51, the surface and bulk resistivity the increased approximately linearly by 122% and 73% respectively with increasing the RFP content from 0% to 20%. However, increasing the RFP beyond 20% resulted in a decrease in the surface and the bulk resistivity by 51% and 48% for the surface and bulk resistivity, respectively (Figure 13a and 14a). This decrease can be explained by investigating Figure 8a where increasing the RFP from 20% to 25% led to increasing the volume of the permeable pore voids from 12.1 to 30.4%. Similar behavior was observed for mixtures having w/c ratio of 0.56 with one-difference; both the surface and bulk resistivities increased significantly with increasing the RFP ratio up to 25% (Figure 13b and 14b). Investigating Figure 6 showed that adding 25% RFP for mixture having w/c of 0.56 did not deteriorate the workability significantly, where at 25% of RFP or sand, the flow was around 40% compared to almost 0% with w/c ratios of 0.51 and 0.42 at the same addition ratio. Hence proper compaction process and high packing density were possible which led to decreased air void.

Two main parameters, air voids between the sand particles and the porosity within the cement paste, affect the electrical resistivity of mortar mixtures. Air voids between the

sand particles can be reduced through optimizing the size and gradation of the sand particles and/or incorporating materials with smaller particle size or different particle geometry and hence RFP with a particle size smaller than sand would be a potential candidate. Porosity within the cement paste can be reduced by reducing the cement content and used w/c in a mixture. Incorporating RFP into a mortar matrix added other contradicting parameters to the resistivity issue making it more challenging. The low electrical conductivity of rubber particles reduces the electrical resistivity of rubberized mortar mixtures (Kaewunruen and Meesit 2016, Si et al. 2018). However, adding rubber to concrete mixture increases its air content (Youssf et al. 2017) and decrease the workability (Figure 6) leading to reductions in concrete electrical resistivity. These contradicting parameters create a fluctuation and inconsistent behavior with different mixture parameters and RFP content.

To isolate the effect of reducing the cement from that of incorporating the RFP in the mortar mixtures on the resistivity, the resistivity values of mixtures included additional sand instead of RFP can be compared to those having RFP. For mixtures with sand addition having w/c of 0.51, the surface and the bulk resistivity decreased approximately linearly by 17% and 41% respectively with increasing the sand content from 0% to 20%. Beyond that and at 25% addition of sand, both the surface and bulk resistivity increased by 68% and 33% compared to the reference mixture, respectively. This increase occurred due to the decrease in the volume of the permeable voids with increasing the sand content (Figure 9a). For mixtures having w/c of 0.56, since the electrical current uses the interconnected void within the cement paste, reducing the cement only and using sand decreased the electrical resistivity slightly compared to the reference mixture. In addition, Figure 9b

shows that at w/c ratio of 0.56, there is a general decreasing trend with increasing both RFP or sand content.

Replacing sand with the RFP without reducing the cement content yielded the highest electrical resistivity compared to the other mixtures with an optimum replacement ratio of 15% (Figure 13a and 14a). Beyond that, the electrical resistivity decreased but still higher or similar to the reference mixture in both the surface and the bulk resistivity respectively. With both w/c ratios of 0.51 and 0.56, adding RFP moved the risk of corrosion from low to negligible per (Chini et al. 2003, Song and Saraswathy 2007, Hornbostel et al. 2013, Sengul 2014, Azarsa and Gupta 2017) where specimens having a bulk resistivity of 20 kΩcm or more have a negligible corrosion risk.

3.5. RAPID CHLORIDE ION PENETRATION (RCPT)

Adding RFP decreased the rapid chloride ion penetration (RCPT) up to 20% RFP (Figure 15). Beyond that the RCPT value significantly increased due to the increase in the volume of the permeable pore space from 12.06 to 30.40% (Figure 9a). A mixture having 20% RFP had an average RCPT of 2667 Coulombs passed through the specimens which represent 76% reduction in the charge passed compared to 10933 Coulombs passed through the reference specimen. Despite the reduction in the RCPT values and except for the mixture with 20% RFP, all mixtures were classified as a high RCPT per (Chini et al. 2003, Hornbostel et al. 2013, Sengul 2014). Adding sand with 5% or higher increased the RCPT values linearly. It is worth noting that the results of the RCPT had a strong correlation to both surface resistivity and bulk electrical resistivity. Eq. 9 was empirically developed to correlate the surface resistivity to the RCPT (Kessler et al. 2005).

The experimental results in this study follow closely the relationship described in Eq. 9 (Figure 16).

$$Surface\ Resistivity = 5801.2(Rapid\ Chloride\ Permeability)^{-0.819} \quad (9)$$

3.6. ACCELERATED CARBONATION

The effect of adding the RFP while reducing the cement content functions in w/c of the mixture (Figs. 17 and 18). For w/c of 0.56, adding up to 25% RFP to the mixtures reduced the carbonation depth (Figure 17b). The carbonation depth started with 13 mm for mixture with 0% rubber content and decreased to approximately 8 mm for mixture with 10% rubber content and then increased to 11 mm for mixture with 25% rubber content. Adding sand, however, significantly increased the carbonation depth. At 5% sand addition, the CO2 had a full penetration into the specimen. The carbonation rate is highly affected by the permeability of concrete that mainly caused by alternating the pore size and distribution (Kulakowski et al. (2009). Therefore, the air void content, particles arrangement, and accompanying air voids in a mixture directly affected the carbonation depth. For relatively low w/c of 0.51, adding RFP or sand increased the carbonation depth. However, this increase was very pronounced in the case of sand compared to RFP.

Adding 5% or higher sand, the carbonation reached a full depth of the specimen. Adding RFP led to an approximately linear increase in the carbonation depth reaching 15 mm at 25% addition of RFP (Figure 18a). This behavior was due to the lack of compaction as a direct result of the relatively low workability of mixtures with w/c ratio of 0.51.

4. SUMMARY, CONCLUSIONS, AND RECOMMENDATIONS

Rubber fiber powder (RFP) was used as an additive to mortar mixtures. The fresh properties, compressive, flexural strength, the hardened density, absorption, and air voids and heat of hydration of rubberized mortar mixtures with six different cement reduction ratios side by side with the addition of RFP of 0, 5, 10, 15, 20, and 25% were investigated. The bulk and surface electrical resistivity, the rapid chloride ion penetration as well as the carbon dioxide penetration were investigated.

Despite the reduction in some of the mechanical properties due to the inclusion of rubber powder in lieu of a portion of the cement, this study disclose that the rubber powder obtained as a solid waste of scrap tires recycling could be used in the mortar as an additive to provide more corrosion resistance and less heat of hydration. In particular, the following points can be concluded:

1. Adding RFP to mortar mixtures decreased mortar workability. For w/c of 0.51 and 0.56. Mortar mixtures with up to 20% RFP addition displayed a good workability reaching flowability of 40%, and 70%, respectively.
2. Decreases in the compressive and flexural strengths were noticed with the increase of RFP ratio. For example, mixtures with w/c of 0.51 at the age of 28 days, the compressive and flexural strength of rubberized cement mortar with 10% RFP decreased by 35%, 27%, and 9%, respectively. However, the compressive and flexural strength of cement mortar with 10% sand addition instead of cement decreased by 76%, and 76%, respectively, which shows the advantage of adding RFP instead of cutting the cement content only.

3. The impact of adding the RFP on the bulk density relates to w/c ratio, workability, and the volume of the permeable voids. Adding 15% RFP reduced the bulk density after immersion and boiling from 2.20, 2.16 and 2.12 to 2.11, 2.02, and 2.06 for mixtures with w/c ratios of 0.42, 0.51 and 0.56 respectively.
4. Adding the RFP lowered and delayed the peak temperature for the heat of hydration compared to reducing the cement content only. The magnitude and the time of the peak heat flow of mixtures with 20% RFP ratios decreased by 25.5% 31.5% respectively.
5. Mortar mixtures with up to 20% RFP showed an improved bulk and surface electrical resistivity values which are a significant indication for better reinforcement corrosion resistance. For example, mixtures with w/c of 0.51 showed a linear increase in the surface and the bulk resistivity from 3.48 and 17.2 to 7.73 and 29.7, respectively, with 20% RFP. Beyond 20% RFP, the bulk and surface resistivity decreased due to the increase in the volume of the permeable voids.
6. The carbon dioxide penetration depth dropped by 38% by adding 10% of RFP to the mortar mixture with w/c ratio of 0.56. However, adding 5% or higher RFP for mixtures having w/c of 0.51 led to a linear increase in the carbonation depth reaching 200% at 25% addition. Furthermore, for both w/c ratios adding RFP was much better than adding sand. Adding 5% or higher sand, carbon dioxide had a full penetration throw the specimens for mixtures with W/C ratio of 0.51 and 0.56 due to the change in air void content, particles arrangement, and accompanying air voids.

7. The results presented in this paper showed that using RFP of 10% to 15% in combination with w/c of 0.51 to 0.56 can yield a workable rubberized mortar with a significant potential for high corrosion resistance.

ACKNOWLEDGEMENTS

This research was supported by the Missouri Department of Natural Resources. However, any opinions, findings, conclusions, and recommendations presented in this paper are those of the authors and do not necessarily reflect the views of the sponsor.

Table 1. Density results of the materials (ASTM B923−16).

Materials	**Density (g/cm^3)**
Rubber powder and nylon fiber (RFP)	1.566
Cement	3.132
Fine aggregate	2.648

Table 2. Test matrix.

Mix ID	Rubber addition (%)	Sand addition (%)	Rubber (kg)	Sand (kg)	Cement (kg)	Water (kg)	w/c	f'c (MPa)	MOR (MPa)
0-0.42	0	0	0.000	9.00	3.00	1.25	0.42	39.4	5.70
R5-0.42	5	0	0.075	9.00	2.85	1.19	0.42	33.5	5.30
R10-0.42	10	0	0.150	9.00	2.70	1.13	0.42	25.2	4.21
R15-0.42	15	0	0.225	9.00	2.55	1.06	0.42	21.7	3.52
R20-0.42	20	0	0.300	9.00	2.40	1.00	0.42	14.4	2.33
R25-0.42	25	0	0.375	9.00	2.25	0.94	0.42	7.40	0.62
S5-0.42	0	5	0.000	9.13	2.85	1.19	0.42	35.5	5.42
S10-0.42	0	10	0.000	9.25	2.70	1.13	0.42	35.9	5.48
S15-0.42	0	15	0.000	9.38	2.55	1.06	0.42	28.2	4.66
S20-0.42	0	20	0.000	9.51	2.40	1.00	0.42	27.2	4.41
S25-0.42	0	25	0.000	9.63	2.25	0.94	0.42	12.2	1.92
0-0.51	0	0	0.000	9.00	3.00	1.53	0.51	44.5	5.84
R5-0.51	5	0	0.075	9.00	2.85	1.46	0.51	37.5	5.76
R10-0.51	10	0	0.150	9.00	2.70	1.38	0.51	32.4	5.30
R15-0.51	15	0	0.225	9.00	2.55	1.30	0.51	26.1	4.52
R20-0.51	20	0	0.300	9.00	2.40	1.23	0.51	25.2	4.08
R25-0.51	25	0	0.375	9.00	2.25	1.15	0.51	20.7	3.32
S5-0.51	0	5	0.000	9.13	2.85	1.46	0.51	12.8	1.77
S10-0.51	0	10	0.000	9.25	2.70	1.38	0.51	10.8	1.52
S15-0.51	0	15	0.000	9.38	2.55	1.30	0.51	8.00	0.80
S20-0.51	0	20	0.000	9.51	2.40	1.22	0.51	6.20	0.51
S25-0.51	0	25	0.000	9.63	2.25	1.15	0.51	6.90	0.46
0-0.56	0	0	0.000	9.00	3.00	1.67	0.56	32.0	5.25
R5-0.56	5	0	0.075	9.00	2.85	1.58	0.56	22.7	3.58
R10-0.56	10	0	0.150	9.00	2.70	1.50	0.56	20.9	3.49
R15-0.56	15	0	0.225	9.00	2.55	1.42	0.56	20.6	3.34
R20-0.56	20	0	0.300	9.00	2.40	1.33	0.56	21.1	3.23
R25-0.56	25	0	0.375	9.00	2.25	1.25	0.56	19.0	3.10
S5-0.56	0	5	0.000	9.13	2.85	1.58	0.56	10.0	1.12
S10-0.56	0	10	0.000	9.25	2.70	1.50	0.56	5.70	0.18
S15-0.56	0	15	0.000	9.38	2.55	1.42	0.56	6.21	0.28
S20-0.56	0	20	0.000	9.51	2.40	1.33	0.56	6.82	0.44
S25-0.56	0	25	0.000	9.63	2.25	1.25	0.56	7.23	0.34
0-0.51S	0	0	0.000	9.00	3.00	1.53	0.51	24.1	3.92
R5-0.51S	5	0	0.266	8.55	3.00	1.53	0.51	22.2	3.71
R10-0.51S	10	0	0.532	8.10	3.00	1.53	0.51	26.2	4.00
R15-0.51S	15	0	0.799	7.65	3.00	1.53	0.51	21.0	3.61
R20-0.51S	20	0	1.065	7.20	3.00	1.53	0.51	16.9	2.85
R25-0.51S	25	0	1.331	6.75	3.00	1.53	0.51	12.5	1.82

Table 3. RCIP in concrete based on charge passed (ASTM C1202-17).

Charge Passed (coulombs)	Chloride Ion Penetrability
>4,000	High
2,000–4,000	Moderate
1,000–2,000	Low
100–1,000	Very Low
<100	Negligible

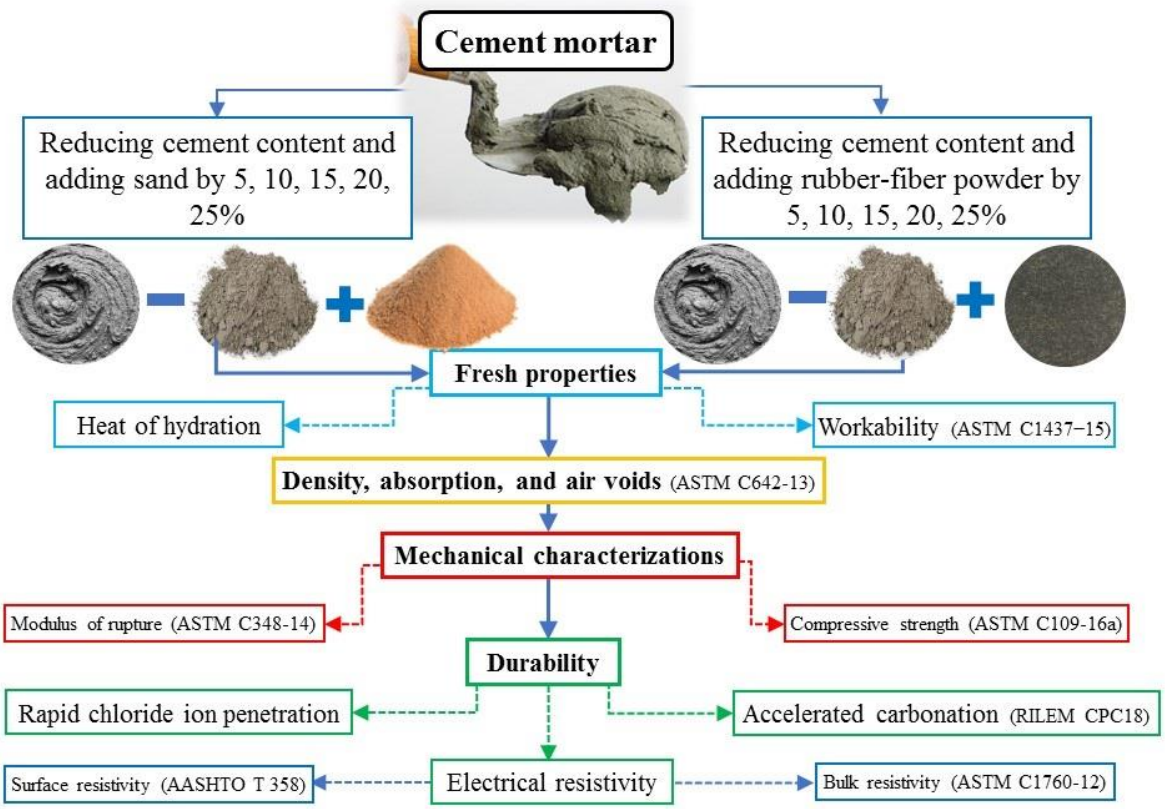

Figure 1. Schematic overview of the work done in this study.

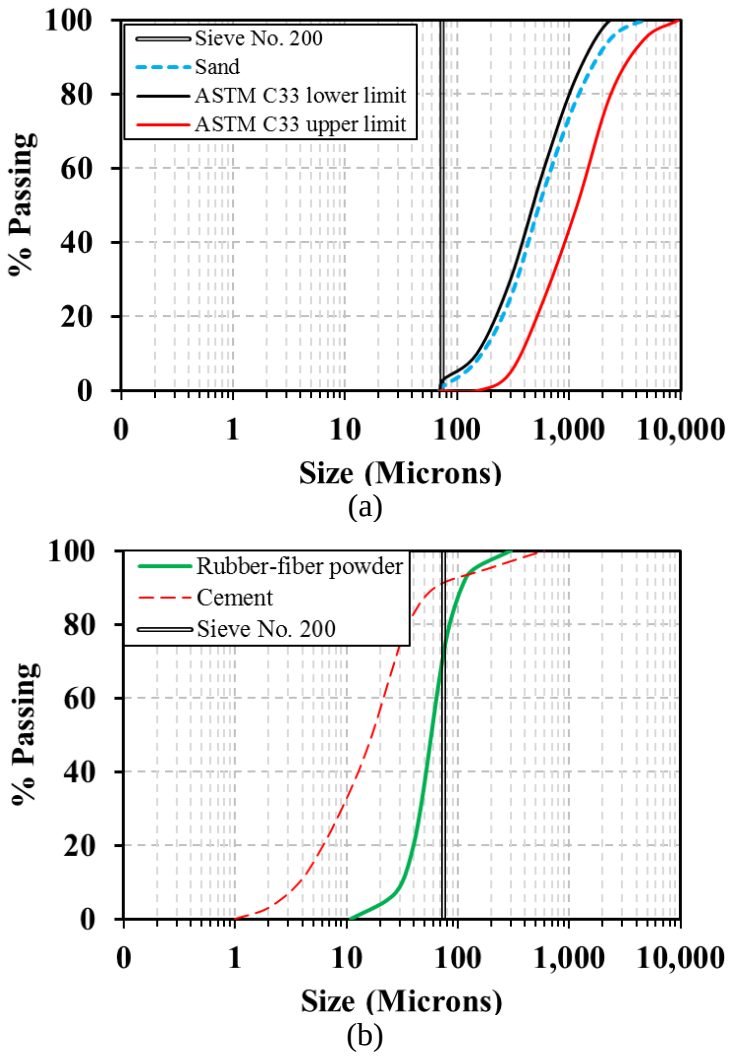

Figure 2. Particles size distribution analysis (a) Sieve analysis of sand, and (b) Laser diffraction analysis of RFP and Cement.

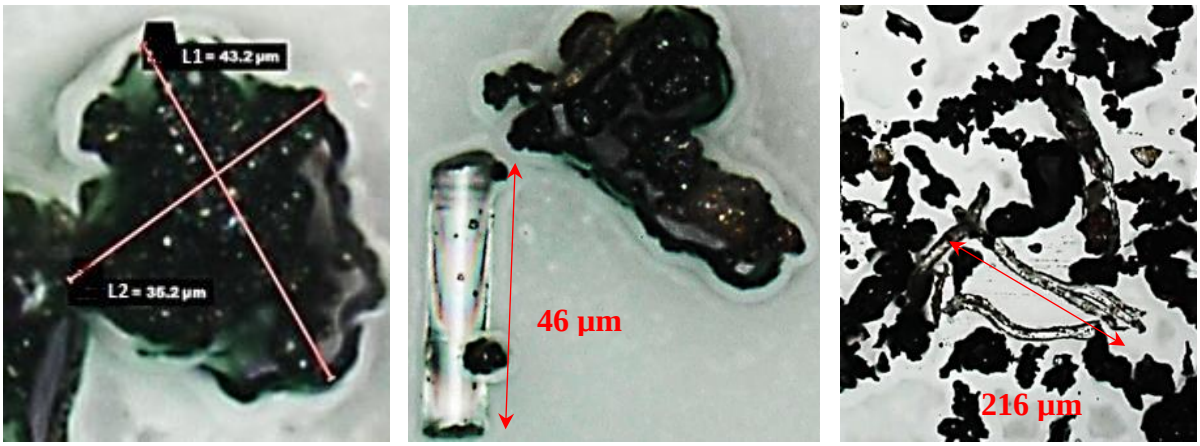

(a) (b) (c)

Figure 3. Microscopic images of rubber powder. (a), (b): The angular irregular shape of the rubber particles and (b), (c): Nylon fiber pieces within the powder.

(a) (b)

Figure 4. Electrical resistivity: (a) Bulk, and (b) Surface.

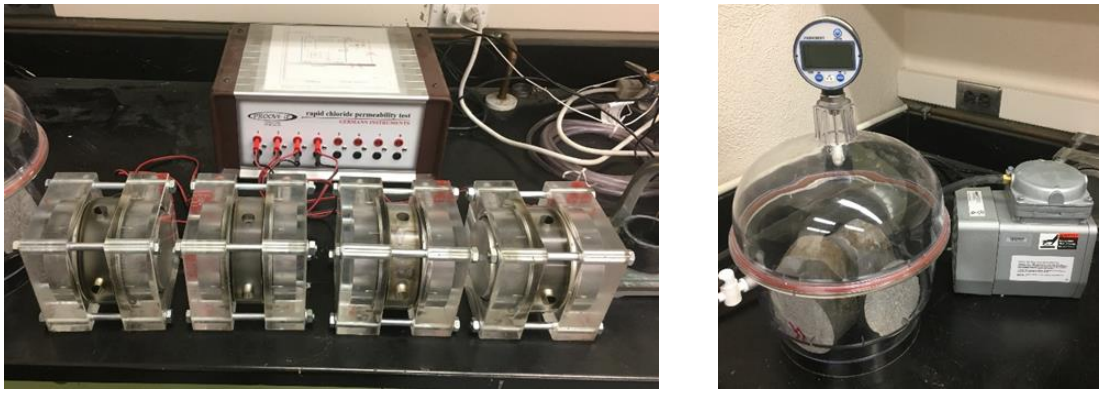

(a) (b)

Figure 5. (a) RICP test device with 4 cells and (b) Vacuum desiccator.

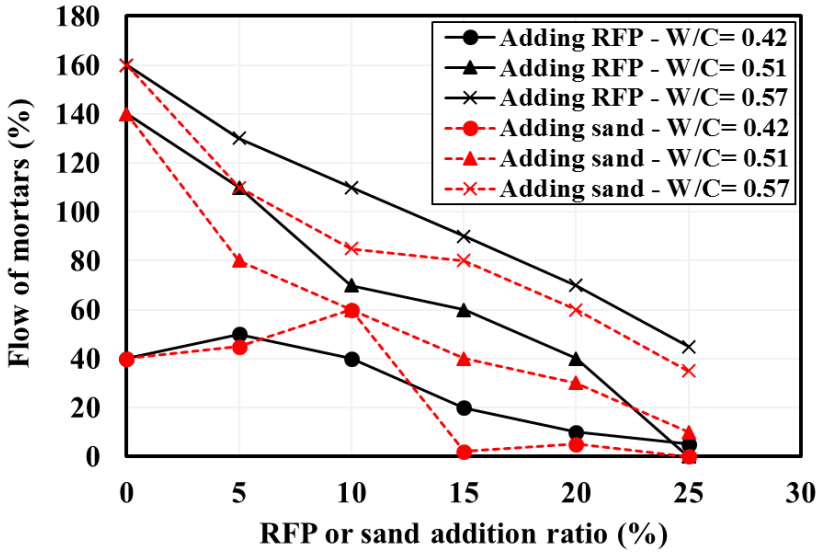

Figure 6. Workability of different mortar mixtures.

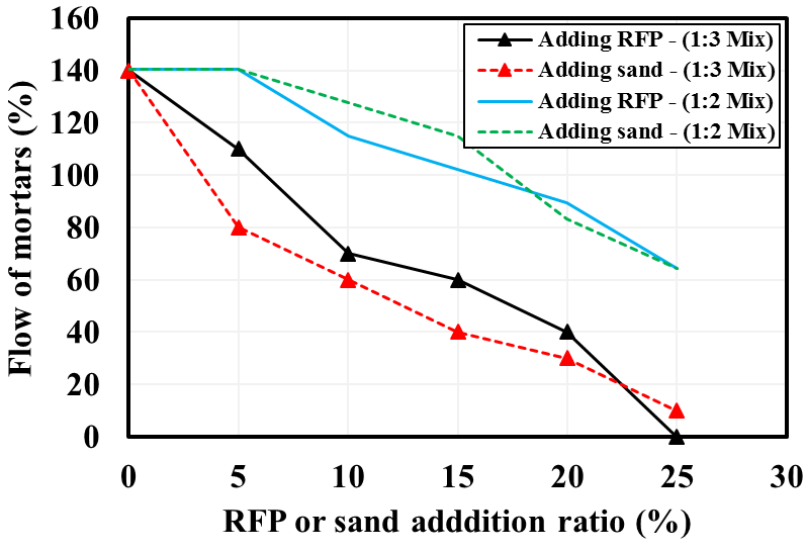

Figure 7. Workability of 1:2 and 1:3 mortar mixtures.

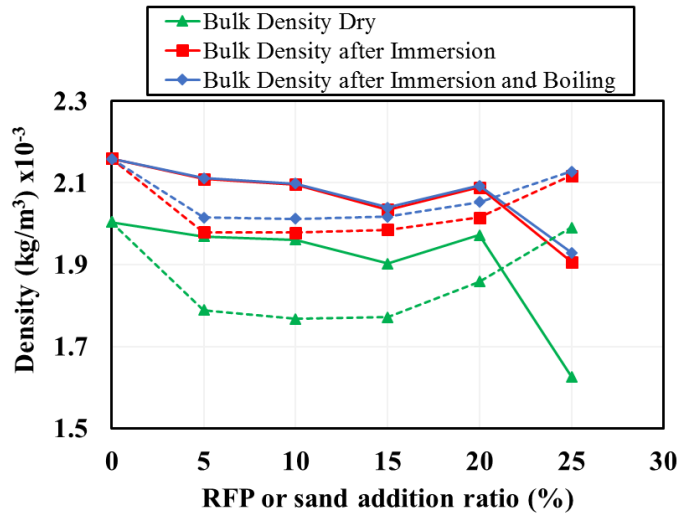

(a)

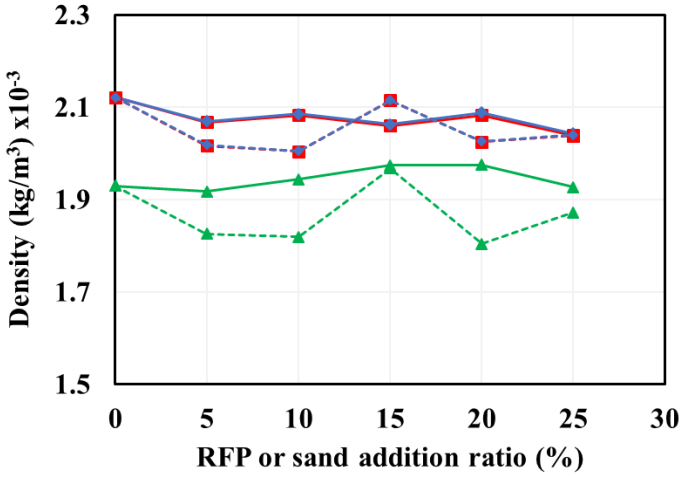

(b)

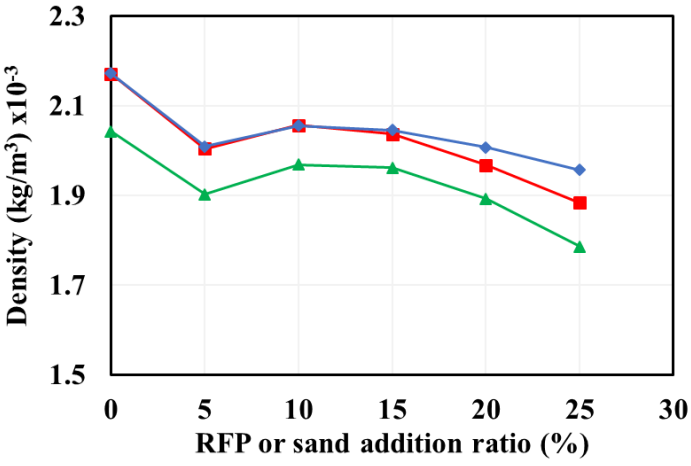

(c)

Figure 8. Different densities of mortar with (a) W/C= 0.51, (b) W/C= 0.56 and (c) RFP was used as a sand replacement. Dotted lines: adding sand; solid lines: adding RFP.

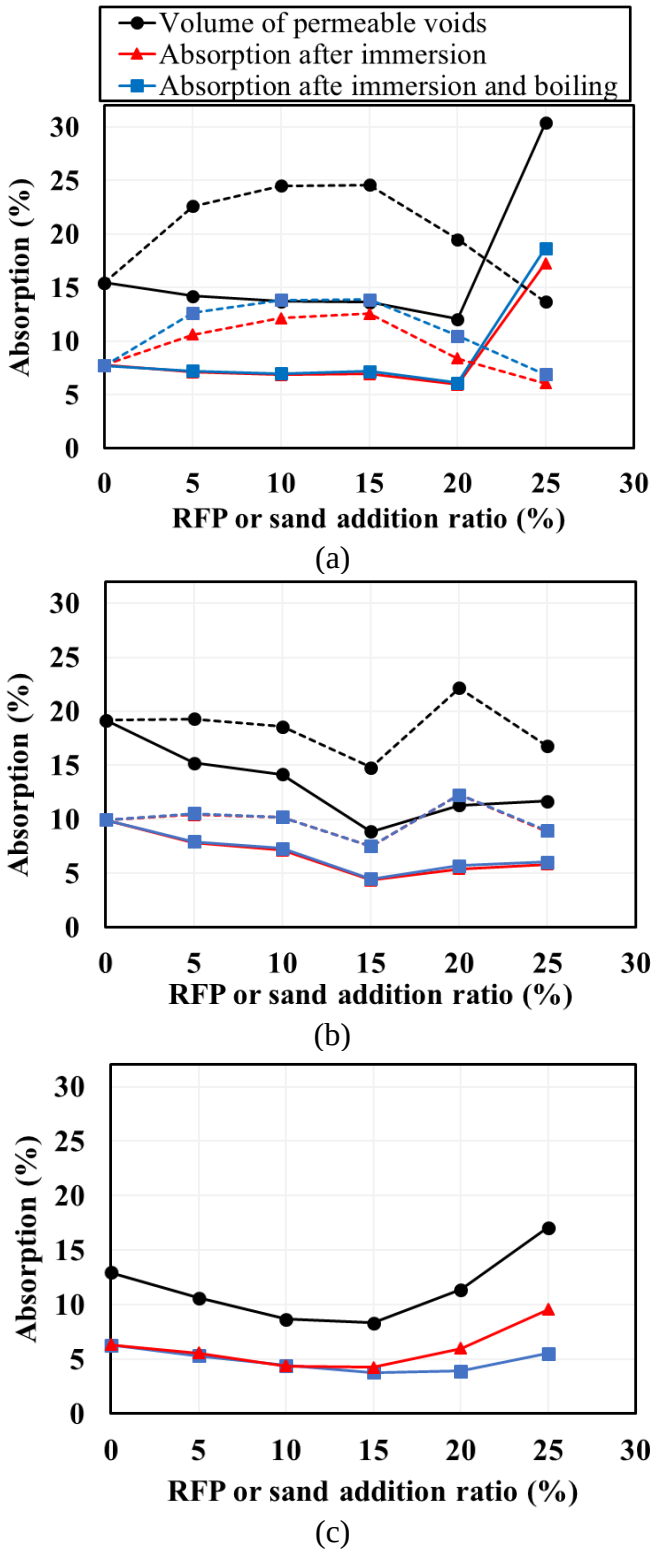

Figure 9. Absorption and air voids of cement mortar with (a) W/C= 0.51, (b) W/C= 0.56, and (c) RFP was used as a sand replacement. Dotted lines: addition of sand, Solid lines: addition of RFP.

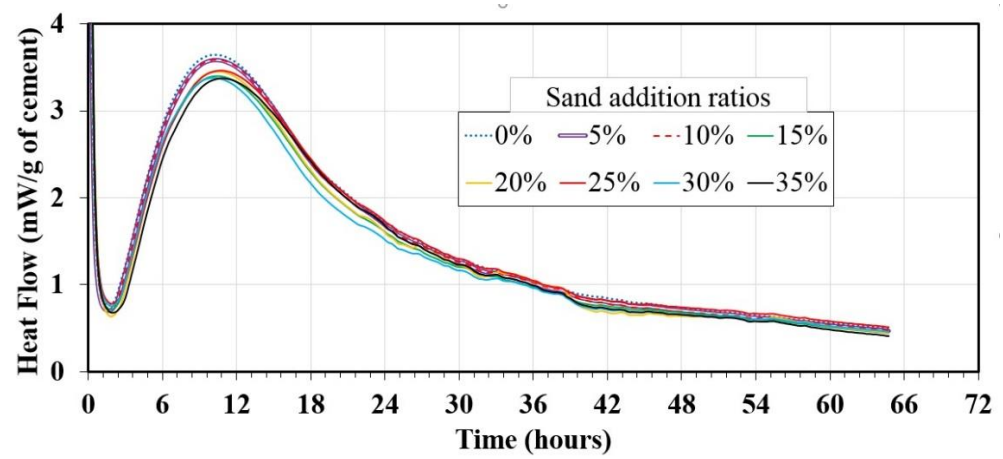

(a)

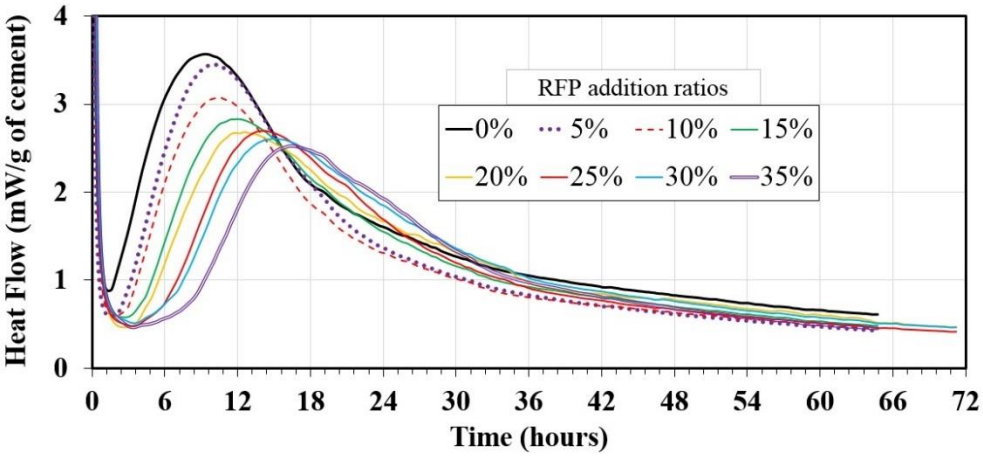

(b)

Figure 10. Heat of hydration (Calorimeter) curves of mortar mixtures with different (a) sand addition and (b) RFP addition ratios.

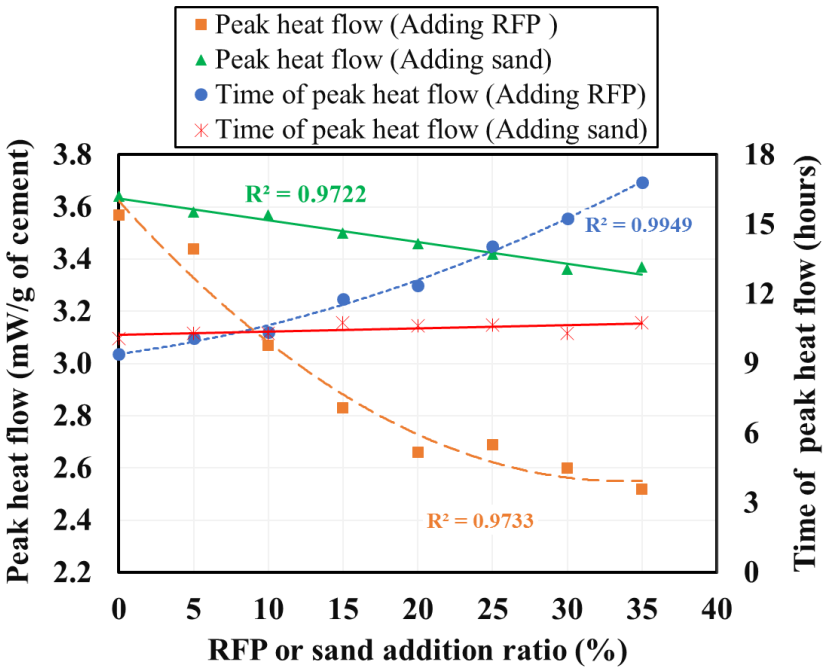

Figure 11. Magnitude of the peak heat flow and induction time of the different mortar mixtures.

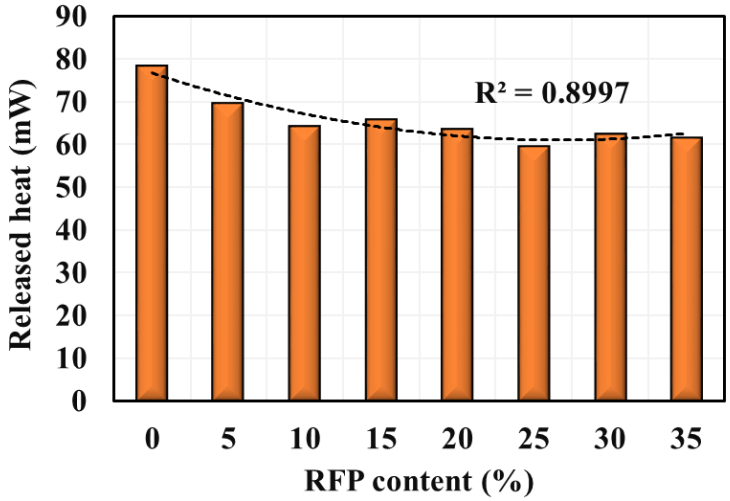

Figure 12. Heat of hydration released of the different mortar mixtures.

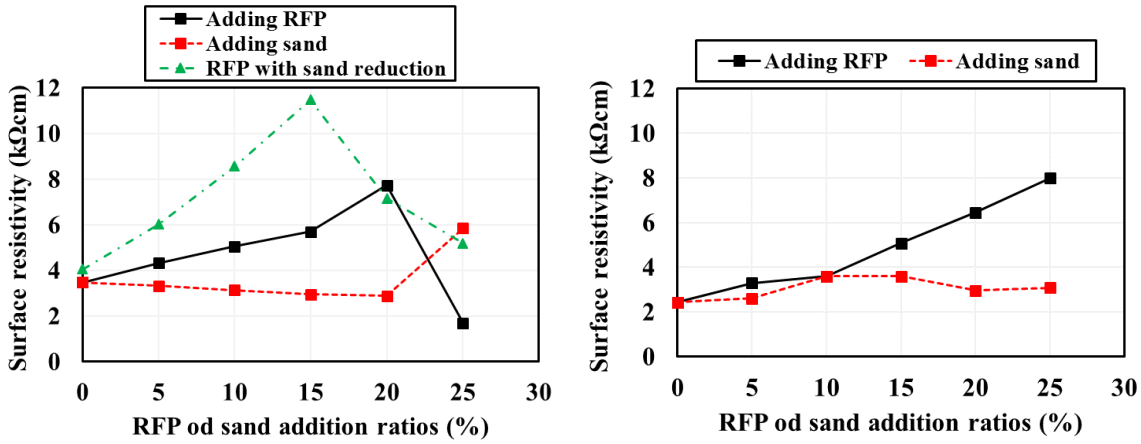

Figure 13. Surface electrical resistivity of mortar mixtures with (a) W/C= 0.51, and (b) W/C= 0.56.

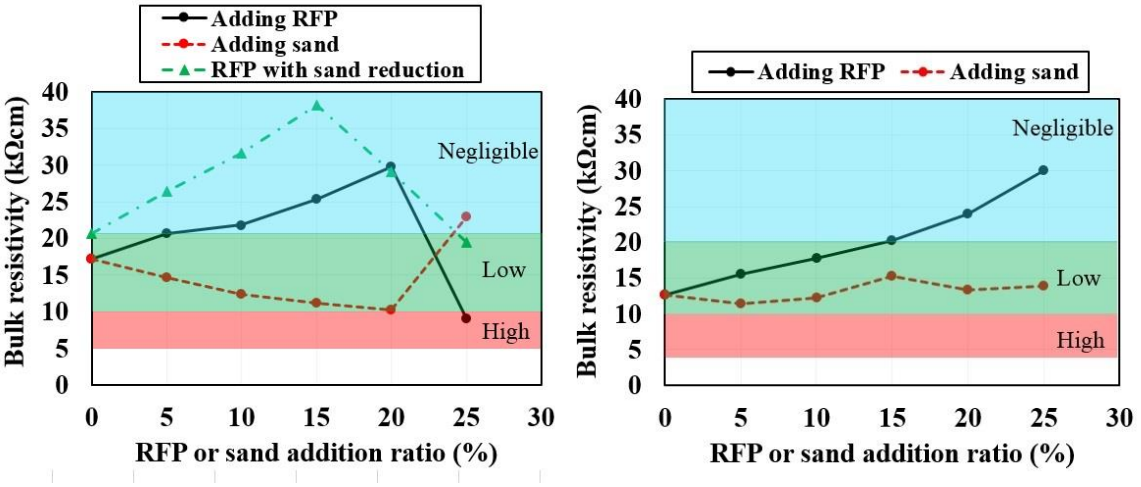

Figure 14. Bulk electrical resistivity of mortar mixtures and its correlation with steel corrosion risk with (a) W/C= 0.51, (b) W/C= 0.56 and (c) RFP was used as a sand replacement .

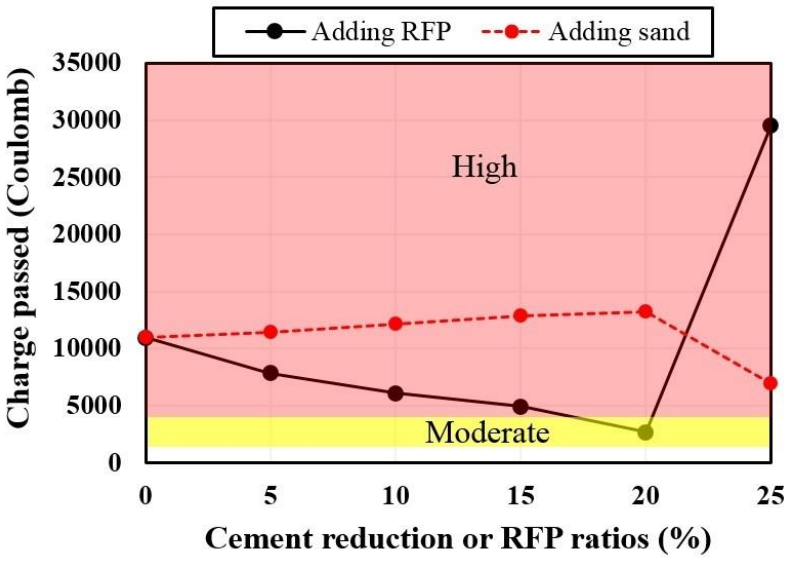

Figure 15. Charge passed through mixture with w/c ratio of 0.51 with adding RFP or sand and its correlation with the RCPT.

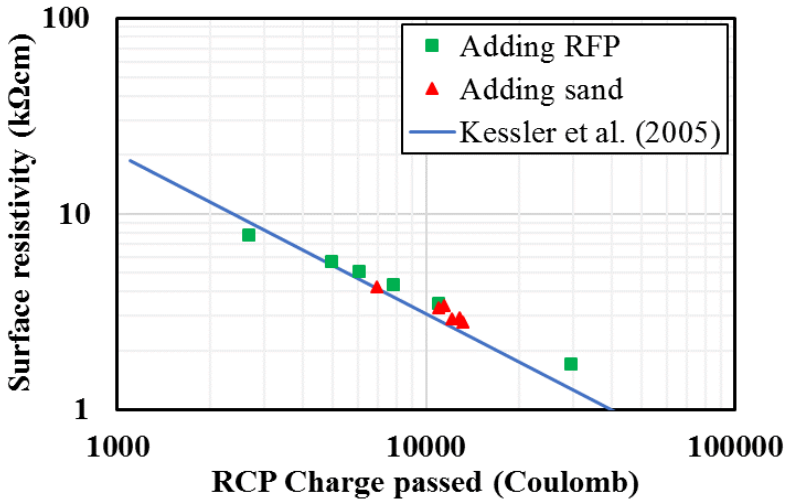

Figure 16. Surface resistivity versus rapid chloride permeability.

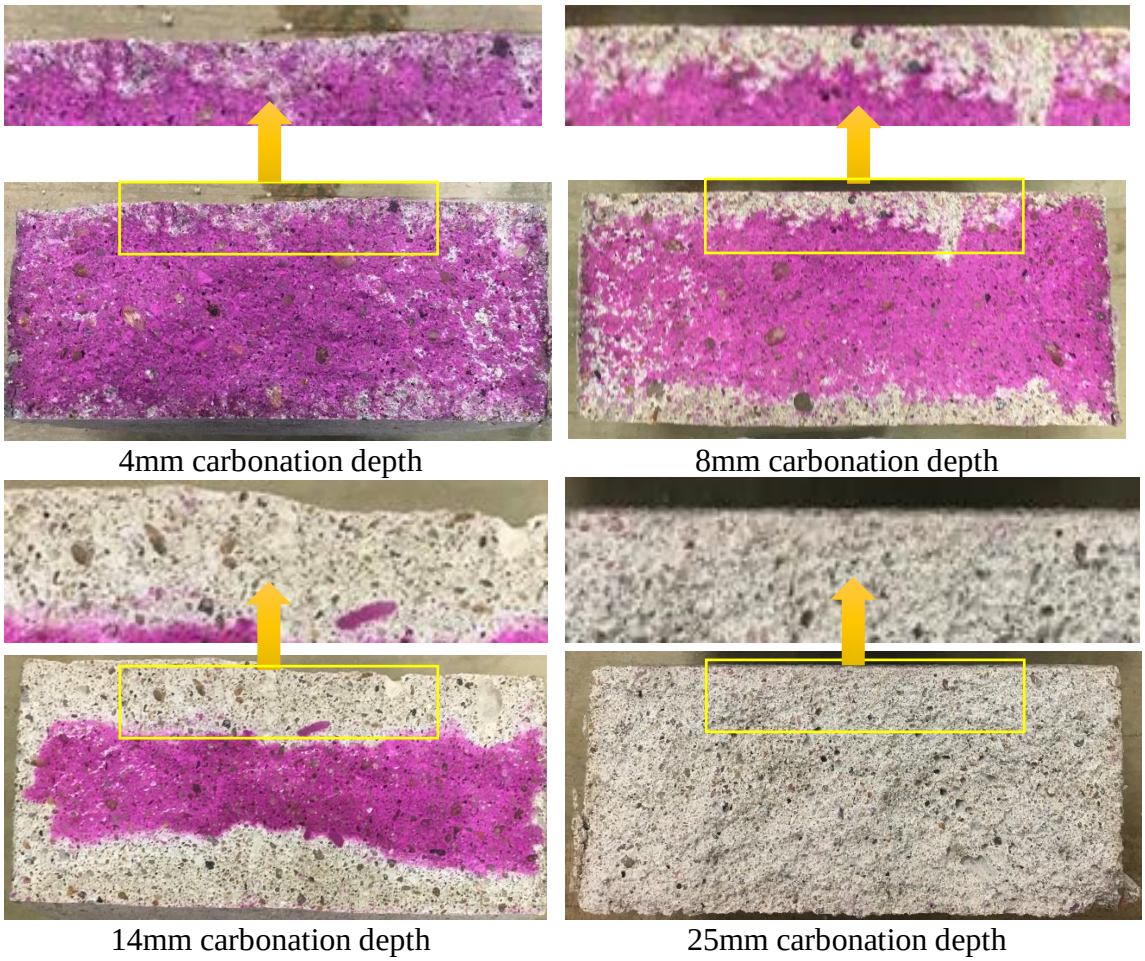

Figure 17. Different carbonation depths with different RFP or sand content.

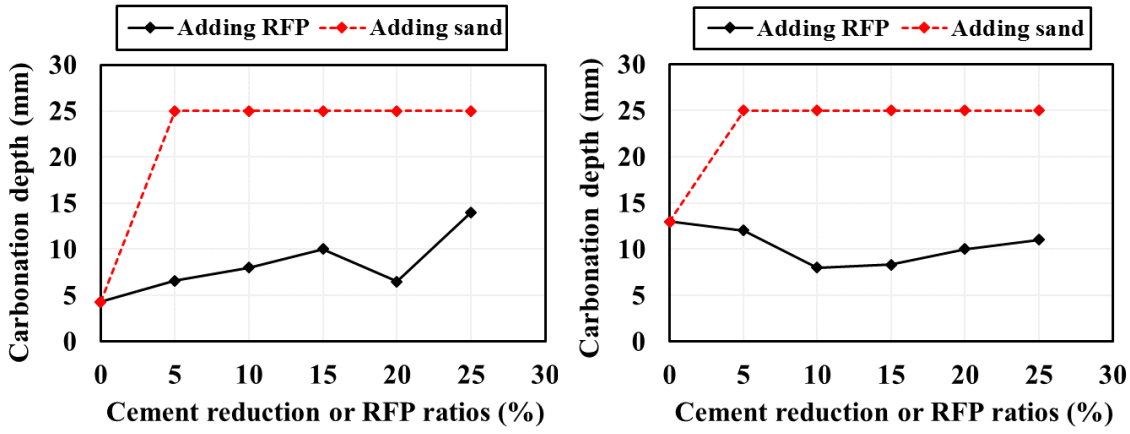

(a) (b)

Figure 18. Accelerated carbonation depth of mortar mixtures with (a) W/C= 0.51, and (b) W/C= 0.56.

REFERENCES

AASHTO (2015). AASHTO T 358:2015Method Of Test For Surface Resistivity Indication Of Concrete'S Ability To Resist Chloride Ion Penetration.

Azarsa, P. and R. Gupta (2017). "Electrical resistivity of concrete for durability evaluation: a review." Advances in Materials Science and Engineering 2017.

Batayneh, M. K., I. Marie and I. Asi (2008). "Promoting the use of crumb rubber concrete in developing countries." Waste Management 28(11): 2171-2176.

Benazzouk, A. and M. Queneudec (2002). Durability of cement-rubber composites under freeze thaw cycles. Proceeding of International congress of Sustainable Concrete Construction, Dundee-Scotland.

Chini, A. R., L. C. Muszynski and J. K. Hicks (2003). Determination of acceptance permeability characteristics for performance-related specifications for Portland cement concrete.

Eldin, N. N. and A. B. Senouci (1993). "Rubber-tire particles as concrete aggregate." Journal of materials in civil engineering 5(4): 478-496.

Fattuhi, N. and L. Clark (1996). "Cement-based materials containing shredded scrap truck tyre rubber." Construction and building materials 10(4): 229-236.

Fedroff, D., S. Ahmad and B. Savas (1996). "Mechanical properties of concrete with ground waste tire rubber." Transportation Research Record: Journal of the Transportation Research Board(1532): 66-72.

Ganjian, E., M. Khorami and A. A. Maghsoudi (2009). "Scrap-tyre-rubber replacement for aggregate and filler in concrete." Construction and Building Materials 23(5): 1828-1836.

Ghaly, A. M. and J. D. Cahill IV (2005). "Correlation of strength, rubber content, and water to cement ratio in rubberized concrete." Canadian Journal of Civil Engineering 32(6): 1075-1081.

Gheni, A. A., M. A. ElGawady and J. J. Myers (2017). "Mechanical Characterization of Concrete Masonry Units Manufactured with Crumb Rubber Aggregate." ACI Materials Journal 114(01).

Gou, M. and X. Liu (2014). "Effect of rubber particle modification on properties of rubberized concrete." Journal of Wuhan University of Technology-Mater. Sci. Ed. 29(4): 763-768.

Granuband Macon, L. (2017). Amount of waste in tire recycling plant after processing scrap tires. A. A. Gheni.

Hesami, S., I. S. Hikouei and S. A. A. Emadi (2016). "Mechanical behavior of self-compacting concrete pavements incorporating recycled tire rubber crumb and reinforced with polypropylene fiber." Journal of cleaner production 133: 228-234.

Hornbostel, K., C. K. Larsen and M. R. Geiker (2013). "Relationship between concrete resistivity and corrosion rate–a literature review." Cement and Concrete Composites 39: 60-72.

Horvath, A. (2004). "Construction materials and the environment." Annu. Rev. Environ. Resour. 29: 181-204.

Kaewunruen, S. and R. Meesit (2016). "Sensitivity of crumb rubber particle sizes on electrical resistance of rubberised concrete." Cogent Engineering 3(1): 1126937.

Kessler, R. J., R. G. Powers and M. P. Mario Paredes (2005). "Resistivity measurements of water saturated concrete as an indicator of permeability." CORROSION 2005.

Khatib, Z. K. and F. M. Bayomy (1999). "Rubberized Portland cement concrete." Journal of materials in civil engineering 11(3): 206-213.

Kulakowski, M. P., F. M. Pereira and D. C. Dal Molin (2009). "Carbonation-induced reinforcement corrosion in silica fume concrete." Construction and Building Materials 23(3): 1189-1195.

Liu, H., X. Wang, Y. Jiao and T. Sha (2016). "Experimental investigation of the mechanical and durability properties of crumb rubber concrete." Materials 9(3): 172.

Moustafa, A. and M. A. ElGawady (2015). "Mechanical properties of high strength concrete with scrap tire rubber." Construction and Building Materials 93: 249-256.

Olorunniwo, A. (1994). Effects of recycled scrap tires and asphalt pavement on the engineering properties of portland cement concrete, University of Texas at Austin.

Richardson, A., K. Coventry, V. Edmondson and E. Dias (2016). "Crumb rubber used in concrete to provide freeze–thaw protection (optimal particle size)." Journal of Cleaner Production 112: 599-606.

RMA, R. M. A. (2016). 2015 U.S. Scrap Tire Management Summary. Wasington, DC.

Savas, B., S. Ahmad and D. Fedroff (1997). "Freeze-thaw durability of concrete with ground waste tire rubber." Transportation Research Record: Journal of the Transportation Research Board(1574): 80-88.

Sengul, O. (2014). "Use of electrical resistivity as an indicator for durability." Construction and Building Materials 73: 434-441.

Shu, X. and B. Huang (2014). "Recycling of waste tire rubber in asphalt and Portland cement concrete: an overview." Construction and Building Materials 67: 217-224.

Si, R., J. Wang, S. Guo, Q. Dai and S. Han (2018). "Evaluation of laboratory performance of self-consolidating concrete with recycled tire rubber." Journal of Cleaner Production 180: 823-831.

Siddique, R. and T. R. Naik (2004). "Properties of concrete containing scrap-tire rubber–an overview." Waste management 24(6): 563-569.

Song, H.-W. and V. Saraswathy (2007). "Corrosion monitoring of reinforced concrete structures-A." Int. J. Electrochem. Sci 2: 1-28.

Thomas, B. S. and R. C. Gupta (2015). "Long term behaviour of cement concrete containing discarded tire rubber." Journal of Cleaner Production 102: 78-87.

Thomas, B. S. and R. C. Gupta (2016). "A comprehensive review on the applications of waste tire rubber in cement concrete." Renewable and Sustainable Energy Reviews 54: 1323-1333.

Thomas, B. S., R. C. Gupta and V. J. Panicker (2016). "Recycling of waste tire rubber as aggregate in concrete: durability-related performance." Journal of Cleaner Production 112: 504-513.

Yang, L.-h., Z. Han and C.-f. Li (2011). "Strengths and flexural strain of CRC specimens at low temperature." Construction and Building Materials 25(2): 906-910.

Youssf, O., M. ElGawady, J. Mills and X. Ma (2014). "Prediction of crumb rubber concrete strength."

Youssf, O., M. A. ElGawady, J. E. Mills and X. Ma (2017). "Analytical modeling of the main characteristics of crumb rubber concrete." Special Publication 314: 1-18.

Yung, W. H., L. C. Yung and L. H. Hua (2013). "A study of the durability properties of waste tire rubber applied to self-compacting concrete." Construction and Building Materials 41: 665-672.

VII. RECYCLED ADDITIVE TO IMPROVE FREEZE-THAW DURABILITY OF HIGH FLY ASH CONTENT MORTAR

Ahmed A. Gheni and Mohamed A. ElGawady

ABSTRACT

Statistics show an increase in using fly ash in concrete to improve both sustainability and performance. However, concrete incorporating high volume fly ash has counters an issue with incompatibility between fly ash and air entraining admixture (AEA). This study investigates using ground recycled rubber (GRR) as an eco-friendly alternative to AEA to improve the freeze-thaw performance of mortar mixtures incorporating two different types and ratios of fly ash. Two different sizes and ratios of GRR were used in this study. The results were compared with mixtures having two different types and dosages of AEA as well as a reference mortar mixture having neither GRR nor AEA. Foam index was investigated for both types of fly ash and compared with cement. The compressive strength retention values of mortar cubes after exposing them to 36 freeze-thaw cycles was determined and related to the air content of each mixture. This study revealed that the GRR outperformed the AEA in terms of the freeze-thaw durability where some of the mixtures exceeded 100% compressive strength retention due to the crystallization of the rubber particles under low temperature.

Keywords: Recycled rubber; Freeze-thaw; Fly ash concrete; Durability; Eco-friendly; Sustainable construction admixture.

1. INTRODUCTION

About sixty million tons of coal combustion products including fly ash, bottom ash, and flue-gas desulfurization were beneficially used in 2016 out of 107 million tons that

were produced. Fly ash is widely used in concrete mainly as a partial cement replacement with 14.4 million tons of fly ash were used during 2016 compared to 10.5 and 11.0 million tons during 2000 and 2010 respectively (ACAA 2017) . Using fly ash in concrete enhances numerous concrete attributes such as strength, durability, heat of hydration, and sustainability (Mehta and Gjørv 1982, Tikalsky et al. 1988, Malhotra 1990, Bilodeau et al. 1994, Naik et al. 1998). In addition to partial replacement, researchers also completely replaced cement with fly ash producing geopolymer concrete (Davidovits 1991, Provis and Bernal 2014, Temuujin et al. 2014, Gomaa et al. 2017, Gomaa et al. 2017, Gomaa et al. 2018, Sargon et al. 2018). Using fly ash in concrete reduces demand on Portland cement, resulting in significant reductions in greenhouse gas emissions.

ACI 318-11 Building Code limits the quantity of fly ash or other C618 pozzolans to 25% max. by weight for a concrete subjected to exposure class F3, which is a very severe freeze-thaw exposure. Based on this, in this manuscript, the authors will refer to mixtures having more than 25% fly ash as high-volume fly ash mixtures. While concrete incorporating fly ash as partial cement replacement has been in use for few decades, comprehensive adoption of concrete incorporating a high-volume fly ash, i.e., more than 25% of cement being replaced, has few barriers including the issue of erratic behavior of concrete due to the uncontrolled constituents of the used fly ash as a by-product material. Researchers reported different air content stability between mixtures having class F and class C fly ash respectively. Other researchers reported an increase in air-entraining admixture demand with the increase of the organic content in fly ash, which cause a higher air content loss with time (Gebler and Klieger 1983, Freeman et al. 1997, Hill et al. 1997). In addition to the organic content, it was reported that the isotropic

(amorphous)/anisotropic (crystalline) carbon ratio is the main reason for the unpredicted demand for air entraining agents (Hill et al. 1997).

Another issue with fly ash concrete , and it is clearer with high-volume fly ash concrete, is the incompatibility between the used fly ash and performance-enhancing admixtures such as air entraining admixture (AEA), which is quite crucial for concrete subjected to freeze-thaw cycles (Ley et al. 2008, Sun and Wu 2013). The most widespread practice toward improving the freeze-thaw durability of concrete is to introduce uniformly scattered air voids, through adding AEA, to the binder matrix to reduce the freezing stress on the matrix by allowing the expanded free water to travel to the added air pockets instead of applying expansion internal stresses that lead to the disintegration of paste structure. However, these AEAs do not yield the anticipated durability improvement once the concrete matrix incorporated fly ash . Gebler and Klieger (1983) recommended a significant increase up to 550% in the AEAs dosages when there are more than1.0% organic materials present within the used fly ash. Other researchers connected the AEA demand to the burning process or the surface area of fly ash (Freeman et al. 1997) However, other study reported that the relation between the loss on ignition, which is an indication for the amount of carbon, and AEA dosage was poorly correlated (Ley et al. 2008).

Another approach to improve freeze-thaw resistance of concrete is to use crumb rubber which work similar to AEA (Savas et al. 1997, Gheni et al. 2017). In addition to the method of tire grinding (i.e., ambient vs cryogenic) and amount of rubber used as admixture within a concrete mixture, the effect of the rubber on freeze-thaw durability has been found to be influenced significantly by the rubber particles' size where the durability of concrete can be further improved should a finer particle size up to 20 μm is used which is comparable

to the size of cement particles (Richardson et al. 2012, Gadkar and Rangaraju 2013, Richardson et al. 2016). However, it is expensive to produce crumb rubber with a particle size smaller than 1.5 mm (Shu and Huang 2014). This study investigated the use of ground recycled rubber (GRR), obtained as a byproduct of tire recycling plant, as admixture to improve the durability of high-volume fly ahs concrete. GRR which is a waste material of tires recycling plant, was used in this study as a sustainable alternative to improve the durability of high-volume fly ash cement mortar. Two different GRR sizes, a size smaller than 74 µm and a size between 149 µm and 74 µm, were used as an additive. The results are compared to those of mortar mixtures incorporating AEA.

1.1. RESEARCH SIGNIFICANCE

This study introduces using GRR as an eco-friendly additive to improve the freeze-thaw performance of high-volume fly ash mortar mixtures. The proposed solution helps in overcoming the issue of the incompatibility between the concrete with a high volume of fly ash from one side and the performance-enhancing admixtures, such as air entraining admixture (AEA) from the other side. In addition, this study introduces a recycled byproduct rubber powder to overcome the high cost of producing and grinding the rubber to a size smaller than 74 µm.

Two grades of GRR and two different types of AEA were investigated during this study as additives to cement mortar with mortar mixtures prepared using two different types of fly ash. The change in the compressive strength of 50 mm mortar cubes was used as an indication to the effects of each additive on the freeze-thaw durability after exposing the specimens to 36 cycles of freeze and thaw similar to those described in ASTM C666 procedure A(ASTM. et al. 2008). In addition, the foam index for each air entraining

admixtures with each type of fly ash was used to evaluate the compatibility and the effectiveness of each admixture.

2. EXPERIMENTAL INVESTIGATION

2.1. MATERIAL PROPERTIES

Well-graded river sand passed through a No. 4 (4.75 mm) sieve was used in this study (Figure 1). Fly ash was sourced from two different coal power plants located in Labadie and Kansas City (Figure 2 c&d), Missouri, USA. The constituents of the fly ash was chemically analyzed and determined using X-ray fluorescence (XRF). Both types were classified as class C per ASTM C618 (Table 1) with calcium content of37.0% and 21.2% for fly ashes obtained from Labadie and Kansas City, respectively. The loss of ignition value, which is the carbon content of the fly ash that is burnt off when subjected to 700 ˚C for two hours, was used to determine the carbon content.

The waste of the scrap tires' processing was collected in a form of rubber dust with fibers from a scrap tire processing factory in Macon, Missouri, USA. The rubber dust was sieved to remove any unwanted particles and to split it into different grades based on their sizes. Two grades of GRR were used during this study. The first grade was for recycled rubber with particles passing sieve No. 100 and retained on sieve No. 200 which led to a particle size between 149 µm and 74 µm (Figure 2b). This grade was comparable to the smallest particles' size in the used fine aggregate. The second grade was for ground recycled rubber particles pass sieve No. 200 which led to a particle size smaller than 74 µm (Figure 2a). This grade has the same maximum particles' size of the used cement. However, it is almost identical with particles' size distribution of both fly ashes. In addition

to the fine aggregate, Figure 1 shows the particle size distribution of both sizes of ground recycled rubber, cement, sand, and the two fly ash types determined using laser diffraction analyzer.

Scanning electron microscope (SEM) was used to investigate the shape and the element analysis of the two grades of the recycled rubber and the two types of fly ash. The rubber particles had a rough and irregular shape for both grades (Figure 3) as it was collected from ambient shredded tires. Fiber pieces were also accompanied the rubber particles. The element analysis of the fiber (Figure 3c) shows that the major component of these fibers was carbon followed by oxygen with a very small amount of silicon which refers to a cellulosic fiber.

Two AEA with different chemistry, neutralized vinsol resin (MasterAir VR 10) and acid salts-based (MasterAir AE 200), were used during the course of this study. Both admixtures meet the requirements of ASTM C 260 (ASTM 2001) and AASHTO M 154 (AASHTO 2011).

2.2. MORTAR TEST MATRIX

Cement mortar mixtures were prepared per ASTM C109/C109M-16a (International 2016) with cementitious materials to sand ratio proportioned by mass equal to 1:2.75 and a constant water/cementitious material of 0.357 to fulfill the required workability of 40% cone flow.

Forty-five mixtures having 0%, 25%, and 50% fly ash as a cement replacement were prepared and grouped into five sets (Table 2). Set 1 included 0% fly ash while sets 2 and 4 included 25% fly ash replacement with the fly ash was sourced from Labadie and Kansas City power plants, respectively. Similarly, sets 3 and 5 included 50% fly ash

replacement with the fly ash was sourced from Labadie and Kansas City power plants, respectively. Set 1 included a reference mixture where neither AEA nor rubber was used. Each of the four sets included mixtures that were prepared with two dosages from each type of the AEA, based on the manufacturer's recommendation, and two rubber ratios from each size of GRR (Table 2).

2.3. FOAM INDEX TEST

In the beginning, the foam index test (Harris et al. 2008) was performed for each type of fly ash as well as the cement. The foam index test procedure can be summarized by placing 20 g of cement with 50 mL of water in a 125 mL glass jar before capping and shaking the jar for 1 minute. Next, adding the AEA solution in a dosage of 2 to 5 drops at a time followed by capping and shaking the jar for 15 seconds with a continues observation to the stability of the foam. The target of the test is finding the minimum amount of AEA needed to produce a stable foam for 45 seconds. Although the foam Index test is not designed to determine the actual AEA dosage rates for concrete, it is an effective way to determine if specific materials will require more or less AEA relative to others. In addition, the foam index test visually showed the presence of unburned carbon, which is as reported before as the main reason for the unstable behavior of the fly ash concrete in terms of the air voids.

2.4. AIR CONTENT OF MORTAR MIXTURES

The air content for each mixture was examined per ASTM C185-15a (ASTM 2015) where the air content was calculated based on the measured density of the fresh mortar using a 400±1 mL cylindrical measure (Figure 5 a), the known densities of the constituents,

and the mixture proportions. Furthermore, ASTM C231/C231M−17a (ASTM 2010) can be used to calculate the air content of freshly mixed concrete by pressure. During this study, the same method was used to calculate the air content of the mortar mixtures using the new version of air meters that manufactured exclusively for mortar mixtures (Figs. 5b and 5c) from observation of the change in volume of mortar with a change in pressure. The test procedure can be summarized by start placing the mortar in the test apparatus bowl in two layers followed by rodding for 25 times for each layer before striking off the top surface. Next, the top part of the air pot was clamped tightly followed by adding water until it raises to the overflow valve. Then, about 1.4 kPa pressure was applied while all valves were closed to read the air content to the nearest 0.1%. Finally, the results from both tests were compared and related to the foam index results as well.

2.5. FREEZE-THAW DURABILITY

Three 50 mm mortar cubes from each mixture were subjected to 36 freeze-thaw cycles (Figure 6) similar to those described in the ASTM C666- procedure A (rapid freezing and thawing in water). After these cycles, the compressive strengths of the exposed cubes were determined and compared to those of reference-unexposed cubes cast from the corresponding mixture and tested at the same age. The strength retention (%) was used then as an indication to the durability performance of each mixture and the impact of the different types and dosages of AEA as well as the different sizes and percentages of recycled rubber.

3. EXPERIMENTAL RESULTS AND DISCUSSION

3.1. FOAM INDEX RESULTS

Figure 7 shows the foam index for the two types of the fly ash and cement. As shown in Figure 7a, there is a significant increase in the foam index for both Kansas City and Labadie fly ash paste compared with the cement paste mixture where the foam indices are three-times and seven-times that of the cement for Kansas City, and Labadie fly ash, respectively when air entraining admixtures type AE 200 was used. The same trend was recorded when air entraining admixtures type VR was used with foam indices of two-times and three-times that of cement paste mixture for Kansas City mixture and Labadie fly ash mixture, respectively. The increase in the foam index with both types of fly ash was related to the presence of unburned carbon within both types of fly ash. In addition to the visual inspection (Figure 4e), increasing the loss on ignition increased the foam index for both types of air entraining admixtures (Figure 7b).

3.2. AIR CONTENT OF MORTAR MIXTURES

Figure 8 shows the calculated air content for all mixtures using the air meter (Figure 8a) and ASTM C185-15a (ASTM 2015) method based on the measured density of the mortar (Figure 8b). The general trend was almost similar in both methods except for the reference mixtures; however, ASTM C185-15a (ASTM 2015) method resulted in higher air content compared to the air meter method. This difference was reported in the literature and was related to the addition of the absolute volume components without considering the dissolve of cement and fly ash in water which leads to increase the volume of paste and

then the volume of air content (Lawrence et al. 1999). As a result, the air meter method (Figure 8a) was considered in the remaining of this manuscript.

In terms of the air entraining admixtures, admixtures VR with lower foam index resulted in higher air content compared to AE 200. The air content for all mixtures with no AEA was between 4.1 and 5.5% with the reference mortar mixture having the highest air-content followed by Labadie fly ash mixtures and finally Kansas City fly ash mixtures. It is also worth noting that with increasing the fly ash content in the mixture the air content decreased.

Adding the AEA increased the air-content up to 13 and 9% with VR and AE200 admixtures respectively. The significant impact of using the fly ash as a replacement of cement on the air content can be noticed in Figs. 8a. Using a dosage of 215 mL/100kg of VR admixture , which is close to the maximum recommended dosage by the manufacturer, increased the air content by 33%, 217%, 160% for mixtures with fly ash ratios of 0%, 50% Kansas City, and 50% Labadie fly respectively.

However, adding AE 200 admixture was less effective in increasing the air content compared to VR admixture resulting in less air content with mixtures with 25 and 50% fly ash compared to the reference mixture. Using a dosage of 75 mL/100kg from AE200 admixture, which is close to the maximum recommended dosage by the manufacturer, increased the air content by only 63% , 90% and 71% for mixtures with fly ash ratios of 0%, 50% Kansas City, and 50% Labadie fly respectively.

3.3. FREEZE-THAW DURABILITY RESULTS.

3.3.1. Freeze-Thaw Performance with Air-Entraining Admixtures. The freeze-thaw durability for the mortar mixtures with different types and ratios of fly ash was evaluated by calculating the normalized compressive strength retention after exposing three cubes from each mixture to 36 freeze-thaw cycles. First, the impact of two types and two dosages of AEA on the compressive strength retention was investigated and the results are presented in Figure 9. The impact of both AEA dosages on the reference mixture with 0% fly ash was consistent where the compressive strength retention increased from 71% to 105% and 95% with VR dosages of 70 and 215 mL/100kg respectively and to 96% and 93% with AE200 dosages of 25 and 75 mL/100kg respectively. These results are compatible with the foam index results (Figure 7a) where the foam index was 1.0 for both AEAs. Although the dosages of both AEAs were tripled, the compressive strength retentions were slightly decreased due to the excessive presence of air void that attracts more water to get into the paste instead of working as an escaping room for the expanded water due to the freezing action.

In terms of Labadie fly ash, which has a foam index higher than Kansas City fly ash, the performance of the mixtures with low VR admixture dosage was better than that with higher VR admixture dosage in both the 25 and 50% fly ash mixtures. This behavior is related to the manufacturer's recommended high dosage of VR, 260 mL/100 kg, compared to that of the AE200 admixture, 98 mL/100 kg, while the foam index results showed opposite trend with a foam index 233% higher for AE200 admixture compared to VR admixture. Both dosages of AE200 admixture showed a similar performance with a

with almost 100% strength retention as the results were within the natural variation of experimental results.

In terms of mixtures with 25% Kansas City fly ash, there was a significant loss of approximately 43%, and 52% in the compressive strength retentions when the VR admixture was used, at a dosage of 70 mL/100 kg and 215 mL/100 kg, compared to using no AEA at all. This loss increased with increasing the fly ash content. Using the manufacturer suggested dosages, that were proposed based on mixtures having cement only as the cementitious material, while the foam index doubled when cement was replaced with Kansas City fly ash. These results are compatible with those in Figure 8, where the mixtures with Kansas City fly ash has a very high air content, which exceeded 10%, when VR admixture was used which attract more water to be stored in the paste matrix and where it was reported before to have a negative impact on the freeze- thaw resistance. At dosages of AE200 admixture equal to 25 mL/100 kg a noticeable decrease in the compressive strength of approximately 28% was recorded compared to using no AEA at all. However, at dosages of AE200 admixture equal to 75 mL/100 kg, mixtures with Kansas City fly ash performed better with almost 100% strength retention as the results were within the natural variation of experimental results. The performance of the mixtures with AE200 admixture was better since this AEA produced a reasonable air content around 6 to 8% (Figure 8).

It is worth noting that air content in concrete containing fly ash is less stable over a period of up to 90 min compared to concrete mixtures with cement only. The air content stability with time is connected to the chemical composition of the fly ash (Gebler and Klieger 1983, Freeman et al. 1997), and the freeze-thaw performance is related to the final retained air content.

3.3.2. Freeze-Thaw Performance with Ground Recycled Rubber. Figure 10 shows the normalized compressive strength retentions of the different mortar mixtures including GRR as an admixture. In general, adding the GRR improved the compressive strength retention after 36 freeze-thaw cycles compared to reference mixtures with 0% GRR and without any air-entraining admixtures. In addition to reaching the full compressive strength of the specimens that were not exposed to freeze-thaw cycles (100% compressive strength retention), All mixtures with both 25 and 50% of Kansas City fly ash exceeded the unexposed compressive strength by up to 26%.In terms of the mixtures with Labadie fly ash, 75% of the specimens with both 25 and 50% exceeded the unexposed compressive strength by up to 30%, while the other 25% reached 90% of the unexposed compressive strength, which is still higher than the reference mixture with 0% GRR.. This increase was due to the fact that rubber get stiffer starting from temperature under 0 ˚C down to -65 ˚C which is the glass transition point of rubber due to the crystallization of the rubber particles (Fuller et al. 2004, Gheni et al. 2017, Gheni et al. 2017). As the rubber particles move to a crystalline condition, their ability to resist and transfer the stresses to the binder matrix increase, which leads to higher compressive strength capacity. In addition to the crystallization of rubber particles under low temperature, the flexibility of the rubber particles helps the concrete matrix to absorb the internal stresses that come from the frozen water (Savas et al. 1997, Gadkar and Rangaraju 2013, Gheni et al. 2017).

The current study showed that the particles' size of GRR did not affect the freeze-thaw resistance of mortar specimens with both 25 and 50% Kansans City fly ash where all mixtures exceeded 100% strength retention and the results were within the natural variation of experimental results. However, when the GRR size was smaller than 74µm instead of

74-149 µm, mixtures with Labadie fly ash showed an average increase in the compressive strength retention of 10 and 11% for mixture with 4 and 8% GRR ratio This occurred as the largest particle size used during this study was 149 µm which represented 30% of the size suggested in the literature. Previous investigations recommended using a rubber with particle size smaller than 500 µm to ensure a consistent, even distribution, and less distance between the particles for the same amount of rubber compared to larger particles (Gadkar and Rangaraju 2013, Richardson et al. 2016).

The irregular shape of the rubber particles (Figure 3) affected the air-entraining system by entrapping more air within and around the rubber particles. These extra air voids have a positive impact on freeze-thaw durability by acting as an entrainment air that provides escaping rooms to release the freezing internal pressure.

4. SUMMARY AND CONCLUSIONS

Two different contents of ground recycled rubber (GRR), with different sizes, were investigated during the course of this study, as a sustainable alternative to air entraining admixtures (AEA) to improve the durability performance of high-volume fly ash mortar mixtures. In addition to the sustainability aspect associated with using GRR, the GRR has the potential to address the issue that air entraining admixture (AEA) are incapable and/or inefficient in creating a stable air entraining in the case of high-volume fly ash mortar. Sixty mortar mixtures having fly ash sourced from two different power plants, two fly ash content ratios, two types and dosages of AEAs, and two sizes and two ratios of GRR were examined. This study revealed the following findings and conclusions:

1. Although the manufacturer suggested dosages of AEAs worked as expected and increased the air entrained and freeze-thaw resistance of the reference mortar

mixture where the cementitious material was solely Portland cement, they failed to do so for high volume fly ash mortar mixtures. This failure occurred due to either excessive or shortage in air entrained amount. Air content of more than 10% caused a significant degradation in the compressive strength retention after being subjected to freeze-thaw cycles while mixtures with air content less than 4% show a poor freeze-thaw resistance.

2. The dosage of AEAs should be optimized based on the chemical composition of the fly ash used in a mixture. In particular, the amount of the unburned carbon was found to influence the amount of air entrained. High loss on ignition value leads to a higher demand for air entraining admixtures.
3. For the neutralized vinsol resin admixture (VR 10), the manufacturer suggested a dosage of three-time that of the acid salts-based admixtures (AE200) to display the same performance. However, the foam index results showed the opposite. The foam indices for AE200 admixture were 150 and 230% of those for VR 10 with mortar mixtures having Kansas City and Labadie fly ash cement replacement, respectively.
4. Using the ground recycled rubber as an additive to mortar mixture with different types and content of fly ash improved the freeze-thaw performance compared to the AEA. Crystallization of rubber particles under low temperature resulted in a compressive strength retention that exceeds 100% of that in unexposed specimens.
5. Since both sizes of ground recycled rubber are smaller than 500 μm, which was recommended in the literature to be used to improve freeze-thaw resistance, there was no clear difference in the performance when GRR with a maximum size of 74 or 149 μm was used.

6. More work is still required on the space factor ,which represent the distribution of the GRR particles as well as air voids within the matrix. The air voids stability with time and its influence on the freeze-thaw performance need to be investigated as well.

ACKNOWLEDGEMENTS

This research was supported by the Missouri Department of Natural Resources. However, any opinions, findings, conclusions, and recommendations presented in this paper are those of the authors and do not necessarily reflect the views of the sponsor.

Table 1. X-Ray fluorescence chemical analysis.

Fly Ash	CaO (%)	Al2O3 (%)	SiO2 (%)	Na2O (%)	MgO (%)	P2O5 (%)	K2O (%)	TiO2 (%)	MnO (%)	Fe2O3 (%)	LOI (%)
Labadie	37.0	14.0	36.9	1.62	4.80	0.70	0.62	0.87	0.03	3.52	1.13
Kansas City	21.2	20.1	43.9	2.87	4.29	0.51	0.70	1.36	0.05	4.96	0.87

Table 2. Test matrix.

		Mix ID	Fly ash (%)	VR (mL/100kg)	AE 200 (mL/100kg)	Rubber (%) 74-149 µm	Rubber (%) <74µm
	0% Fly ash	R	0	0	0	0	0
		0F-70VR	0	70	0	0	0
		0F-215VR	0	215	0	0	0
		0F-25AE	0	0	25	0	0
		0F-75AE	0	0	75	0	0
		0F-4R100	0	0	0	4	0
		0F-8R100	0	0	0	8	0
		0F-4R200	0	0	0	0	4
		0F-8R200	0	0	0	0	8
Labadie Fly ash	25% Fly ash	25F1	25	0	0	0	0
		25F1-70VR	25	70	0	0	0
		25F1-215VR	25	215	0	0	0
		25F1-25AE	25	0	25	0	0
		25F1-75AE	25	0	75	0	0
		25F1-4R100	25	0	0	4	0
		25F1-8R100	25	0	0	8	0
		25F1-4R200	25	0	0	0	4
		25F1-8R200	25	0	0	0	8
	50% Fly ash	50F1	50	0	0	0	0
		50F1-70VR	50	70	0	0	0
		50F1-215VR	50	215	0	0	0
		50F1-25AE	50	0	25	0	0
		50F1-75AE	50	0	75	0	0
		50F1-4R100	50	0	0	4	0
		50F1-8R100	50	0	0	8	0
		50F1-4R200	50	0	0	0	4
		50F1-8R200	50	0	0	0	8
Kansas City Fly ash	25% Fly ash	25F2	25	0	0	0	0
		25F2-70VR	25	70	0	0	0
		25F2-215VR	25	215	0	0	0
		25F2-25AE	25	0	25	0	0
		25F2-75AE	25	0	75	0	0
		25F2-4R100	25	0	0	4	0
		25F2-8R100	25	0	0	8	0
		25F2-4R200	25	0	0	0	4
		25F2-8R200	25	0	0	0	8
	50% Fly ash	50F2	50	0	0	0	0
		50F2-70VR	50	70	0	0	0
		50F2-215VR	50	215	0	0	0
		50F2-25AE	50	0	25	0	0
		50F2-75AE	50	0	75	0	0
		50F2-4R100	50	0	0	4	0
		50F2-8R100	50	0	0	8	0
		50F2-4R200	50	0	0	0	4
		50F2-8R200	50	0	0	0	8

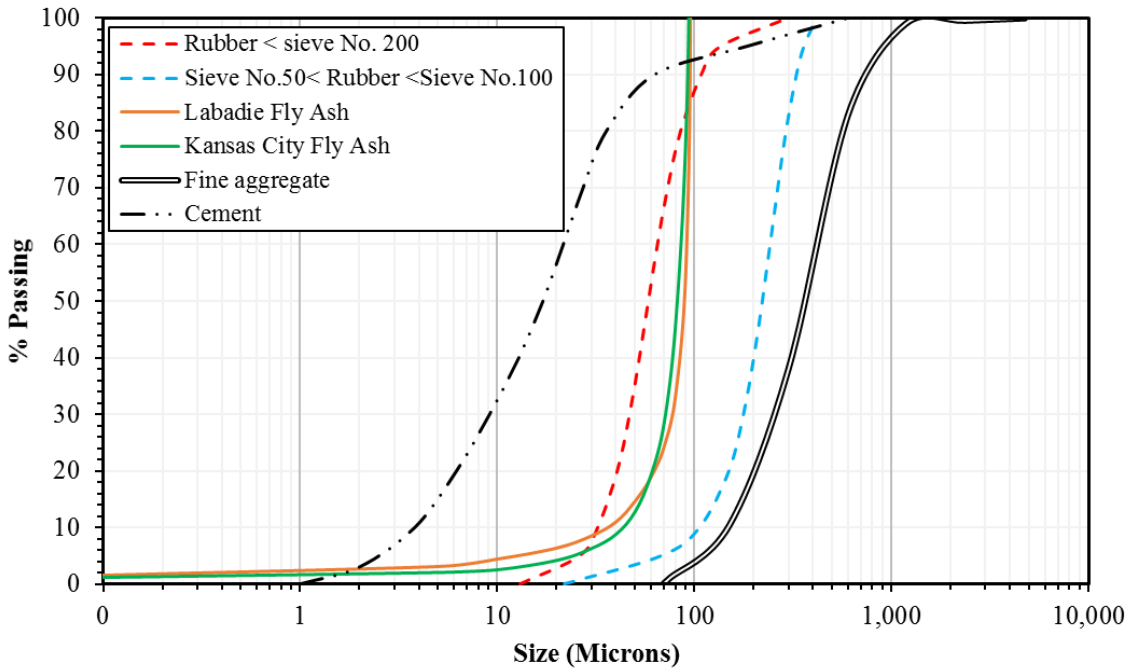

Figure 1. Sieve analysis of the fine aggregate, cement, rubber, and fly ash.

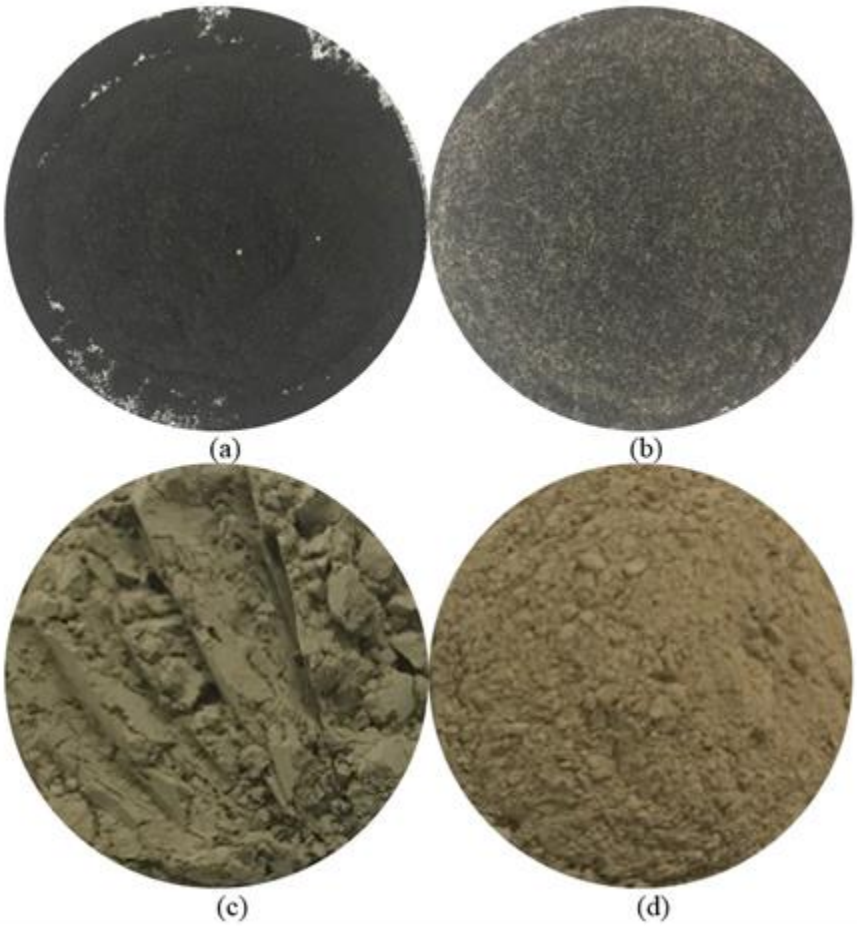

Figure 2. Images of the used materials (a) GRR with max. size of 74 µm, (b) GRR with max. size of 149 µm, (c) Labadie fly ash, and (d) Kansas City fly ash.

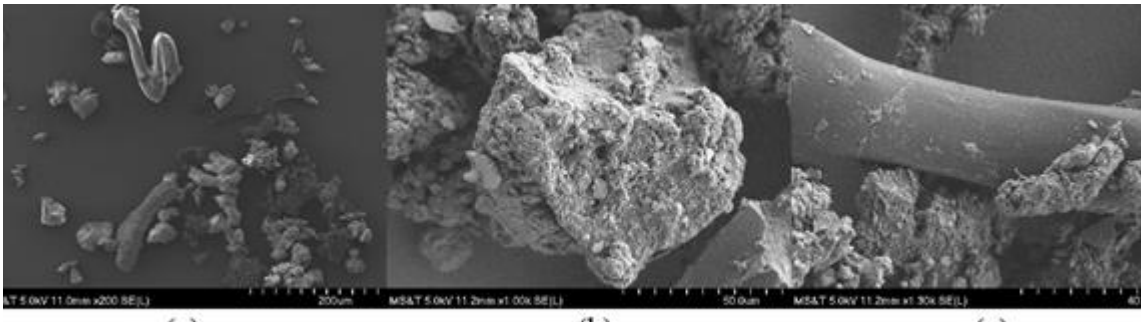

Figure 3. SEM analysis of ground recycled rubber (a) the whole compositions (b) rubber particles, and (c) fiber particles.

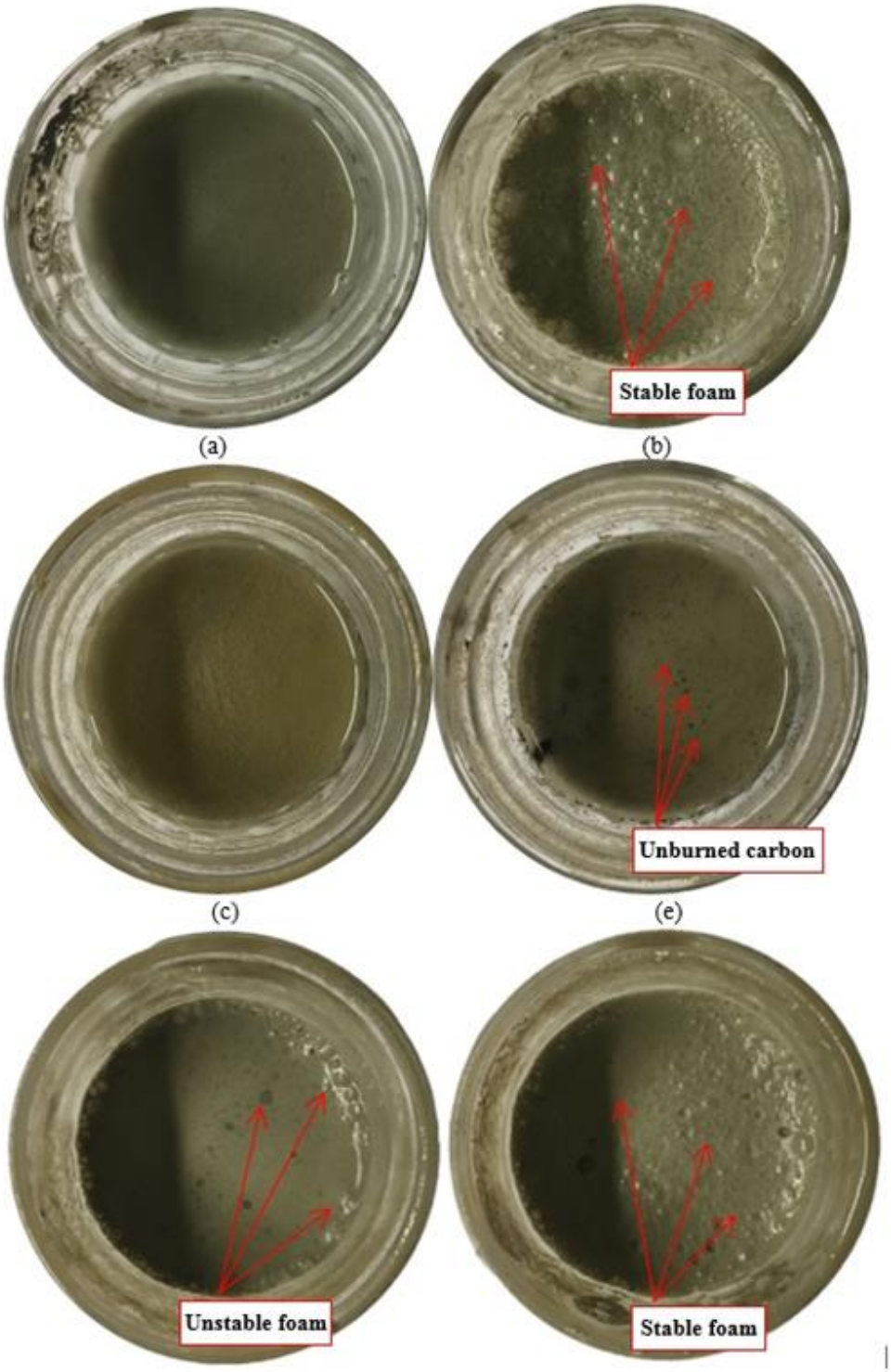

Figure 4. Foam index test (a) cement before adding AEA (b) cement after adding the required AEA dosage (c) fly ash before adding AEA with low carbon content, (e) fly ash before adding AEA with high carbon content (f) fly ash with unstable foam, and (g) fly ash with stable foam.

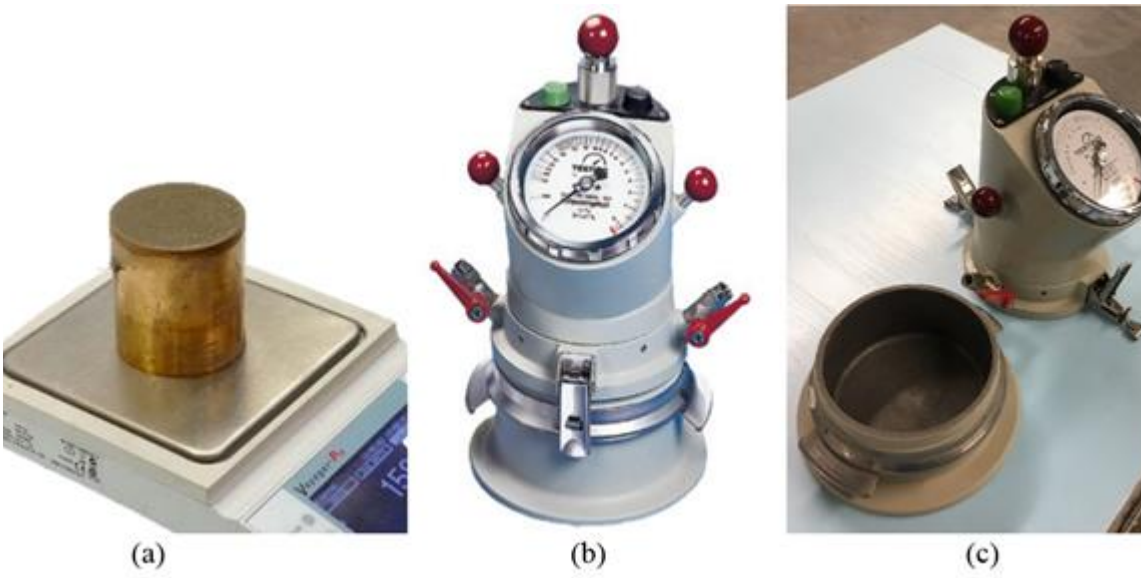

Figure 5. Air content of cement mortar (a) ASTM C185-15a method (b) overview, and (c) detailed view of air entrainment meters for mortar.

Figure 6. Test specimens in a freeze-thaw durability chamber.

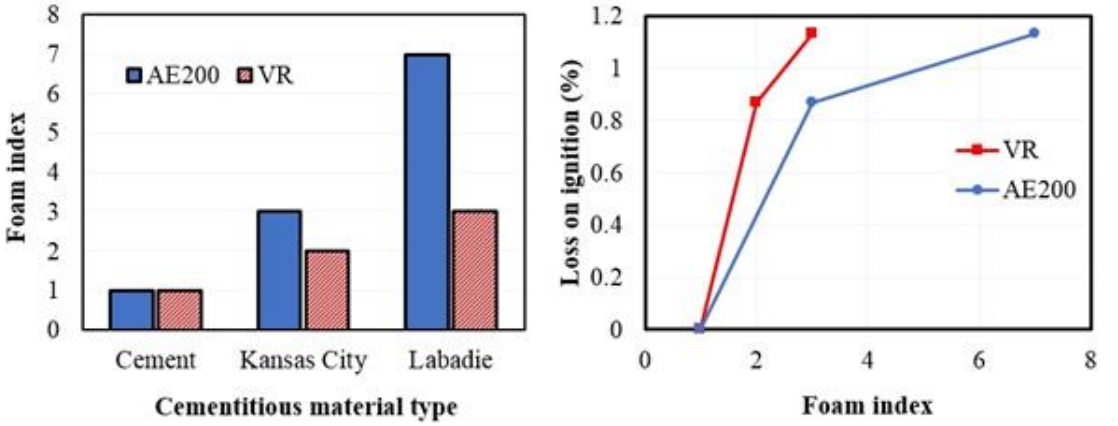

Figure 7. Foam index results (a) foam index for different types of cementitious material, and (b) the relation between the foam index and loss on ignition.

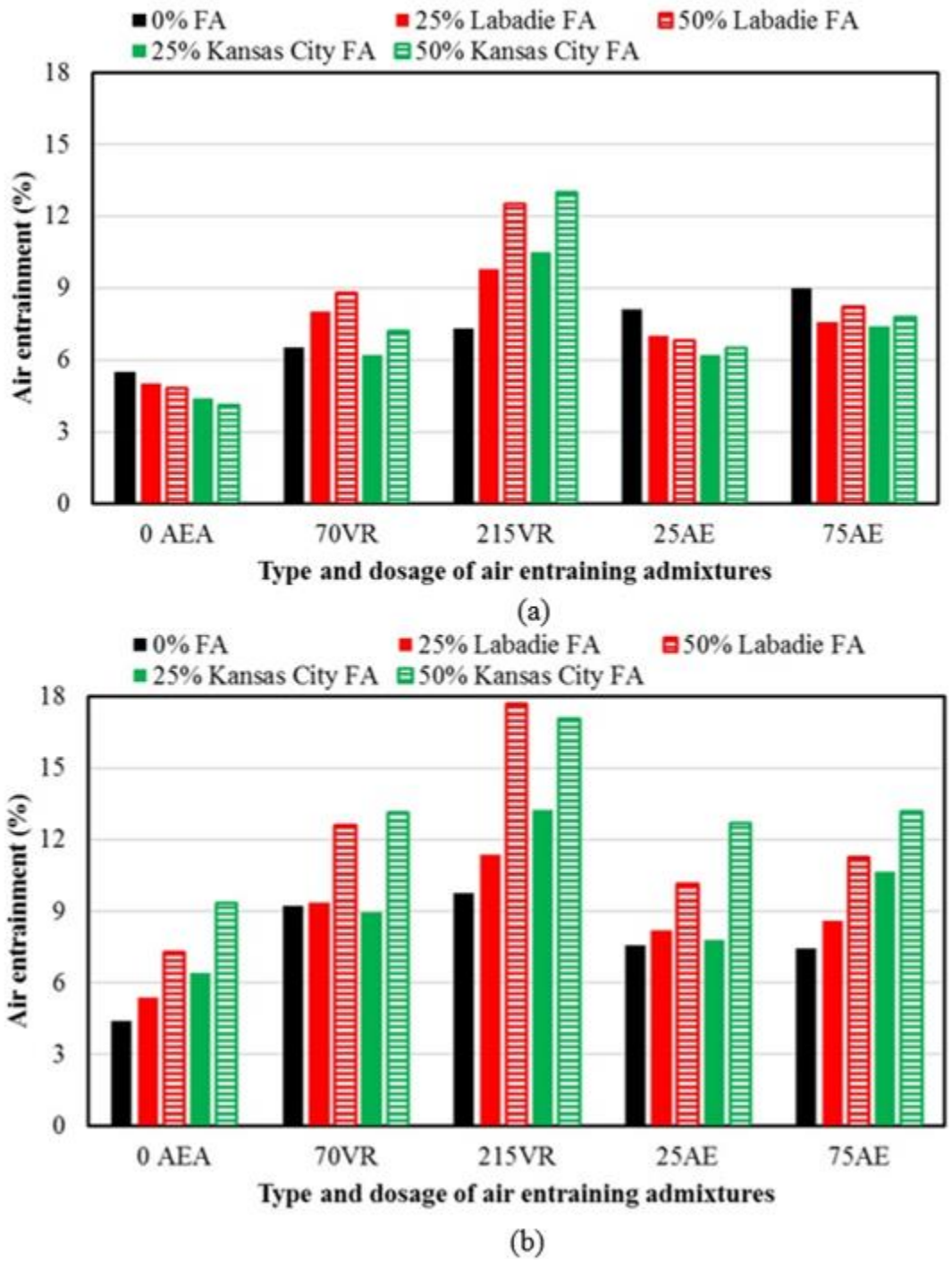

Figure 8. Air content of all mortar mixtures using (a) air meters (adopted ASTM C231/C231M−17a method) and (b) ASTM C185-15a method.

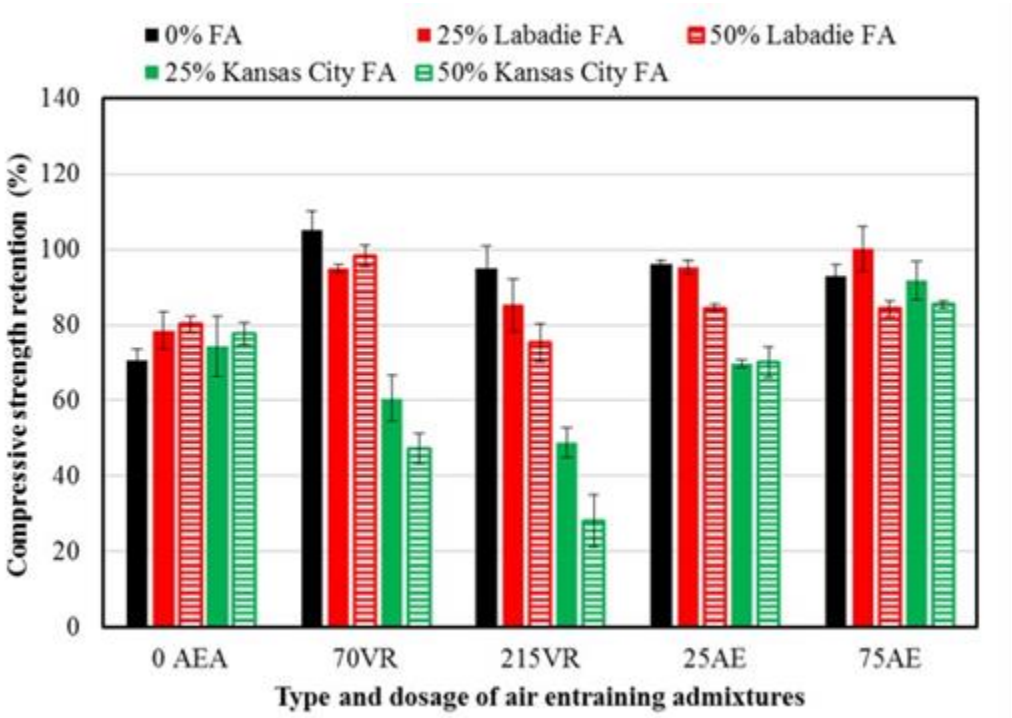

Figure 9. Normalized compressive strength retention after 36 freeze-thaw cycles for mortar mixtures with different ratios and types of fly ash and different dosages and types of AEA.

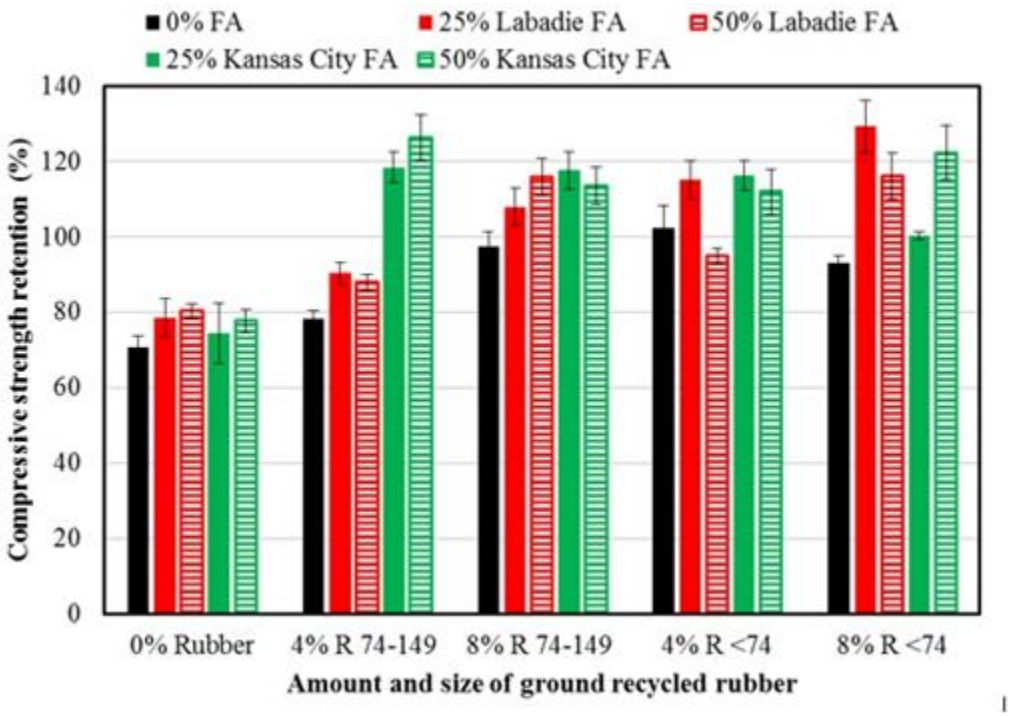

Figure 10. Normalized compressive strength retention after 36 freeze-thaw cycles for mortar mixtures with different ratios and types of fly ash and different ratios and sizes of ground recycled rubber.

REFERENCES

1. ACAA, "2016 Coal Combustion Product (CCP) Production and Use Survey,," *Book 2016 Coal Combustion Product (CCP) Production and Use Survey,*, Editor, ed.^eds., American Coal Ash Association, City, 2017, pp.

2. Bilodeau A, Sivasundaram V, Painter K, Malhotra V, "Durability of concrete incorporating high volumes of fly ash from sources in the USA," *Materials Journal*, V. 91, No. 1. 1994, pp. 3-12.

3. Mehta P, Gjørv O, "Properties of portland cement concrete containing fly ash and condensed silica-fume," *Cement and Concrete Research*, V. 12, No. 5. 1982, pp. 587-95.

4. Malhotra V, "Durability of concrete incorporating high-volume of low-calcium (ASTM Class F) fly ash," *Cement and Concrete Composites*, V. 12, No. 4. 1990, pp. 271-7.

5. Naik TR, Singh SS, Ramme BW, "Mechanical properties and durability of concrete made with blended fly ash," *Materials Journal*, V. 95, No. 4. 1998, pp. 454-62.

6. Tikalsky P, Carrasquillo P, Carrasquillo R, "Strength and durability considerations affecting mix proportioning of concrete containing fly ash," *ACI Materials Journal*, V. 85, No. 6. 1988, pp. 505-11.

7. Temuujin J, Minjigmaa A, Davaabal B, Bayarzul U, Ankhtuya A, Jadambaa T, et al., "Utilization of radioactive high-calcium Mongolian flyash for the preparation of alkali-activated geopolymers for safe use as construction materials," *Ceramics International*, V. 40, No. 10. 2014, pp. 16475-83.

8. Provis JL, Bernal SA, "Geopolymers and related alkali-activated materials," *Annual Review of Materials Research*, V. 44. 2014, pp. 299-327.

9. Davidovits J, "Geopolymers: inorganic polymeric new materials," *Journal of Thermal Analysis and calorimetry*, V. 37, No. 8. 1991, pp. 1633-56.

10. Gomaa E, Sargon S, Kashosi C, ElGawady M, "Fresh properties and early compressive strength of alkali-activated high calcium fly ash paste," *Book Fresh properties and early compressive strength of alkali-activated high calcium fly ash paste*, Editor, ed.^eds., Springer, City, 2017, pp. 497-507.

11. Gomaa E, Sargon S, Kashosi C, Gheni A, ElGawady M, "Effect of Different Class C Fly Ash Compositions on the Properties of the Alkali-Activated Concrete," *Book Effect of Different Class C Fly Ash Compositions on the Properties of the Alkali-Activated Concrete*, Editor, ed.^eds., Springer, City, 2018, pp. 541-7.

12. Gomaa E, Sargon S, Kashosi C, ElGawady M, "Fresh properties and compressive strength of high calcium alkali activated fly ash mortar," *Journal of King Saud University-Engineering Sciences*, V. 29, No. 4. 2017, pp. 356-64.

13. Sargon SP, Gomaa EY, Kashosi C, Gheni AA, ElGawady MA, "Effect of Curing Temperatures on Zero-Cement Alkali-Activated Mortars," *Book Effect of Curing Temperatures on Zero-Cement Alkali-Activated Mortars*, Editor, ed.^eds., Springer, City, 2018, pp. 549-55.

14. Gebler S, Klieger P, "Effect of fly ash on the air-void stability of concrete," *Special Publication*, V. 79. 1983, pp. 103-42.

15. Hill RL, Sarkar SL, Rathbone RF, Hower JC, "An examination of fly ash carbon and its interactions with air entraining agent," *Cement and Concrete Research*, V. 27, No. 2. 1997, pp. 193-204.

16. Freeman E, Gao Y-M, Hurt R, Suuberg E, "Interactions of carbon-containing fly ash with commercial air-entraining admixtures for concrete," *Fuel*, V. 76, No. 8. 1997, pp. 761-5.

17. Sun P, Wu H-C, "Chemical and freeze–thaw resistance of fly ash-based inorganic mortars," *Fuel*, V. 111. 2013, pp. 740-5.

18. Ley MT, Harris NJ, Folliard KJ, Hover KC, "Investigation of air-entraining admixture dosage in fly ash concrete," *ACI Materials Journal*, V. 105, No. 5. 2008, pp. 494.

19. Savas B, Ahmad S, Fedroff D, "Freeze-thaw durability of concrete with ground waste tire rubber," *Transportation Research Record: Journal of the Transportation Research Board*, No. 1574. 1997, pp. 80-8.

20. Gheni AA, ElGawady MA, Myers JJ, "Mechanical Characterization of Concrete Masonry Units Manufactured with Crumb Rubber Aggregate," *ACI Materials Journal*, V. 114, No. 01, 1/1/2017. 2017.

21. Richardson A, Coventry K, Edmondson V, Dias E, "Crumb rubber used in concrete to provide freeze–thaw protection (optimal particle size)," *Journal of Cleaner Production*, V. 112. 2016, pp. 599-606.

22. Richardson AE, Coventry KA, Ward G, "Freeze/thaw protection of concrete with optimum rubber crumb content," *Journal of Cleaner Production*, V. 23, No. 1. 2012, pp. 96-103.

23. Gadkar S, Rangaraju PR, "The Effect of Crumb Rubber on Freeze-Thaw Durability of Portland Cement Concrete," *Advances in Civil Engineering Materials*, V. 2, No. 1. 2013, pp. 566-85.

24. Shu X, Huang B, "Recycling of waste tire rubber in asphalt and portland cement concrete: An overview," *Construction and Building Materials*, V. 67. 2014, pp. 217-24.

25. ASTM., Concrete CC-o, Aggregates C, "Standard test method for resistance of concrete to rapid freezing and thawing." ASTM International; 2008.

26. ASTM C, "260. Standard Specification for Air-Entraining Admixtures for Concrete," *Book 260. Standard Specification for Air-Entraining Admixtures for Concrete*, Editor, ed.^eds., West Conshohocken, PA: ASTM International, City, 2001, pp.

27. AASHTO, "Standard Specification for Air-Entraining Admixtures for Concrete," *Book Standard Specification for Air-Entraining Admixtures for Concrete*, Editor, ed.^eds., American Association of State Highway and Transportation Officials (AASHTO), City, 2011, pp. 2.

28. International A, "ASTM C109 / C109M-16a, Standard Test Method for Compressive Strength of Hydraulic Cement Mortars (Using 2-in. or [50-mm] Cube Specimens)," *Book ASTM C109 / C109M-16a, Standard Test Method for Compressive Strength of Hydraulic Cement Mortars (Using 2-in. or [50-mm] Cube Specimens)*, Editor, ed.^eds., ASTM International, City, 2016, pp.

29. Harris N, Hover K, Folliard K, Ley M, "The Use of the Foam Index Test to Predict AEA Dosage in Concrete Containing Fly Ash: Part I—Evaluation of the State of Practice." 2008.

30. ASTM A, "Standard test method for air content of hydraulic cement mortar." 2015.

31. ASTM, "Standard test method for air content of freshly mixed concrete by the pressure method." 2010.

32. Lawrence P, Ringot E, Husson B, "About the measurement of the air content in mortar," *Materials and Structures*, V. 32, No. 8. 1999, pp. 618-21.

33. Fuller K, Gough J, Thomas A, "The effect of low-temperature crystallization on the mechanical behavior of rubber," *Journal of Polymer Science Part B: Polymer Physics*, V. 42, No. 11. 2004, pp. 2181-90.

34. Gheni A, ElGawady MA, Myers JJ, "Thermal Characterization of Cleaner and Eco-Efficient Masonry Units Using Sustainable Aggregates," *Journal of Cleaner Production*. 2017.

VIII. ECO-FRIENDLY THERMAL AND ACOUSTIC RETROFITTING OF MASONRY ELEMENTS USING RUBBER-FIBER POWDER

Ahmed A. Gheni and Mohamed A. ElGawady

ABSTRACT

The low thermal and sound insulation capacity of concrete masonry unit motivated the researchers to investigate the impact of using rubber-fiber powder (RFP), which comes from scrap tires recycling process, as a partial replacement for cement or sand in cement in plastering mortar. Using recycled rubber has the potential to produce more sustainable construction and reduces the buildings' energy consumption. An experimental investigation was conducted to investigate the impact of using various thicknesses of plastering having varies ratios of RFP in plastering cement mortar on the thermal conductivity and the sound insulation. The thermal conductivity of the new proposed plastering materials was measured according to ASTM D5334-14 and for thermally retrofitted masonry units according to the ASTM C1363−11. The sound absorption test was performed according to the requirements of ASTM E1050 using a tube, two microphones, and a digital frequency analysis system. Plastering mortar mixtures with up to 40% of the cement or sand replaced by rubber-fiber powder did not show any difficulties to mix and apply with different thicknesses on the masonry units. The results indicated that adding rubber-fiber powder as a replacement for cement or sand in plastering mortar has a positive impact on reducing the thermal conductivity of the masonry unit and then reducing the heating energy consumption. Compared to conventional masonry units without any plastering, a reduction varied from 11 to 53% was achieved in thermal conductivity of masonry unit based on the size and amount of RFP as well as the thickness of the plastering

lawyer. Finally, the new rubberized plastering material exhibited a clear increase in sound absorption and noise reduction compared to standard conventional masonry units.

Keywords: Masonry; Thermal insulation; rubber powder; Sustainable material; Eco-friendly; Sound absorption.

1. INTRODUCTION

According to the Energy Information Administration (EIA 2016), Energy usage of buildings, in both residential and commercial sectors, in the United States accounts for 40% of total energy usage. During the year of 2009, about 65.4% of the residential demand of US household was used of for heating and cooling, which makes it 26.2% of the United States energy use (Dehghanpour and Afsharnia 2015). These statistics present the demand and importance of enhancing the energy efficiency of buildings and how this enhancement will lead to a significant cut in the energy use. Many techniques were proposed or used by the construction companies to improve the thermal insulation of building, however, most of the suggested materials have a high embodied energy, which leads to higher CO2 emissions. Using recycled solid waste materials to improve the thermal insulation of buildings will reduce both operating and embodied energy and at the same time utilizing and finding a new home for solid waste material.

Meanwhile, the world is facing a serious threat dealing with scrap tires especially with the continuous increase in the number of vehicles, which is directly connected to the increase in the global population. According to the most recent statistics, there are more than 1.1 billion vehicles on the roads and this number is expected to double by 2040 (Sperling and Gordon 2008, Sperling and Gordon 2009). This enormous number of vehicles across the world led to a global yearly production of tires of 1.7 billion and caused

a yearly generation of 1.0 billion scrap tires (Forrest 2014), which put a significant pressure on the environment and motivated the authors to use the recycled rubber that comes from scrap tires as a replacement for some of the conventional component of the cement plastering mortar.

Recycled rubber was used before as a partial replacement of virgin row construction material to improve the sustainability and some of the mechanical properties (Siddique and Naik 2004, Mohammed et al. 2012, Abu-Lebdeh et al. 2014, Moustafa and ElGawady 2015, Youssf et al. 2016, Gheni et al. 2017, Gheni et al. 2017, Gheni et al. 2017, Moustafa et al. 2017). In terms of fresh properties, it was reported that using crumb rubber has a direct impact on lowering the fresh density and the workability and increasing the air-entrainment (Najim and Hall 2010, Najim and Hall 2012, Gou and Liu 2014). The compressive strength, flexural strength, and the modulus of elasticity of hardened concrete were decreased with the increase of rubber content, however, the ductility and toughness of rubberized concrete were higher than that in conventional concrete (Ganjian et al. 2009, Ho et al. 2012). The water absorption and the porosity were increased with the increase of rubber content due to the increased air voids which led to lower unit weight(Siddique and Naik 2004, Onuaguluchi and Panesar 2014). Using crumb rubber helped to produce more durable concrete by enhancing the abrasion resistance, frost resistance, acid attack and chloride ion penetration (Richardson et al. 2012, Zhu et al. 2012, Gesoğlu et al. 2014, Richardson et al. 2016, Thomas and Gupta 2016), however, the effect of rubber on the carbonation resistance was varied based on the rubber content (Gesoğlu and Güneyisi 2011, Gupta et al. 2014).

Incorporating the crumb rubber within the concrete improved the sound absorption under deferent environmental condition (Mohammed et al. 2012, Holmes et al. 2014). The ultrasonic sound velocity was dropped by 65% with the use of 30% rubber content, which reflected on the sound transmission within the concrete.

There was an obvious influence of using rubber on the thermal characterization of concrete and this influence was mainly related to the amount and the particle size of rubber (Abu-Lebdeh et al. 2014, Fadiel et al. 2014, Kashani et al. 2017). As rubber content increases, the thermal conductivity of concrete decrease due to the relatively low thermal conductivity of rubber compared to concrete and the accompanying entrapped air that been created with the present of rubber particles within concrete (Turgut and Yesilata 2008, Sukontasukkul 2009, Hall et al. 2012). The thermal insulation of a model room was improved when the crumb rubber was used in its walls (Yesilata et al. 2011). Furthermore, low-rise buildings were modified to meet the thermal UK Building Regulations by only involving the crumb rubber in within the construction materials (Paine and Dhir 2010).

In terms of cutting the heating energy consumption, a reduction of 45% was achieved when 37% of the natural aggregate in masonry units was replaced with crumb rubber (Gheni et al. 2017). Varied thickness of thermally insulating materials was used as an energy retrofitting material to improve the fire resistance of masonry walls and it was proven that increasing the thickness result more effective thermal retrofitting (Triantafillou et al. 2017). The effectiveness of any thermal retrofitting system can be influenced by several factors such as the system orientation, climate, and type and thickness of the thermal insulation materials (Huang et al. 2013). Applying the thermal retrofitting system on both external and internal faces of masonry walls has a positive impact on cutting the

energy consumption, however, applying the thermal insulation system externally caused an extra 8% cut in the energy consumption compared to the internally applied thermal insulation (Kolaitis et al. 2013).

Plastering mortar is a functional material rather than a structural material, and mainly plays the role of protecting the wall, in addition to leveling the wall. The main problems existing in plastering mortar are cracking which is a direct result of low ultimate strain. Good plastering mortar can play a protective role in buildings and walls. It can resist the erosion of natural environment such as wind, rain, and snow to buildings, and can improve the durability of buildings. The component materials of plastering mortar are basically the same as those of masonry mortar. However, in order to prevent cracking of mortar layer, sometimes there is a need to add some fibrous materials; sometimes, in order to make it have certain features, such as waterproofing or insulation and other functions, there is a need to select special aggregates or admixtures to improve the crack resistance ability rather than strength.

Even though most of the thermal retrofitting systems have a direct impact on cutting the consumption of operation energy of buildings, most of the retrofitting systems increase the embodied energy of the building because of using conventional unsustainable materials. This paper proposes a new sustainable thermal and acoustic system by incorporating the double recycled rubber powder in a plastering cement mortar.

Two grades of double recycled rubber that were collected as a byproduct from the scrap tire recycling plant were used in this study as a cement or fine aggregate replacement in plastering cement mortar. Ratios of 0, 10, 20, 30, and 40% of rubber powder were use as volume replacement of cement and fine aggregate respectively. The physical

characterizations of the new proposed materials were studied first including compressive strength, flexure strength, direct tensile strength, strain energy, toughness, drying shrinkage, thermal conductivity, heat resistivity, sound absorption, and sound absorption. The thermal and acoustic retrofitting performance were investigated for masonry units with a layer of the proposed material. Plastering layers with varied ratios of rubber powder replacement and varied thicknesses were used in this study. The effectiveness of the proposed retrofitting system was evaluated in cold and hot condition to determine the effect of climate. In terms of the acoustic retrofitting, the sound absorption coefficient and the noise reduction factor were investigated under a varied range of frequency from 0 to 5000 Hz. All the above characterizations were compared with the performance of conventional and lightweight masonry units.

2. MATERIAL PROPERTIES

The waste of the scrap tires' processing was collected in a form of rubber dust with fibers from a scrap tire processing factory in Macon, Missouri, USA. The rubber dust was sieved to remove any unwanted particles and to split it to different grades based on the size. Two grades of recycled rubber were used during this study. The first grade was a recycled rubber with particles pass sieve No. 50 and retained on sieve No. 100 which leads to a particle size between 0.297 and 0.149 mm. Based on the size, this grade was used as a replacement of fine aggregate. The second grade was for recycled rubber particles pass sieve No. 200 which leads to a particle size smaller than 0.074 mm (74 μm). Based on the size, this grade was used as a replacement for cement powder. Figure 1 shows the particle size distribution of both sizes of recycled rubber in addition to cement using the laser diffraction analyzer.

Scanning electron microscope (SEM) was used to explore the shape and the element analysis of the two grades of recycled rubber. As shown in Figure 2, the rubber particles have a rough and irregular shape for both grades. In addition, pieces of fiber were accompanied with the rubber particles. The element analysis of the fiber (Figure 2b) shows that the major component of these fibers is carbon followed by oxygen with a very small amount of silicon which refers to a cellulosic fiber. Well-graded river sand passed through a No. 4 (4.75 mm) sieve was used in this study.

3. EXPERIMENTAL PROGRAM

Two sets of cement mortar mixture with varied rubber ratios were prepared (Table 1). Rubber powder with particles passing sieve No. 200 (74 μm) was used in the first set as a replacement for the cement with volume replacement ratios of 0, 10, 20, 30, and 40%. In the second set, rubber powder with particles passing sieve No. 50 (297 μm) and retaining on sieve No. 100 (149 μm) was used as a replacement for the fine aggregate with volume replacement ratios of 0, 10, 20, 30, and 40%.

3.1. MECHANICAL PROPERTIES OF RUBBERIZED MORTAR

3.1.1. Density, Water Absorption, and Air Voids. Concrete cylinders, 100×200 mm, out of each mixture were used to measure the density and voids in hardened mortar according to ASTM C642-13 method which can be used to deduce concrete permeability attribute and it yields results similar to that of vacuum saturation method; however, the former approach is more versatile. The test procedure can be summarized as follows: the oven-dried masses of all specimens were determined followed by saturating them in water and determine their surface-dry masses after immersion for not less than 48 hrs. After

boiling the specimens in water for 5 hours, the soaked, boiled, and surface-dried masses were determined. Finally, after suspending the specimens in water, the apparent masses in water after immersion and boiling were determined. Based on the results from this procedure, the following characteristics can be calculated:

$$\text{Absorption after immersion, \%} = [(B - A)/A] \times 100 \quad (1)$$

$$\text{Absorption after immersion and boiling, \%} = [(C - A)/A] \times 100 \quad (2)$$

$$\text{Bulk density, dry} = [A/(C - D)].\rho = g_1 \quad (3)$$

$$\text{Bulk density after immersion} = [B/(C - D)].\rho \quad (4)$$

$$\text{Bulk density after immersion and boiling} = [C/(C - D)].\rho \quad (5)$$

$$\text{Apparent density} = [A/(A - D)].\rho = g_2 \quad (6)$$

$$\text{Volume of permeable pore space (voids), \%} = (g_1 - g_2)/g_2 \times 100 \quad (7)$$

Where: A = mass of oven-dried sample in air, B = mass of surface-dry sample in air after immersion, C = mass of surface-dry sample in air after immersion and boiling, D = apparent mass of sample in water after immersion and boiling, g_1 = dry bulk density, g_2= apparent density, and ρ = density of water.

3.1.2. Compressive Strength. Three 50 mm mortar cubes were prepared and tested for each mixture. The compressive strength test was performed according to ASTM C109-16a at the ages of 28, and 56 days. For a given mixture, the testing result of any specimen with a range of 8.7% or more from the average of the results of the three cubes of that mixture were excluded from the average.

3.1.3. Flexural Strength and Toughness. The modulus of rupture, at the ages of 28 and 56 days, of each mixture, was determined using a three-point bending test (Figure 4) carried out on three 40×40×160 mm prisms constructed out of that mixture per ASTM

C348–14. After discarding the strength values that differed by more than 10% from the average value of all test specimens for given mixture, the flexural strength was calculated in MPa as follows:

$$S_f = 0.0028\,P \tag{8}$$

where

S_f = flexural strength, MPa, and

P = total maximum load, N.

In addition to the modulus of rupture, the modulus of toughness was measured. The toughness of a material is the ability to absorb energy within the plastic region without rupture, and it represents the balance between the strength and the ductility. For the behavior shown in Figure 3b, the toughness is calculated as the area under the curve. The toughness factor, T.F., was taken equal to the toughness of the rubberized beam-to-the toughness of the reference beam. The toughness was then calculated as the area under the load-deflection curve. In addition, the brittleness of the new rubberized mortar could be represented by the brittleness coefficient which is defined as the ratio of the compressive strength to the flexural strength.

3.1.4. Tensile Strength and Strain Energy. Three 3-inch length dog-bone-shaped cement mortar specimens (Figure 4a) were cast for each rubber replacement ratio. Special clips were used to hold the specimens to the tensile strength testing machine (Figure4b). The test was performed according to ASTM C307 with a loading speed of 6 mm/min. As shown in Figure 4c, 2 inches digital extensometer was mounted at the middle of the specimens to measure the axial elongation within the test specimens. Based on the displacement readings from the digital extensometer, the strain and later the modulus of

resilience were calculated from the strain-stress curve. The modulus of resilience is defined as the maximum energy that can be absorbed per unit volume without creating a permanent distortion. It can be calculated by integrating the stress-strain curve from zero to the elastic limit (Figure 4d).

3.2. THERMAL CHARACTERIZATION OF RUBBERIZED CEMENT MORTAR AT DIFFERENT TEMPERATURES

Three thicknesses of rubberized mortar with cement or sand replaced with five different ratios of rubber-fiber powder of 0, 10, 20, 30 and 40% were used as a plastering layer on conventional concrete masonry units (Figure 5). The thermal conductivity of the new proposed plastering materials was measured according to ASTM D5334-14, while the thermal conductivity of the plastered masonry units was examined according to ASTM C1363−11 in order to determine the steady-state thermal performance of construction units exposed to a constant heat source.

3.2.1. Thermal Needle Probe Method for Plastering Materials. This test was performed according to ASTM D5334-14 using a transient heat method. This test measures the thermal conductivity using a metal probe that contains both a heating source element and temperature-measuring element. By inserting the probe in the sample, the heating element raises the temperature with time, and the temperature-measuring element recorded the change over a period of time. The temperature decay with time after the cessation of heating was recorded to be included in the calculations to minimize the effects of temperature drift during measurement. The thermal conductivity was calculated after two heating and cooling cycles. All the measurements and the analysis were performed using a fully portable field and lab thermal properties analyzer (Figure 6). The analyzer

uses the transient line heat source method to measure thermal conductivity, resistivity, diffusivity, and specific heat. This test was originally designed to determine the thermal conductivity of soil and soft rock by inserting the thermal needle probe in the soft material using hand pressure without creating any prior hole. Since it is impossible to insert the thermal needle probe in hard materials such as concrete or mortar using hand pressure, a modified method that uses the same technology as in ASTM D5334-14 was used. The modification came from using a 4 mm rotary hammer drill bit to create a properly sized pilot hole. Thermal grease was then squeezed up around the thermal probe (Figure 6b) before inserting the probe in the hole to ensure full contact between the thermal needle probe and the tested material. Using thermal grease eliminates any air gaps between the concrete and the probe surface due to the drilling action. To examine the thermal performance of the newly proposed rubberized mortar under different temperatures, which simulate different seasons, the thermal needle probe test was performed temperature of 22° C and -10° C.

3.2.2. The Guarded Hot Box Method. A guarded hot box was constructed in accordance with ASTM C1363−11 in order to determine the steady-state thermal performance of building units exposed to a constant heat source. The box was constructed using 12.7 mm thick homogeneous plywood plates. The box was insulated from the inside by 50.8 mm thick Styrofoam with an R-value equal to 10 to eliminate any heat loss (Figure 7). All of the parts were glued, tightened together, and inspected to minimize any heat leaks. It was very important to make sure that the expected transferred heat would only go through the masonry unit without any undesirable heat leaks through any gap between the masonry unit and the Styrofoam layer. Therefore, the Styrofoam sheets were shaped and

engraved so that the plastered concrete masonry unit fit in tightly, which eliminate any manufacturing tolerance in the masonry units. The tested plastered masonry unit was located on one of the six sides of the guarded hot box. This test represented a close simulation of the thermal insulation of a building. The heat source was kept inside the box to keep the temperature between 48°C and 52°C, which represented a very hot weather during the Summer season. The temperature outside the box was kept between 18°C and 20° C using the lab AC system to represent semi-cool temperature inside a building. This test system shows the amount of the saved energy by comparing the power consumption required to keep the temperature between 45°C and 55°C using masonry block with plastering mortar layer with varied RFP content. Since the tested masonry unit represented one of the six walls of the box and the consumed power was calculated for the whole box, calculating the energy that was consumed by the masonry unit only was necessary. This was done by using a unit that was fabricated using Styrofoam sheets (Figure 6-b). This unit gave an ultimate insulation with an R factor of more than 30 to find the energy consumed by the guarded box itself to keep the temperature between 45° C and 55° C. The energy consumed by the guarded box itself then was subtracted from the total consumption during the test. The energy consumptions were then calculated for masonry units with rubberized plastering and compared with the conventional masonry unit. Fourier heat conduction equation (Eq.9) was used to calculate the thermal conductivity for each type of masonry blocks. The heat flow at steady state was assumed to be the same as the rate of heat output from the heat source. It was computed as 3.41 times the rate of the inputted electrical energy to the heat source. A sensitive meter was used to monitor and record the energy consumption during each test to obtain the most accurate measurement of electrical

energy consumption. The inside and outside temperature data were collected using two thermocouple wires that connected to a computerized data acquisition system. During the test, the guarded hot box was checked for heat leaking using a sensitive thermal camera. As shown in Figure 6d, the heat was escaping out of the box through the tested specimen only.

The net exposed area of the tested masonry unit was calculated. The thermal conductivity factor was calculated using the measured heat flow and temperatures on both sides of masonry as follows:

$$k = \left(-\frac{qL}{A(t_1 - t_2)} \right) \tag{9}$$

Heat resistivity was then calculated as follows:

$$r = \frac{L}{k} \tag{10}$$

where:

k: thermal conductivity factor, (W/m K).

r: heat resistivity, (m2 K /W).

L: thickness of the tested specimen, (m).

A: area of the tested specimen, (m2).

t1: the temperature of hot plate face in contact with the specimen, K.

t2: the temperature at the heat collecting plate on the top face of the sample, K.

q: heat flow rate within the tested specimen, W/m2. (q = 3.41 times the rate of electrical energy input to the hot plate, Watts).

3.3. ACOUSTIC CHARACTERIZATION OF RUBBERIZED CEMENT MORTAR

3.3.1. Sound Absorption. The ability of a material to absorb sound can be measured using the sound absorption coefficient (α). According to ASTM E1050−12, the Acoustical Properties of Materials and Systems (ACUPRO) was used to measure both absorption coefficient under varied frequencies and noise reduction coefficient. The plane wave tube was carefully machined using stainless steel tube with a wall thickness of 3.2 mm for an accurate measurement of sound pressure amplitude and phase (Figure 8a). The phase response of the tube is less than 0.1 degrees over the operating range from 50-5650 Hz. The precision machined flanges, side ports, and microphone holders accurately maintain microphone alignment. A 16-ohm high-frequency compression JBL compression driver was used to produce sound (Figure 8b). Two 13 mm high accuracy microphones were used with microphone holders to ensure stable posting the testing apparatus (Figure 8c). A fully integrated ACUPRO Software and DT 9837A data acquisition module was used to collect and analyze the output data from the testing apparatus (Figure 8d).

Since the sound absorption of materials is varied under different frequency ranges, it required using a single value that evaluates the sound absorption of the particular material. To solve this problem, the noise reduction coefficient (NRC) was calculated for each masonry material with different rubber ratio using Eq. 11. The NRC can be calculated using the following equation (Thumann and Miller 1986, Sukontasukkul 2009):

$$NRC = (\alpha_{250} + \alpha_{500} + \alpha_{1000} + \alpha_{2000})/4 \tag{11}$$

Where α250, α500, α1000, α2000 are the sound absorption coefficients (α) at 250, 500, 1000, and 2000 Hz respectively.

3.3.2. Sound Transmission. In addition to sound absorption, sound transmission and later transmission loss of retrofitted masonry materials can be measured. This test is similar to the sound absorption test method (ASTM E1050-12) in that it also uses a tube with a sound source connected to one end and the test sample mounted in the tube. However, for sound transmission, four microphones instead of two, at two locations on each side of the sample were used. Plane waves are generated in the testing tube using a broadband signal from a noise source. The resulting standing wave pattern is decomposed into forwarding- and backward-traveling components by measuring sound pressure simultaneously at the four locations and examining their relative amplitude and phase. The acoustic transfer matrix is calculated from the pressure and particle velocity, or equivalently the acoustic impedance, of the traveling waves on either side of the specimen. Finally, A fully integrated ACUPRO software and DT 9837A data acquisition module was used to collect and analyze the output data from the testing apparatus (Figure 9).

The tested specimens were prepared by using a high precision water jet cutter (Figure 10a) to cut masonry specimens that fit tightly inside the ACUPRO testing system (Figure 10b).

4. EXPERIMENTAL RESULTS AND DISCUSSION

4.1. MECHANICAL PROPERTIES

4.1.1. Density, Water Absorption, and Air Voids. Figure 11 shows the influence of using varied RFP ratios and sizes on each of the apparent and bulk dry densities. Adding RFP with a size smaller than 75 μm (R200) up to 20%, decreased the apparent and bulk densities. Replacing 20% of cement with RFP decreased both apparent and bulk dry densities by 17 and 12% respectively. However, using RFP with a size between 150 and

300 µm (R50) as a sand replacement was more influential on both densities and it continued up to 40% replacement of sand. Replacing 20% of sand with RFP decreased both apparent and bulk dry densities by 23 and 20% respectively. Although it was anticipated to have a lower bulk density in the case of increasing the RFP content due to the relatively low density of RFP compared to sand or cement, adding RFP beyond a certain amount did not change the density due to changing the mortar packing density, which leads to a more condense mixture. However, there was no consistent trend since the w/c ratio was changed with adding the RFP as a cement or sand replacement. The high influence of the RFP with particles size between 150 and 300 µm (R50) on the density compared to RFP with particle size smaller than 75 µm (R200) is attributed to the total ratio of RFP within the mortar matrix since the sand represent 78% of the volume reference mortar matrix compared to 22% for the cement. For example, replacing 20% of cement with RFP (R200) leading to a total RFP within the mortar matrix of 4.4% compared to 15.6% when the 20% of sand was replaced with RFP (R50).

4.1.2. Compressive Strength. Figure 12 shows the compressive strength at age of 28 days for the different mortar mixtures with error bars that represent the statistical range of the results. A systematic reduction in the compressive strength was recorded with increasing the RFP replacement ratio. This reduction was expected as a result of replacing a portion of the cementitious material with a non-reactive material in the case of replacing cement or replacing sand with low stiffness material. Figure 12 shows that according to strength per ASTM C270−14a, replacing up to 30% of cement with RFP maintain a class M requirement, which is the highest grade of mortar that requires a minimum compressive

strength of 17.2 MPa at the age of 28 days. In the case of replacing the sand, class M mortar was achieved by replacing up to 25% of sand with RFP.

4.1.3. Flexural and Tensile Strength. Figure 13 shows the modulus of rupture (MOR) of the rubberized mortar prisms with varied RFP replacement ratios. The test was performed on three prisms for each RFP replacement ratio at the age of 28 days. A systematic reduction was noticed with the flexural strength in both cases of replacing cement or sand with up to 40% RFP.

Regarding the tensile strength, the results of the direct tensile strength of dog bone shape mortar specimens with varied RFP sizes and replacement ratios are presented in Figure 14. As shown in Figure 14a, increasing the amount of RFP replacement in the mortar decreased the tensile strength with a relatively higher reduction when cement was replaced compare to the case of replacing sand with RFP. For example, replacing 20% of cement with RFP decreased the tensile strength from 3.80 to 2.76 MPa which represent a reduction of 27%, while replacing 20% of sand with RFP resulted in a reduction of 21%. However, increasing the RFP content increased the ultimate strain of rubberized mortar (Figure 14b). Mixtures with 40% RFP had an increase in the ultimate strain of 63 and 122% when cement and sand replacement respectively. In terms of using the rubberized cement mortar for plastering and since it exposed to continues cycles of thermal expansion rather than a direct physical load, increasing the ultimate strain is more advantages and recommended compared to increasing the strength.

Although there was a reduction in the tensile and flexure strength, the modulus of toughness showed an increase of 19 and 16% when sand was replaced by 30 and 40% respectively (Fig 15). These results show that increasing RFP ratio will increase the strain

energy that the rubberized mortar can absorb just before it fractures, which address the main cause of using plaster mortar. The modulus of resilience showed relatively slight reduction with all RFP replacement ratios. These results show that increasing RFP ratio will approximately maintain the same amount of strain energy that the rubberized mortar can absorb without permanent deformation.

4.2. THERMAL CONDUCTIVITY

4.2.1. The Thermal Needle Probe Method for Plastering Materials. The relationship between the rubber replacement ratio and the thermal conductivity factor was approximately consistent (Figure 16). At a temperature of 25˚ C, replacing 10, 20, 30 and 40% of cement with RFP (R200) reduced the thermal conductivity factor of rubberized plastering mortar by 29, 41, 47, and 52% respectively. Higher reduction in thermal conductivity was noticed when sand was replaced partially with RFP. At a temperature of 25˚ C, replacing 10, 20, 30 and 40% of sand with RFP (R50) reduced the thermal conductivity factor of rubberized plastering mortar by 35, 53, 63, and 64% respectively. Like the explanation in the density section, the high influence of the RFP with particles size between 150 and 300 µm (R50) on the thermal conductivity compared to RFP with particle size smaller than 75 µm (R200) is attributed to the total ratio of RFP within the mortar matrix since the sand represent 78% of the volume reference mortar matrix compared to 22% for the cement. For example, replacing 20% of cement with RFP (R200) leading to a total RFP within the mortar matrix of 4.4% compared to 15.6% when the 20% of sand was replaced with RFP (R50).

The coefficient of thermal conductivity showed a systematic reduction at low temperature. For example, at a temperature of -10˚ C, RFP ratio of 20%, the coefficient of

thermal conductivity decreased by 57 and 62% when cement and sand were replaced respectively.

4.2.2. Thermal Conductivity of Plaster Masonry Units Using the Guarded Hot Box Method. Figure 17 shows the influence of applying three different thicknesses of mortar plastering with varied RFP ratios. Using RFP in plastering mortar as a partial replacement for either cement or sand had a significant effect on lowering the thermal conductivity of plastered masonry units based on the size and the amount of RFP within the plastering matrix. Applying 0.25-inch thick mortar plastering with 40% of the cement replaced by RFP decreased the thermal conductivity of the plastered unit from 1.02 to 0.9 (w/m·k). Simultaneously, by applying 0.75-inch thick mortar plastering with 40% of the cement replaced by RFP the thermal conductivity of the plastered unit decreased from 0.96 to 0.72 (w/m·k). These results represent a reduction of 12% and 25% in thermal conductivity respectively. The influence of replacing sand instead of cement was higher on the thermal conductivity. For example, using 0.25, 0.50, and 0.75-inch thick mortar plastering with 40% of the sand replaced by RFP decreased the thermal conductivity by 34, 41, and 48% respectively compared to 12, 19, and 25% respectively, when the cement was replaced at the same ratio. Comparing these results with the conventional masonry units without any plastering shows that a reduction varied from 11 to 53% can be achieved in thermal conductivity of masonry unit based on the size and amount of RFP as well as the thickness of the plastering lawyer. These reductions in thermal conductivity will be reflected in the same trend on the energy consumption of building using this type of rubberized mortar plastering. Figure 18 shows the effect of using RFP as a sand

replacement on the reduction in energy consumption of masonry units with three plastering thicknesses.

4.3. SOUND ABSORPTION

Figure 19 shows the sound absorption coefficients of unflustered and plastered masonry units with varied RFP content under frequency ranges from 50-5650 Hz. As shown in Figure 19, applying rubberized plastering mortar improved the sound absorption especially with frequencies up to 3000 Hz. In addition, the results also being compared with unflustered masonry units where all plastered units behaved acoustically better than the unplasterd unit.

Figure 20 present the noise reduction factor of unplastered and plastered masonry units with varied RFP content. The noise reduction factor increased with applying the plastering layer with varied RFP content. However, plastering layer with 10% RFP showed the best noise reduction of 0.34% compared with 0.2 for a layer of mortar plastering with 0% RFP and 0.19 for unplastered masonry unit. This behavior was related to other factors that affect the noise reduction coefficient such as the packing density and the surface texture of the plastering layers.

5. CONCLUSIONS

Rubber-fiber powder (RFP) came as a byproduct of the scrap tires recycling process was used as a partial replacement of cement or sand in plastering mortar mixtures. Despite the reduction in some of the mechanical properties due to the inclusion of rubber powder in lieu of a portion of the cement or sand, this study disclose that the rubber powder obtained as a solid waste of scrap tires recycling could be used in the plastering mortar as an Eco-

friendly additive to provide better crack resistance, thermal and acoustical insulation based on the thickness of plastering layer from one side and the size and content of RFP within the plastering layer. Based on the experimental investigation, the following points can be concluded:

1. Plastering mortar mixtures with up to 40% of the cement or sand replaced by RFP did not show any difficulties to mix and apply with the required plastering thickness compared to the reference mortar mixture.
2. Adding RFP with a size smaller than 75 µm up to 20% of cement, decreased the apparent and bulk densities. However, using RFP with a size between 150 and 300 µm as a sand replacement was more influential on both densities and it continued up to 40% replacement of sand.
3. Although there was a reduction in the compressive, tensile and flexure strength, the modulus of toughness showed an increase of 19 and 16% when sand was replaced by 30 and 40% respectively, while the modulus of resilience showed relatively slight reduction with all RFP replacement ratios. These results show that increasing RFP ratio will increase the strain energy that the rubberized mortar can absorb just before it fractures, which address the main cause of using plaster mortar.
4. At a temperature of 25˚ C, replacing 10, 20, 30 and 40% of cement with RFP reduced the thermal conductivity factor of rubberized plastering mortar by 29, 41, 47, and 52% respectively. Higher reduction in thermal conductivity was noticed when sand was replaced partially with RFP.
5. The coefficient of thermal conductivity showed a systematic reduction at low temperature. At a temperature of -10˚ C, mixtures with RFP ratio of 20% showed a

reduction in coefficient of thermal conductivity of 57 and 62% when cement and sand were replaced respectively compared to 41 and 53% at 25˚ C.

6. Compared to conventional masonry units without any plastering, a reduction varied from 11 to 53% was achieved in thermal conductivity of masonry unit based on the size and amount of RFP as well as the thickness of the plastering lawyer.
7. Applying rubberized plastering mortar improved the sound absorption especially with frequencies up to 3000 Hz. Simultaneously, the noise reduction factor increased by applying the plastering layer with varied waste rubber powder content. Plastering layer with 10% waste rubber powder showed the best noise reduction of 0.34% compared with 0.2 for a layer of mortar plastering with 0% waste rubber powder and 0.19 for unplastered masonry unit.

ACKNOWLEDGEMENTS

This research was supported by the Missouri Department of Natural Resources. However, any opinions, findings, conclusions, and recommendations presented in this paper are those of the authors and do not necessarily reflect the views of the sponsor.

Table 1. Mix proportions for cement mortar mixes with cement or fine aggregate replacement by recycled rubber powder.

	Mix ID	Cement		Fine aggregate		Rubber		Total volume	Water	W/C ratio
		Weight (kg)	*Volume (cm^3)*	*Weight (kg)*	*Volume (cm^3)*	*Weight (kg)*	*Volume (cm^3)*	*(cm^3)*	*Volume (liter)*	
	0% R	6.80	2152	20.4	7701	0.00	0.00	9852	2.90	0.43
Set 1	10%R200	6.12	1937	20.4	7701	0.21	217	9852	2.89	0.47
Set 1	20%R200	5.44	1722	20.4	7701	0.42	434	9852	2.95	0.54
Set 1	30%R200	4.76	1506	20.4	7701	0.62	641	9852	2.95	0.62
Set 1	40%R200	4.08	1291	20.4	7701	0.83	857	9852	2.95	0.72
Set 2	10%R50	6.80	2152	18.4	6926	0.75	775	9852	3.27	0.48
Set 2	20%R50	6.80	2152	16.3	6161	1.49	1539	9852	3.67	0.54
Set 2	30%R50	6.80	2152	14.3	5386	2.24	2314	9852	3.99	0.59
Set 2	40%R50	6.80	2152	12.2	4611	2.99	3089	9852	4.60	0.72

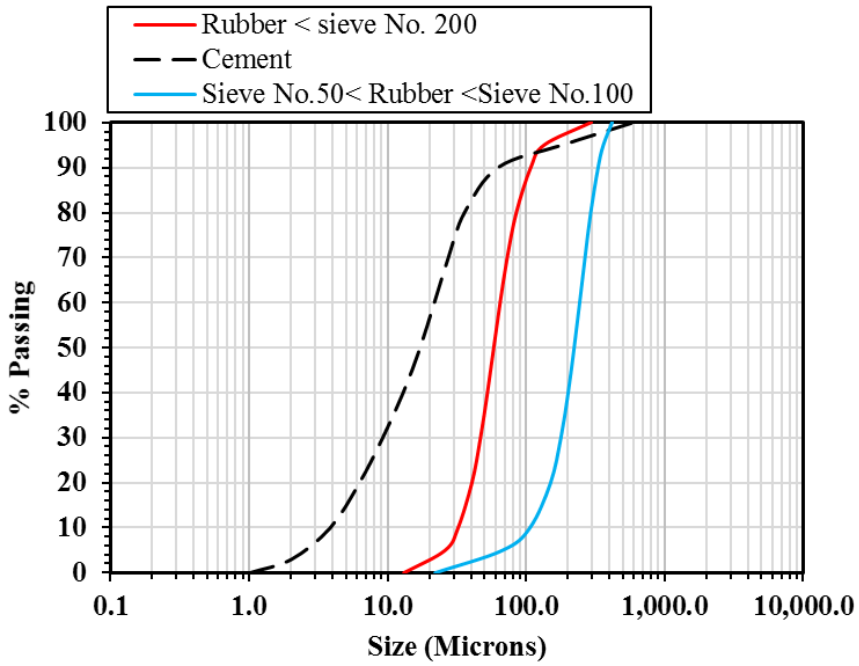

Figure 1. Sieve analysis of the two grades of rubber and cement.

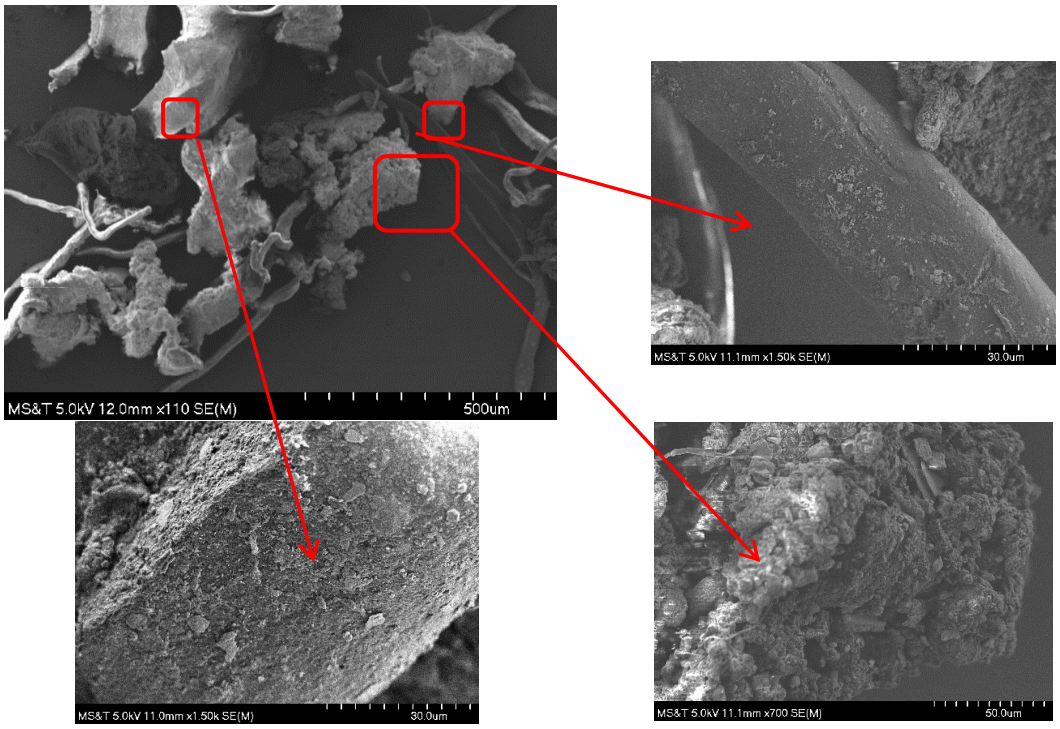

(a)

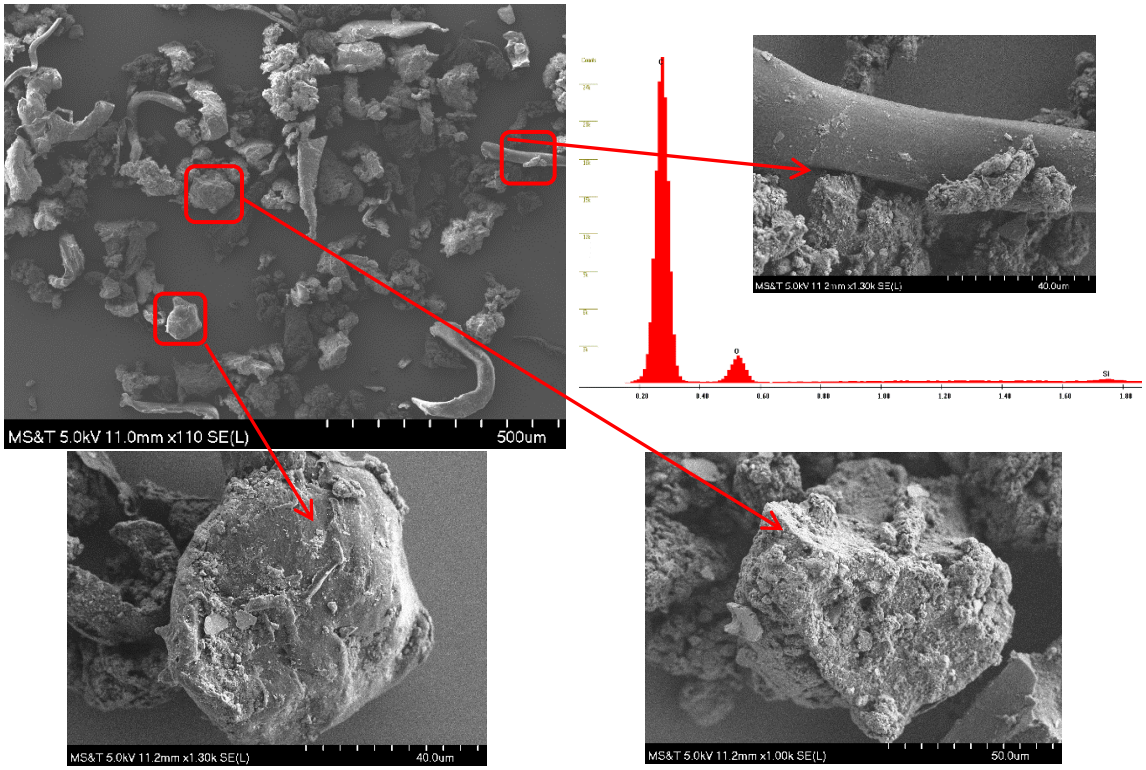

(b)

Figure 2. SEM analysis of the two grades of rubber (a) rubber < sieve No. 200 and (b) rubber between sieves No. 50 and 100.

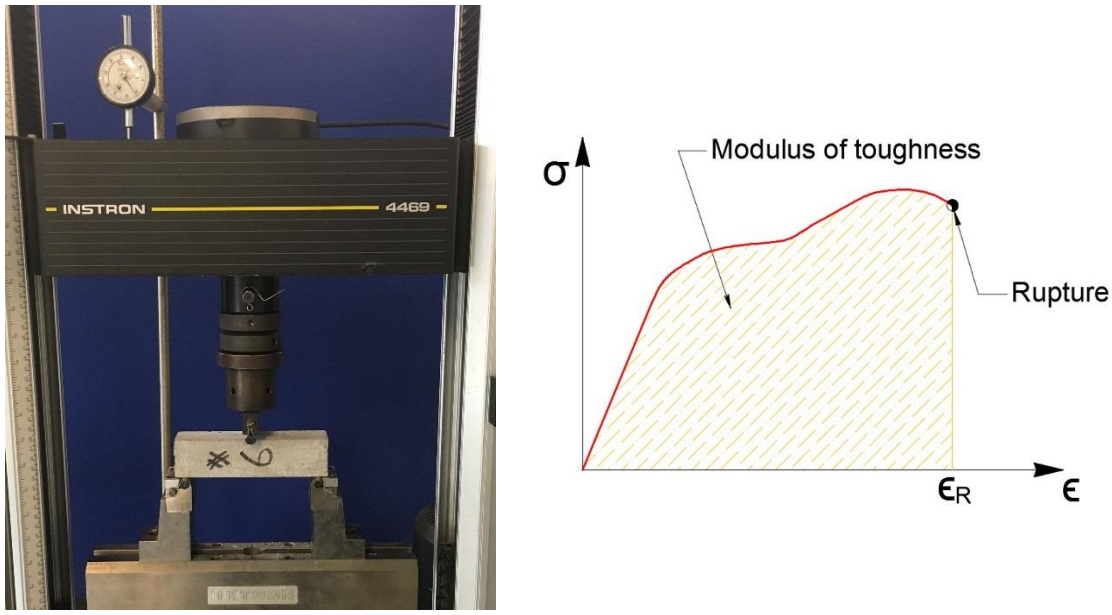

Figure 3. Flexural strength and toughness (a) Flexural strength test setup and (b) modulus of toughness calculation.

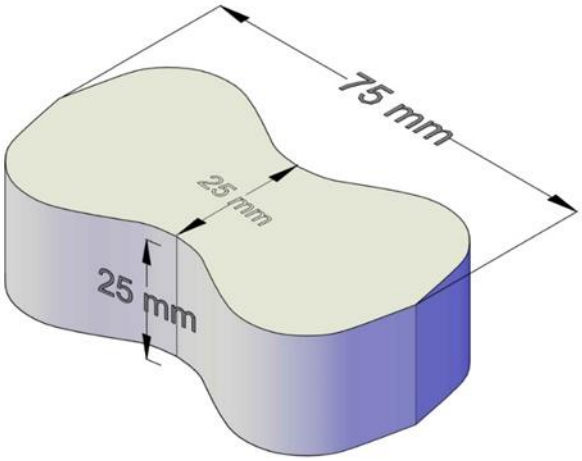

(a)

(b)

(c)

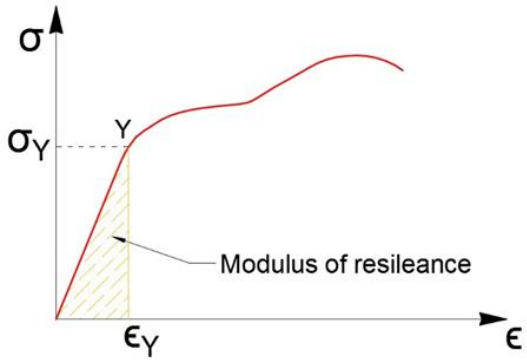

(d)

Figure 4. Tensile strength and resilience (a) test specimen (b) test setup, (c) digital extensometer for strain measurement, and (d) modulus of resilience calculation.

Figure 5. Different thicknesses of rubberized mortar plaster with five different ratios of RFP.

(a) (b)

Figure 6. Thermal needle probe test (a) testing mortar specimen with KD2 PRO portable thermal properties analyzer and (b) thermal needle probe with and without thermal grease.

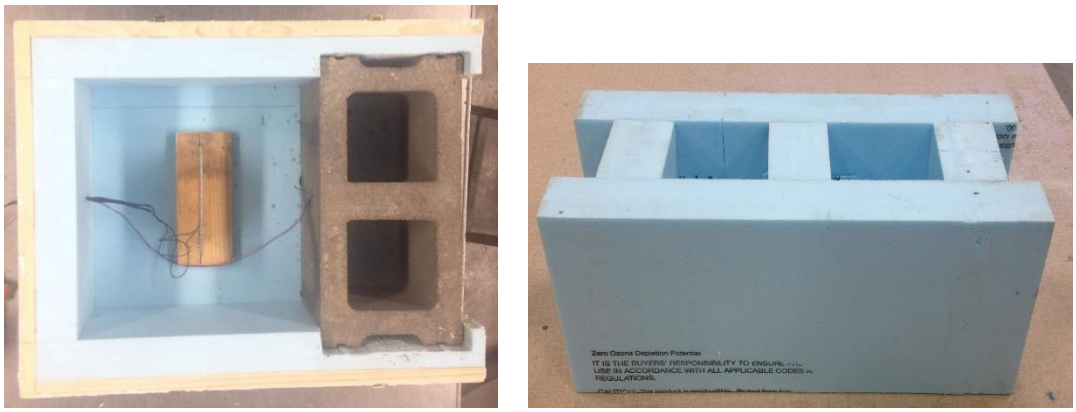

(a) (b)

(c) (d)

Figure 7. The guarded hot box system (a) guarded hot box with heat source (b) calibration Styrofoam block (c) view of the guarded hot box during the test, and (d) thermal image of the test setup.

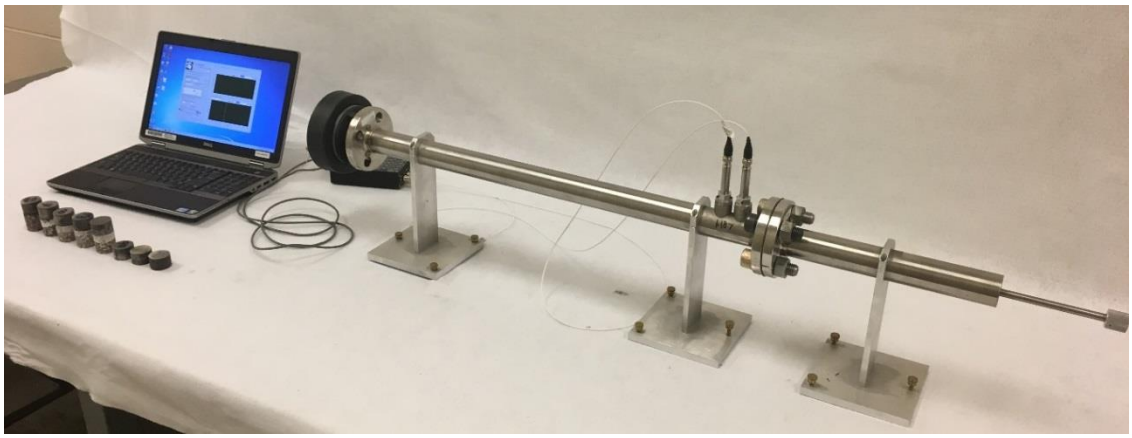

(a)

(b)

(c)

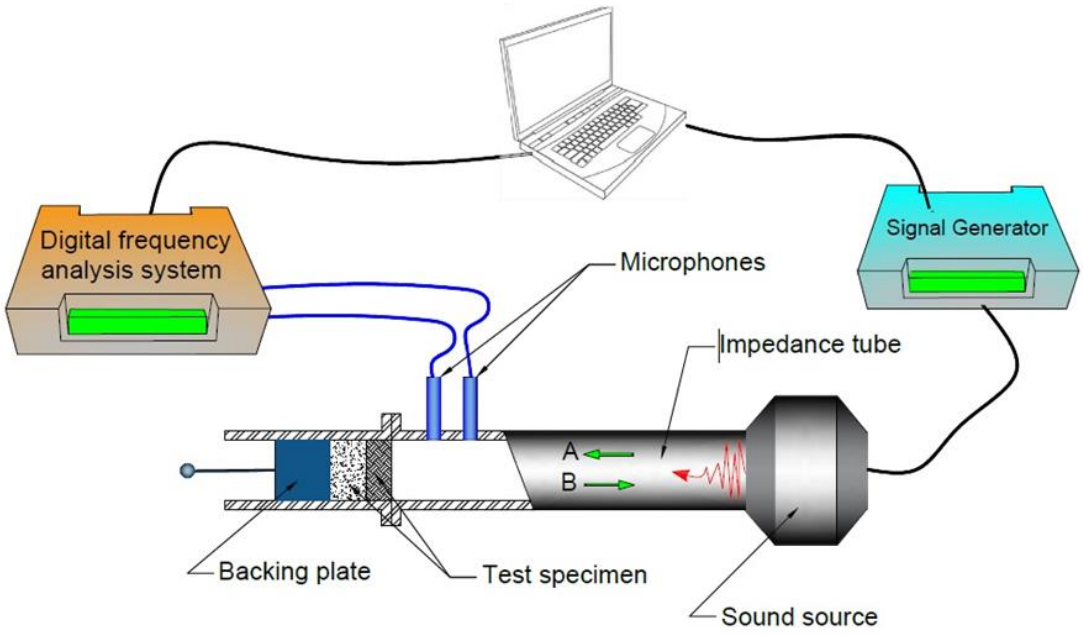

(d)

Figure 8. Acoustic absorption test: (a) testing apparatus, (b) sound source (compression driver), (c) microphones with holders, (d) ACUPRO Software with data acquisition module.

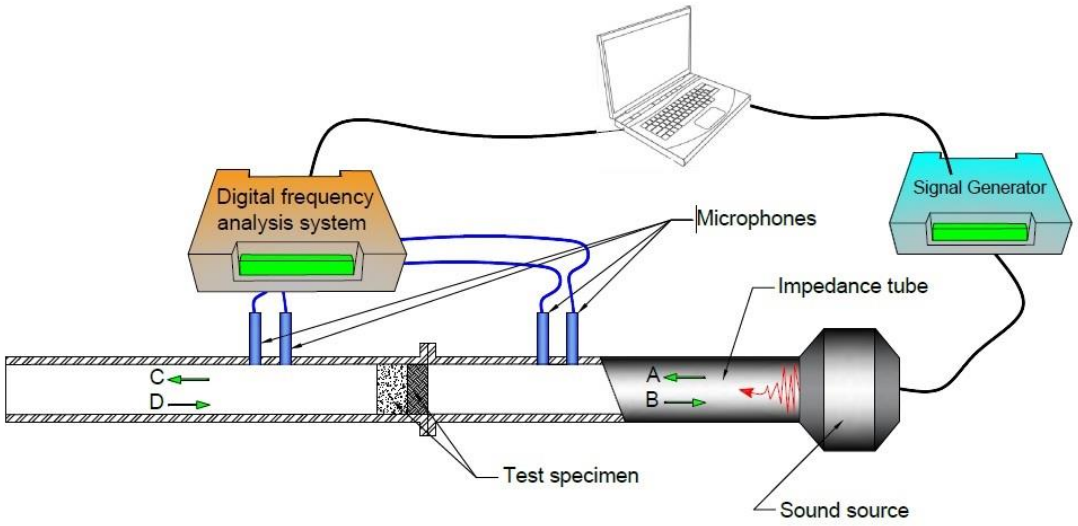

Figure 9. Sound transmission testing apparatus.

(a)

(b)

Figure 10. (a) using water jet cutter to cut masonry specimens and (b) masonry specimen to be used in ACUPRO testing system.

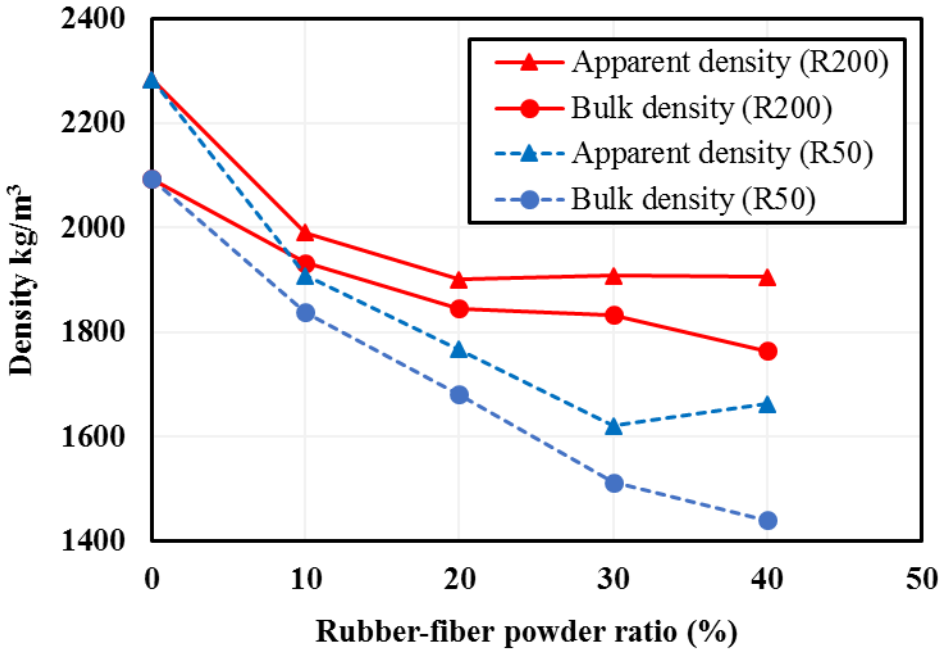

Figure 11. Apparent and bulk densities of rubberized plastering mortar with varied sizes and ratios of rubber-fiber powder.

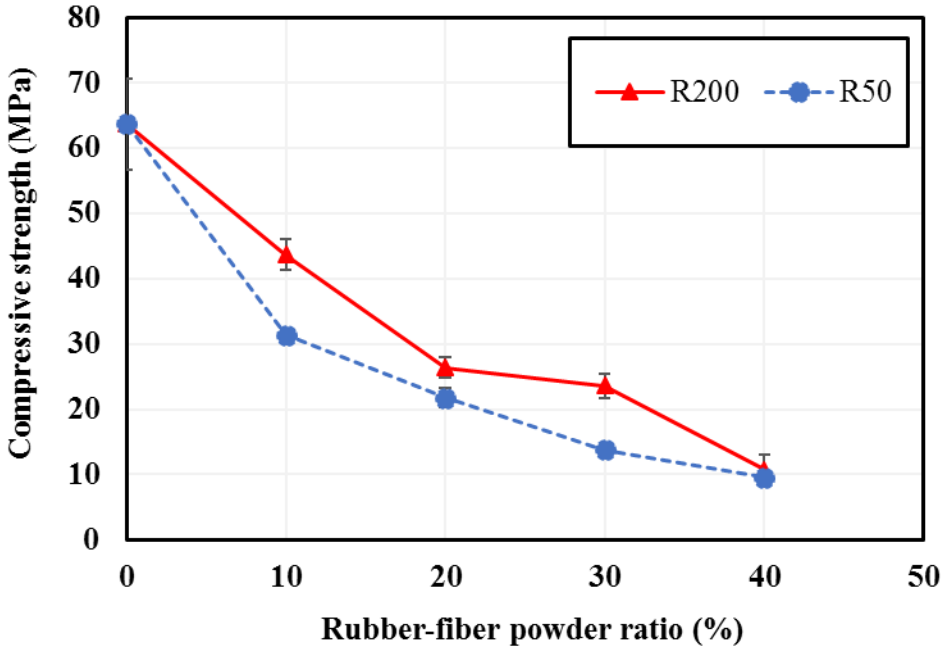

Figure 12. Compressive strength of rubberized plastering mortar with varied sizes and ratios of rubber-fiber powder.

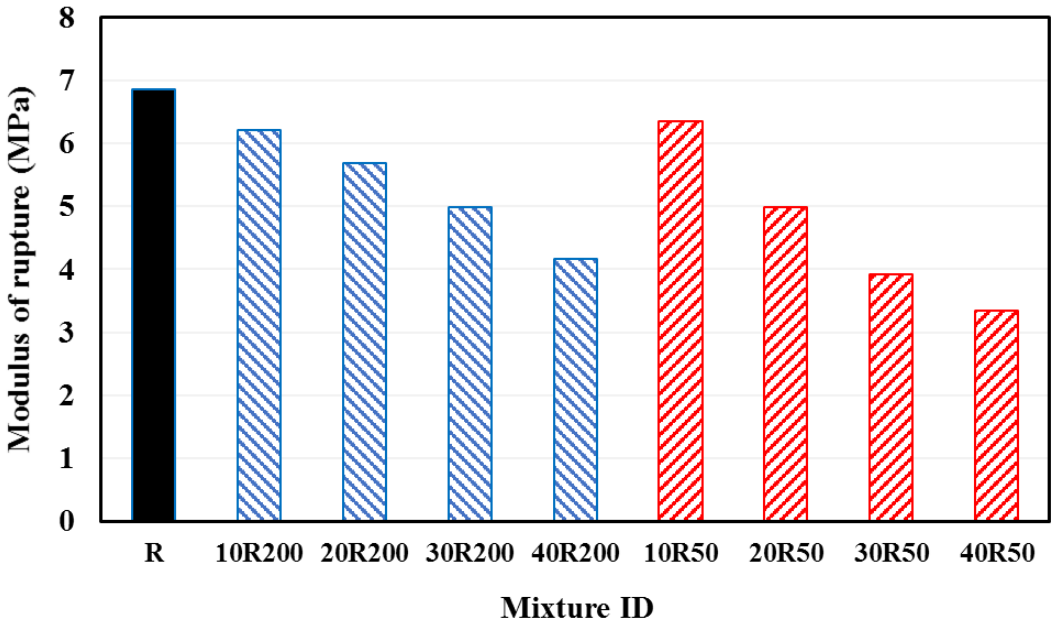

Figure 13. Flexural strength of rubberized plastering mortar with varied sizes and ratios of rubber-fiber powder.

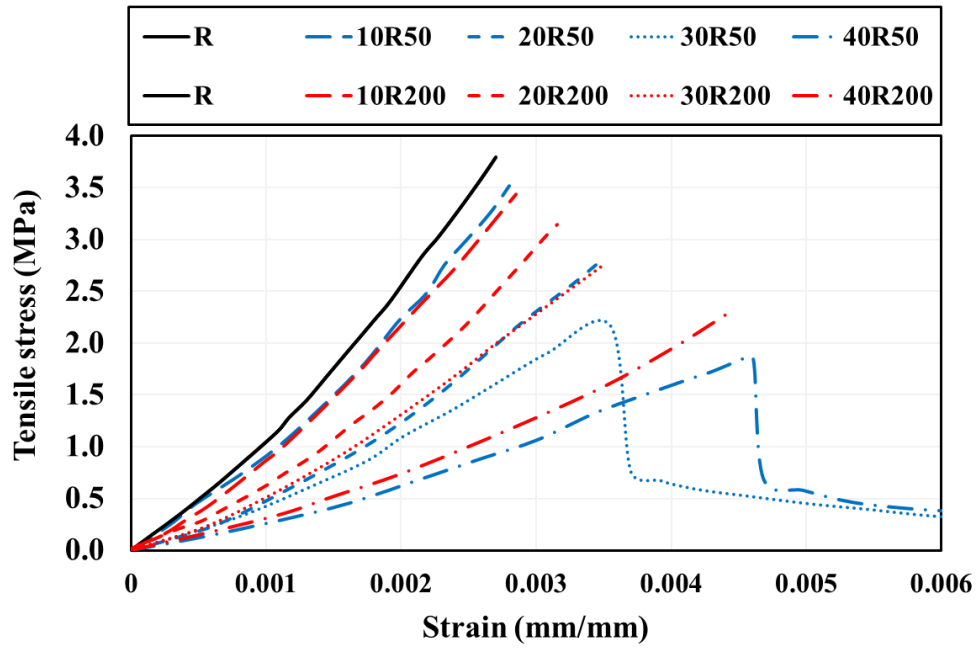

(a)

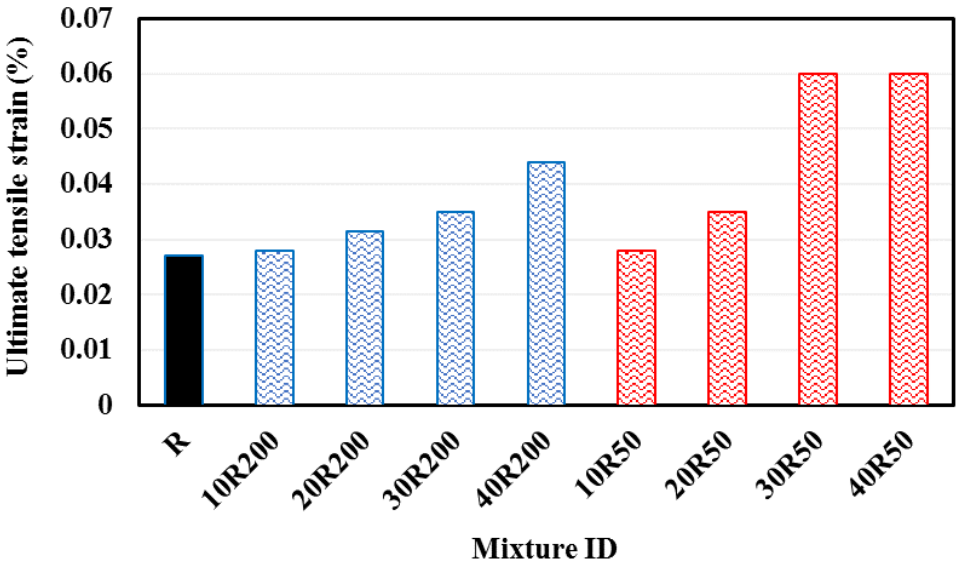

(b)

Figure 14. Tensile strength test: (a) stress-strain behavior of cement mortar with different rubber powder sizes and content and (b) the ultimate strain of cement mortar with different rubber powder sizes and content .

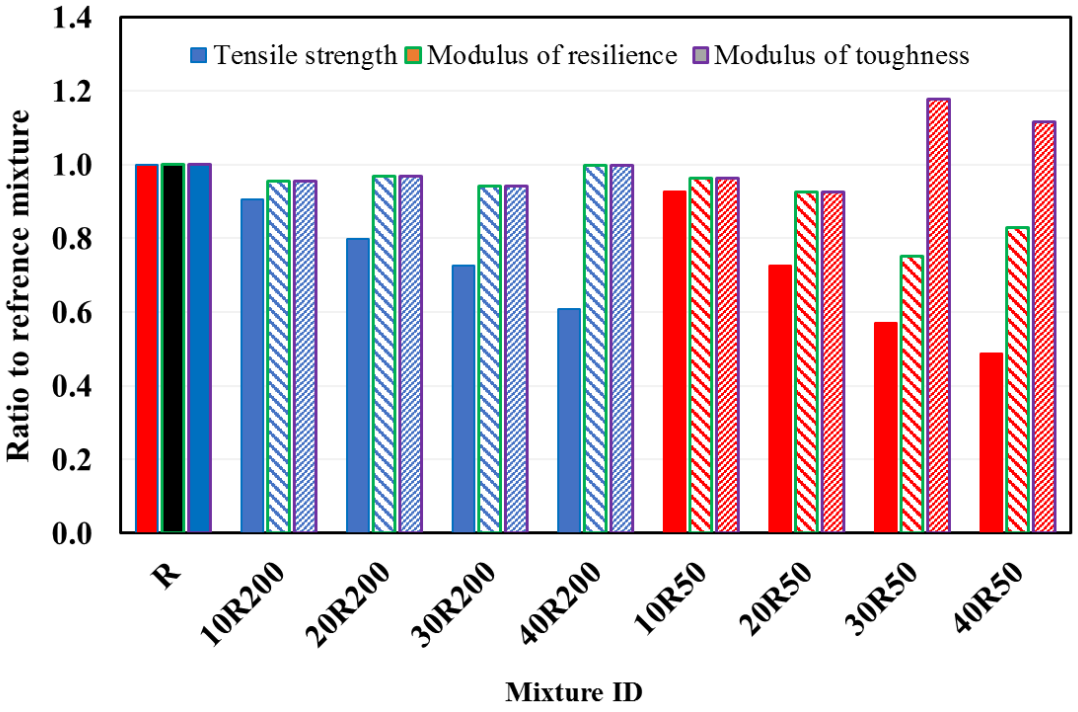

Figure 15. Compressive strength of rubberized plastering mortar with varied sizes and ratios of rubber-fiber powder.

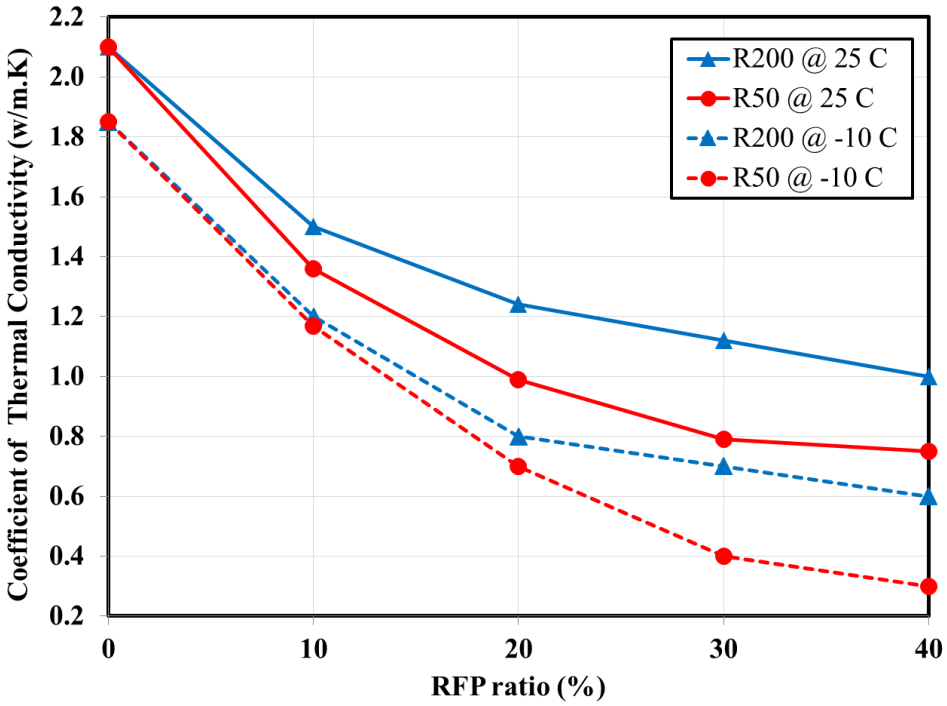

Figure 16. Thermal conductivity factor for rubberized mortar with different sizes and ratios of RFP.

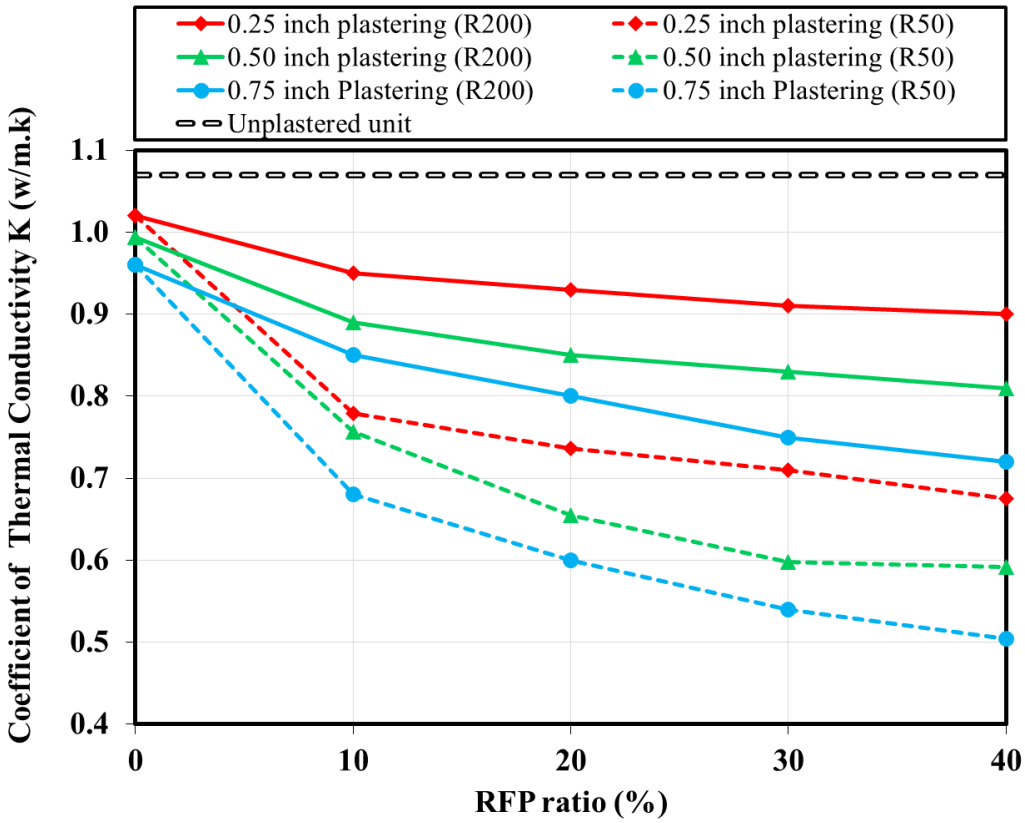

Figure 17. Thermal conductivity coefficients of masonry units with three plastering thicknesses and varied RFP sizes and content.

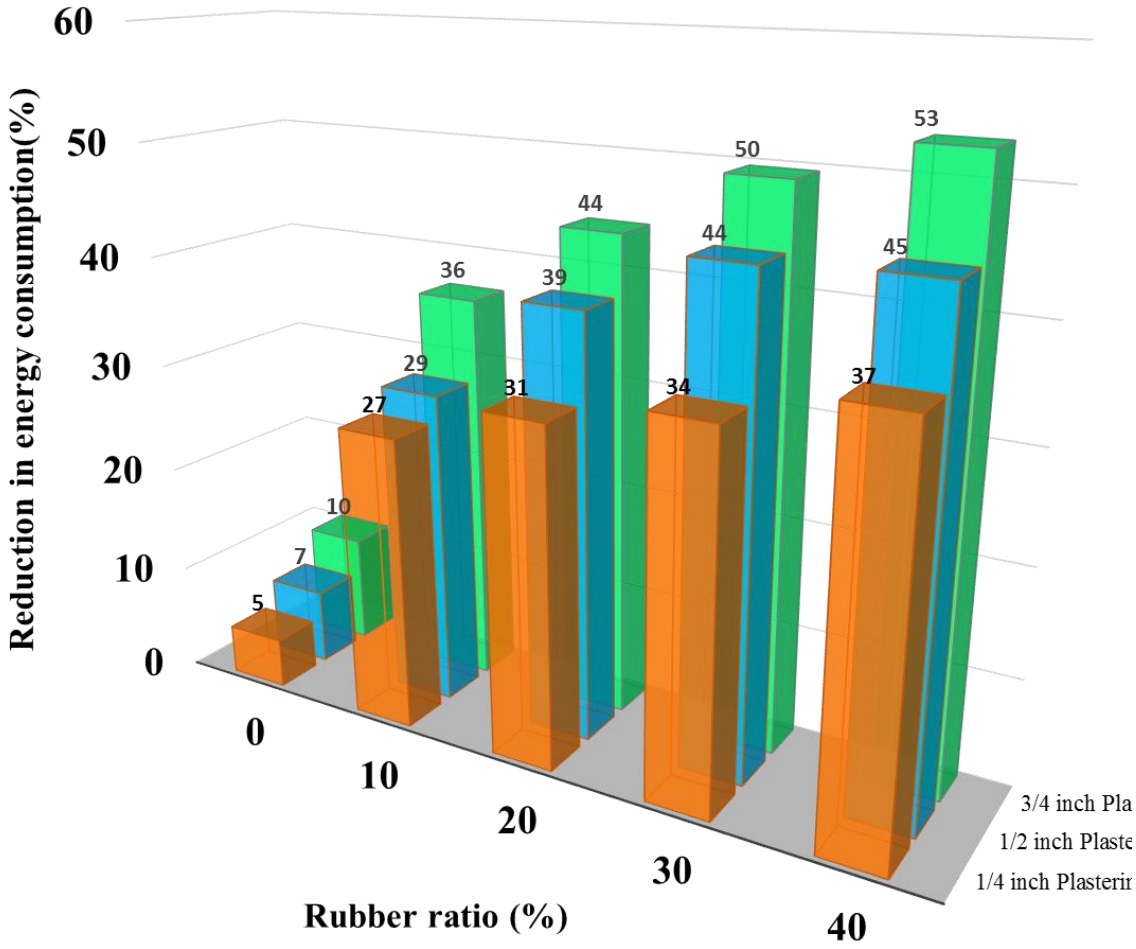

Figure 18. Effect of using RFP as a sand replacement on the reduction in energy consumption of masonry units with three plastering thicknesses.

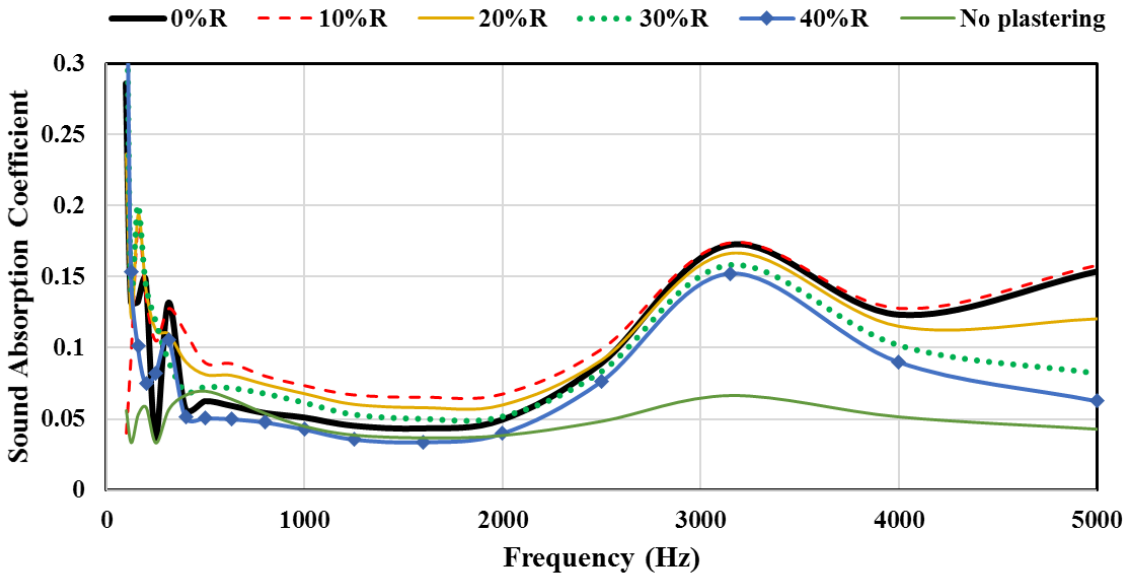

Figure 19. Sound absorption coefficient of plastered masonry units with varied RFP ratios.

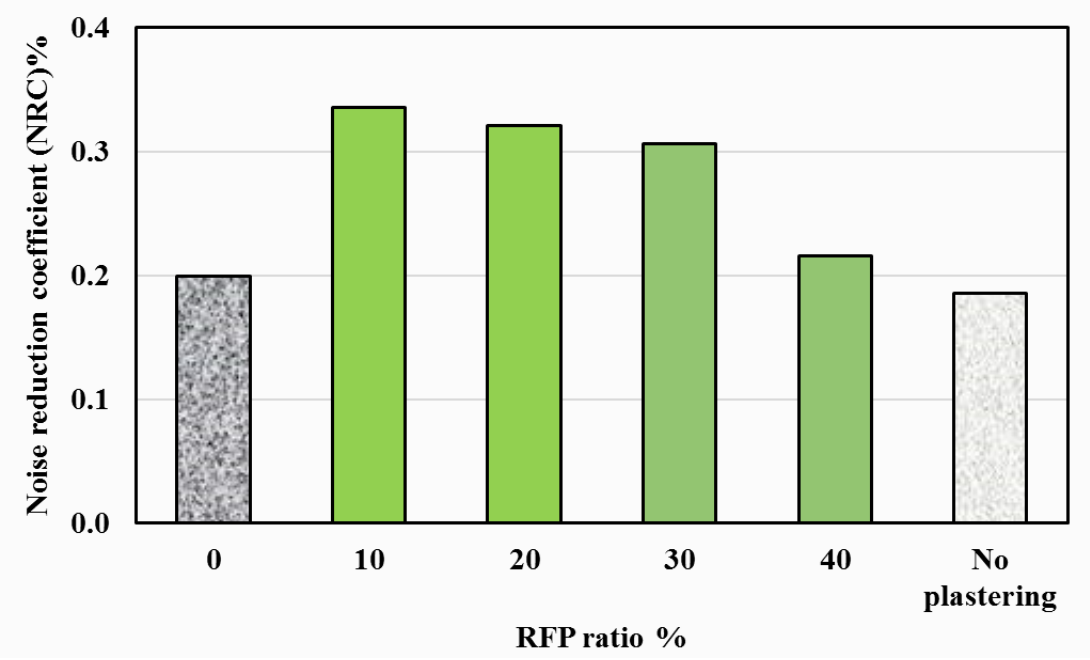

Figure 20. Noise reduction coefficient of plastered masonry units with varied RFP ratios.

REFERENCES

AASHTO (2011). Standard Specification for Air-Entraining Admixtures for Concrete. Air entraining admixtures shall be added to the mixer in the amount necessary to produce the specified air content, American Association of State Highway and Transportation Officials (AASHTO): 2.

AASHTO (2015). AASHTO T 358:2015Method Of Test For Surface Resistivity Indication Of Concrete'S Ability To Resist Chloride Ion Penetration.

Abe, H., A. Tamai, J. Henry and J. Wambold (2001). "Measurement of pavement macrotexture with circular texture meter." Transportation Research Record: Journal of the Transportation Research Board(1764): 201-209.

Abu-Lebdeh, T., E. Fini and A. Fadiel (2014). "Thermal conductivity of rubberized gypsum board." Am. J. Eng. Applied Sci 7: 12-22.

ACAA (2017). 2016 Coal Combustion Product (CCP) Production and Use Survey,. Production & Use Reports. ACAA. Farmington Hills, MI, American Coal Ash Association.

Amirkhanian, S. N. (2001). "Utilization of crumb rubber in asphaltic concrete mixtures–South Carolina's Experience." See ref 3: 163-174.

Ang, G. and V. Marchal (2013). "Mobilising private investment in sustainable transport: The case of land-based passenger transport infrastructure." OECD Environment Working Papers(56): 0_1.

ASTM (2010). "Standard test method for air content of freshly mixed concrete by the pressure method."

ASTM (2011). ASTM D7000 Standard Test Method for Sweep Test of Bituminous Emulsion Surface Treatment Samples,. ASTM International, West Conshohocken, PA.

ASTM, A. (2011). "D7000-08 Standard test method for sweep test of bituminous emulsion surface treatment samples." American Society for Testing and Materials, West Conshohocken, PA.

ASTM, A. (2015). "Standard test method for air content of hydraulic cement mortar."

ASTM, C. (2001). 260. Standard Specification for Air-Entraining Admixtures for Concrete, West Conshohocken, PA: ASTM International.

ASTM., C. C.-o. Concrete and C. Aggregates (2008). Standard test method for resistance of concrete to rapid freezing and thawing, ASTM International.

Atahan, A. O. and A. Ö. Yücel (2012). "Crumb rubber in concrete: static and dynamic evaluation." Construction and Building Materials 36: 617-622.

Azarsa, P. and R. Gupta (2017). "Electrical resistivity of concrete for durability evaluation: a review." Advances in Materials Science and Engineering 2017.

Banerjee, A., A. de Fortier Smit and J. A. Prozzi (2012). "Modeling the effect of environmental factors on evaporative water loss in asphalt emulsions for chip seal applications." Construction and Building Materials 27(1): 158-164.

Batayneh, M. K., I. Marie and I. Asi (2008). "Promoting the use of crumb rubber concrete in developing countries." Waste Management 28(11): 2171-2176.

Beck, P. E., Robert (2006). A Basic Emulsion Manual. Asphalt Institute Manual Series MS-19. Salida, Colorado, Colorado Department of Transportation.

Bekhiti, M., H. Trouzine and A. Asroun (2014). "Properties of Waste Tire Rubber Powder." Engineering, Technology & Applied Science Research 4(4): pp. 669-672.

Benazzouk, A. and M. Queneudec (2002). Durability of cement-rubber composites under freeze thaw cycles. Proceeding of International congress of Sustainable Concrete Construction, Dundee-Scotland.

Berrueco, C., E. Esperanza, F. Mastral, J. Ceamanos and P. García-Bacaicoa (2005). "Pyrolysis of waste tyres in an atmospheric static-bed batch reactor: Analysis of the gases obtained." Journal of Analytical and Applied Pyrolysis 74(1): 245-253.

Bilodeau, A., V. Sivasundaram, K. Painter and V. Malhotra (1994). "Durability of concrete incorporating high volumes of fly ash from sources in the USA." Materials Journal 91(1): 3-12.

Brown, E. R. (1988). "Preventative maintenance of asphalt concrete pavements." National Center for Asphalt Technology, Auburn, AL.

Cabeza, L. F., C. Barreneche, L. Miró, J. M. Morera, E. Bartolí and A. I. Fernández (2013). "Low carbon and low embodied energy materials in buildings: A review." Renewable and Sustainable Energy Reviews 23: 536-542.

Caltrans (2006). Method of Test for Vialit Test for Aggregate Retention in Chip Seals: “French Chip”. California Department of Transportation.

Caltrans, O. o. P. P. (2003). Maintenance Technical Advisory Guide (TAG). Division of Maintenance, Caltrans.

Carder, C. and R. M. Construction (2004). "Rubberized concrete." Colorado: Rocky Mountain Construction.

Chini, A. R., L. C. Muszynski and J. K. Hicks (2003). Determination of acceptance permeability characteristics for performance-related specifications for Portland cement concrete.

Choubane, B., C. Holzschuher and S. Gokhale (2004). "Precision of locked-wheel testers for measurement of roadway surface friction characteristics." Transportation Research Record: Journal of the Transportation Research Board(1869): 145-151.

Davidovits, J. (1991). "Geopolymers: inorganic polymeric new materials." Journal of Thermal Analysis and calorimetry 37(8): 1633-1656.

Do, M.-T., H. Zahouani and R. Vargiolu (2000). "Angular parameter for characterizing road surface microtexture." Transportation Research Record: Journal of the Transportation Research Board(1723): 66-72.

Eldin, N. N. and A. B. Senouci (1993). "Rubber-tire particles as concrete aggregate." Journal of materials in civil engineering 5(4): 478-496.

Elseifi, M. A., L. N. Mohammad and S. B. Cooper III (2011). "Laboratory evaluation of asphalt mixtures containing sustainable technologies." Journal of the Association of Asphalt Paving Technologists 80.

EN, B. (2003). "12272-3. Surface dressing." Test methods-determination of binder aggregate adhesivity by the vialit plate shock test method.

Epps, J. and L. Mason (1994). Uses of recycled rubber tires in highways: A synthesis of highway practice. Final report, National Cooperative Highway Research Program, Washington, DC (United States).

Fadiel, A. (2013). Use of Crumb Rubber to Improve Thermal Efficiency of Construction Materials, North Carolina Agricultural and Technical State University.

Fadiel, A., F. Al Rifaie, T. Abu-Lebdeh and E. Fini (2014). "Use of crumb rubber to improve thermal efficiency of cement-based materials." American Journal of Engineering and Applied Sciences 7(1): 1-11.

Fattuhi, N. and L. Clark (1996). "Cement-based materials containing shredded scrap truck tyre rubber." Construction and building materials 10(4): 229-236.

Fedroff, D., S. Ahmad and B. Savas (1996). "Mechanical properties of concrete with ground waste tire rubber." Transportation Research Record: Journal of the Transportation Research Board(1532): 66-72.

Flintsch, G., E. de León, K. McGhee and I. AI-Qadi (2003). "Pavement surface macrotexture measurement and applications." Transportation Research Record: Journal of the Transportation Research Board(1860): 168-177.

Forster, S. W. (1981). Aggregate microtexture: Profile measurement and related frictional levels.

Freeman, E., Y.-M. Gao, R. Hurt and E. Suuberg (1997). "Interactions of carbon-containing fly ash with commercial air-entraining admixtures for concrete." Fuel 76(8): 761-765.

Fuller, K., J. Gough and A. Thomas (2004). "The effect of low-temperature crystallization on the mechanical behavior of rubber." Journal of Polymer Science Part B: Polymer Physics 42(11): 2181-2190.

Gadkar, S. and P. R. Rangaraju (2013). "The Effect of Crumb Rubber on Freeze-Thaw Durability of Portland Cement Concrete." Advances in Civil Engineering Materials 2(1): 566-585.

Ganjian, E., M. Khorami and A. A. Maghsoudi (2009). "Scrap-tyre-rubber replacement for aggregate and filler in concrete." Construction and Building Materials 23(5): 1828-1836.

Gebler, S. and P. Klieger (1983). "Effect of fly ash on the air-void stability of concrete." Special Publication 79: 103-142.

Ghaly, A. M. and J. D. Cahill IV (2005). "Correlation of strength, rubber content, and water to cement ratio in rubberized concrete." Canadian Journal of Civil Engineering 32(6): 1075-1081.

Gheni, A., O. I. Abdelkarim, X. Liu, M. Abdulazeez, M. Lusher, K. Liu, M. ElGawady, H. Shi and J. Wang (2017). Mechanical and Environmental Performance of Eco-Friendly Chip Seal with Recycled Crumb Rubber.

Gheni, A., M. A. ElGawady and J. J. Myers (2017). "Thermal Characterization of Cleaner and Eco-Efficient Masonry Units Using Sustainable Aggregates." Journal of Cleaner Production.

Gheni, A., X. Liu, M. A. ElGawady, H. Shi and J. Wang (2018). "Leaching Assessment of Eco-Friendly Rubberized Chip Seal Pavement." Transportation Research Record: 0361198118758688.

Gheni, A. A., O. I. Abdelkarim, M. M. Abdulazeez and M. A. ElGawady (2017). "Texture and design of green chip seal using recycled crumb rubber aggregate." Journal of Cleaner Production 166: 1084-1101.

Gheni, A. A., M. A. ElGawady and J. J. Myers (2017). "Mechanical Characterization of Concrete Masonry Units Manufactured with Crumb Rubber Aggregate." ACI Materials Journal 114(01).

Gomaa, E., S. Sargon, C. Kashosi and M. ElGawady (2017). "Fresh properties and compressive strength of high calcium alkali activated fly ash mortar." Journal of King Saud University-Engineering Sciences 29(4): 356-364.

Gomaa, E., S. Sargon, C. Kashosi and M. ElGawady (2017). Fresh properties and early compressive strength of alkali-activated high calcium fly ash paste. Congrès International de Géotechnique–Ouvrages–Structures, Springer.

Gomaa, E., S. Sargon, C. Kashosi, A. Gheni and M. ElGawady (2018). Effect of Different Class C Fly Ash Compositions on the Properties of the Alkali-Activated Concrete. International Congress on Polymers in Concrete, Springer.

Gou, M. and X. Liu (2014). "Effect of rubber particle modification on properties of rubberized concrete." Journal of Wuhan University of Technology-Mater. Sci. Ed. 29(4): 763-768.

Gransberg, D. (2006). "Correlating chip seal performance and construction methods." Transportation Research Record: Journal of the Transportation Research Board(1958): 54-58.

Gransberg, D. and D. James (2005). "Chip Seal Best Practices, National Cooperative Highway Research Program Synthesis 342." Transportation Research Board, National Academies, Washington, DC.

Gransberg, D. D. and D. M. James (2005). Chip seal best practices, Transportation Research Board.

Granuband Macon, L. (2017). Amount of waste in tire recycling plant after processing scrap tires. A. A. Gheni.

Hall, M. R., K. B. Najim and C. J. Hopfe (2012). "Transient thermal behaviour of crumb rubber-modified concrete and implications for thermal response and energy efficiency in buildings." Applied thermal engineering 33: 77-85.

Hammond, G. P. and C. I. Jones (2008). "Embodied energy and carbon in construction materials." Proceedings of the Institution of Civil Engineers-Energy 161(2): 87-98.

Hanson, D., J. Epps and R. Hicks (1996). "Construction Guidelines for Crumb Rubber Modified Hot Mix Asphalt." Federal Highway Administration Report DTFH61-94-C-00035.

Hanson, D. I., J. Epps and R. G. Hicks (1996). Construction Guidelines for Crumb Rubber Modified Hot Mix Asphalt: Interim Report, National Center for Asphalt Technology.

Hanson, D. I. and B. D. Prowell (2004). Evaluation of circular texture meter for measuring surface texture of pavements, the Center.

Harris, N., K. Hover, K. Folliard and M. Ley (2008). "The Use of the Foam Index Test to Predict AEA Dosage in Concrete Containing Fly Ash: Part I—Evaluation of the State of Practice."

Henry, J. J. (2000). Evaluation of pavement friction characteristics, Transportation Research Board.

Hernandez-Olivares, F., G. Barluenga, M. Bollati and B. Witoszek (2002). "Static and dynamic behaviour of recycled tyre rubber-filled concrete." Cement and concrete research 32(10): 1587-1596.

Hesami, S., I. S. Hikouei and S. A. A. Emadi (2016). "Mechanical behavior of self-compacting concrete pavements incorporating recycled tire rubber crumb and reinforced with polypropylene fiber." Journal of cleaner production 133: 228-234.

Hill, R. L., S. L. Sarkar, R. F. Rathbone and J. C. Hower (1997). "An examination of fly ash carbon and its interactions with air entraining agent." Cement and Concrete Research 27(2): 193-204.

Hornbostel, K., C. K. Larsen and M. R. Geiker (2013). "Relationship between concrete resistivity and corrosion rate–a literature review." Cement and Concrete Composites 39: 60-72.

Horvath, A. (2004). "Construction materials and the environment." Annu. Rev. Environ. Resour. 29: 181-204.

Howard, I. L. and G. Baumgardner (2009). US Highway 84 Chip Seal Field Trials and Laboratory Test Results, Mississippi Department of Transportation.

Huang, B., L. Mohammad, P. Graves and C. Abadie (2002). "Louisiana experience with crumb rubber-modified hot-mix asphalt pavement." Transportation Research Record: Journal of the Transportation Research Board(1789): 1-13.

International, A. (2016). ASTM C109 / C109M-16a, Standard Test Method for Compressive Strength of Hydraulic Cement Mortars (Using 2-in. or [50-mm] Cube Specimens). West Conshohocken, PA, 2016, www.astm.org, ASTM International.

Islam, S. and M. Hossain (2011). "Chip seal with lightweight aggregates for low-volume roads." Transportation Research Record: Journal of the Transportation Research Board(2205): 58-66.

Isler, J. W. (2012). Assessment of concrete masonry units containing aggregate replacements of waste glass and rubber tire particles, University of Colorado Denver.

Isler, J. W. (2012). Assessment of concrete masonry units containing aggregate replacements of waste glass and rubber tire particles, University of Colorado at Denver.

Jensen, W. and M. Abdelrahman (2006). Use of crumb rubber in performance graded binder.

Jordan III, W. S. and I. L. Howard (2011). "Applicability of Modified Vialit Adhesion Test for Seal Treatment Specifications." Journal of Civil Engineering and Architecture 5(3).

Kaewunruen, S. and R. Meesit (2016). "Sensitivity of crumb rubber particle sizes on electrical resistance of rubberised concrete." Cogent Engineering 3(1): 1126937.

Kandhal, P. S. and J. B. Motter (1991). Criteria for accepting precoated aggregates for seal coats and surface treatments.

Karasahin, M., B. Aktas, A. Gungor, F. Orhan and C. Gurer (2014). "Laboratory and In Situ Investigation of Chip Seal Surface Condition Improvement." Journal of Performance of Constructed Facilities 29(2): 04014047.

Kearby, J. (1953). Tests and theories on penetration surfaces. Highway Research Board Proceedings.

Kessler, R. J., R. G. Powers and M. P. Mario Paredes (2005). "Resistivity measurements of water saturated concrete as an indicator of permeability." CORROSION 2005.

Khatib, Z. K. and F. M. Bayomy (1999). "Rubberized Portland cement concrete." Journal of materials in civil engineering 11(3): 206-213.

Kotek, P. and M. Kováč (2015). "Comparison of Valuation of Skid Resistance of Pavements by two Device with Standard Methods." Procedia Engineering 111: 436-443.

Kulakowski, M. P., F. M. Pereira and D. C. Dal Molin (2009). "Carbonation-induced reinforcement corrosion in silica fume concrete." Construction and Building Materials 23(3): 1189-1195.

LaForce, R. F. (1983). "Squeegee Seal and Crumb Rubber Chip Seal Sapinero-East." Colorado Department of Transportation, CDH-DTP.

LaForce, R. F. (1986). "Crumb rubber chip seal east of Punkin Center."

Lawrence, P., E. Ringot and B. Husson (1999). "About the measurement of the air content in mortar." Materials and Structures 32(8): 618-621.

Lee, S.-J., C. K. Akisetty and S. N. Amirkhanian (2008). "The effect of crumb rubber modifier (CRM) on the performance properties of rubberized binders in HMA pavements." Construction and Building Materials 22(7): 1368-1376.

Lewis, P. (1980). "Laboratory testing of rubber durability." Polymer Testing 1(3): 167-189.

Ley, M. T., N. J. Harris, K. J. Folliard and K. C. Hover (2008). "Investigation of air-entraining admixture dosage in fly ash concrete." ACI Materials Journal 105(5): 494.

Liu, H., X. Wang, Y. Jiao and T. Sha (2016). "Experimental investigation of the mechanical and durability properties of crumb rubber concrete." Materials 9(3): 172.

Liu, L., W. Xie, Y. Wang and S. Wu (2018). "Evaluation of significant factors for aggregate retention in chip seals based on mesostructured finite element model." International Journal of Pavement Research and Technology.

Malhotra, V. (1990). "Durability of concrete incorporating high-volume of low-calcium (ASTM Class F) fly ash." Cement and Concrete Composites 12(4): 271-277.

Masad, E. (2007). Test methods for characterizing aggregate shape, texture, and angularity, Transportation Research Board.

Mataei, B., H. Zakeri, M. Zahedi and F. M. Nejad (2016). "Pavement Friction and Skid Resistance Measurement Methods: A Literature Review." Open Journal of Civil Engineering 6(04): 537.

Maupin Jr, G. (1996). "Hot mix asphalt rubber applications in Virginia." Transportation Research Record: Journal of the Transportation Research Board(1530): 18-24.

McHattie, R. L. (2001). Asphalt surface treatment guide, Alaska Department of Transportation and Public Facilities.

McLeod, N. W., C. Chaffin, A. Holberg, C. Parker, V. Obrcian, J. Edwards, W. Campen and W. Kari (1969). A general method of design for seal coats and surface treatments. Association of Asphalt Paving Technologists Proc.

Mehta, P. and O. Gjørv (1982). "Properties of portland cement concrete containing fly ash and condensed silica-fume." Cement and Concrete Research 12(5): 587-595.

Mertens, E. and J. Wright (1959). Cationic asphalt emulsions: How they differ from conventional emulsions in theory and practice. Highway Research Board Proceedings.

Micelli, F. and J. Myers (2008). "Durability of FRP-confined concrete." Proceedings of the ICE-Construction Materials 161(4): 173-185.

Milne, G. and C. Reardon (2005). "Embodied energy." Your Home Technical Manual: Australia's guide to environmentally sustainable homes. Commonwealth of Australia.

Mohammad, L. N., S. B. Cooper Jr and M. A. Elseifi (2011). "Characterization of HMA mixtures containing high reclaimed asphalt pavement content with crumb rubber additives." Journal of Materials in Civil Engineering 23(11): 1560-1568.

Mohammed, B. S., K. M. A. Hossain, J. T. E. Swee, G. Wong and M. Abdullahi (2012). "Properties of crumb rubber hollow concrete block." Journal of Cleaner Production 23(1): 57-67.

Mohammed, S., K. Hossain, J. Swee, G. Wong and M. Abdullahi (2012). "Properties of crumb rubber hollow concrete block." Journal of Cleaner Production 23(1): 57-67.

Mohseni, A. (1998). LTPP seasonal asphalt concrete (AC) pavement temperature models.

Moustafa, A. and M. A. ElGawady (2015). "Mechanical properties of high strength concrete with scrap tire rubber." Construction and Building Materials 93: 249-256.

Moustafa, A. and M. A. ElGawady (2016). "Strain rate effect on properties of rubberized concrete confined with glass fiber–reinforced polymers." Journal of Composites for Construction 20(5): 04016014.

Moustafa, A. and M. A. ElGawady (2017). "Dynamic properties of high strength rubberized concrete." ACI Spec. Publ 314: 1-22.

Moustafa, A., A. Gheni and M. A. ElGawady (2017). "Shaking-Table Testing of High Energy–Dissipating Rubberized Concrete Columns." Journal of Bridge Engineering 22(8): 04017042.

Naik, T. R., S. S. Singh and B. W. Ramme (1998). "Mechanical properties and durability of concrete made with blended fly ash." Materials Journal 95(4): 454-462.

Najim, K. and M. Hall (2010). "A review of the fresh/hardened properties and applications for plain-(PRC) and self-compacting rubberised concrete (SCRC)." Construction and building materials 24(11): 2043-2051.

Nehdi, M. and A. Khan (2001). "Cementitious composites containing recycled tire rubber: an overview of engineering properties and potential applications." Cement, concrete and aggregates 23(1): 3-10.

O'Brien, L. G. (1989). Evolution and benefits of preventive maintenance strategies.

Olorunniwo, A. (1994). Effects of recycled scrap tires and asphalt pavement on the engineering properties of portland cement concrete, University of Texas at Austin.

Pacheco-Torgal, F., P. B. Lourenço, J. Labrincha and S. Kumar (2014). Eco-efficient masonry bricks and blocks: design, properties and durability, Woodhead Publishing.

Pacheco-Torgal, F., P. B. Lourenço, J. Labrincha and S. Kumar (2015). Eco-efficient masonry bricks and blocks: design, properties and durability, Woodhead Publishing.

Page, G. C. (1992). "Florida's initial experience utilizing ground tire rubber in asphalt concrete mixes." Journal of the Association of Asphalt Paving Technologists 61.

Paine, K. A. and R. K. Dhir (2010). "Research on new applications for granulated rubber in concrete." Proceedings of the institution of civil engineers: construction materials 163(1): 7-17.

Papadopoulos, A. M. and E. Giama (2007). "Environmental performance evaluation of thermal insulation materials and its impact on the building." Building and environment 42(5): 2178-2187.

Papagiannakis, A. and T. Lougheed (1995). "Review of Crumb-Rubber Modified Asphalt Concrete Technology."

Papagiannakis, A. and T. Lougheed (1995). A REVIEW OF CRUMB-RUBBER MODIFIED ASPHALT CONCRETE TECHNOLOGY. RESEARCH REPORT.

Poole Jr, S. (1998). Scrap and Shredded Tire Fires Special Report.

Praticò, F. G., R. Vaiana and T. Iuele (2015). "Macrotexture modeling and experimental validation for pavement surface treatments." Construction and Building Materials 95: 658-666.

Presti, D. L. (2013). "Recycled tyre rubber modified bitumens for road asphalt mixtures: a literature review." Construction and Building Materials 49: 863-881.

Provis, J. L. and S. A. Bernal (2014). "Geopolymers and related alkali-activated materials." Annual Review of Materials Research 44: 299-327.

Pusca, A., S. Bobancu and A. Duta (2010). "MECHANICAL PROPERTIES OF RUBBER- AN OVERVIEW." Bulletin of the Transilvania University of Brasov. 3(107): 2010.

Rada, E. C., M. Ragazzi, R. Dal Maschio, M. Ischia and V. N. Panaitescu (2012). "Energy recovery from tyres waste through thermal option." Scientific Bulletin, Politehnica University of Bucharest, Series D, Mechanical Engineering 74: 201-210.

Rahman, F., M. Islam, H. Musty and M. Hossain (2012). "Aggregate retention in chip seal." Transportation Research Record: Journal of the Transportation Research Board(2267): 56-64.

Rangaraju, P. and S. Gadkar (2012). "Durability evaluation of crumb rubber addition rate on Portland cement concrete." Department of Civil Engineering, Clemson University, Clemson: 1-126.

Richardson, A., K. Coventry, V. Edmondson and E. Dias (2016). "Crumb rubber used in concrete to provide freeze–thaw protection (optimal particle size)." Journal of Cleaner Production 112: 599-606.

Richardson, A. E., K. A. Coventry and G. Ward (2012). "Freeze/thaw protection of concrete with optimum rubber crumb content." Journal of Cleaner Production 23(1): 96-103.

RMA, R. M. A. (2018). 2017 U.S. Scrap Tire Management Summary. Wasington, DC.

Sadek, D. M. and M. M. El-Attar (2015). "Structural behavior of rubberized masonry walls." Journal of Cleaner Production 89: 174-186.

Sajwani, A. and Y. Nielsen (2017). "THE APPLICATION OF THE ENVIRONMENTAL MANAGEMENT SYSTEM AT THE ALUMINUM INDUSTRY IN UAE." International Journal 12(30): 1-10.

Sargon, S. P., E. Y. Gomaa, C. Kashosi, A. A. Gheni and M. A. ElGawady (2018). Effect of Curing Temperatures on Zero-Cement Alkali-Activated Mortars. International Congress on Polymers in Concrete, Springer.

Savas, B., S. Ahmad and D. Fedroff (1997). "Freeze-thaw durability of concrete with ground waste tire rubber." Transportation Research Record: Journal of the Transportation Research Board(1574): 80-88.

Sengul, O. (2014). "Use of electrical resistivity as an indicator for durability." Construction and Building Materials 73: 434-441.

Shu, X. and B. Huang (2014). "Recycling of waste tire rubber in asphalt and portland cement concrete: An overview." Construction and Building Materials 67: 217-224.

Shuler, S. (1998). "DESIGN AND CONSTRUCTION OF CHIP SEALS FOR HIGH TRAFFIC." Flexible Pavement Rehabilitation and Maintenance 1348: 96.

Shuler, S. (2011). Manual for emulsion-based chip seals for pavement preservation, Transportation Research Board.

Shuler, S. (2011). Use of Waste Tires, Crumb Rubber, on Colorado Highways, Colorado Department of Transportation, DTD Applied Research and Innovation Branch.

Si, R., J. Wang, S. Guo, Q. Dai and S. Han (2018). "Evaluation of laboratory performance of self-consolidating concrete with recycled tire rubber." Journal of Cleaner Production 180: 823-831.

Siddique, R. and T. R. Naik (2004). "Properties of concrete containing scrap-tire rubber–an overview." Waste management 24(6): 563-569.

Song, H.-W. and V. Saraswathy (2007). "Corrosion monitoring of reinforced concrete structures-A." Int. J. Electrochem. Sci 2: 1-28.

Stockton, W. R. and J. A. Epps (1975). ENGINEERING ECONOMY AND ENERGY CONSIDERATIONS. SEAL COAT ECONOMICS AND DESIGN.

Sukontasukkul, P. (2009). "Use of crumb rubber to improve thermal and sound properties of pre-cast concrete panel." Construction and Building Materials 23(2): 1084-1092.

Sukontasukkul, P. and C. Chaikaew (2006). "Properties of concrete pedestrian block mixed with crumb rubber." Construction and Building Materials 20(7): 450-457.

Sun, P. and H.-C. Wu (2013). "Chemical and freeze–thaw resistance of fly ash-based inorganic mortars." Fuel 111: 740-745.

Temuujin, J., A. Minjigmaa, B. Davaabal, U. Bayarzul, A. Ankhtuya, T. Jadambaa and K. MacKenzie (2014). "Utilization of radioactive high-calcium Mongolian flyash for the preparation of alkali-activated geopolymers for safe use as construction materials." Ceramics International 40(10): 16475-16483.

Testa, D. M. and M. Hossain (2014). Kansas Department of Transportation 2014 Chip Seal Manual, Kansas Department of Transportation.

Thomas, B. S. and R. C. Gupta (2013). "Mechanical properties and durability characteristics of concrete containing solid waste materials." Journal of Cleaner Production.

Thomas, B. S. and R. C. Gupta (2015). "Long term behaviour of cement concrete containing discarded tire rubber." Journal of Cleaner Production 102: 78-87.

Thomas, B. S. and R. C. Gupta (2016). "A comprehensive review on the applications of waste tire rubber in cement concrete." Renewable and Sustainable Energy Reviews 54: 1323-1333.

Thomas, B. S., R. C. Gupta and V. J. Panicker (2016). "Recycling of waste tire rubber as aggregate in concrete: durability-related performance." Journal of Cleaner Production 112: 504-513.

Thumann, A. and R. K. Miller (1986). "Fundamentals of noise control engineering."

Tikalsky, P., P. Carrasquillo and R. Carrasquillo (1988). "Strength and durability considerations affecting mix proportioning of concrete containing fly ash." ACI Materials Journal 85(6): 505-511.

Transportation, M. D. o. (2016). Missouri Standard Specifications for Highway Construction AGGREGATE FOR SEAL COATS, Missouri Highway and Transportaion Commission.

Troy, K., P. Sebaaly and J. Epps (1996). "Evaluation systems for crumb rubber modified binders and mixtures." Transportation Research Record: Journal of the Transportation Research Board(1530): 3-10.

Turgut, P. and B. Yesilata (2008). "Physico-mechanical and thermal performances of newly developed rubber-added bricks." Energy and Buildings 40(5): 679-688.

Tuwair, H., J. Volz, M. ElGawady, M. Mohamed, K. Chandrashekhara and V. Birman (2016). "Behavior of GFRP bridge deck panels infilled with polyurethane foam under various environmental exposure." Structures 5: 141-151.

USEPA (2010). Scrap Tires: Handbook on Recycling Applications and Management for the U.S. and Mexico. O. o. R. C. a. Recovery. Washington DC, United States Environmental Protection Agency.

Way, J. R. S. G. B. (2012). Asphalt-Rubber Chip Seal and Polymer Modified Asphalt-Rubber Two Layer System, Case Studies. Asphalt Rubber Conference Munich, Rubberized Asphalt Foundation.

Wood, T. J., D. W. Janisch and F. S. Gaillard (2006). Minnesota seal coat handbook 2006.

Xincheng, P. (2012). Super-High-Strength High Performance Concrete, CRC Press.

Xue, J. and M. Shinozuka (2013). "Rubberized concrete: A green structural material with enhanced energy-dissipation capability." Construction and Building Materials 42: 196-204.

Yandell, W. (1971). "A new theory of hysteretic sliding friction." Wear 17(4): 229-244.

Yandell, W. and S. Sawyer (1994). "Prediction of tire-road friction from texture measurements." Transportation Research Record(1435).

Yang, L.-h., Z. Han and C.-f. Li (2011). "Strengths and flexural strain of CRC specimens at low temperature." Construction and Building Materials 25(2): 906-910.

Yesilata, B., H. Bulut and P. Turgut (2011). "Experimental study on thermal behavior of a building structure using rubberized exterior-walls." Energy and Buildings 43(2): 393-399.

Youssf, O., M. ElGawady, J. Mills and X. Ma (2014). "Prediction of crumb rubber concrete strength."

Youssf, O., M. A. ElGawady and J. E. Mills (2015). Experimental investigation of crumb rubber concrete columns under seismic loading. Structures, Elsevier.

Youssf, O., M. A. ElGawady and J. E. Mills (2016). "Static cyclic behaviour of FRP-confined crumb rubber concrete columns." Engineering Structures 113: 371-387.

Youssf, O., M. A. ElGawady, J. E. Mills and X. Ma (2017). "Analytical modeling of the main characteristics of crumb rubber concrete." Special Publication 314: 1-18.

Yung, W. H., L. C. Yung and L. H. Hua (2013). "A study of the durability properties of waste tire rubber applied to self-compacting concrete." Construction and Building Materials 41: 665-672.

Zheng, L., X. S. Huo and Y. Yuan (2008). "Experimental investigation on dynamic properties of rubberized concrete." Construction and building materials 22(5): 939-947.

SECTION

3. SUMMARY, CONCLUSIONS AND RECOMMENDATIONS

This section summarizes the findings of all investigations.

3.1. SUMMARY AND CONCLUSIONS OF RESEARCH

This research aimed to investigate the feasibility of using recycled rubber in new construction applications. Based on particle size, recycled rubber was selected to match its natural counterpart which leads to three grades namely, recycled coarse aggregate, recycled fine aggregate, and recycled powder. For each one of these grades, new application was proposed, investigated, and evaluated.

Different ratios of recycled rubber were used as a fine aggregate replacement in masonry units. The mechanical and physical characteristics as well as the durability of rubberized concrete masonry units having 0%, 10%, 20%, and 37% crumb rubber were investigated. Furthermore, the thermal conductivity and the energy efficiency of the newly proposed masonry unit were investigated using four different approaches. Based on the experimental investigation of this application, the following conclusions can be drawn:

1. Producing rubberized concrete masonry units (RCMUs) in a typical masonry plant was undertaken successfully. Crumb rubber can be used up to 20% partial replacement for fine natural aggregate to produce RCMUs that meet the requirements of the ASTM C90.
2. The RCMUs have a lower unit weight; however, they have higher water absorption rate compared to those of conventional masonry units.

3. Despite the reduction in the compressive strength of RCMUs with increasing the rubber content, using 20% rubber replacement in RCMU resulted in a reduction of 6% in compressive strength of masonry prism. However, a significant reduction in the initial stiffness was observed causing a 34% reduction in initial stiffness when 20% rubber replacement was used.
4. RCMUs displayed significantly higher ultimate strain compared to those of conventional masonry units.
5. The addition of 20% rubber as a partial replacement of fine aggregate improved the durability of RCMUs by increasing the compressive strength after cycles of extreme environmental conditions.
6. Rubberized CMUs displayed a reduction in the ultrasonic pulse velocity and sound transmission. However, farther investigations are needed to study the impact of rubber on sound absorption, reflection, and energy reduction.
7. Scanning electron microscope (SEM) analysis of the interfacial transition zone (ITZ) showed that rubber particles have a weaker bond with cement paste than natural aggregates, which explained the systematic reduction in the compressive strength of the rubberized masonry blocks.
8. The specific heat of RCMUs increased linearly with increasing the rubber content. Increasing the rubber content from 0% to 37% increased the specific heat by an average of 19% depending on the experiment temperature. For example, at 45 °C, the specific heat increased from 950 J/kg.K to 1150 J/kg.K with increasing rubber content in cement paste from 0% to 37%. A similar trend was measured at 30 °C and 60 °C.

9. The thermal conductivity measured at the material level for rubberized masonry linearly decreased with increasing the rubber content. While the absolute values of the measured thermal conductivity varied depending on the used measuring method, both the thermal needle probe and guarded hot plate showed a reduction of 44.9% and 42.5% in the thermal conductivity, respectively, when the rubber content increased from 0% to 37%.
10. The thermal conductivity measured at the masonry unit level showed a nonlinear decrease with increasing the rubber content. Adding small rubber content of 10% reduce the thermal diffusivity of the block resulted in a significant drop of 22% in the thermal conductivity. Beyond that adding more rubber decreased the thermal conductivity at a smaller rate. Increasing the rubber content from 10% to 37% decreased the thermal conductivity by 16%.
11. A reduction in energy consumption was measured when RCMU was used in lieu of CMU. Replacing the fine aggregate with 10%, 20%, and 37% crumb rubber reduced the energy consumption that is needed to keep the temperature constant inside the hot box by 9.4%, 20%, and 45% respectively.
12. At the steady state, RCMUs had higher differences between the inner and outer temperatures compared to that of the CMUs. While the differences in inner and outer temperatures were 14.3 ℃ for CMU it increased to 24 ℃ for RCMU having 37% rubber content. Furthermore, the time to reach steady state heat flow was higher in the case of RCMUs compared to that of CMU. Increasing the rubber content from 0% to 37% increased the time required to reach steady state by 49%.

The second innovative application was using recycled rubber as a full or partial replacement of coarse aggregate in chip seal pavement surfacing. A broad investigation on the retention of the new aggregate with four asphalt-based binders was examined and compared to the performance of two mineral aggregates. In addition, the impact of using recycled rubber aggregate on the chip seal's micro and macro texture and their impacts on the skid resistance and driving safety was studied. Besides the physical performance, the environmental impact of using rubber aggregate in chip seal pavement in terms of leaching under different pH conditions was examined and evaluated based on the EPA drinking water standards. Based on the experimental investigation of this application, the following conclusions can be drawn:

1. The crumb rubber can be used as a mineral aggregate replacement; however, it is recommended to increase the curing time based on the crumb rubber replacement percentage. For a crumb rubber replacement percentage of 50% and above, curing time of six hours is required before sweeping.
2. For mineral aggregate, a minimum curing time of five hours is required before sweeping the chip seal.
3. Based on the microtexture analysis and the environmental impact, the ambient crumb rubber is recommended over the cryogenic crumb rubber because it has a much rougher surface and lower energy consumption during the production process. For example, the ambiently processed rubber tested in this study had a surface area 1.19 times that of the cryogenic rubber.
4. The standard sweep test, which specifies only one hour of curing time, does not give enough data to estimate the time to open the road. Therefore, the test should

be performed with a range of curing times to decide the best time of curing that causes less aggregate loss.

5. Chip seals with 100% crumb rubber aggregate, river gravel, or traprock passed the standard Vialit test with 100% aggregate retention. However, when the number of drops was increased to 40, the crumb rubber aggregate had 100% retention versus 65% to 90% for the mineral aggregates when emulsions were used, and 40% to 50% for the mineral aggregates when asphalt cement were used.
6. The Pennsylvania test showed that the crumb rubber had better retention than the mineral aggregates. The knock-off weight loss was between 1% to 3% for crumb rubber versus 7% to 12% for mineral aggregates for both emulsions 1 and 2.
7. Ambient processed crumb rubber displayed 20% higher surface area compared to that of cryogenically processed crumb rubber. This resulted in significant improvement in the microtexture of crumb rubber aggregates with higher contact area with tires which increases the adhesion component in skid resistance by 20%. Hence, it is recommended to use ambient processed rubber as aggregate.
8. Sand patch and section image processing showed that replacing mineral aggregates with crumb rubber improves the macrotexture of chip seal. An Increase of 25% and 33% in mean texture depth (MTD) was observed when 100% of the trap rock and creek gravel was replaced with crumb rubber, respectively.
9. While both micro and macrotexture showed significant improvements when crumb rubber was used as aggregate, a reduction ranging from 1.5% to 20% in the British Pendulum number (BPN) for specimens with rubber replacement ratios ranging from 25% to 100% was recorded. It should be noted that the BPN is not reliable for

a rough surface such as chip seal. Hence, more advanced techniques are required to measure the skid resistance of crumb rubber-based chip seal. Furthermore, under high temperatures, crumb rubber-based chip seal outperformed mineral aggregate-based chip seal. Specimens with 100% rubber did not show any loss in BPN under an elevated temperature of 65 °C while 10% loss was recorded in mineral aggregate-based chip seal.

10. A virtual 3D pyramid shape can be used to simulate aggregate particles to find the required binder application rate that produces chip seal with an embedment depth ranging from 50% to 80% of the average aggregate least dimension.
11. Using the crumb rubber that comes from scrap tires as a mineral aggregate replacement in chip seal pavement does not have a negative environmental impact in terms of heavy metal leaching. The toxic heavy metals leached from the recycle rubber or rubberized chip seal are below EPA drinking water standards.
12. The major leached heavy metal from the recycled bare rubber particles is Zn, which is consistent with the tire component. However, Zn is not regulated in primary drinking water regulations.
13. Under different pH conditions, a significant reduction of heavy metal leaching was recorded when rubber is used with emulsion in the form of chip seal pavement because asphalt is hydrophobic and prohibited the contact of tire and solution. About a 50% reduction of Zn leaching was recorded with chip seal specimens compared with the leaching from bare crumb rubber.
14. The metal leaching in all types of samples including rubber, asphalt emulsion, and chip seal decreased with the increase in pH value.

15. The cryogenic crumb rubber has a different metal leaching behavior than the ambient crumb rubber, depending on the pH value.

The third application was utilizing the waste of scrap tire processing in a form of rubber- fiber powder (RFP) as a sustainable alternative to produce rubberized mortar. The fresh and hardened properties of rubberized mortar with different RFP ratios were investigated as well as the durability of the new rubberized mortar mixtures and its ability to increase the corrosion protection for the steel reinforcement. In addition, RFP was used as an eco-friendly additive to improve the freeze-thaw performance of high-volume fly ash mortar mixtures. This application helps in overcoming the issue of the incompatibility between concrete mixtures with high volume fly ash and the air-entraining admixture. Finally, RFP was used as a partial replacement for sand in plastering mortar with a potential to improve both thermal and acoustic performance as well as reducing the buildings' energy consumption. Based on the experimental investigation of this application, the following conclusions can be drawn:

1. Adding RFP to mortar mixtures decreased mortar workability. For w/c of 0.51 and 0.56. Mortar mixtures with up to 20% RFP addition displayed a good workability reaching flowability of 40%, and 70%, respectively.
2. Decreases in the compressive and flexural strengths were noticed with the increase of RFP ratio. For example, mixtures with w/c of 0.51 at the age of 28 days, the compressive and flexural strength of rubberized cement mortar with 10% RFP decreased by 35%, 27%, and 9%, respectively. However, the compressive and flexural strength of cement mortar with 10% sand addition instead of cement

decreased by 76%, and 76%, respectively, which shows the advantage of adding RFP instead of cutting the cement content only.

3. The impact of adding the RFP on the bulk density relates to w/c ratio, workability, and the volume of the permeable voids. Adding 15% RFP reduced the bulk density after immersion and boiling from 2.20, 2.16 and 2.12 to 2.11, 2.02, and 2.06 for mixtures with w/c ratios of 0.42, 0.51 and 0.56 respectively.
4. Adding the RFP lowered and delayed the peak temperature for the heat of hydration compared to reducing the cement content only. The magnitude and the time of the peak heat flow of mixtures with 20% RFP ratios decreased by 25.5% 31.5% respectively.
5. Mortar mixtures with up to 20% RFP showed an improved bulk and surface electrical resistivity values which are a significant indication for better reinforcement corrosion resistance. For example, mixtures with w/c of 0.51 showed a linear increase in the surface and the bulk resistivity from 3.48 and 17.2 to 7.73 and 29.7, respectively, with 20% RFP. Beyond 20% RFP, the bulk and surface resistivity decreased due to the increase in the volume of the permeable voids.
6. The carbon dioxide penetration depth dropped by 38% by adding 10% of RFP to the mortar mixture with w/c ratio of 0.56. However, adding 5% or higher RFP for mixtures having w/c of 0.51 led to a linear increase in the carbonation depth reaching 200% at 25% addition. Furthermore, for both w/c ratios adding RFP was much better than adding sand. Adding 5% or higher sand, carbon dioxide had a full penetration throw the specimens for mixtures with W/C ratio of 0.51 and 0.56 due

to the change in air void content, particles arrangement, and accompanying air voids.

7. The results showed that using RFP of 10% to 15% in combination with w/c of 0.51 to 0.56 can yield a workable rubberized mortar with a significant potential for high corrosion resistance.
8. Using the ground recycled rubber as an additive to mortar mixture with different types and content of fly ash improved the freeze-thaw performance compared to the AEA. Crystallization of rubber particles under low temperature resulted in a compressive strength retention that exceeds 100% of that in unexposed specimens.
9. There was no clear difference in the freeze-thaw performance when RFP with a maximum size of 74 or 149 µm was used.
10. Plastering mortar mixtures with up to 40% of the cement or sand replaced by RFP did not show any difficulties to mix and apply with the required plastering thickness compared to the reference mortar mixture.
11. Adding RFP with a size smaller than 75 µm up to 20% of cement, decreased the apparent and bulk densities. However, using RFP with a size between 150 and 300 µm as a sand replacement was more influential on both densities and it continued up to 40% replacement of sand.
12. Although there was a reduction in the compressive, tensile and flexure strength, the modulus of toughness showed an increase of 19 and 16% when sand was replaced by 30 and 40% respectively, while the modulus of resilience showed relatively slight reduction with all RFP replacement ratios. These results show that increasing

RFP ratio will increase the strain energy that the rubberized mortar can absorb just before it fractures, which address the main cause of using plaster mortar.

13. At a temperature of 25˚ C, replacing 10, 20, 30 and 40% of cement with RFP reduced the thermal conductivity factor of rubberized plastering mortar by 29, 41, 47, and 52% respectively. Higher reduction in thermal conductivity was noticed when sand was replaced partially with RFP.

14. The coefficient of thermal conductivity showed a systematic reduction at low temperature. At a temperature of -10˚ C, mixtures with RFP ratio of 20% showed a reduction in coefficient of thermal conductivity of 57 and 62% when cement and sand were replaced respectively compared to 41 and 53% at 25˚ C.

15. Compared to conventional masonry units without any plastering, a reduction varied from 11 to 53% was achieved in thermal conductivity of masonry unit based on the size and amount of RFP as well as the thickness of the plastering lawyer.

16. Applying rubberized plastering mortar improved the sound absorption especially with frequencies up to 3000 Hz. Simultaneously, the noise reduction factor increased by applying the plastering layer with varied waste rubber powder content. Plastering layer with 10% waste rubber powder showed the best noise reduction of 0.34% compared with 0.2 for a layer of mortar plastering with 0% waste rubber powder and 0.19 for unplastered masonry unit.

3.2. RECOMMENDATIONS FOR FUTURE WORK

Extensive research was carried out to investigate the feasibility of using recycled rubber in new construction applications. Based on the sizes of crumb rubber particles, the following issues need to be investigated in future work:

Recycled rubber as a powder:

• The effect of incorporating rubber powder particles on the maximum packing density of concrete.

• The effect of space factor on the durability of rubberized mortar mixture. The space factor represents the distribution of the particles of the rubber powder as well as air voids within the matrix. The stability of air voids with time and its influence on the freeze-thaw performance need to be investigated as well.

•The effect of bond of rubberized mortar with different substrates on rubberized mortar as a plastering material.

Recycled rubber as a fine aggregate:

• The effect of rubber particle's size on the mechanical characterization of RCMUs.

• The effect of rubber particle's size on the thermal characterization of RCMUs. Furthermore, the effects of these measured characteristics on the overall energy consumption of RCMU buildings need to be addressed.

• The effect of rubber ratio and its effect on different rubber applications.

• The effect of using rubberized masonry units on the seismic performance of structural elements.

Recycled rubber as a coarse aggregate:

• The effect of different environmental and driving speed conditions as well as snow plowing on the temporal aggregate retention at the micro level

• The effect of average rubber particle's size on the long-term retention.

• The effect of different types of binders on the long-term aggregate retention.

• The effect of different chip seal parameters on the different components of the surface friction resistance, i.e., hysteresis forces and adhesion. The current standard tests such as British Pendulum tester does not simulate the real case scenario when tires have been in contact with chip seal surface.

• The effect of vehicle speed on the measured friction values.

• The effect of aggregate shape models such as the proposed pyramid shape model on the predicted mean texture depth for different aggregate sizes and types.

REFERENCES

Abu-Lebdeh, T., E. Fini and A. Fadiel (2014). "Thermal conductivity of rubberized gypsum board." Am. J. Eng. Applied Sci 7: 12-22.

Amirkhanian, S. N. (2001). "Utilization of crumb rubber in asphaltic concrete mixtures–South Carolina's Experience." See ref 3: 163-174.

Ang, G. and V. Marchal (2013). "Mobilising private investment in sustainable transport: The case of land-based passenger transport infrastructure." OECD Environment Working Papers(56): 0_1.

Atahan, A. O. and A. Ö. Yücel (2012). "Crumb rubber in concrete: static and dynamic evaluation." Construction and Building Materials 36: 617-622.

Batayneh, M. K., I. Marie and I. Asi (2008). "Promoting the use of crumb rubber concrete in developing countries." Waste Management 28(11): 2171-2176.

Benazzouk, A. and M. Queneudec (2002). Durability of cement-rubber composites under freeze thaw cycles. Proceeding of International congress of Sustainable Concrete Construction, Dundee-Scotland.

Eldin, N. N. and A. B. Senouci (1993). "Rubber-tire particles as concrete aggregate." Journal of materials in civil engineering 5(4): 478-496.

Epps, J. and L. Mason (1994). Uses of recycled rubber tires in highways: A synthesis of highway practice. Final report, National Cooperative Highway Research Program, Washington, DC (United States).

Fadiel, A., F. Al Rifaie, T. Abu-Lebdeh and E. Fini (2014). "Use of crumb rubber to improve thermal efficiency of cement-based materials." American Journal of Engineering and Applied Sciences 7(1): 1-11.

Fattuhi, N. and L. Clark (1996). "Cement-based materials containing shredded scrap truck tyre rubber." Construction and building materials 10(4): 229-236.

Fedroff, D., S. Ahmad and B. Savas (1996). "Mechanical properties of concrete with ground waste tire rubber." Transportation Research Record: Journal of the Transportation Research Board(1532): 66-72.

Ganjian, E., M. Khorami and A. A. Maghsoudi (2009). "Scrap-tyre-rubber replacement for aggregate and filler in concrete." Construction and Building Materials 23(5): 1828-1836.

Gou, M. and X. Liu (2014). "Effect of rubber particle modification on properties of rubberized concrete." Journal of Wuhan University of Technology-Mater. Sci. Ed. 29(4): 763-768.

Gransberg, D. D. and D. M. James (2005). Chip seal best practices, Transportation Research Board.

Hall, M. R., K. B. Najim and C. J. Hopfe (2012). "Transient thermal behaviour of crumb rubber-modified concrete and implications for thermal response and energy efficiency in buildings." Applied thermal engineering 33: 77-85.

Hanson, D., J. Epps and R. Hicks (1996). "Construction Guidelines for Crumb Rubber Modified Hot Mix Asphalt." Federal Highway Administration Report DTFH61-94-C-00035.

Hernandez-Olivares, F., G. Barluenga, M. Bollati and B. Witoszek (2002). "Static and dynamic behaviour of recycled tyre rubber-filled concrete." Cement and concrete research 32(10): 1587-1596.

Isler, J. W. (2012). Assessment of concrete masonry units containing aggregate replacements of waste glass and rubber tire particles, University of Colorado at Denver.

Karasahin, M., B. Aktas, A. Gungor, F. Orhan and C. Gurer (2014). "Laboratory and In Situ Investigation of Chip Seal Surface Condition Improvement." Journal of Performance of Constructed Facilities 29(2): 04014047.

Khatib, Z. K. and F. M. Bayomy (1999). "Rubberized Portland cement concrete." Journal of materials in civil engineering 11(3): 206-213.

Lee, S.-J., C. K. Akisetty and S. N. Amirkhanian (2008). "The effect of crumb rubber modifier (CRM) on the performance properties of rubberized binders in HMA pavements." Construction and Building Materials 22(7): 1368-1376.

Liu, H., X. Wang, Y. Jiao and T. Sha (2016). "Experimental investigation of the mechanical and durability properties of crumb rubber concrete." Materials 9(3): 172.

Maupin Jr, G. (1996). "Hot mix asphalt rubber applications in Virginia." Transportation Research Record: Journal of the Transportation Research Board(1530): 18-24.

Mohammed, B. S., K. M. A. Hossain, J. T. E. Swee, G. Wong and M. Abdullahi (2012). "Properties of crumb rubber hollow concrete block." Journal of Cleaner Production 23(1): 57-67.

Moustafa, A. and M. A. ElGawady (2017). "Dynamic properties of high strength rubberized concrete." ACI Spec. Publ 314: 1-22.

Moustafa, A. and M. A. ElGawady (2015). "Mechanical properties of high strength concrete with scrap tire rubber." Construction and Building Materials 93: 249-256.

Moustafa, A. and M. A. ElGawady (2016). "Strain rate effect on properties of rubberized concrete confined with glass fiber–reinforced polymers." Journal of Composites for Construction 20(5): 04016014.

Moustafa, A., A. Gheni and M. A. ElGawady (2017). "Shaking-Table Testing of High Energy–Dissipating Rubberized Concrete Columns." Journal of Bridge Engineering 22(8): 04017042.

Najim, K. and M. Hall (2010). "A review of the fresh/hardened properties and applications for plain-(PRC) and self-compacting rubberised concrete (SCRC)." Construction and building materials 24(11): 2043-2051.

Pacheco-Torgal, F., P. B. Lourenço, J. Labrincha and S. Kumar (2014). Eco-efficient masonry bricks and blocks: design, properties and durability, Woodhead Publishing.

Page, G. C. (1992). "Florida's initial experience utilizing ground tire rubber in asphalt concrete mixes." Journal of the Association of Asphalt Paving Technologists 61.

Paine, K. A. and R. K. Dhir (2010). "Research on new applications for granulated rubber in concrete." Proceedings of the institution of civil engineers: construction materials 163(1): 7-17.

Papagiannakis, A. and T. Lougheed (1995). A REVIEW OF CRUMB-RUBBER MODIFIED ASPHALT CONCRETE TECHNOLOGY. RESEARCH REPORT.

Presti, D. L. (2013). "Recycled tyre rubber modified bitumens for road asphalt mixtures: a literature review." Construction and Building Materials 49: 863-881.

Rangaraju, P. and S. Gadkar (2012). "Durability evaluation of crumb rubber addition rate on Portland cement concrete." Department of Civil Engineering, Clemson University, Clemson: 1-126.

Richardson, A., K. Coventry, V. Edmondson and E. Dias (2016). "Crumb rubber used in concrete to provide freeze–thaw protection (optimal particle size)." Journal of Cleaner Production 112: 599-606.

RMA, R. M. A. (2018). 2017 U.S. Scrap Tire Management Summary. Wasington, DC.

Sadek, D. M. and M. M. El-Attar (2015). "Structural behavior of rubberized masonry walls." Journal of Cleaner Production 89: 174-186.

Savas, B., S. Ahmad and D. Fedroff (1997). "Freeze-thaw durability of concrete with ground waste tire rubber." Transportation Research Record: Journal of the Transportation Research Board(1574): 80-88.

Shu, X. and B. Huang (2014). "Recycling of waste tire rubber in asphalt and Portland cement concrete: an overview." Construction and Building Materials 67: 217-224.

Shuler, S. (2011). Use of Waste Tires, Crumb Rubber, on Colorado Highways, Colorado Department of Transportation, DTD Applied Research and Innovation Branch.

Siddique, R. and T. R. Naik (2004). "Properties of concrete containing scrap-tire rubber–an overview." Waste management 24(6): 563-569.

Sukontasukkul, P. (2009). "Use of crumb rubber to improve thermal and sound properties of pre-cast concrete panel." Construction and Building Materials 23(2): 1084-1092.

Sukontasukkul, P. and C. Chaikaew (2006). "Properties of concrete pedestrian block mixed with crumb rubber." Construction and Building Materials 20(7): 450-457.

Thomas, B. S. and R. C. Gupta (2015). "Long term behaviour of cement concrete containing discarded tire rubber." Journal of Cleaner Production 102: 78-87.

Thomas, B. S. and R. C. Gupta (2013). "Mechanical properties and durability characteristics of concrete containing solid waste materials." Journal of Cleaner Production.

Thomas, B. S., R. C. Gupta and V. J. Panicker (2016). "Recycling of waste tire rubber as aggregate in concrete: durability-related performance." Journal of Cleaner Production 112: 504-513.

Troy, K., P. Sebaaly and J. Epps (1996). "Evaluation systems for crumb rubber modified binders and mixtures." Transportation Research Record: Journal of the Transportation Research Board(1530): 3-10.

Turgut, P. and B. Yesilata (2008). "Physico-mechanical and thermal performances of newly developed rubber-added bricks." Energy and Buildings 40(5): 679-688.

Xue, J. and M. Shinozuka (2013). "Rubberized concrete: A green structural material with enhanced energy-dissipation capability." Construction and Building Materials 42: 196-204.

Yang, L.-h., Z. Han and C.-f. Li (2011). "Strengths and flexural strain of CRC specimens at low temperature." Construction and Building Materials 25(2): 906-910.

Yesilata, B., H. Bulut and P. Turgut (2011). "Experimental study on thermal behavior of a building structure using rubberized exterior-walls." Energy and Buildings 43(2): 393-399.

Youssf, O., M. A. ElGawady and J. E. Mills (2015). Experimental investigation of crumb rubber concrete columns under seismic loading. Structures, Elsevier.

Youssf, O., M. A. ElGawady and J. E. Mills (2016). "Static cyclic behaviour of FRP-confined crumb rubber concrete columns." Engineering Structures 113: 371-387.

Youssf, O., M. A. ElGawady, J. E. Mills and X. Ma (2017). "Analytical modeling of the main characteristics of crumb rubber concrete." Special Publication 314: 1-18.

Yung, W. H., L. C. Yung and L. H. Hua (2013). "A study of the durability properties of waste tire rubber applied to self-compacting concrete." Construction and Building Materials 41: 665-672.

Zheng, L., X. S. Huo and Y. Yuan (2008). "Experimental investigation on dynamic properties of rubberized concrete." Construction and building materials 22(5): 939-947.

VITA

Ahmed Adnan Gheni was born in Basrah, Iraq. He received his Bachelor of Civil Engineering degree in 2000 and his Master of Science in Structural Engineering degree in 2010 both from Tikrit University, Iraq. During his Master coursework, he conducted a research on the dynamic response of lightweight concrete beams. He was granted a PhD scholarship by the Higher Committee for Education Development in Iraq (HCED) and began his PhD at Missouri University of Science and Technology in January 2013.

After graduation with his Bachelor degree, he worked in the construction industry for more than 12 years managing, supervising, and designing different construction projects in the field of education, health, and infrastructures. Finally, he worked as a consultant engineer at University of Tikrit, Iraq with a duties of structural design checking, in site nondestructive tests, structures assessments and strengthening for the new and old building of the university.

Ahmed has been a member of many professional organizations such as; American Concrete Institute (ACI), American Society of Civil Engineering (ASCE), The Masonry Society (TMS) as well as various honor society such as Chi Epsilon Honor Society, Tau Beta Pi Honor Society, Blue Key Honor Society, and Associated General. His research has focused on the short and long-term performance of sustainable infrastructure where recycled scrap tires replaced mineral fine aggregates in concrete, masonry, and chip seal.

In May 2019, he received his Ph.D. in Civil Engineering from Missouri University of Science and Technology.